HOW DNA PACKAGING AND PROCESSING PROTEINS AFFECT DYNAMIC DNA ALKYLATION

by
Shane R. Byrne

A dissertation submitted to Johns Hopkins University in conformity with the requirements for the degree of Doctor of Philosophy

Baltimore, Maryland
October 2019

Abstract

DNA alkylating agents are commonly considered toxic due to the irreversible nature of the lesions that they form and the failure of DNA repair enzymes to remove their lesions. However, compounds that alkylate DNA in a reversible manner may not share the same toxicity as irreversible alkylating agents. Quinone methides (QMs) are a class of transient electrophiles that reversibly alkylate DNA. A bifunctional QM conjugated to the DNA intercalator acridine (bisQMAcr) has previously been synthesized in order to examine the dynamics of reaction with DNA. BisQMAcr's reversible chemistry facilitates its stepwise migration from one end of a duplex DNA to the other in a bipedal manner. However, bisQMAcr requires 7 days to traverse 10 base pairs, which may be too slow to be effective *in vivo* to evade DNA repair.

Two monofunctional QMs were linked together using a flexible polyammonium alkyl chain (diQMs) to potentially facilitate faster QM migration. Additionally, BisQMs conjugated to weakly intercalative quinoxalines were synthesized to avoid the strength of acridine's intercalation that may have suppressed QM migration. However, neither of the new QMs alkylated DNA reversibly. Thus, bisQMAcr remains the most dynamic QM synthesized to date.

The environment within cells likely influences the potency of QMs' reversible DNA alkylation, since cellular DNA is packaged around histone proteins to form nucleosomes. The assembly of DNA into nucleosomes weakens QMs' potency as DNA alkylating agents by 90% relative to DNA free in solution. Nucleosomes possess an additional protective function against bisQMAcr's DNA alkylation, as the histone proteins serve as terminal acceptors of bisQMAcr's DNA adducts. BisQMAcr can release from its adducts on DNA and alkylate the

histones, leaving the DNA unmodified. However, QM alkylation of the histones does not interfere with their assembly into nucleosomes, as adducts formed in the core regions of the protein that may not disrupt with the necessary DNA-protein contacts for nucleosome formation.

The ability of DNA polymerases and helicases to modulate the dynamics of bisQMAcr's DNA alkylation and of bisQMAcr's crosslinks to inhibit replication was also investigated to determine whether biological machines may hasten QM migration. The Klenow Exo⁻ and φ29 DNA polymerases were unable to cause bisQMAcr's crosslinks to break apart and failed to extend DNA primers in the presence of the crosslinks. However, the T7 bacteriophage gene 4 protein (T7GP4) DNA helicase was able to unwind DNA containing reversible QM crosslinks. The helicase induced dissociation of only 40% of bisQMAcr's crosslinks, while the remaining 60% remained intact. Irreversible DNA crosslinks formed by mechlorethamine completely resisted unwinding by the T7GP4 helicase, suggesting that only reversible crosslinks separate during DNA unwinding. Reversible QM crosslinks may not pose an absolute block to replication like many irreversible crosslinking agents do. The ability of a helicase to remove QM adducts from DNA essentially affords DNA repair without relying on specific DNA repair proteins.

This work describes the potency of reversible QM alkylation in a biological setting. Transfer of reversible adducts to the histone proteins and loss of DNA adducts by helicases' translocation may afford their repair by means of their intrinsic reversible chemistry.

Thesis Advisor: Dr. Steven E. Rokita

Readers: Dr. Marc M. Greenberg, Dr. Evangelos Moudrianakis

Acknowledgements

I would not have had the experience that I had throughout my graduate school career without my advisor, Dr. Rokita. I would like to thank him for his guidance, support, mentorship, grace, respect, and kindness throughout my time at Hopkins. He was the best fit for me as an advisor, and was instrumental to my success throughout graduate school and my development as an independent scientist. He has always showed concern for my development as a scientist, student, and as a person. He respected my abilities as a scientist and treated me as a "partner" throughout the research project, rather than as a subordinate. He let me drive the project in the directions that peaked my interest, but never failed to draw me back in to think about the overall goal of the project and how to best achieve it. We could share ideas with each other, and learn from each other throughout the process, as opposed to me only learning from him. He respected the attributes that I could contribute to the research, and allowed the research to change directions based on my interests. I cannot thank him enough for the motivation and inspiration that he instilled in me. He always knows how to see the best in negative situations. Almost every time that I showed him a result that I deemed negative, he would exclaim "that's not as bad as you think, because at least we learned something from the data". His passion for learning, rather than solely obtaining results inspired me to learn as much as possible throughout my time here and to push further than I thought was possible. I cannot thank him enough for his mentorship and I hope to lead by his example in my future endeavors.

I would like to thank the members of my thesis committee for their support, guidance, and suggestions along the way. Dr. Greenberg, Dr. Bailey, and Dr. Bryant provided many helpful suggestions and directions for my research throughout the past few years, and always

materials at the last minute. Additionally, they always were very supportive and helpful with planning events, such as providing me suggestions for the student happy hours and always placing the orders for me and making amazing flyers to advertise the events. I would also like to thank Renee Eastwood for her support during the past year and for her dedication to advocating for graduate students' needs. I want to thank Boris Steinberg for always displaying kindness and never failing to fix any issues that were brought to his attention. He always provided great conversations to lighten the mood and never failed to listen to whatever it was that I had to say. Running into Boris always improved the mood of my day.

I would like to thank some of the current and former members of the Rokita Lab for their collegiality. Zuodong Sun and Qi Su have been the senior members of the lab for the past few years and were always a pleasure to interact with. I wish them both luck in their next endeavors and with their upcoming dissertation defenses. Qi's smile was very infectious and it was always great to pass by him and receive a very "bubbly" hello. I would like to acknowledge Ravina Moirangthem for her willingness to learn about me and hear what I have to say. I would like to thank Bing Xu and Daniel Lemen for their immense kindness and for always treating those around them in the most respectful way. I hope that they are able to inspire others with their kindness and respect the way that they inspired me. Dr. Mark Hutchinson was such a pleasure to work with for the short time that we worked together and has since become a great friend. He trained me and helped integrate me into the lab when I first joined. He was instrumental in providing me the skills needed for success in my research. I would also like to acknowledge Dr. Jonathan Musila for his kindness, support, and assistance with protein purification. He was always a pleasure to talk with during his year here and he has great foresight.

I would like to thank my friends and classmates that really helped to make this an enjoyable experience. It was always nice to have their support and to get a break from the lab by interacting with them. Whether it was through coffee, lunch, or just chatting in the hallway, all of my friends and classmates at Hopkins made a huge difference and made my experience here great. Lastly, I would like to thank my parents, grandparents, and the rest of my family for all of their guidance, support, and love that helped get me to where I am now.

Table of Contents

List of Tables

List of Figures

List of Schemes

List of Supporting Figures

List of Abbreviations

A- adenine

AP- abasic site

BcPh- benzo[c]-phenanthrene

BER- base excision repair

BHT- butylated hydroxytoluene

bisQM- bifunctional quinone methide

bisQMP- bifunctional quinone methide precursor

bisQMPAcr- bifunctional quinone methide precursor conjugated to acridine

BisQMPQuin- bis-quinone methide precursor conjugated to a quinoxaline

BSA- bovine serum albumin

C- cytosine

conc- concentration

dAN6- N6 position of adenine

DCM- dichloromethane

ddNTP- dideoxynucleotide triphosphate

dGN1- N1 position of guanine

dGN2- N2 position of guanine

dGN7- N7 position of guanine

$DiQMPN_2$- di-quinone methide precursor conjugated to a diammonium linker

$DiQMPN_3$- di-quinone methide precursor conjugated to a triammonium linker

DMF- dimethylformamide

DNA- deoxyribonucleic acid

dNTP- deoxynucleotide triphosphate

ebisQMAcr- electron-rich analogue of the bis-quinone methide conjugated to acridine

EDC- 1-Ethyl-3-(3-dimethylaminopropyl)carbodiimide

ESI- electron spray ionization

Et 743- Ecteinascidin 743

FAB- fast atom bombardment

G- guanine

h- hours

HN2- mechlorethamine

HRMS- high resolution mass spectrometry

ICL- inter-strand crosslink

IDT- Integrated DNA Technologies

min- minutes

monoQM- monofunctional quinone methide

MsCl- methanesulfonyl chloride

NCP- nucleosome core particle

NER- nucleotide excision repair

NMR- nuclear magnetic resonance

NO- nitric oxide

NSAID- nonsteroidal anti-inflammatory drugs

OD- oligodeoxynucleotide

PAGE- polyacrylamide gel electrophoresis

PEI- polyethylenimine

ppm- parts per million

p-TsOH- *para*-toluenesulfonic acid

QM- quinone methide

sat- saturated

sec- seconds

T- thymine

T7GP4- T7 Bacteriophage Gene 4 Protein

TBDMS- *tert*-butyl-dimethylsilyl

TFA- trifluoroacetic acid

TLC- thin layer chromatography

TLS- translesion synthesis

UPLC-MS- Ultra Performance liquid chromatography-mass spectrometry

UV- ultra-violet

WRN- Werner syndrome

Chapter 1: Introduction

1.1 DNA Damage

Deoxyribonucleic acid (DNA) encodes all of the genetic information that regulates an organism's chemical and biochemical processes, as well as their phenotypic characteristics. However, DNA is susceptible to various forms of damage that can interfere with the processing of the information contained in DNA. This damage can arise from many sources that are both exogenously and endogenously generated. As such, our DNA is constantly exposed to agents that can wreak havoc on our cells (Figure 1.1). Chemicals found in the environment, such as acrolein which is a constituent of cigarette smoke, may act as electrophiles that react with the nucleophilic bases within DNA.[1] Polycyclic aromatic hydrocarbons (PAHs) are widespread in the environment, as they are generated from the burning of fuel.[2] Once ingested, PAHs require metabolic activation via oxidation to unleash their toxicity through DNA damage.[3] Exposure to the sun's UV light can result in skin cancer via the formation of bulky photochemical DNA lesions.[4] In addition, organisms are exposed to ionizing radiation produced from the sun, lightning, nuclear reactors, and x-ray tubes.[5] Ionizing radiation induces DNA damage via radical-mediated hydrogen atom abstraction that causes DNA strand scission.[6] Lastly, countless drugs damage our DNA, either as their mechanism of action or as an undesired side effect. Many anticancer drugs, such as temozolomide and chlorambucil, function as alkylating agents that transfer an alkyl group to DNA to induce apoptosis of diseased cells.[7, 8]

Damage can occur to DNA's phosphodiester backbone as well as on its nucleobases. This compromises DNA's structural integrity by strand scission, which will lead to a loss of
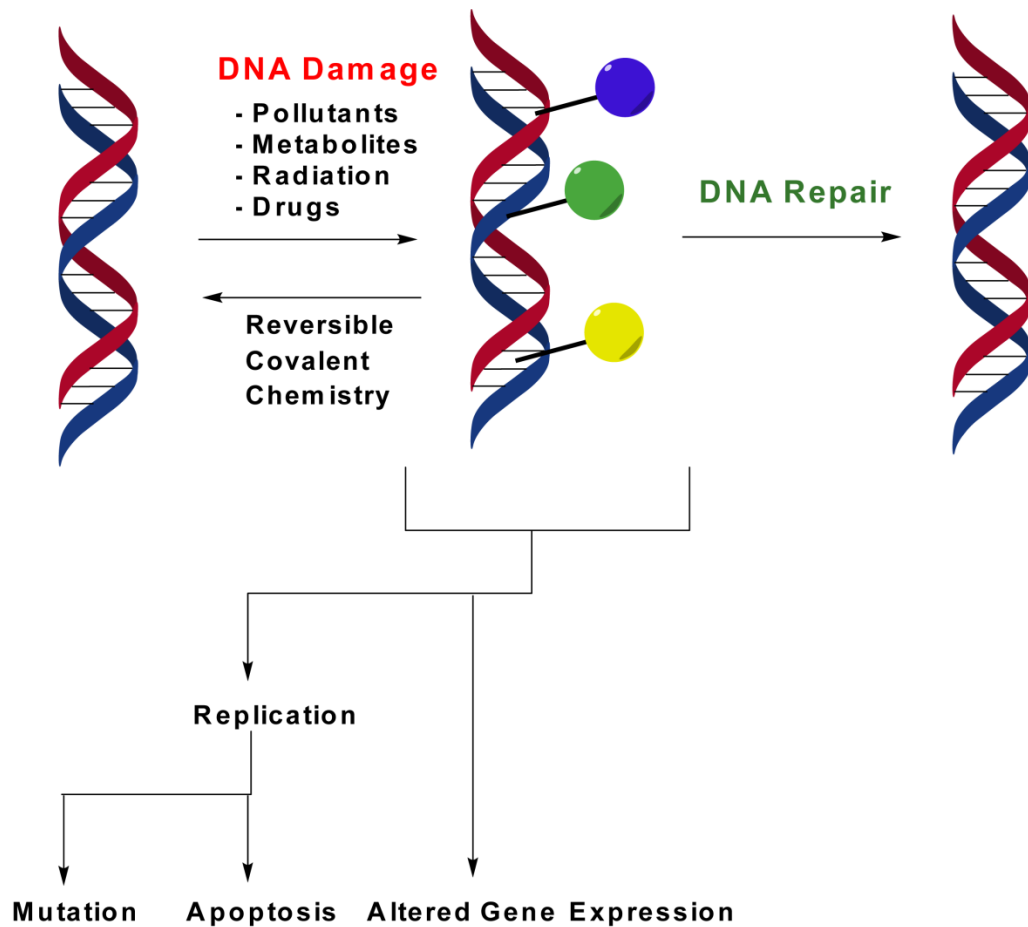
Figure 1.1 Sources and impact of DNA damage.[9]

genetic information or improper regulation of the genome. Although the half-life for

spontaneous hydrolytic strand cleavage is greater than 30,000,000 years, alkaline conditions

and enzymes can hydrolyze the phosphodiester backbone with rate enhancements on the

order of 10^{17}.[10] Hydrolysis can also damage the nucleobases to create mutations in the DNA

sequence. For instance, hydrolytic deamination of cytosine (C) generates uracil (U), a non-

native DNA base that may lead to mutations in the genetic code. Uracil forms Watson-Crick

base pairs with adenine (A), and will create C:G to T:A transversions in the DNA sequence

after DNA replication. Lesions on the nucleobases may not only interfere with hydrogen-

bonding between the nucleobases within duplex DNA, but also disrupt replication,

transcription, and translation of an organism's genetic information. Oxidative damage to the bases can also change the hydrogen bonding pattern with DNA, resulting in mutations. For example, oxidation of guanine to form 8-oxo-guanine creates G to T substitutions in DNA by forming Watson- Crick base pairs with adenine instead of cytosine after replication.[11] Adducts on the bases can also disrupt transmission of the genetic code by polymerases and helicases that act on DNA. Covalent DNA crosslinks generated by bifunctional DNA alkylating agents are considered toxic to cells due to posing blocks to DNA replication.[12] DNA crosslinks prevent strand separation, which is required for the transmission of the genetic information encoded by an organism's DNA.[13]

1.2 Impact of DNA Damage

Any form of DNA damage has the potential to impair the chemical and biochemical processes that regulate transmission of the genetic code (Figure 1.1). Some forms of DNA damage may not harm cells, but others may lead to effects as drastic as apoptosis. Small modifications to the nucleobases, such as oxidation of cytosine to 5-hydroxy-C, may not affect cellular viability if they do not impair DNA replication. However, incorrect replication of modified bases may result in mutations due to the formation of incorrect base pairs. For instance, 5-hydroxy-C will produce a C to T transition via formation of the highly miscoding 5-hydroxy-U following deamination.[14] Base transitions will not cause apoptosis, but the point mutations that result may affect protein folding or abolish essential protein activities.[15]

Cells contain repair mechanisms to reverse the deleterious effects of DNA damage. Different repair pathways have evolved for different types of lesions, with numerous steps and enzymes often required to afford repaired DNA. The simplest mechanism is direct reversal of the DNA damage. However, only a handful of enzymes exist that repair a few

specific types of DNA damage without further deconstructing the DNA. O^6-Methyl guanine methyltransferase removes a methyl group from the O^6- position of guanine to generate the unmodified nucleobase, while the oxygenase AlkB restores adenine and cytosine from N^1- methyl adenine and N^3-methyl cytosine, respectively.[16] Most lesions are repaired by the creation of strand breaks in the DNA, before restoration of the DNA to its unmodified state. Small, non-bulky lesions on the nucleobases are repaired by base excision repair (BER).[17] BER involves the action of specific glycosylases, the enzymes responsible for cleaving the glycosidic bond of damaged nucleobases, for specific DNA lesions.[17] Thus, BER is restricted to only those specific lesions that are recognized by a particular DNA glycosylase. Nucleotide excision repair (NER) is less stringent for repairing DNA lesions, as one network of enzymes recognizes a wide variety of lesions. Generally, bulky lesions and some inter-strand crosslinks are repaired by NER via a complex and well-coordinated network of enzymes that recognize and excise the damage before restoring the resulting gap in the DNA sequence.[18] Lesions that create double strand breaks in DNA have the potential to cause significant damage to cells by fragmenting an organism's genome, and therefore are repaired by a well-synchronized network of enzymes during homologous recombination. Although no universal mechanism for repair of one of the most deleterious DNA lesions, DNA inter-strand crosslinks (ICLs), exists, a wide array of processes repair ICLs.[19, 20] A complex network of proteins from various pathways, such as those associated with Fanconi Anemia and translesion synthesis polymerases, function to repair ICLs. However, ICL repair does not always succeed due to the bulk of their lesions, their presence on both strands of duplex DNA, and their severe distortion of DNA's structure.[19] As a consequence, cells may enter apoptosis or cancer may develop as a result of ICLs. Investigating the biological

consequences of DNA ICLs may provide an assessment of their role in the development of disease and their potential as a chemotherapeutic mechanism.

Some forms of damage may not require repair and may not cause toxicity to cells. Some lesions, such as ICLs, are considered toxic due to the irreversibility of their DNA adducts in the absence of DNA repair pathways. However, DNA adducts that form reversibly may not harm cells in such a manner. These adducts may not require the cell's repair mechanisms, as their intrinsic reversible covalent chemistry may afford their removal from DNA. On the other hand, reversible chemistry may enhance the lesion's toxicity if the reactive moiety were regenerated and able to react with a new site on the DNA molecule after its removal from its first site of reaction. Reversible DNA lesions warrant investigations to evaluate their toxicity, which may inform the development of drugs that function with reversible covalent chemistry.

1.3 DNA Alkylation

Alkylating agents not only contain electrophiles for covalent DNA modification, but also often possess a moiety that directs their binding to DNA. Without localization to DNA, alkylating agents' potency will suffer due to off-target reactions with other nucleophiles present in cells. Bifunctional alkylating agents, or crosslinking agents, predominate over
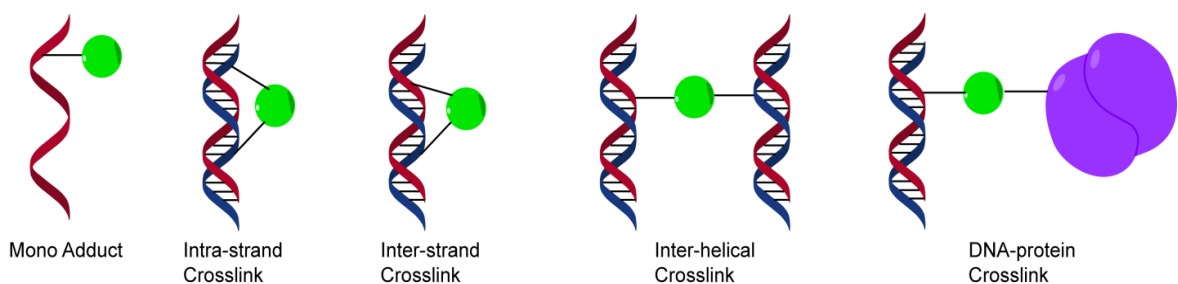
Figure 1.2 Types of DNA adducts formed by DNA alkylating agents.

monofunctional alkylating agents in the clinic since DNA ICLs are more deleterious than

mono adducts. ICLs affect both DNA strands in the duplex, while monoadducts damage only

one strand and may be more easily repaired. Crosslinking agents form a variety of adducts

with biological nucleophiles (Figure 1.2). Mono adducts form when only one electrophile

reacts with DNA to form an adduct that may be less challenging to repair than DNA

crosslinks. A variety of crosslinks can form, depending on which DNA strand reacts with the

electrophile. ICLs are considered more deleterious than intra-strand crosslinks because they

prevent separation of DNA's strands, which is necessary for replication and transcription.

DNA inter-helical and DNA-protein crosslinks may pose even greater challenges for cells to

overcome than DNA ICLs by interfering with the proteins that process DNA and posing

large roadblocks DNA processing. In particular, DNA-protein crosslinks are large, toxic

lesions that impede chromatin-based processes such as transcription and DNA unwinding.[21]

The ICLs generated by DNA crosslinking agents serve as a chemotherapeutic

mechanism. Crosslinking agents selectively and irreversibly alkylate the DNA in cancerous
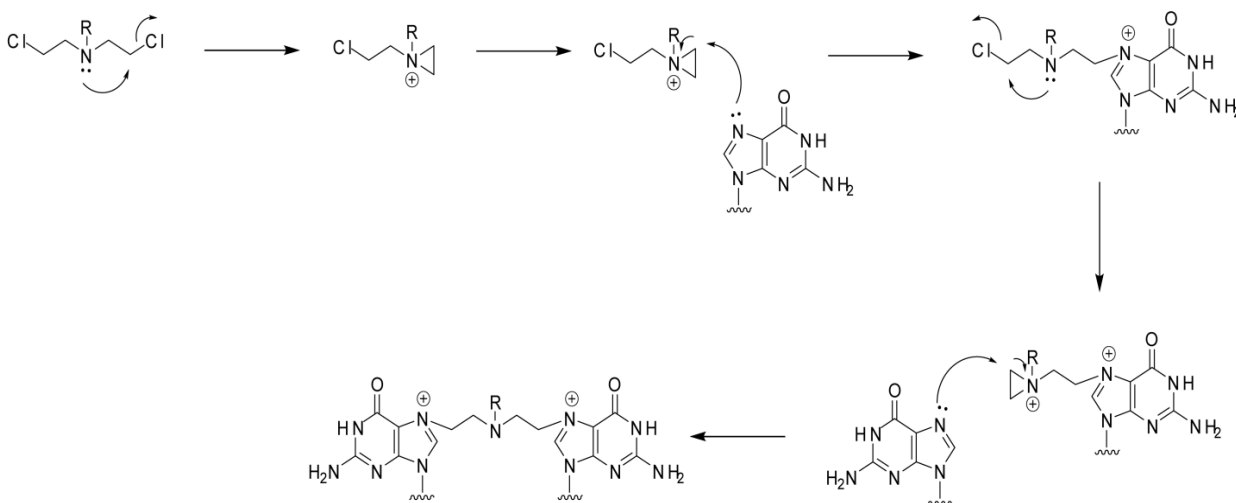
Scheme 1.1 Mechanism of DNA crosslinking by nitrogen mustards.

cells to induce their apoptosis. Several exogenous crosslinking agents have been developed as therapeutic agents that are used in the clinic. Nitrogen mustards are among one of the earliest classes of alkylating agents to be used as chemotherapeutics. Nitrogen mustards react irreversibly at the N7 position of guanines (dGN7) in 5'-GNC-3' sequences (Scheme 1.1).[13, 22] The nitrogen mustard first undergoes an intramolecular substitution reaction to generate the reactive aziridinium ion. The resulting positive charge assists in localizing the compound to DNA for reaction. The nucleophilic dGN7 then reacts with the aziridinium ion to form a nitrogen mustard- DNA mono adduct. Subsequent formation of a second aziridinium and nucleophilic substitution with a second dGN7 generates the DNA ICL.

Mitomycin C is another chemotherapeutic agent that functions by forming irreversible DNA ICLs. Unlike the nitrogen mustards, mitomycin C requires reductive activation to uncover the electrophilic species capable of alkylating DNA (Scheme 1.2).[23, 24] Mitomycin C's selectivity for cancer cells arises from the hypoxic conditions characteristic of some tumor cells. Upon reduction, mitomycin C binds DNA's minor groove to position the resulting electrophilic quinone methide (QM) to react with the N2 position of guanine
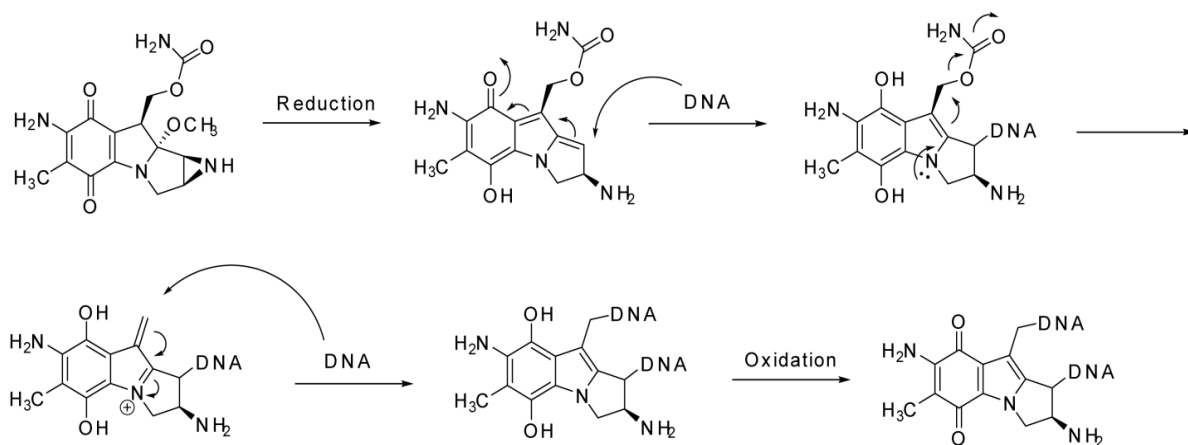
Scheme 1.2 Mechanism of DNA ICL formation by mitomycin C.

(dGN2). Subsequent loss of carbamate unveils a second electrophile that reacts with a second dGN2 to form an irreversible ICL. The irreversible ICLs generated by nitrogen mustards and mitomycin C halt biochemical processes that require separation of DNA's strands. Both compounds suffer from off-target reactions with DNA from healthy cells, which limits their efficacy.

The effectiveness of chemotherapeutic DNA alkylating agents often suffers from repair of their lesions by the cell's repair mechanisms. However, drugs that alkylate DNA reversibly may improve their potency. Once repaired, the alkylating agent may be able to regenerate its reactive moiety. This would allow a reversible alkylating agent to alkylate DNA again, either at the same site or at a different nucleophilic site within DNA. The natural product Ecteinascidin 743 (Et 743) reversibly alkylates DNA at dGN2s (Figure 1.3). Repeated capture and release of Et 743 by reversible covalent reaction with DNA permits its migration from sites of greatest kinetic selectivity to sites of greatest thermodynamic stability.[25] Et 743's diffusion through DNA essentially extends the drug's effective lifetime.
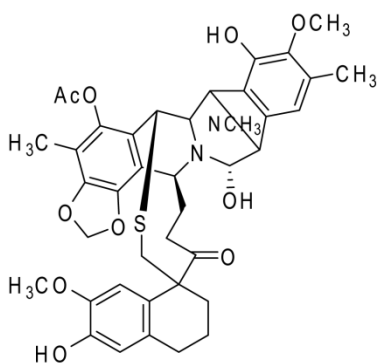
Ecteinascidin 743

Figure 1.3 Structure of Ecteinascidin 743.

Thus, Et 743's intrinsic reversible chemistry may enhance its potency as a chemotherapeutic drug by permitting it to evade repair of its DNA adducts.

The endogenously generated alkylating agent acrolein also forms reversible adducts with DNA.[26] Acrolein is a toxic component of cigarette smoke that is produced *in vivo* from oxidation of the glycerol contained in cigarettes.[27] Acrolein forms DNA ICLs by initially reacting with dGN2 via Michael addition, before subsequent addition of a second dGN2 to the aldehyde (Scheme 1.3).[28] In addition, acrolein can react intramolecularly with the N1 position of guanine (dGN1) to form an adduct on a single guanine residue. These adducts cause mutagenic stress on cells that triggers DNA repair pathways or apoptosis.[29, 30] However, the reversibility of acrolein's DNA adduct may reduce acrolein's toxicity. Regeneration of acrolein will leave the DNA unmodified, essentially affording repair of the DNA. Acrolein may then re-alkylate the DNA, causing more damage, or alkylate another nucleophile present in cells. Thus, the reversibility of some alkylating agents may either enhance their toxicity by extending the electrophile's effective lifetime, or reduce their toxicity by affording DNA repair.
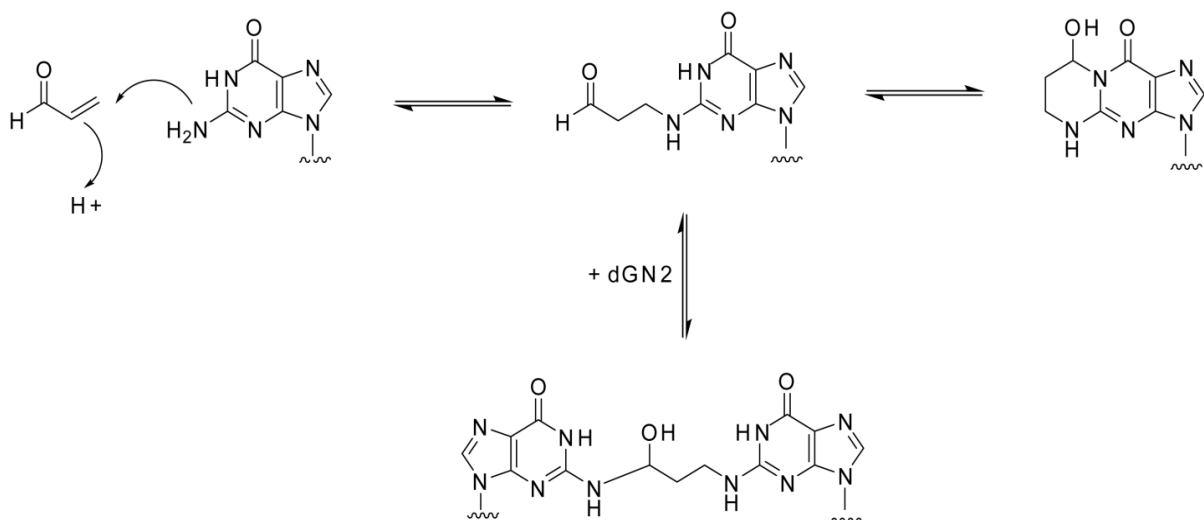
Scheme 1.3 Alkylation of DNA by acrolein.

9

1.4 Quinone Methides

Quinone methides (QMs) are another class of endogenously generated electrophiles that alkylate DNA. QMs are transient electrophilic intermediates that are often formed *in vivo* following metabolic activation.[31] QMs are involved in plant lignification and are components of natural products, such as the taxodiones and celastrol.[31] Drugs, such as tamoxifen, mitomycin C, and some of the nitric oxide (NO)-precursors to the non-steroidal anti-inflammatory drugs (NSAIDs), and the food additive butylated hydroxytoluene (BHT) form QMs upon metabolic activation (Figure 1.4).[23, 32-35] QMs may form as a result of oxidation, ester hydrolysis, or photochemical activation.[36] Once generated, QMs act as both desired metabolites that assist in a drug's mechanism of action, and as undesired byproducts of metabolism. BHT, contained in many processed foods, forms a potentially toxic QM upon oxidation. The BHT-QM may then interfere with cellular processes by alkylating DNA and protein nucleophiles.

QMs react as Michael acceptors with a wide variety of nucleophiles found in biological systems, such as thiols, water, amino acids, and DNA's nucleobases. QMs form either as the *para*-QM isomer, or the more reactive *ortho*-QM isomer (Figure 1.4).[36] QMs are unique alkylating agents, as their alkylation can be either reversible or irreversible, depending on the pKa of the conjugate base of the QM-adduct and the electronics of the QM. *Ortho*-QMs form a variety of reversible and irreversible adducts with DNA (Scheme 1.4).[37] The strong nucleophiles within DNA form reversible adducts with QMs due to the low pKa of the adduct's conjugate base. The kinetically favorable, reversible QM-DNA adducts evolve over time to form the thermodynamically stable, irreversible adducts. Owing to their reversible DNA alkylation and relative ease of activation, QMs may find application as
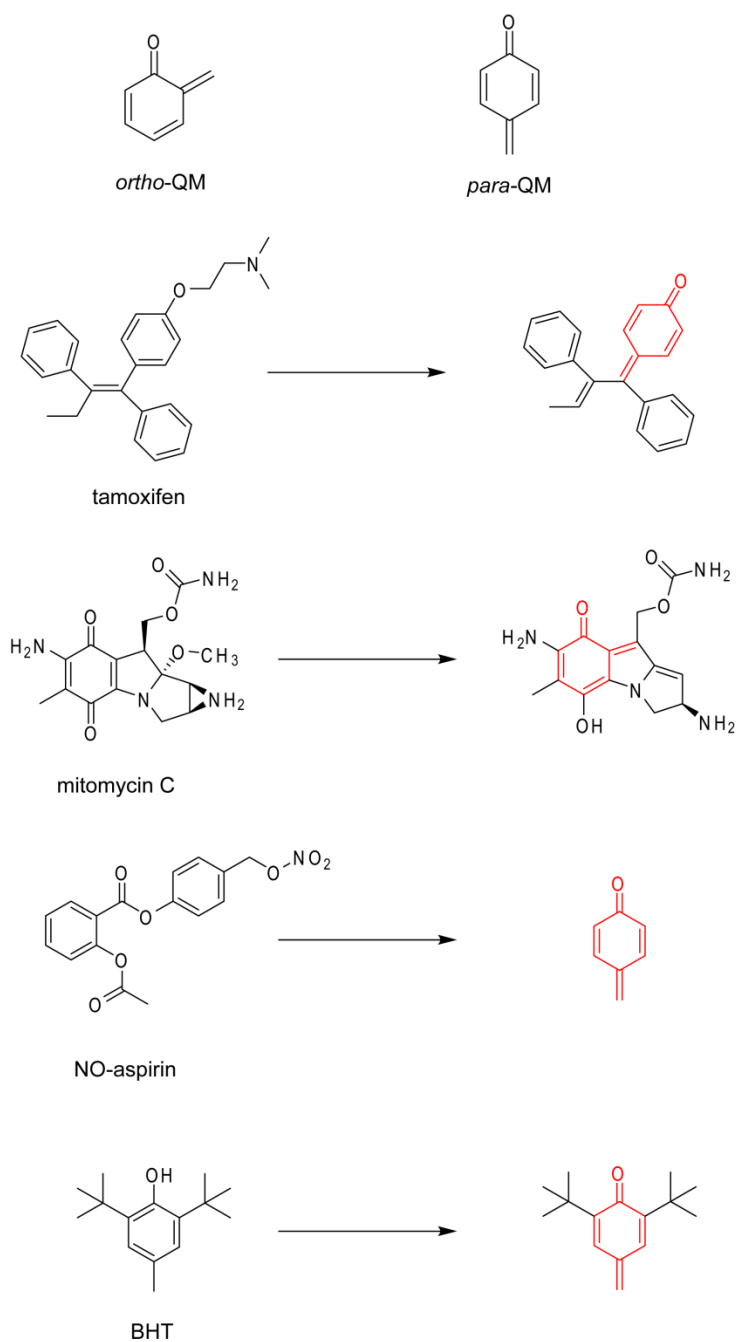
Figure 1.4 Structures and formation of quinone methides from drugs and food additives. The QM moiety is highlighted in red.

potential chemotherapeutic agents. However, QMs also exist as naturally occurring

electrophiles with the potential to create toxicity for cells. Thus, understanding how their
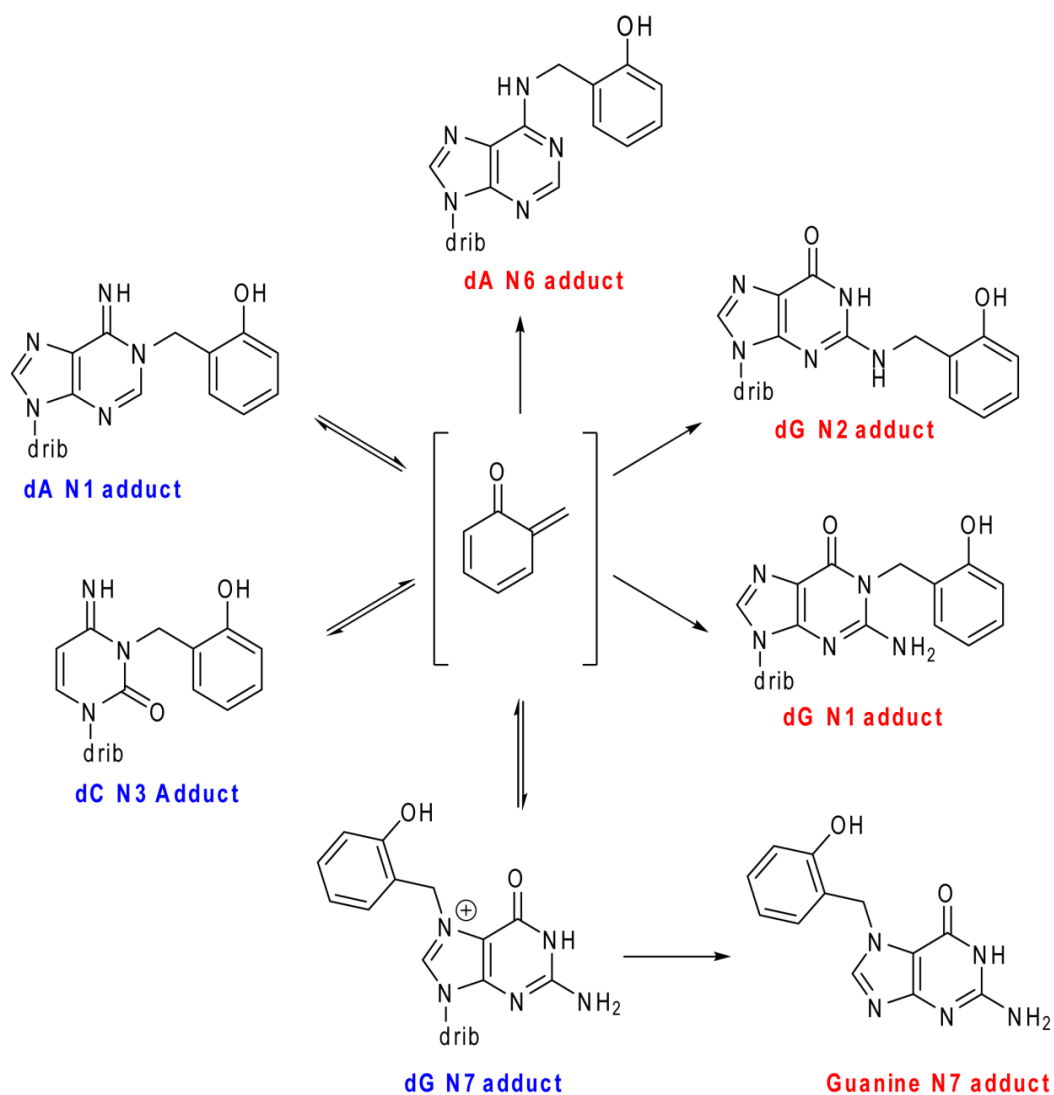
Scheme 1.4 DNA adducts formed by *ortho*-QMs. Reversible adducts are labeled in blue, while irreversible adducts are labeled in red.[38]

reversible alkylation modulates their effects on a biological system may reveal new

mechanisms by which reversible chemistry interferes with biochemical processes.

Bifunctional QMs (bisQMs) have been synthesized to explore reversible DNA ICLs.

However, bisQMs must be generated from their stable precursors (bisQMPs) bearing a silyl

protecting group, due to the transient lifetime of QMs. Fluoride activates the reactive QM

upon removal of the silyl protecting group (Scheme 1.5).[39] To increase bisQM's affinity for

DNA, the intercalator acridine was appended to the bisQMP scaffold (bisQMPAcr) (Figure

1.5). Acridine positions the bisQM within close proximity to DNA's nucleophiles for DNA

alkylation, rather than reaction with the surrounding water molecules.[40, 41] BisQMAcr's

reversible alkylation of DNA was demonstrated by its ability to isomerize from an intra-

strand DNA crosslink to a DNA ICL in the presence of complementary DNA sequences.[42]
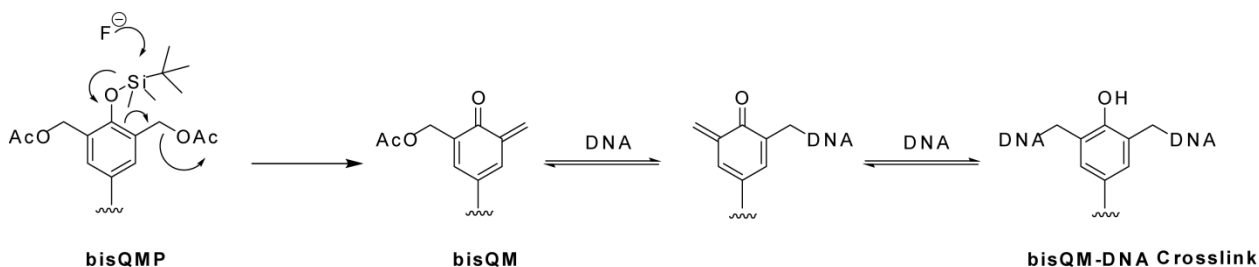
Scheme 1.5 Activation of bisQMs from their stable precursors through fluoride-mediated silyl group deprotection.

BisQMAcr's reversible alkylation prolonged its lifetime, as evidenced by the observation that

its DNA adducts survived multiple exchanges of DNA strands.[43]

BisQMAcr possesses the ability to migrate along a DNA duplex by reacting

reversibly at dGN7s to traverse duplex DNA in a bipedal fashion.[41] Migration was only

possible when the methylene bridged linkage to the acridine was replaced with an electron-

rich ether linkage. Increased electron density hastens the rate of QM regeneration to facilitate

migration. BisQMAcr's ability to migrate along DNA may be a promising attribute for the

development of a chemotherapeutic agent. Nevertheless, the impact of its reversible covalent

chemistry on a biological system is not known. QM migration was demonstrated *in vitro*

using DNA free in solution. However, the environment in cells may affect bisQMAcr's

migration along DNA. Cells contain numerous nucleophiles, such as thiols, water,

BisQMPAcr
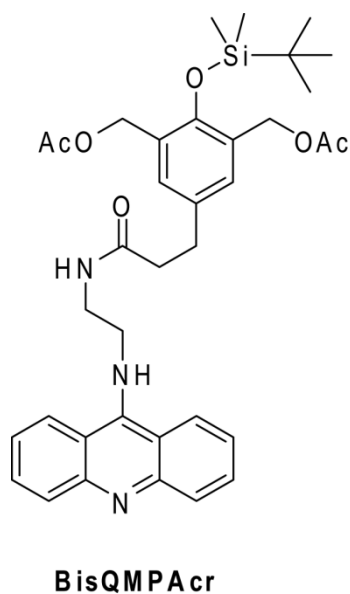
Figure 1.5 Structure of the *tert*-butyl-dimethylsilyl protected precursor to bisQMAcr.

deoxynucleotide triphosphates (dNTPs), and amino acids, which may compete with DNA for bisQMAcr's alkylation. BisQMAcr's migration may occur too slowly to impact cellular survival, as DNA repair would occur more quickly than QM regeneration. In addition, cellular DNA is intricately packaged with proteins as chromosomes. DNA packaging may alter bisQMAcr's profile of DNA alkylation and may affect its ability to bind and react with duplex DNA. Thus, how bisQMAcr responds to components of a cell's *in vivo* environment must be assessed in order to determine its potential potency.

The goal of this dissertation is to understand how the proteins involved in DNA packaging and processing affect bisQMAcr's dynamic DNA alkylation. The development of QMs with hastened migration along DNA was pursued to enhance the potential toxicity of QMs in a biological setting. BisQMAcr's migration may occur too slowly to be effective as a chemotherapeutic *in vivo*. Thus, a QM that migrates on a faster timescale would provide the most relevant compound to study biochemically. To begin to understand the biological

14

consequences of QMs' dynamic DNA alkylation, the response of QMs to DNA packaging was investigated. DNA in eukaryotic cells is not free in solution, but rather packaged around histone proteins to form nucleosomes. These investigations also addressed the question of whether nucleophiles found in proteins would react with QMs when both DNA and proteins are present. Finally, the effect of QM alkylation on DNA processing was investigated to probe how QMs may affect regulation and repair of the genetic code in cells. Numerous proteins that process DNA, such as polymerases and helicases, act as biological machines, with the potential to modulate QMs' migration through DNA. This dissertation will contribute to understanding the effects of dynamic alkylation on the proteins that are involved in DNA packaging and processing. The findings presented here may expand the design of chemotherapeutic agents based on dynamic DNA alkylation by evaluating how such drugs may respond to DNA processing and packaging by histones, polymerases, and helicases.

Chapter 2: Development of Bifunctional QMs for Migration along DNA

2.1 Introduction

DNA crosslinking can be detrimental to cells, but may also be leveraged as a mechanism for treating diseases. Many anticancer drugs are based on the cytotoxicity of DNA crosslinking agents. However, drugs such as nitrogen mustards and cisplatin often form a wide spectrum of products, with DNA crosslinks representing only a small fraction of these. Additionally, these drugs often lack specificity for specific cell types and biomolecules. Thus, efforts are needed to design crosslinking agents conjugated to ligands that direct reaction to DNA in order to limit undesired off-target reactions.

Compounds that form reversible DNA crosslinks may be advantageous over drugs that react irreversibly since any off-target adducts may not persist. Conjugation of a bisQM to the intercalator acridine localizes the reactive species to DNA to limit undesired quenching by water.[40] BisQMAcr requires a 100-fold lower concentration than a bisQM lacking acridine to crosslink DNA to the same extent (50 μM vs 5 mM).[41] BisQMAcr's dynamics of DNA crosslinking extended the lifetime of the reactive QM and allowed for crosslinks to transfer between different DNA targets (Scheme 2.1).[42-43] BisQMs' dynamic covalent crosslinking of DNA may be a promising attribute for the design of a chemotherapeutic drug. Regeneration of a drug's reactive intermediate may allow the drug to re-alkylate DNA at a different site once the original crosslink is repaired by DNA repair enzymes. Dynamic DNA crosslinking may increase a drug's potency by essentially allowing the compound to evade
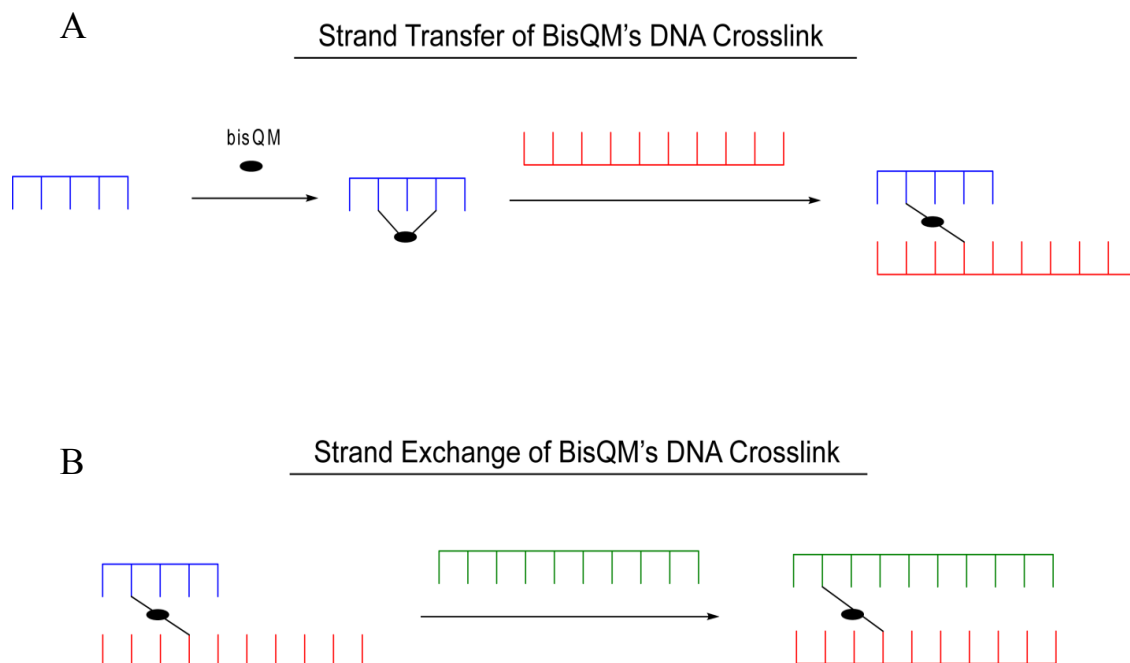
Scheme 2.1 Dynamics of bisQM's DNA crosslinks. A) A single-stranded oligonucleotide is treated with bisQM to form an intra-strand DNA crosslink. Upon addition of the complementary DNA strand, bisQM's crosslink isomerizes to form an inter-strand DNA crosslink. B) A bisQM DNA inter-strand crosslink is formed, with one of the strands containing a toe-hold region. Upon addition of a DNA strand complementary to the strand containing the toe-hold, bisQM's original DNA crosslink dissociates and transfers to form a new DNA crosslink.

repair of its own DNA adducts.

Migration of crosslinks through DNA signifies that the alkylating agent regenerates its reactive species from an initial crosslink to eventually form a new crosslink downstream of the original adduct. However, only an electron-rich analogue of bisQMAcr (ebisQMAcr), but not bisQMAcr could migrate through DNA (Scheme 2.2).[41] The addition of an electron-donating group to the QM's ring system increases the rate of QM formation and regeneration from its DNA adducts.[44] Furthermore, the added electron density increases the stability of the QM intermediate, which slows its rate of alkylation.[5] Thus, the QM has more time to diffuse and adjust its orientation within duplex DNA to alkylate adjacent nucleophiles. Improper

OTBDMS

AcO

OAc

O

HN

X

NH
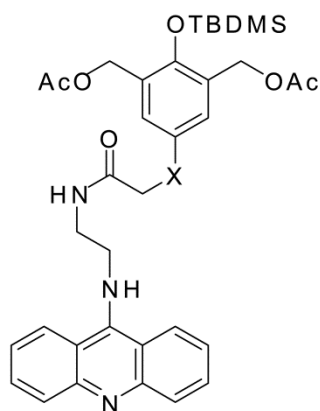
BisQMPAcr X=-CH₂-
eBisQMPAcr X=-O-

Scheme 2.2 Structures of the *tert*-butyl-dimethylsilyl protected precursors to bisQMAcr and ebisQMAcr.

orientation of the QM may lead to irreversible reaction with water, which will hinder its migration along duplex DNA. Migration of ebisQMAcr's crosslink through DNA occurred in a bipedal manner by reacting reversibly with dGN7s. However, migration occurred slowly, as ebisQMAcr required 7 days to traverse 7-10 base pairs within DNA (Figure 2.1).[41] The net rate of migration occurred too slowly to be effective *in vivo*, since DNA is processed on a much faster time scale by repair and processing enzymes. The thermodynamics of acridine's intercalation may have retarded migration, since acridine might be required to dissociate from the DNA in order for migration to occur. In addition, bisQMs' sequential formation of its two reactive intermediates may also slow the rate of migration, since one electrophile must react before the other QM is generated. To address the slow kinetics of migration, bisQMs conjugated to di- and tri-alkylammonium chains were synthesized (bisQMN$_2$ and bisQMN$_3$, respectively) (Scheme 2.3).[45-46] These bisQMs were designed to localize to DNA's phosphodiester backbone via electrostatic, rather than intercalative interactions, which was hypothesized to hasten their migration along DNA. However, neither bisQMN$_2$ and bisQMN$_3$, nor their electron-rich analogues were able to migrate along DNA. The
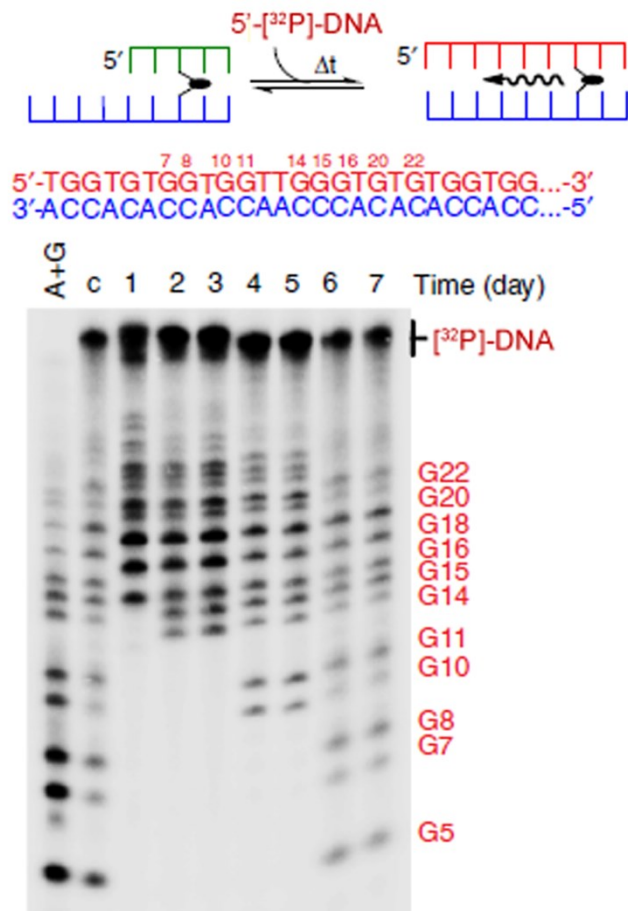
Figure 2.1 Migration of ebisQMAcr's crosslinks along duplex DNA from Fakhari *et al.*[41] Migration was observed by the appearance of new DNA fragments over time, following piperidine cleavage of the alkylated DNA.

compounds transferred their alkylation between DNA strands to isomerize from an intra- to inter-strand crosslink, but in lower yields than that observed for bisQMAcr. The ammonium-linked bisQMs may bind the DNA in a manner that directs the QM to react to form irreversible DNA adducts.[45-47] More efforts are needed to explain the ammonium-linked bisQMs' failure to migrate along DNA and to further elucidate the effect of conjugated ligands on QM's dynamic DNA crosslinking.

Additionally, bifunctional QMs linked to alkylammonium chains in which the reactive QM intermediates are separated onto distinct aromatic ring systems (diQMs) were

synthesized in order to investigate the hypothesis that sequential QM formation may hinder bisQMs' migration along DNA.[45, 46, 48, 49] Separation of the QM intermediates in diQMs may permit independent QM reactions.[48, 49] Previous work suggests that photoinducible diQMs form DNA ICLs at lower concentrations than their bisQM counterparts.[50] Thus, diQMs could hasten QM migration along DNA, as well as increase the yield of QM crosslinks that are able to migrate.

Here, we compare the efficiency, kinetics, and dynamics of DNA crosslinking by ammonium-linked diQMs relative to their bisQM counterparts. In addition, bisQMs linked to weakly intercalative quinoxalines were synthesized and their DNA alkylation profile was
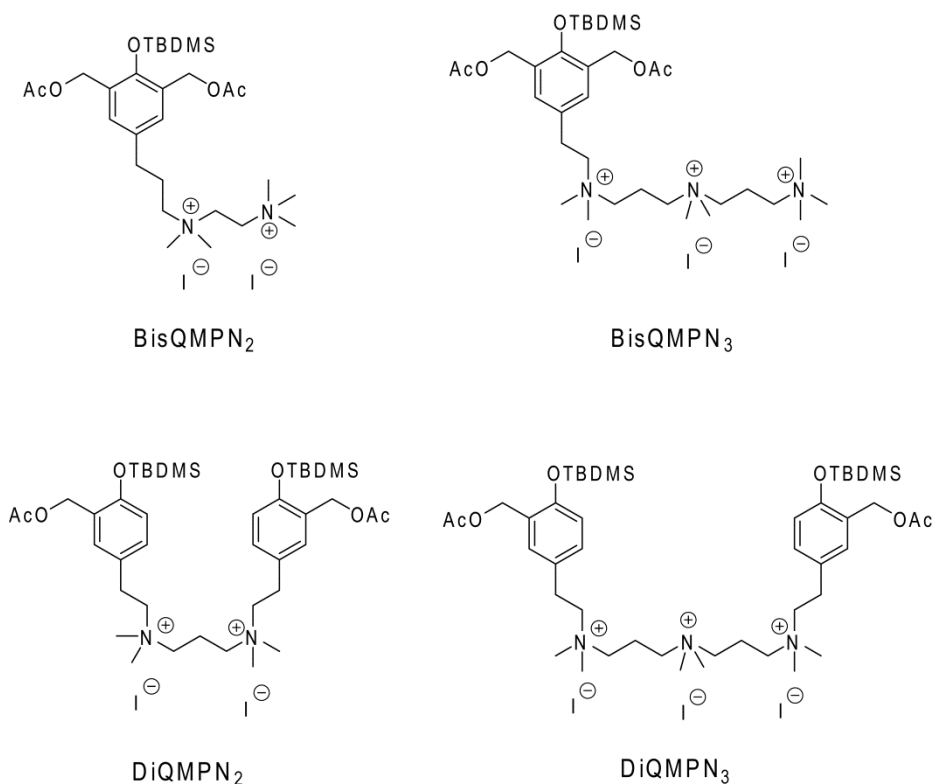
Scheme 2.3 A) Structures of the *tert*-butyl-dimethylsilyl protected precursors to bisQMN$_2$ and bisQMN$_3$. B) Structures of the *tert*-butyl-dimethylsilyl protected precursors to diQMN$_2$ and diQMN$_3$.

studied to determine weak intercalators enhance QM migration relative to acridine. Our results provide insight into how different ligands alter QMs' reaction with DNA and highlight the importance of a DNA-binding ligand for facilitating DNA crosslinking.

2.2 Results and Discussion

2.2.1 Decoupled QM Formation for Crosslinking Duplex DNA

DiQMPN$_2$ and diQMPN$_3$ were synthesized by Dr. Mark Hutchinson, as described previously, in order to examine the reversibility of reaction with DNA in the absence of the geometric constraints of a bisQM.[45, 46] The kinetics of DNA alkylation by diQMs was investigated to determine their efficiency of DNA crosslink formation. Duplex OD1/[^{32}P]-OD2 in MES (10 mM) and NaF (10 mM) was treated alternatively with diQMPN$_2$ (500 μM) and diQMPN$_3$ (50 μM) for 0- 24 h (Figure 2.2A). Both compounds were slow to react with DNA, requiring 4 h before any adducts were observed by denaturing polyacrylamide gel electrophoresis (PAGE) (Figure 2.2B). BisQMN$_2$ and bisQMN$_3$ react faster than the corresponding diQMs, as adducts were detected within 1 h and complete crosslinking of the DNA was achieved by 4 h. DiQMN$_2$ required a 10-fold higher concentration than diQMN$_3$ to form a similar yield of DNA adducts. The tri-ammonium chain likely binds DNA with greater affinity than the di-ammonium chain due to its increased positive charge. The disparity in concentrations required for alkylation is not surprising, as a similar trend was evident for the ammonium-linked bisQMs.[45] Both diQMs reacted to form < 50% yield of DNA crosslinks after 24 h. In addition, the diQMs reacted to form a mixture of both DNA ICLs and single-stranded DNA alkylation. The presence of bands that smear on the gel and their retarded migration relative to single-stranded DNA is consistent with sequential

21

monalkylation.[40] One reactive intermediate may alkylate the DNA, while the other arm reacts

with water. Another diQM molecule may then alkylate the same DNA strand, leaving

multiple mono-adducts on the DNA. Additionally, the diQMs may react to form intra-strand

rather than inter-strand DNA crosslinks, which could also result in bands that smear on the

gel. Samples containing DiQMPN$_3$ were treated with hot piperidine to determine whether the
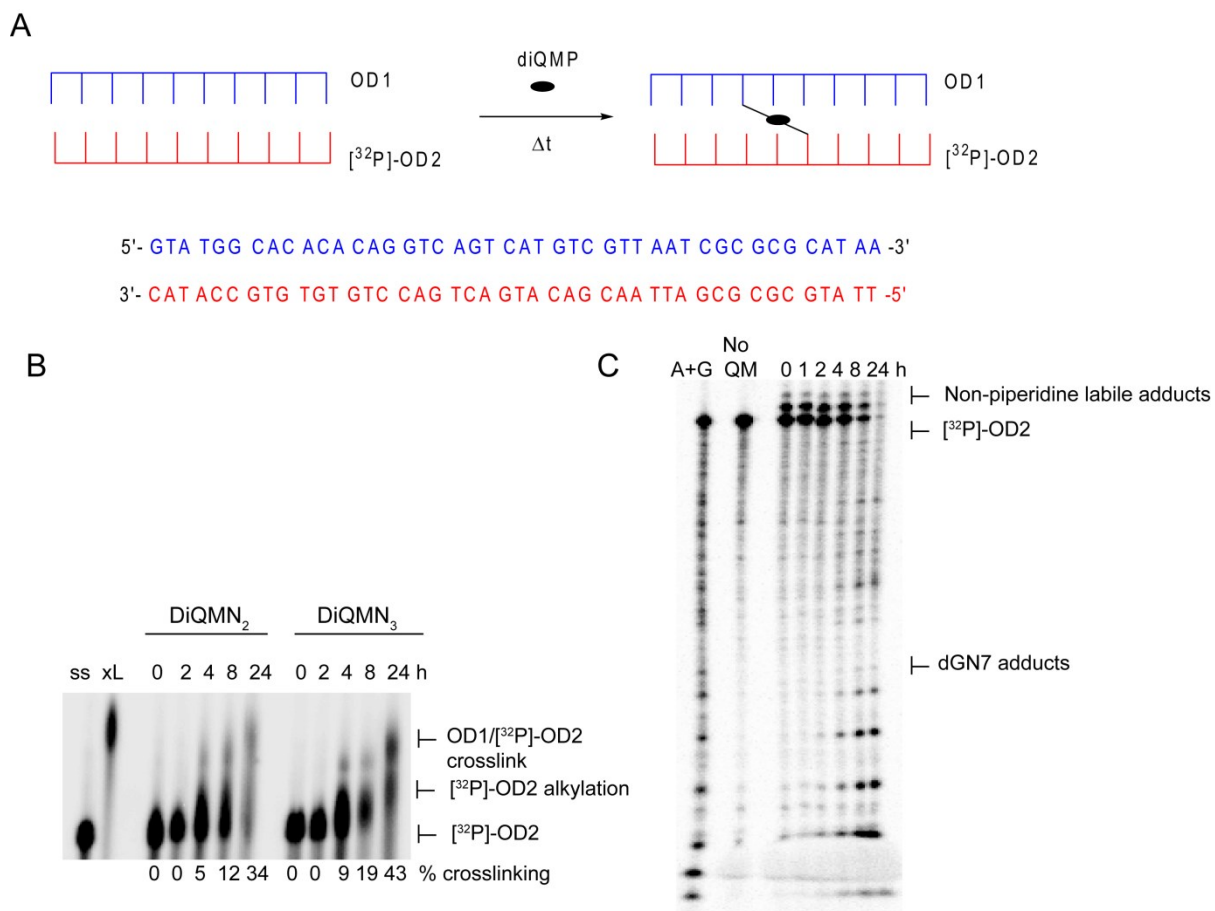
Figure 2.2 Kinetics of DNA alkylation by diQMN$_2$ and diQMN$_3$. A) Scheme depicting the experimental setup. B) Duplex OD1/[^{32}P]-OD2 DNA(3 μM) in MES (10 mM, pH 7) and NaF (10 mM) was treated alternatively with diQMPN$_2$ (500 μM) and diQMPN$_3$ (50 μM) in 20% acetonitrile for 0- 24 h at room temperature. Products were separated by denaturing PAGE (20%) and quantified by phosphorimagery. "SS" and "xL" samples contain OD1/[^{32}P]-OD2 in MES (10 mM, pH 7), NaF (10 mM), and 20% acetonitrile with and without bisQMPN$_3$ (100 μM), respectively. Samples were incubated for 24 h. C) Piperidine-induced fragmentation of DNA treated with diQMPN$_3$ for 0-24 h. Samples were treated with piperidine (10%) for 30 min after reaction to induce fragmentation at sites of dGN7 alkylation. Products were separated by denaturing PAGE (20%), visualized and quantified by phosphorimagery.

diQM reacts to form reversible dGN7 adducts. Preferential reaction at dGN7s will be vital for facilitating the diQM's migration along DNA through dynamic covalent chemistry. DiQMN$_3$ reacted at dGN7s after 4 h, but also reacted at other nucleophilic sites within DNA to form persistent non-piperidine labile adducts (Figure 2.2C). Reaction at sites that form non-piperidine labile adducts occurred more rapidly than at dGN7. The appearance of adducts at time zero indicates that reaction occurred so quickly that adducts formed within the minutes required to set up, freeze, and thaw samples. The appearance of multiple bands that migrate more slowly than the parent DNA lends support to diQMN$_3$'s sequential monoalkylation of DNA.

The ammonium-linked diQMs react more slowly and form a lower yield of crosslinks than their bisQM counterparts (Figure 2.2B, xL lane). The bisQMs primarily form DNA ICLs, whereas the diQMs also react to form a series of sequential monoadducts in addition to a low yield of ICLs. These differences in the profile of DNA alkylation between the bisQMs and diQMs suggests that decoupled QM formation does alter the QM's reactivity by allowing the two reactive intermediates to react independently of one another. However, the independence of the two QMs lowers the yield of crosslinking by permitting the formation of monoadducts, intra-strand crosslinks, or irreversible quenching by water. Additionally, diQMN$_3$ possesses conformational flexibility that may allow the two reactive QMs to react with a wide range of sites within DNA. The two electrophiles in bisQMs cannot alter their orientation relative to one another due to the rigid, planar ring system connecting them. Thus, bisQMs are constrained to react at two nucleophiles within spatial proximity to one another, while the diQMs are flexible to react with nucleophiles covering a wider spatial array.

It is vital to determine the length of time required for full quenching of QMs by water in order to ensure that the results of strand transfer and exchange experiments are actually a result of reversible alkylation, and not alkylation by free QM that had persisted in solution (Scheme2.1). DiQMPN$_3$ was incubated in aqueous buffer and NaF for 0-72 h, at which point the duplex DNA OD1/[^{32}P]-OD2 was added, and incubated for an additional 24 h (Figure 2.3A). DiQMN$_3$ was not fully quenched by water after 72 h, as DNA alkylation was still observed (Figure 2.3B). Water may react with one of the reactive QM intermediates, but not the other. This would allow DiQMN$_3$ to alkylate DNA after a 72 h incubation in aqueous buffer. In order to overcome the slow quenching, excess QM were removed via ethanol precipitation prior to examining its reversibility.

The dynamics of diQMN$_3$'s DNA alkylation were assessed by isomerization of its
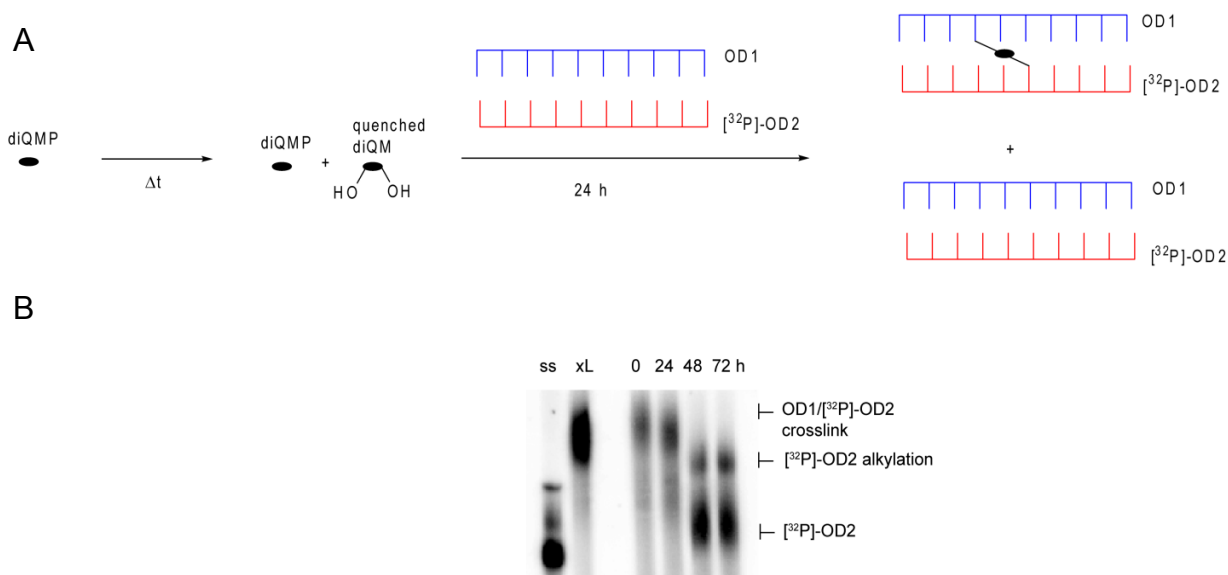
Figure 2.3 Quenching of diQMN$_3$ by water. A) Scheme depicting the experimental setup. B) DiQMPN$_3$ (50 µM) was incubated in MES (10 mM, pH 7), NaF (10 mM), and 20% acetonitrile for 0-72 h. After the indicated time, duplex DNA OD1/[^{32}P]-OD2 (3 µM) was added for an additional 24 h. Products were separated by denaturing PAGE (20%) and visualized by phosphorimagery.

adducts from an intra- to an inter-strand DNA crosslink. $DiQMN_3$ was initially trapped with single-stranded OD3 for 24 h before removal of excess QM via ethanol precipitation. $[^{32}P]$-OD2 was added to determine whether $DiQMN_3$'s DNA adducts on OD3 would dissipate and allow regenerated $DiQMN_3$ to react with the newly added DNA strand (Figure 2.4A). No DNA ICLs were observed, but a new band appeared on the gel that migrated slightly more slowly than parent OD2 (Figure 2.4B). This band signifies monoadducts, indicating that $DiQMN_3$ can reversibly alkylate, but not crosslink DNA. $DiQMN_3$ may transfer its adducts as monoadducts, rather than crosslinks, due to quenching of one reactive QM by water, while the other QM alkylates DNA. Both reactive intermediates may release simultaneously from their initial DNA adducts due to the independent formation of the QMs and flexibility of the QMs' conformation that is inherent to diQMs. $DiQMN_3$ will essentially behave as a monoQM once water quenches one of its electrophiles. The bisQM counterpart to $diQMN_3$ transfers its adducts to form ICLs rather than monoadducts, but forms a similar yield of ICLs as that for $diQMN_3$'s adducts. The preference for transferring its alkylation as monoadducts rather than ICLs likely stems from decoupling of the reactive QM intermediates. Both $diQMN_3$ and $bisQMN_3$ transfer their DNA adducts in a lower yield than that for bisQMAcr.[41] The ammonium chains may cause a lower yield of reversible QM-DNA adducts, which highlights the importance of ligands for directing reaction to dGN7s to form reversible DNA adducts.

DiQMN$_3$ is primarily captured by nucleophiles that result in non-piperidine labile adducts, rather than by dGN7 (Figure 2.4C). These adducts are irreversible, which will halt diQMN$_3$'s migration along DNA. The ammonium chain likely localizes diQMN$_3$ to the

5'- AT GTC GTT AAT CGC GCG CAT AA -3'

3'- CAT ACC GTG TGT GTC CAG TCA GTA CAG CAA TTA GCG CGC GTA TT -5'
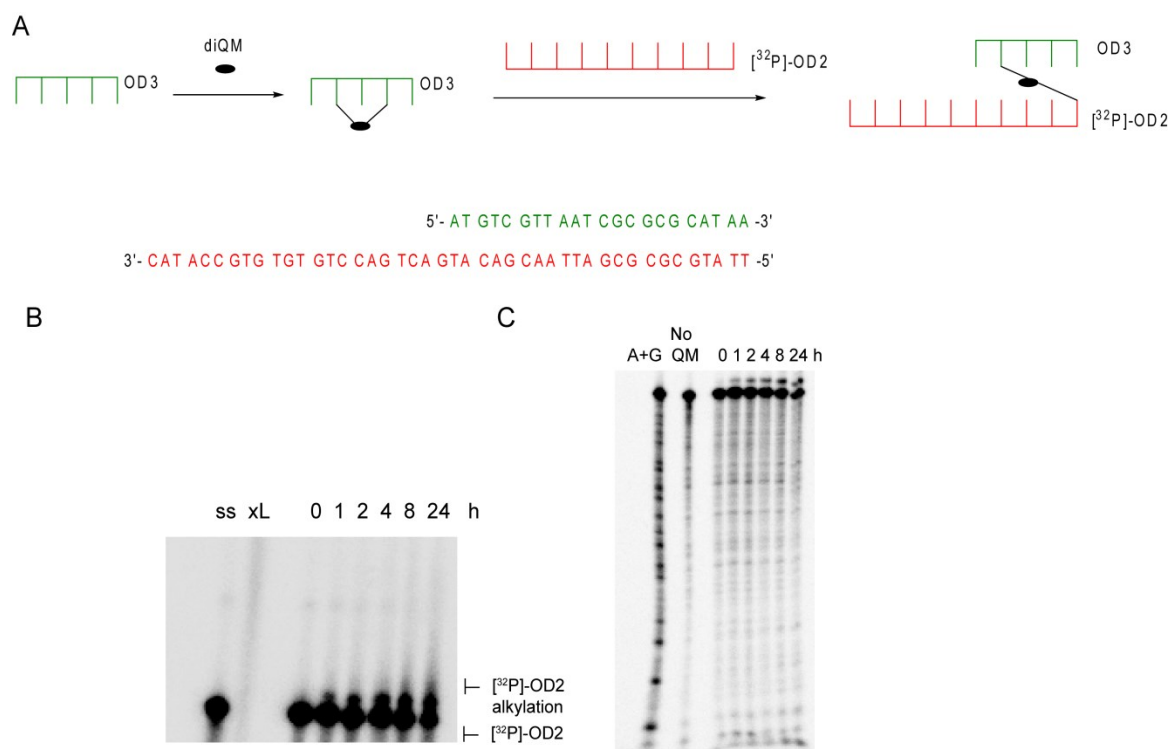
Figure 2.4 Transfer of DiQMN$_3$'s adducts between DNA strands. A) Scheme depicting the experimental setup. B) OD3 (3 µM) in MES (10 mM, pH 7) and NaF (10 mM) was treated with diQMPN$_3$ (50 µM) for 24 h. Excess QM was removed from the DNA by ethanol precipitation. The precipitated DNA was resuspended in buffer and [^{32}P]-OD2 was added and the reaction was incubated for 0-24 h. The products were separated by denaturing PAGE (20%) and visualized by phosphorimagery. C) Piperidine-induced fragmentation of the samples from (B). Samples were treated with piperidine (10%) for 30 min after reaction to induce fragmentation at sites of dGN7 alkylation. Products were separated by denaturing PAGE (20%) and visualized by phosphorimagery.

minor groove of DNA, where it will have access to nucleophiles that form irreversible QM-

DNA adducts. Crystal structures exist of polyammonium compounds bound to DNA's minor

groove, suggesting minor groove binding as the means by which these compounds recognize
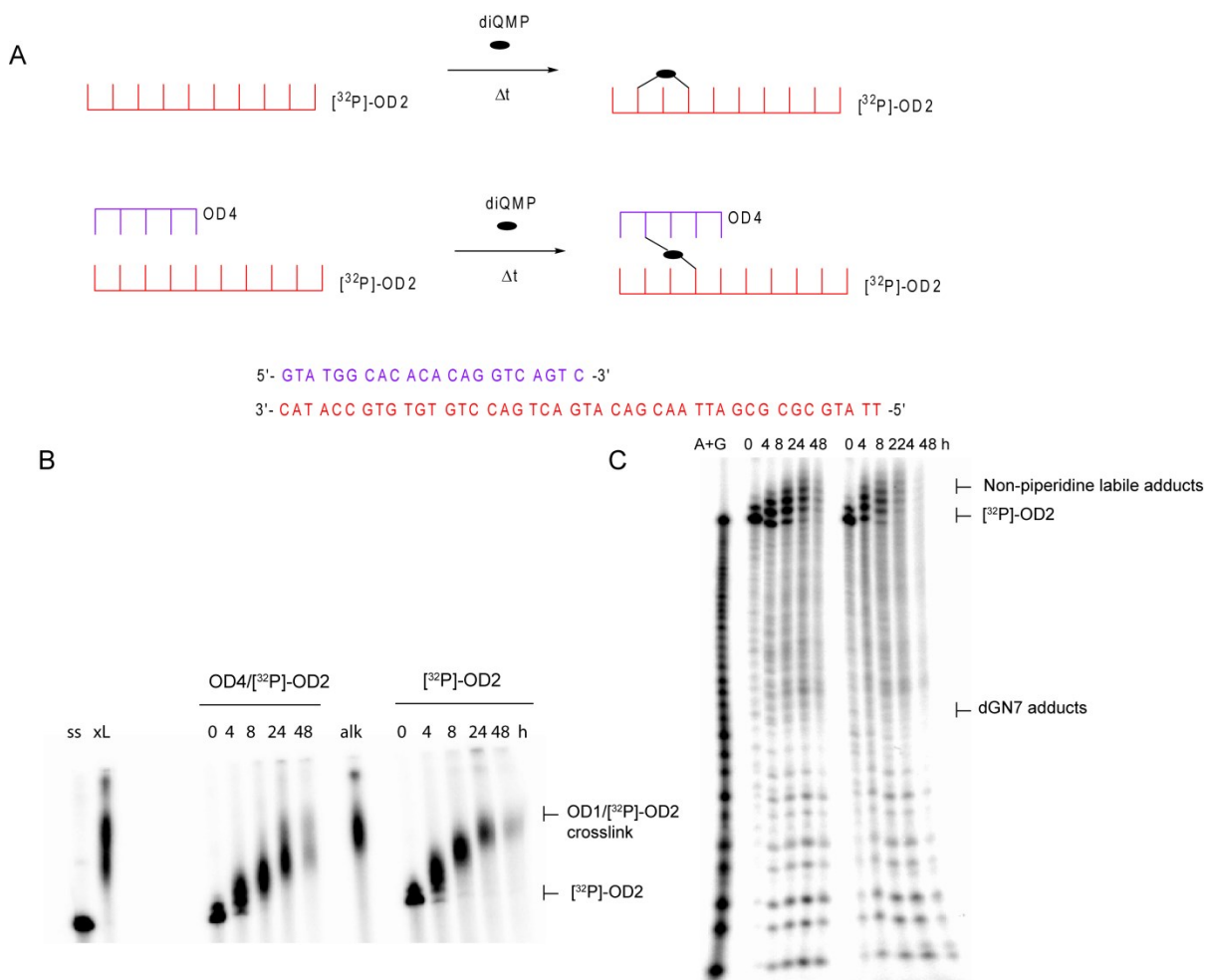
Figure 2.5 Alkylation of single-stranded and duplex DNA by $diQMN_3$. A) Scheme depicting the experimental setup. B) Either OD4/[^{32}P]-OD2 duplex DNA or single-stranded [^{32}P]-OD2 in MES (10 mM, pH 7) and NaF (10 mM) was treated with $diQMPN_3$ (50 μM) in 20% acetonitrile for 0-48 h. Products were separated by denaturing PAGE (20%). "Ss" and "xL" samples contain OD4/[^{32}P]-OD2 in MES (10 mM, pH 7), NaF (10 mM), and acetonitrile (20%) with and without $bisQMPN_3$ (100 μM) for 24 h. The "alk" sample contains [^{32}P]-OD2 in MES (10 mM, pH 7), NaF (10 mM), and acetonitrile (20%) with $bisQMPN_3$ (100 μM) for 24 h. C) Piperidine-induced fragmentation of the samples from (B). Samples were treated with piperidine (10%) for 30 min after reaction to induce fragmentation at sites of dGN7 alkylation. Products were separated by denaturing PAGE (20%) and visualized by phosphorimagery.

27

DNA.[51, 52] Furthermore, bisQMN$_3$ also formed irreversible DNA adducts, most likely by binding DNA's minor groove.[45, 46] On the other hand, acridine likely delivers bisQMAcr to the major groove of DNA where the dGN7 nucleophile is available to form reversible QM-DNA adducts. Thus, the disparity between bisQMAcr's and bisQMN$_3$'s and diQMN$_3$'s abilities to transfer their DNA adducts likely stems from the binding mode of their ligands.

A low yield of strand transfer could also occur if the initial oligonucleotide used to trap diQMN$_3$ were over-alkylated and prevented annealing of the complementary target sequence. DiQMN$_3$'s alkylation of single-stranded and duplex DNA was compared to determine whether diQMN$_3$'s low yield of transfer results from over-alkylation of single-stranded DNA. Single-stranded [^{32}P]-OD2 and duplex [^{32}P]-OD2/OD4 were alternatively treated with diQMN$_3$ before separation of the products by denaturing PAGE (Figure 2.5A). Reaction in both single-stranded and duplex DNA produced products with similar migration on the gel (Figure 2.5B). In both cases, the band's migration retards over time, consistent with sequential monoalkylations.[40] DiQMN$_3$ likely behaves as a monoQM in both single-stranded and duplex DNA, as the majority of its products represent sequential monoadducts rather than DNA ICLs. Treatment of the samples with piperidine confirmed the sequential adduct formation in both single-stranded and duplex DNA, as several distinct non-piperidine labile bands were observed (Figure 2.5C). The presence of several distinct high molecular weight bands suggests that diQMN$_3$ over- alkylates the DNA, which may prevent hybridization of the complementary strand and preclude strand transfer.

To determine whether diQMN$_3$'s dynamics continue beyond transfer of its adducts to a new DNA strand, its ability retain its DNA adducts upon an exchange of DNA strands was measured. Upon formation of diQMN$_3$ adducts on OD2 via strand transfer as described
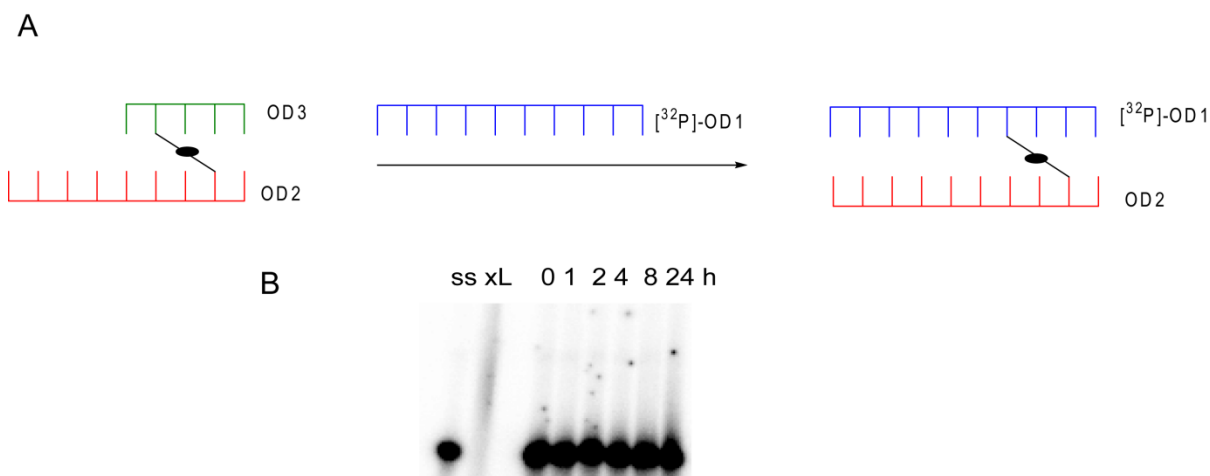
Figure 2.6 Exchange of diQMN$_3$'s alkylation between DNA strands. A) Scheme depicting the experimental setup. B) Initial DNA adducts were formed by treating OD3 (3 μM) in MES (10 mM, pH 7), NaF (10 mM), and 20% acetonitrile with diQMPN$_3$ (50 μM) for 24 h. Excess QM was removed via ethanol precipitation and OD2 (3 μM) was then added and incubated for 24 h. [^{32}P]-OD1 (3 μM) was then added for 0-24 h. Products were separated by denaturing PAGE (20%) and visualized by phosphorimagery.

above, [^{32}P]-OD1 was added to determine whether diQMN$_3$'s adducts exchanged to alkylate OD1 (Figure 2.6A). However, no alkylation of OD1 was apparent, lending further support to the notion that the non-piperidine labile adducts observed from strand transfer represent irreversible QM-DNA adducts (Figure 2.6B). The dynamics of diQMN$_3$'s DNA alkylation are not maintained beyond transfer between complementary DNA sequences. DiQMN$_3$ does not support exchange of adducts between multiple DNA strands, as bisQMAcr had.[43] The formation of irreversible DNA adducts will prevent diQMN$_3$'s migration along DNA, as ebisQMAcr required reversible adducts to extend its lifetime for further reaction.

To circumvent diQMN$_3$'s preference for forming irreversible DNA adducts, duplex DNA containing sticky ends was utilized to measure diQMN$_3$'s diffusion through DNA. OD5/OD6 duplex DNA was initially treated with diQMN$_3$ to trap initial QM-DNA adducts

before removing excess QM via ethanol precipitation. The preannealed duplex [^{32}P]-OD7/OD8 was then added to observe diffusion of diQMN$_3$ through DNA (Figure 2.7A). New adducts were evident by PAGE in as few as 4 h, with the yield increasing over 96 h. The majority of products formed were monoadducts, with a 3% yield of DNA ICLs detected (Figure 2.7B). DiQMN$_3$ reacted with dGN7s to form reversible adducts and with the weak nucleophiles such as dGN2, dAN6, and dGN1 to form irreversible adducts (Figure 2.7C). DiQMN$_3$'s yield of adducts may be low due to the evolution of its reversible adducts to irreversible adducts. Formation of irreversible adducts prevents further QM reaction. DiQMN$_3$ diffuses freely through duplex DNA, as opposed to migrating in a bipedal manner like ebisQMAcr. A monoQM linked to acridine (monoQMAcr) migrated through DNA via free diffusion.[53, 54] Once regenerated from a DNA-adduct, a monoQM is not anchored to the DNA in the same manner than a bisQM is. Thus, monoQMs may diffuse through the DNA before reacting to form a new adduct. DiQMN$_3$'s migration resembles that of a monoQM, rather than a bisQM. DiQMN$_3$ essentially functions as a monofunctional QM, since water quenches one of its reactive intermediates. Ultimately, diQMN$_3$ may migrate along DNA and do so quite rapidly, but as a monoalkylating agent, rather than a crosslinking agent. Even so, its migration stops after the formation of irreversible adducts. Efforts would be needed to improve diQMN$_3$'s yield of reversible adduct formation in order to enhance its potential effectiveness *in vivo*.
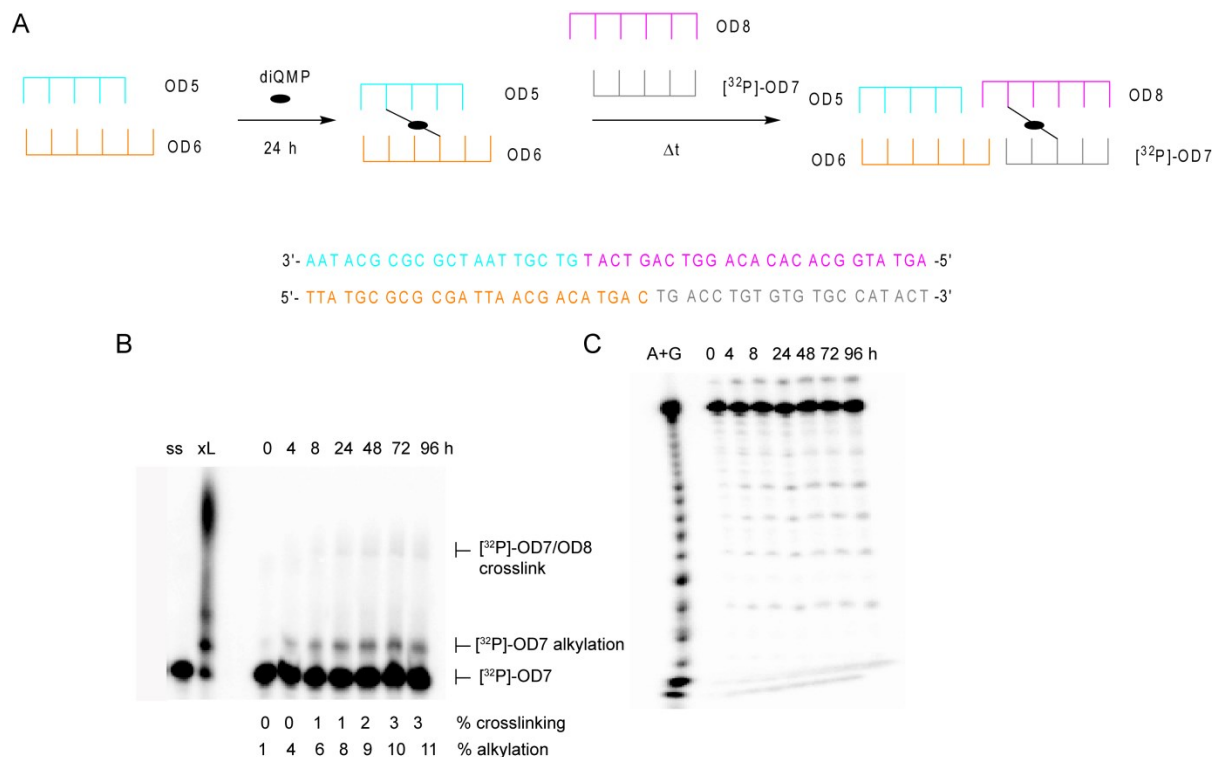
Figure 2.7 Migration of diQMN$_3$ along DNA containing sticky ends. A) Scheme depicting the experimental setup. B) Duplex DNA OD5/OD6 (3 µM) in MES (10 mM, pH 7), NaF (10 mM), and 20% acetonitrile was treated with diQMPN$_3$ (50 µM) for 24 h. Excess QM was removed via ethanol precipitation. [^{32}P]-OD7/OD8 was then added for 0-96 h. Products were separated by denaturing PAGE (20%) and visualized by phosphorimagery. C) Piperidine-induced fragmentation of the samples from (B). Samples were treated with piperidine (10%) for 30 min after reaction to induce fragmentation at sites of dGN7 alkylation. Products were separated by denaturing PAGE (20%), visualized, and quantified by phosphorimagery.

31

2.2.2 Synthesis of an Electron-Rich Analogue of DiQMPN$_3$

DiQMN$_3$'s dynamic DNA alkylation suffered from irreversible quenching by water and a lack of specificity for forming reversible adducts. Addition of electron density to the QM ring systems may improve target selectivity by decreasing the rate of Michael addition.[41, 44, 45]The synthesis of an electron-rich analogue of diQMPN$_2$ was not pursued due to the low affinity for and alkylation of DNA by diQMN$_2$. Synthesis of the electron-rich analogue of diQMPN$_3$ (ediQMPN$_3$) was performed similarly to that of diQMPN$_3$ (Scheme 2.4).[45, 46] The synthesis was initiated with mono-hydroxymethylation of 2-(4-hydroxyphenoxy) acetic acid **1**. Hydroxymethylation was initially attempted using phenylboronic acid and formaldehyde.[55] However, hydroxymethyl signals at approximately
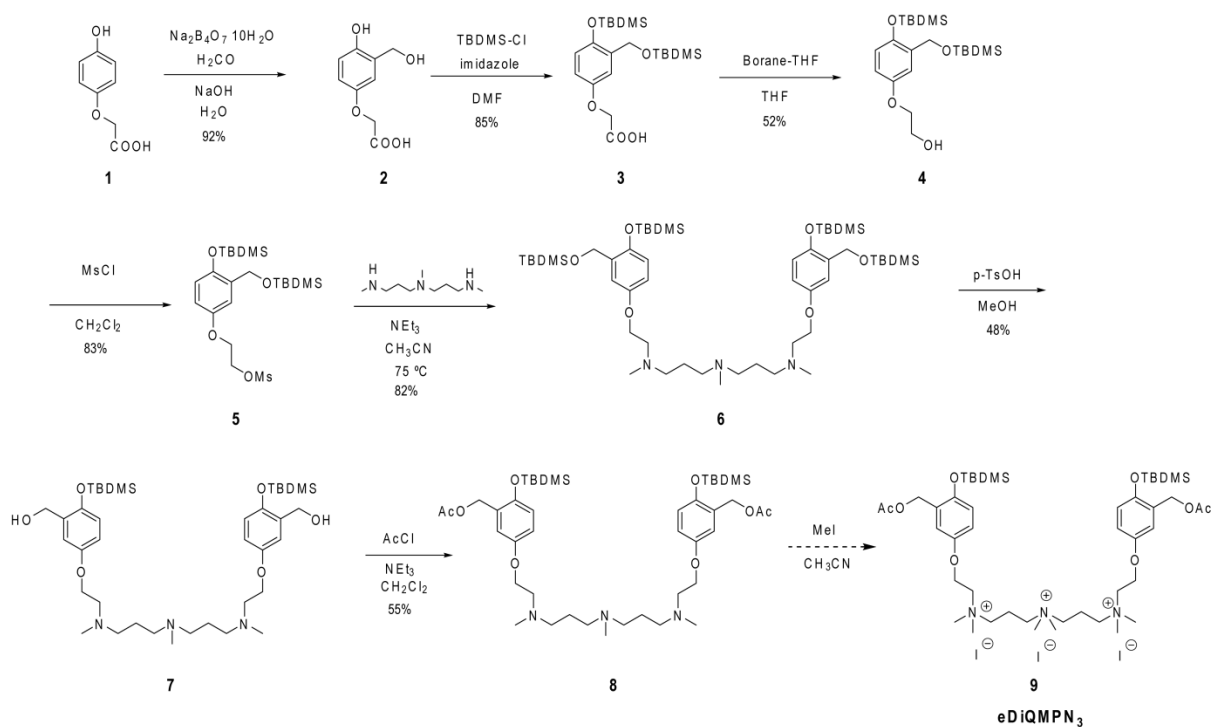
Scheme 2.4 Synthesis of ediQMPN$_3$.

4.5 ppm were never evident by ^{1}H NMR. The phenylboronic acid may have chelated the carboxylic acid, preventing the formation of the hydroxymethyl- phenylboronic acid

32

intermediate. The use of sodium tetraborate successfully resulted in monohydroxymethylation to yield intermediate **2**, which did not require purification.[56]

The phenolic and benzylic alcohols were then protected with a *tert*-butyldimethylsilyl (TBDMS) protecting group. The product was carried forth without further purification despite the presence of TBDMS-OH byproducts in the ^{1}H NMR spectrum. The product was purified after reduction with borane-THF, since the conversion of a carboxylic acid to its corresponding alcohol facilitates silica column flash chromatography. The primary alcohol was activated as a leaving group using methanesulfonyl chloride (MsCl) to facilitate subsequent nucleophilic substitution with the alkylamine.[57]

Nucleophilic substitution of the mesylated alcohol **5** with the alkylamine was performed overnight at 75 °C using 1 equivalent of the alkylamine to 2 equivalents of mesylated alcohol **5**.[50] Product **6** was purified from unreacted starting material **5** by flash column chromatography. A 1:1 mixture of hexanes:ethyl acetate was first used to remove unreacted starting material and any residual TBDMS-OH that remained from prior steps, followed by elution of the desired product with a mixture of 99% methanol/1% triethylamine. The TBDMS-protected benzylic alcohols were then unmasked for their eventual acetylation. Selective deprotection of the benzylic, but not secondary, phenolic TBDMS-protected alcohols was achieved using *para*-toluenesulfonic acid (p-TsOH).[58] A 1.5-fold excess of p-TsOH was needed since p-TsOH could also protonate the amines. Product **7** was separated from the resulting TBDMS-OH via a hexane:methanol wash. Product **7** partitioned into the methanol layer, while the byproducts remained in the hexanes layer. The benzylic alcohols were then acetylated using acetyl chloride and triethylamine, and the product was purified by

flash column chromatography by washing with ethyl acetate, followed by elution with a mixture of 99% methanol/1% triethylamine to afford pure **8**.

Methylation of the amines to afford ediQMPN$_3$ proved challenging and could not be accomplished successfully (Table 2.1). Methylation with methyl iodide was performed for 2 min, as opposed to the 1 h reaction time required for diQMPN$_3$, since methylation of ebisQMPN$_3$ was complete within this time frame.[45, 46] Methylation of ebisQMPN$_3$ had proven to be more difficult to achieve than that for bisQMPN$_3$. Following the 2 min reaction time, solvent was immediately removed and the crude residue was purified using a C-18 reverse phase Sep Pak by washing with a gradient of acetonitrile. However, attempted purification did not change the purity of the crude mixture. A myriad of products were evident by ^{1}H NMR, including the appearance of new signals in the aromatic region. A downfield shift of the methylene protons at 1.78 ppm, which would have indicated quaternization of the amines, was not evident. Methyl iodide most likely reacts with the aromatic enol leading to a spectrum of products that may result in dearomatization, as well as cleavage of the alkylamine chain. Although decomposition was evident for this step of the synthesis of ebisQMPN$_3$ as well, the issue was less severe than for ediQMPN$_3$. EdiQMPN$_3$ contains two aromatic enols that magnified the decomposition observed following the 2 min reaction. Neither decreasing the reaction time to 30 sec nor conducting the reaction under anhydrous conditions led to any improvements in the product purity. In order to reduce the reaction rate to attempt to shift the selectivity of methylation to the amines rather than the enol, the reaction was performed at 0 °C. But, decomposition still occurred. Next, the number of equivalents of methyl iodide was reduced in order to try to gain selectivity for N-methylation. One equivalent of MeI per amine did not lead to reaction, while some

decomposition and unreacted starting material were detected when 2 equivalents of MeI per amine were used. Neither the more reactive dimethylsulfate (DMS) nor DMSO with triethylamine and formaldehyde yielded the desired product either, as both reagents produced mixtures whose ^{1}H NMR spectra showed even more decomposition than reactions with methyl iodide, possibly due to the elevated temperatures that were required for reaction and the greater reactivity of the methylating agents.[59-61] Next, MeI was once again utilized but with added LiBr. The lithium cations may chelate the oxygen atom, preventing its reaction and directing methylation to the amines. Selectivity for N-methylation over O-methylation was achieved via lithium chelation of aminoalcohols.[62] However, the desired product was not generated, as decomposition was still evident by ^{1}H NMR.

To achieve selectivity for N-alkylation rather than O-alkylation, ethyl iodide, rather than methyl iodide was used, since it is a less reactive alkylating agent. Ethylation was attempted using 100 equivalents of ethyl iodide per amine and stirring for 2 h at room temperature. The ^{1}H spectrum contained fewer products after 2 h reaction with ethyl iodide than were detected for reactions with methyl iodide. New signals did not appear in the aromatic region of the ^{1}H NMR spectra, as had been the case for reaction with methyl iodide. Reaction with ethyl iodide may lead to less decomposition than that observed in prior experiments due to the slower rate of reaction. The reaction mixture was subjected to cation exchange chromatography to remove any undesired byproducts and unreacted starting material. However, no product was recovered from the column, indicating that the desired alkylation of the amines was likely not attained. The synthesis of ediQMPN$_3$ was abandoned at this point.

Table 2.1 Conditions attempted for the methylation of product **8**

Reagent	Equivalents	Time	Temperature	Notes
MeI	300	2 min	Room temp.	
MeI	300	30 sec	Room temp.	
MeI	300	2 min	Room temp.	Anhydrous
MeI	300	30 sec	Room temp.	Anhydrous
MeI	300	30 sec	0 ℃	Anhydrous
MeI	300	2 min	0 ℃	Anhydrous
MeI	3	2 min	Room temp	Anhydrous
MeI	6	2 min	Room temp	Anhydrous
DMS	9	2 h	50 ℃	
DMSO	300	24 h	150 ℃	
MeI/LiBr	300 (MeI) 5 (LiBr)	2 min	Room temp.	
MeI/LiBr	6 (MeI) 5 (LiBr)	2 min	Room temp.	
EtI	300	2 h	Room temp.	
EtI	300	2 h	Room temp.	Cation exchange purification
EtI	6	2 h	Room temp.	Cation exchange purification

2.2.3 Synthesis and DNA Alkylation of Quinoxaline-linked BisQMs

BisQMAcr's ability to dynamically alkylate and migrate along DNA, and the failure

of bisQMPN$_2$ and bisQMP$_3$ to migrate along DNA suggests that intercalation, rather than

electrostatic interactions with DNA's backbone may be the ideal binding mode to promote

dynamic QM reaction with DNA. However, acridine may intercalate too strongly to promote

migration that is fast enough to be effective *in vivo*. Quinoxalines are "minimal intercalators"

that weakly intercalate DNA .[63] A bisQM conjugated to a quinoxaline may migrate more quickly than ebisQMAcr, as the thermodynamics governing its association and dissociation from DNA may be weaker than that for acridine. Furthermore, the quinoxaline scaffold offers many opportunities for functionalization to modulate its binding to DNA.[64] Here, we synthesized four quinoxaline-conjugated bisQMs and assessed their ability to dynamically alkylate DNA.

2.2.3.1 Synthesis and DNA Alkylation of BisQMPQuin1

We first synthesized a bisQMP linked to quinoxaline-2-carboxylic acid **17** in order to determine the ability of an unfunctionalized quinoxaline to localize bisQMs to DNA to form reversible adducts. The succinimide activated ester of bisQMP was synthesized as previously described, in order to couple the bisQMP to the quinoxalines (Scheme 2.5).[40] To activate the quinoxaline as a nucleophile, the carboxylic acid was activated with succinimide to facilitate amide bond formation with mono-Boc-protected diaminopropane **16** (Scheme 2.6).[65]
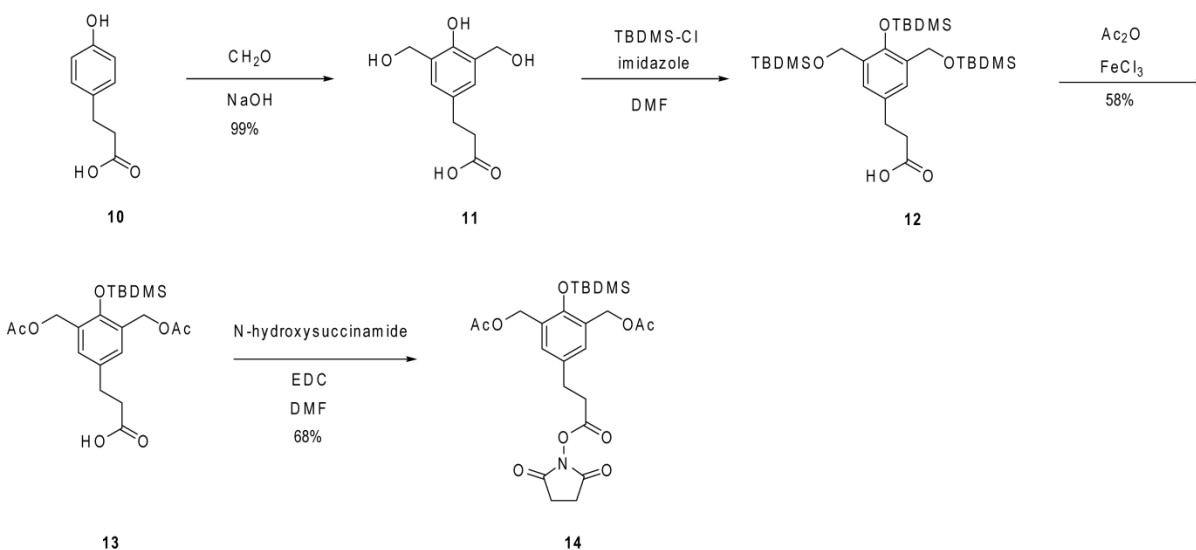
Scheme 2.5 Synthesis of the succinimide activated ester of bisQMP intermediate **14**
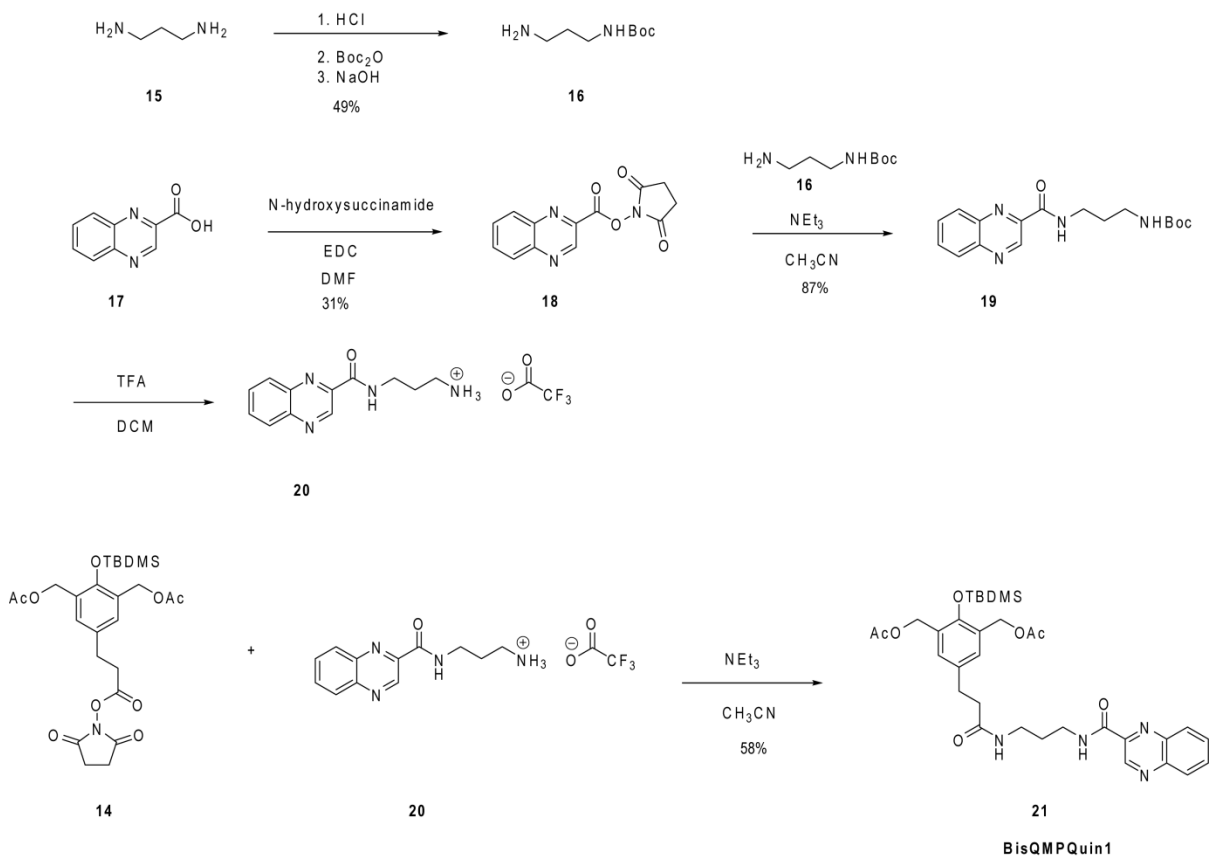
Scheme 2.6 Synthesis of bisQMPQuin1

The Boc protecting group was then removed using trifluoroacetic acid (TFA) to yield the

TFA salt of the aminoquinoxaline **20** (Scheme 2.6). The coupling of **20** to **14** was achieved

by employing an excess of triethylamine in order to produce the nucleophilic amine and a

salt between TFA and triethylamine. The salt was removed via aqueous washes, and pure

bisQMPQuin1 was obtained following organic extraction.
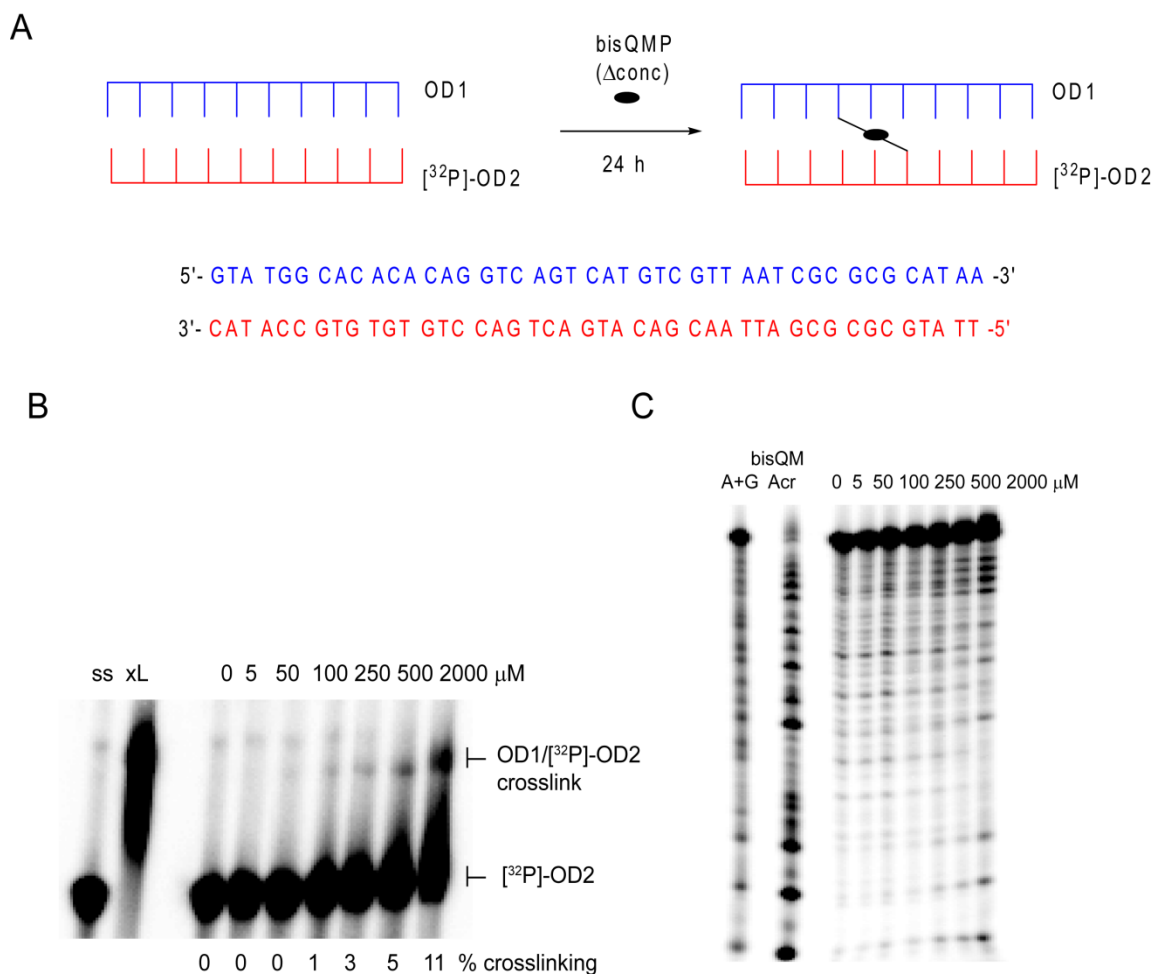
Figure 2.8 Dependence of DNA crosslinking on the concentration of bisQMQuin1. A) Scheme depicting the experimental setup. B) OD1/[^{32}P]-OD2 (3 µM) was treated with varying concentrations of bisQMPQuin1 for 24 h in MES (10 mM, pH 7), NaF (10 mM), and 20% acetonitrile at room temperature. Products were separated by denaturing PAGE (20%). "Ss" and "xL" samples include OD1/[^{32}P]-OD2, MES (10 mM, pH 7), NaF (10 mM), and 20% acetonitrile in the presence and absence of bisQMPAcr (100 µM), respectively. C) Piperidine-induced fragmentation of the samples from (B). Samples were treated with piperidine (10%) for 30 min after reaction to induce fragmentation at sites of dGN7 alkylation. Products were separated by denaturing PAGE (20%), visualized, and quantified via phosphorimagery.

The efficiency of DNA ICL formation by bisQMQuin1 was determined by treating duplex DNA OD1/[^{32}P]-OD2 with increasing concentrations of bisQMPQuin1 (0- 2000 µM) for 24 h (Figure 2.8A). DNA ICLs formed with increasing concentrations of bisQMQuin1

(Figure 2.8B). Crosslink formation occurred with a yield of 11% with 2 mM of the QM, much less efficient than bisQMAcr's 100% yield of crosslink formation at 100 μM of QM. Quinoxaline may not have a strong affinity for DNA, which could explain the low yield of DNA crosslinking, even at high QM concentrations. BisQMQuin1 primarily alkylated dGN7s to form reversible QM-DNA adducts (Figure 2.8C).

Intercalators recognize and bind to noncanonical DNA structures, such as bulges, mismatches and abasic sites, due to the distortion created in the DNA. These sites provide increased space for the intercalator to bind, and facilitate the local DNA unwinding that intercalation induces. Thus, bisQMQuin1 may bind more easily to, and hence react with a greater yield with DNA containing noncanonical structures. The dependence of DNA crosslinking on bisQMPQuin1's concentration was examined using the duplex DNA OD1/[^{32}P]-OD9, which contained a T-T bulge in the sequence (Figure 2.9A). ICL formation at 2 mM of bisQMPQuin1 occurred in approximately 50% yield, a dramatic improvement over the 11% yield using a standard DNA duplex (Figure 2.9B). Piperidine fragmentation of the alkylated DNA indicated that bisQMQuin1 preferentially alkylates dGN7s adjacent to the T-T bulge (Figure 2.9C). The presence of the bulge improves bisQMQuin1's binding affinity to DNA at this region by providing a pocket for intercalation. Furthermore, the preference for alkylating dGN7s at the T-T bulge suggests that bisQMQuin1 intercalates the DNA and that intercalation directs the QM to dGN7s for covalent reaction. However, BisQMQuin1 will likely not improve the rate of migration of bisQMs along DNA, due to the low yields of ICLs formed and the high concentration of QM required to form ICLs. Functionalization of the quinoxaline scaffold may improve binding to and reaction with DNA.
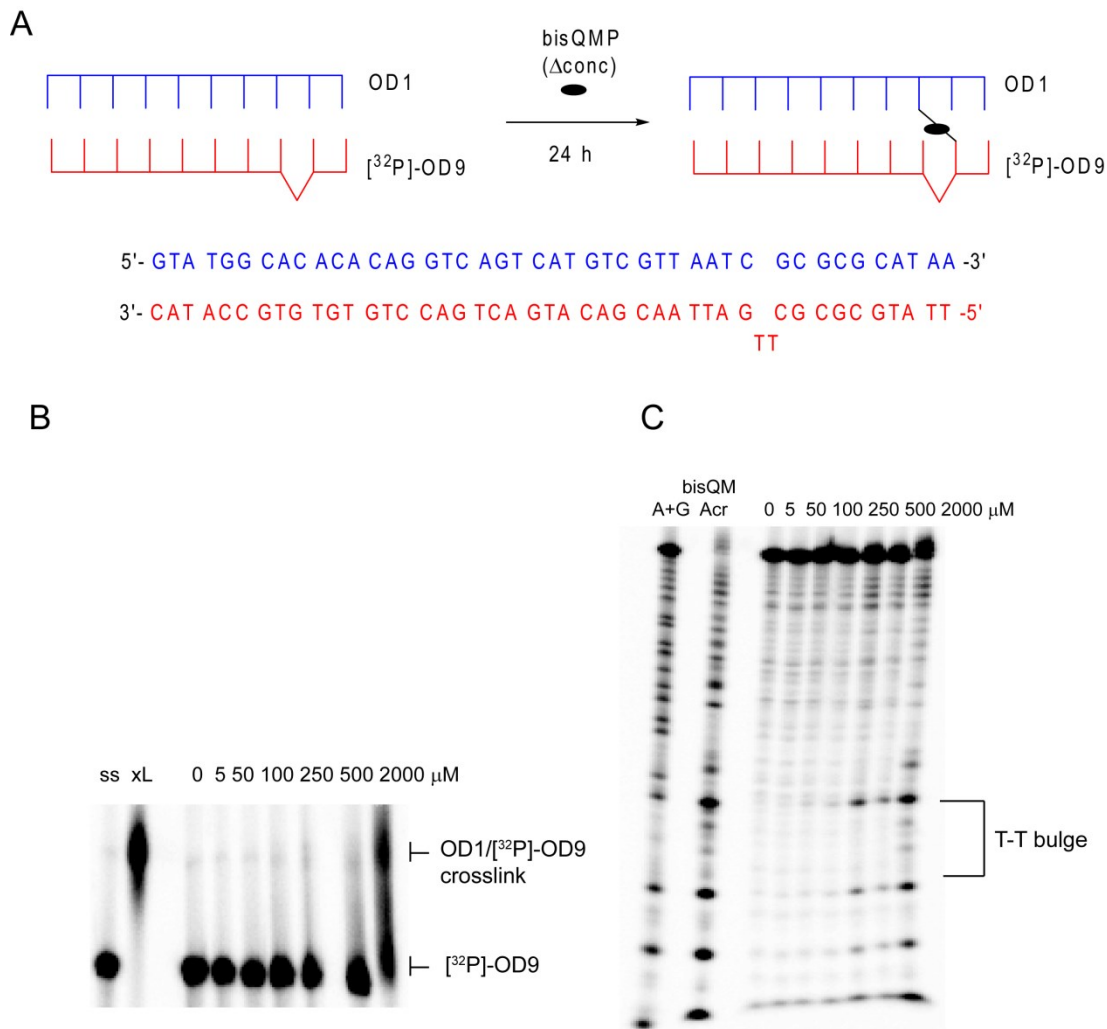
Figure 2.9 Inter-strand crosslink formation by bisQMQuin1 with DNA containing a T-T bulge. A) Scheme depicting the experimental setup. B) OD1/[^{32}P]-OD9 (3 μM) was treated with varying concentrations of bisQMPQuin1 for 24 h in MES (10 mM, pH 7), NaF (10 mM), and 20% acetonitrile. Products were separated by denaturing PAGE (20%). "Ss" and "xL" samples include OD1/[^{32}P]-OD9, MES (10 mM, pH 7), NaF (10 mM), and 20% acetonitrile in the presence and absence of bisQMPAcr (100 μM), respectively. C) Piperidine-induced fragmentation of the samples from (B). Samples were treated with piperidine (10%) for 30 min after reaction to induce fragmentation at sites of dGN7 alkylation. Products were separated by denaturing PAGE (20%) and visualized by phosphorimagery.

2.2.3.2 Synthesis and DNA Alkylation of BisQMPQuin2

Mahata *et al* reported that the benzyl moiety in quinoxaline compounds acts as an intercalation switch that permits quinoxalines to not only bind, but intercalate DNA.[63] Thus, we synthesized a new quinoxaline-linked bisQMP (bisQMPQuin2) that contains a benzyl moiety in order to improve association of the compounds to DNA. The synthesis began with a nucleophilic aromatic substitution reaction to substitute benzylamine for a chloride on 1,2-dichloroquinoxaline (Scheme 2.7).[66] Intermediate **23** was purified from unreacted starting material **22** via flash column chromatography. The remaining steps of the synthesis proceeded analogously to those for bisQMPQuin1.

The efficiency of DNA crosslinking by bisQMQuin2 was assessed by treating OD1/[^{32}P]-OD2 with increasing concentrations of bisQMPQuin2 for 24 h (Figure 2.10A).
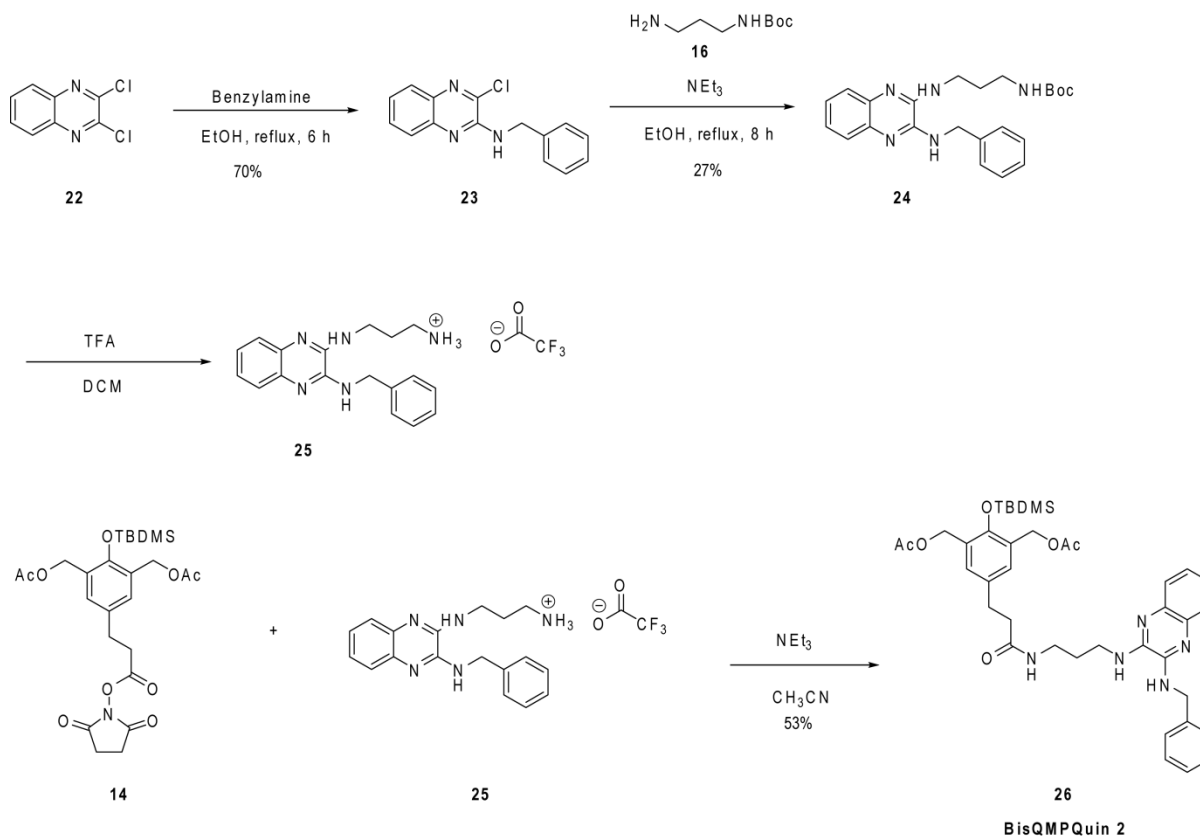
Scheme 2.7 Synthesis of bisQMPQuin 2

42

Surprisingly, no ICLs were detected with as high as 2 mM of bisQMPQuin2 (Figure 2.10B). BisQMQuin2 may bind DNA, but in a conformation that precludes QM alkylation. The benzyl moiety may bind the DNA place the QM aromatic ring too far from the bases to alkylate them.

A

bisQMP
(Δconc)

OD1

[^{32}P]-OD2

24 h

OD1

[^{32}P]-OD2

5'- GTA TGG CAC ACA CAG GTC AGT CAT GTC GTT AAT CGC GCG CAT AA -3'

3'- CAT ACC GTG TGT GTC CAG TCA GTA CAG CAA TTA GCG CGC GTA TT -5'

B

ss xL   0 5 50 100 250 500 2000 µM

⊢ OD1/[^{32}P]-OD2
crosslink
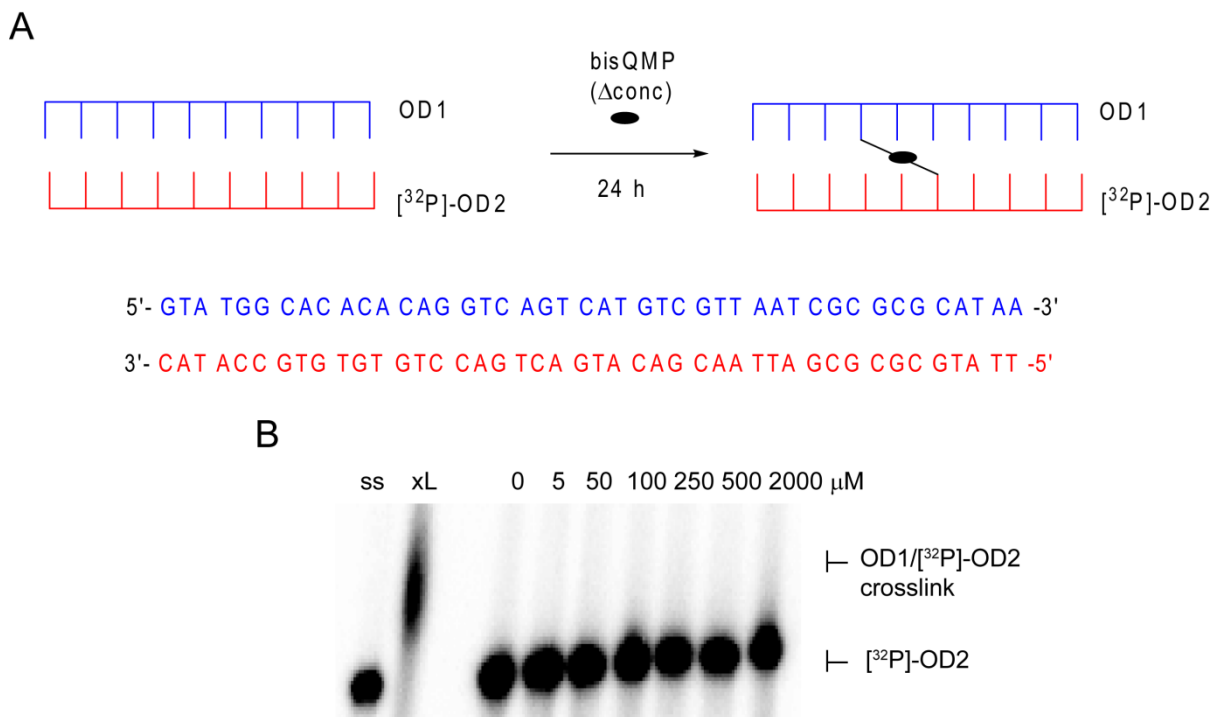
⊢ [^{32}P]-OD2

Figure 2.10 Dependence of DNA crosslinking on the concentration of bisQMQuin2. A) Scheme depicting the experimental setup. B) OD1/[^{32}P]-OD2 (3 µM) was treated with varying concentrations of bisQMPQuin1 for 24 h in MES (10 mM, pH 7), NaF (10 mM), and 20% acetonitrile. "Ss" and "xL" samples include OD1/[^{32}P]-OD2, MES (10 mM, pH 7), NaF (10 mM), and 20% acetonitrile in the presence and absence of bisQMPAcr (100 µM), respectively. Products were separated by denaturing PAGE (20%) and visualized by phosphorimagery.

2.2.3.3 Synthesis and DNA Alkylation of BisQMPQuin3

BisQMPAcr is linked to acridine via a two carbon diamino-linker, as opposed to the three carbon diamino-linker used for bisQMPQuin1 and bisQMPQuin2. Thus, using the two

carbon diamino-linker to conjugate quinoxaline to the bisQMP may improve its ability to alkylate DNA by placing QM closer to the nucleophiles of DNA. BisQMPQuin3 was synthesized in the same manner as bisQMPQuin1 (Scheme 2.8).

To determine the effect of the amine linker length of DNA alkylation, OD1/[^{32}P]-OD2 was treated with increasing concentrations of bisQMPQuin3 for 24 h. BisQMPQuin3 reacted to form a mixture of both crosslinking and monoalkylation at as low as 100 μM of the QM (Figure 2.11A). The shorter linker length afforded a significant improvement in DNA alkylation, as the total yield of reaction was greater than 50% with 2 mM of bisQMPQuin3. BisQMQuin3 may have overcome the low yields of DNA alkylation achieved by bisQMQuin1 and bisQMQuin2 by decreasing the distance between the QM and DNA's
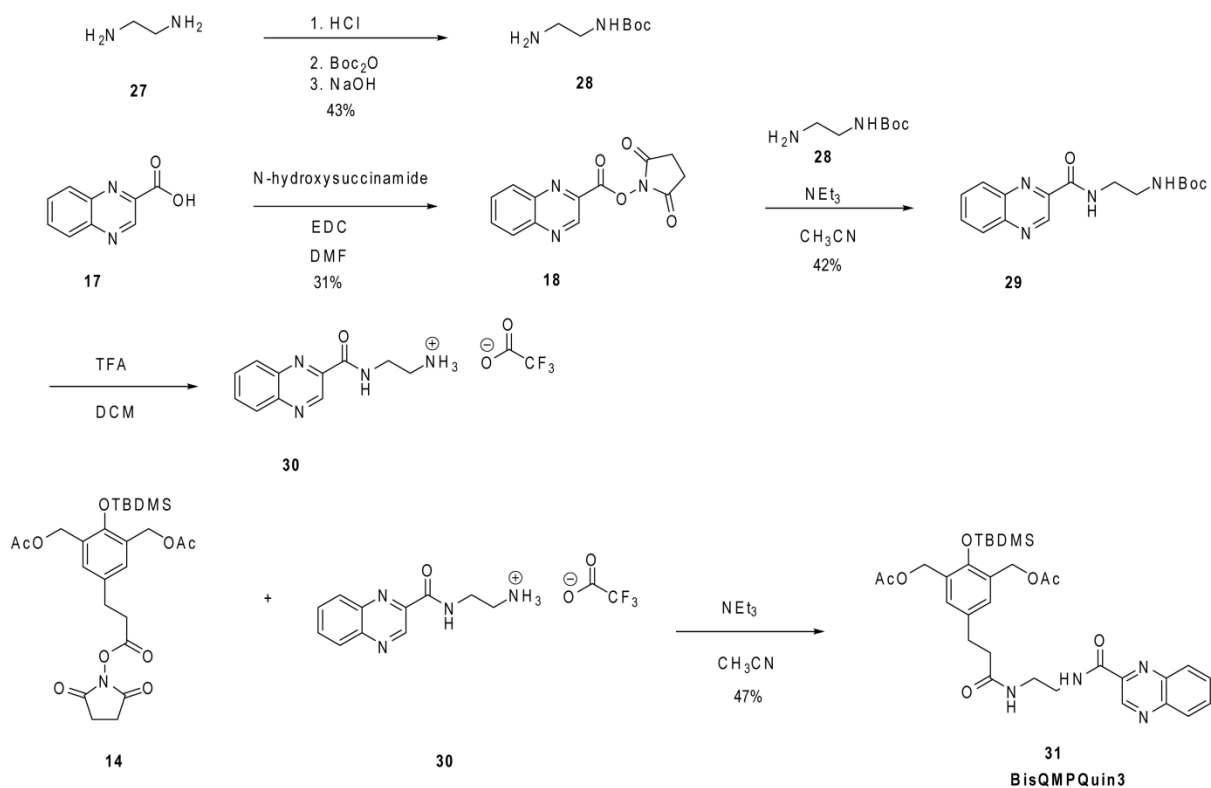
Scheme 2.8 Synthesis of bisQMPQuin3

44

nucleophilies to facilitate alkylation. BisQMQuin3 reacted primarily at dGN7s to form reversible DNA, but also at DNA's weaker nucleophiles to form irreversible, non-piperidine labile adducts in a small, but noticeable yield (Figure 2.11B).

BisQMQuin3's relatively high efficiency of ICL formation prompted an investigation of its dynamics of crosslinking. OD3 was treated with bisQMPQuin3 for 24 h to trap the QM's initial adducts and to ensure that any unreacted QM had been fully quenched by water (Appendix B, Figure B.32). [^{32}P]-OD2 was then added to the reaction to capture bisQMQuin3 once it regenerates from its adducts with OD3. No ICLs were detected after 24 h, indicating that bisQMQuin3's DNA alkylation is not dynamic (Figure 2.12). The failure to transfer its adducts between DNA strands is surprising given that bisQMQuin3 primarily alkylates dGN7s in duplex DNA (Figure 2.11B). However, bisQMQuin3 may bind single-stranded DNA differently than duplex DNA, as intercalation would be impaired with a single DNA sequence. A different binding mode with single-stranded DNA could lead different sites of reaction. BisQMQuin3 may form irreversible adducts in single-stranded DNA, which would prevent its ability to transfer its adducts between DNA strands. Mahata *et al* reported that quinoxalines lacking a benzyl group do not intercalate DNA, but rather bind in a non-intercalation event.[63] Thus, combination of the shorter diamino-linker with the addition of a benzyl group may not only improve bisQMQuins' affinity for DNA, but also its efficiency of reversible adduct formation.

A

bisQMP
(Δconc)

OD1 → OD1

[32P]-OD2 → 24 h → [32P]-OD2

5'- GTA TGG CAC ACA CAG GTC AGT CAT GTC GTT AAT CGC GCG CAT AA -3'

3'- CAT ACC GTG TGT GTC CAG TCA GTA CAG CAA TTA GCG CGC GTA TT -5'

B

ss xL   0 5 50 100 250 500 2000 µM

⊢ OD1/[32P]-OD2 crosslink

⊢ [32P]-OD2

0 0 2 3 8 13 25 % crosslinking

C

A+G   0 5 50 100 250 500 2000 µM

⊢ non-piperidine labile adducts

⊢ [32P]-OD2

⊢ dGN7 adducts
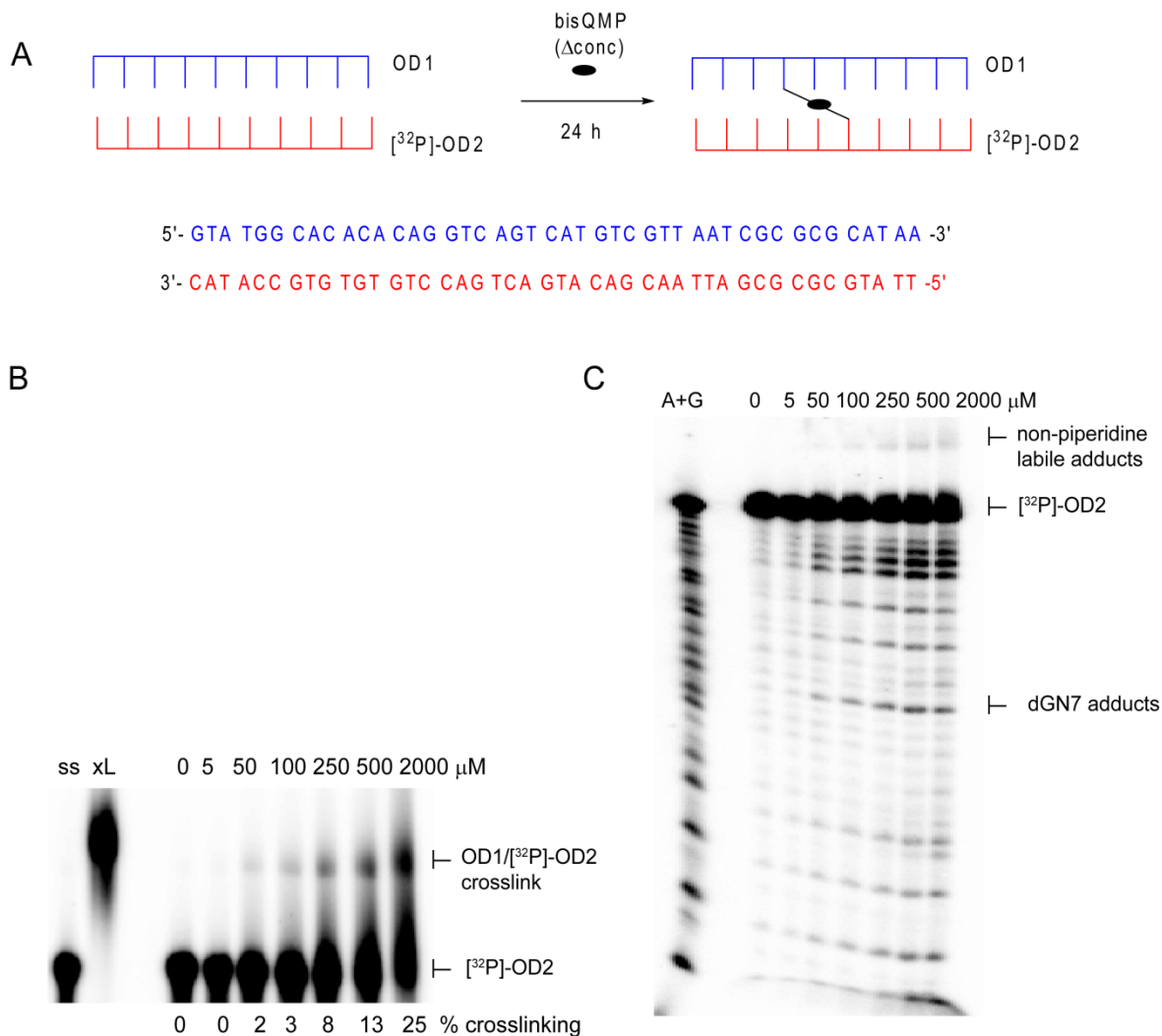
Figure 2.11 Dependence of DNA crosslinking on the concentration of bisQMQuin3. A) Scheme depicting the experimental setup. B) OD1/[32P]-OD2 (3 µM) was treated with varying concentrations of bisQMPQuin1 for 24 h in MES (10 mM, pH 7), NaF (10 mM), and 20% acetonitrile. Products were separated by denaturing PAGE (20%). "Ss" and "xL" samples include OD1/[32P]-OD2, MES (10 mM, pH 7), NaF (10 mM), and 20% acetonitrile in the presence and absence of bisQMPAcr (100 µM), respectively. C) Piperidine-induced fragmentation of the samples from (B). Samples were treated with piperidine (10%) for 30 min after reaction to induce fragmentation at sites of dGN7 alkylation. Products were separated by denaturing PAGE (20%), visualized, and quantified by phosphorimagery.

Figure 2.12 Transfer of bisQMQuin3's adducts between DNA strands. A) Scheme depicting the experimental setup. B) OD3 (3 µM) in MES (10 mM, pH 7) and NaF (10 mM) was treated with diQMPN$_3$ (50 µM) for 24 h. Excess QM was removed from the DNA by ethanol precipitation. The precipitated DNA was resuspended in buffer and [^{32}P]-OD2 was added and the reaction was incubated for 0-24 h. The products were separated by denaturing PAGE (20%) and visualized by phosphorimagery.

2.2.3.4 Synthesis and DNA Alkylation of BisQMPQuin4

A shorter diamino-linker between the quinoxaline and bisQMP fragments improved DNA alkylation efficiency. Thus, addition of a benzyl group to bisQMPQuin4 may further improve the yield of alkylation and direct alkylation to dGN7s via intercalation. BisQMPQuin4 was synthesized using the synthetic procedures established for synthesizing bisQMPQuin2 (Scheme 2.9). Treatment of OD1/[^{32}P]-OD2 with increasing concentrations of bisQMPQuin4 revealed very little DNA alkylation (Figure 2.13A). BisQMQuin4 forms ICLs with an approximate yield of 10% when 2 mM of the QM is utilized (Figure 2.13B). However, the yield of ICLs is too low to pursue further studies with this compound, despite improvements in alkylation efficiency over bisQMQuin2. Regardless, the detection of alkylation by bisQMQuin4 supports the hypothesis that the benzyl moiety may result in
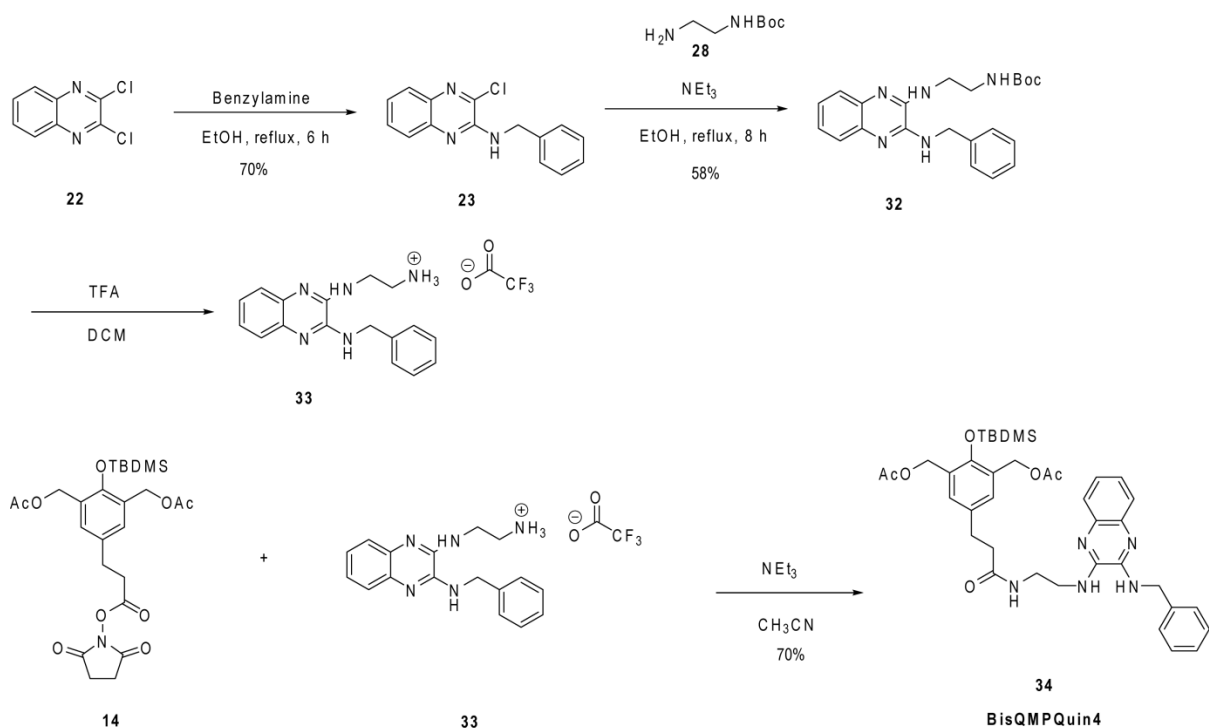
Scheme 2.9 Synthesis of bisQMPQuin4.

binding of the quinoxaline to DNA in a manner that precludes QM reaction. Shortening the linkage between the QMP and the quinoxaline may have improved the alkylation efficiency by placing the QMP in closer proximity to both the quinoxaline and the DNA once it was bound.

Additional functionalization of the quinoxaline scaffold will be necessary in order to develop a bisQM that migrates along DNA on a physiologically relevant time scale. Nitro-functionalized quinoxalines are abundant in the literature as DNA intercalators, probes for live cell imaging, and anti-cancer, anti-fungal, and anti-tuberculosis agents.[67, 68] Several quinoxalines have been designed that contain the nitro-functionality, in addition to other functional groups that may direct binding to DNA, such as the naphthyl group. A former

A

bisQMP
(Δconc)

OD1

[³²P]-OD2

24 h

OD1

[³²P]-OD2

5'- GTA TGG CAC ACA CAG GTC AGT CAT GTC GTT AAT CGC GCG CAT AA -3'

3'- CAT ACC GTG TGT GTC CAG TCA GTA CAG CAA TTA GCG CGC GTA TT -5'

B

ss xL   0 5 50 100 250 500 2000 μM

OD1/[³²P]-OD2
crosslink
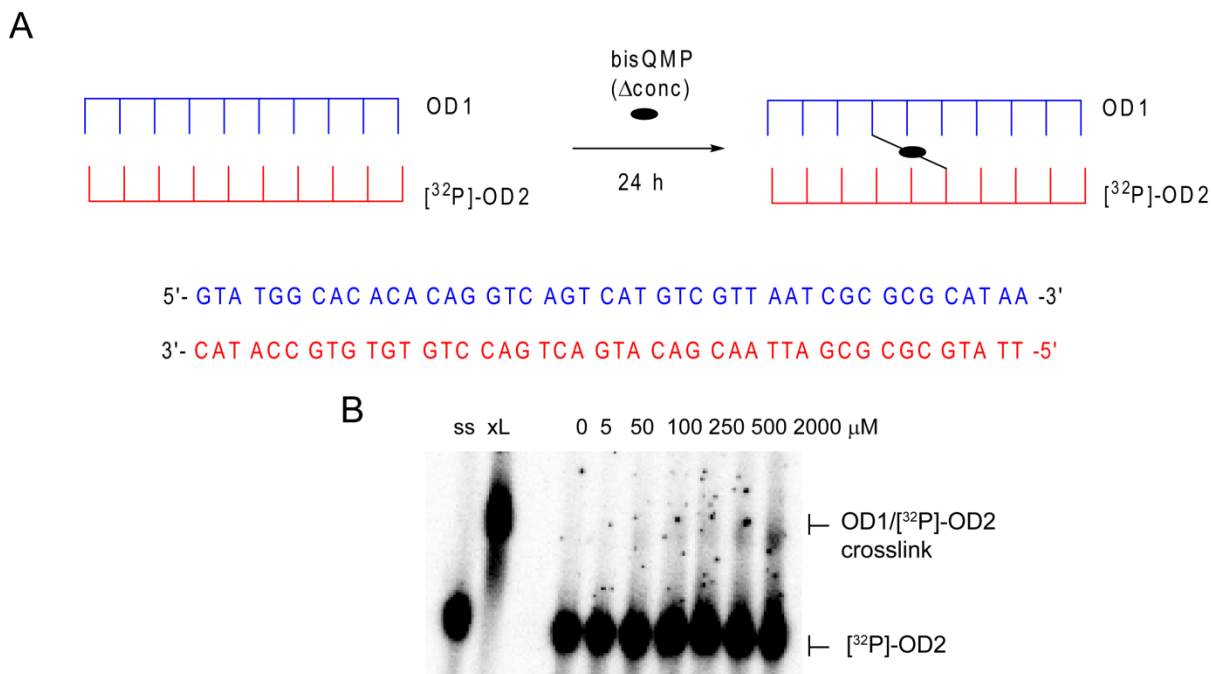
[³²P]-OD2

Figure 2.13 Dependence of DNA crosslinking on the concentration of bisQMQuin4. A) Scheme depicting the experimental setup. B) OD1/[³²P]-OD2 (3 μM) was treated with varying concentrations of bisQMPQuin1 for 24 h in MES (10 mM, pH 7), NaF (10 mM), and 20% acetonitrile. Products were separated by denaturing PAGE (20%). "Ss" and "xL" samples include OD1/[³²P]-OD2, MES (10 mM, pH 7), NaF (10 mM), and 20% acetonitrile in the presence and absence of bisQMPAcr (100 μM), respectively.

undergraduate student in the Rokita Lab worked on the synthesis and DNA alkylation efficiencies of several new bisQMPQuins, none of which dynamically alkylate DNA.

2.3 Summary

DiQMs conjugated to alkylammonium chains were evaluated as dynamic DNA alkylating agents and compared with their bisQM counterparts. DiQMs primarily behaved as monoalkylating agents, as one of the QM intermediates reacted irreversibly with water. DiQMN₃ alkylated DNA dynamically by transferring its adducts between DNA strands. However, its adducts transferred as monoadducts, rather than ICLs. The ability of monoQMs

to diffuse through DNA may have accounted for diQMN$_3$'s higher yield of strand transfer compared with that for bisQMN$_3$. Once released from its initial DNA adduct, diQMN$_3$ is free to diffuse through the DNA, while bisQMs are still anchored to the DNA strand by one of their two reactive QMs. DiQMN$_3$'s dynamics of alkylation ceased upon transfer of its adducts to a new DNA strand, as it transferred irreversible sites on the acceptor strand, preventing its further migration along DNA. However, diQMN$_3$'s behavior as a monoQM permitted its migration through DNA containing sticky ends by means of free diffusion upon regeneration from its original adduct. However, migration occurred through sequential monoalkylations, rather than via new ICL formation, as was the case for ebisQMAcr. The evolution of diQMN$_3$'s reversible DNA adducts to irreversible adducts prevent migration. Moreover, conjugation to alkylammonium chains likely directs the QM to nucleophiles in the minor groove that will react irreversibly. Our findings suggest that ebisQMAcr's migration along DNA was facilitated by acridine's delivery of the QM to the major groove for reversible reaction at dGN7.

Weakly intercalative quinoxalines were conjugated to bisQMs to hasten their migration by facilitating more facile dissociation from DNA than acridine. However, the quinoxalines likely bind DNA too weakly to enable QM alkylation. The quinoxalines may not even intercalate with DNA, but rather bind the grooves, as both reversible adducts at dGN7 and irreversible adducts with DNA's weak nucleophiles were formed.

Our efforts failed to develop a bifunctional QM with hastened migration along DNA via dynamic covalent chemistry. Our studies of ammonium-linked diQMs and quinoxaline-linked bisQMs highlight the delicate balance between DNA binding and reactivity that is necessary to achieve dynamic DNA alkylation. An alternate approach to facilitating QM

50

migration through DNA may draw from the use of biological machines that generate mechanical force while traversing DNA. Such an enzyme may be able to catalyze bisQMAcr's migration along DNA by providing a mechanical "push".

2.4 Materials and Methods

2.4.1 Materials

Organic reagents and starting materials were purchased from Sigma- Aldrich and Acros Organics and used without further purification. Solvents and salts were purchased from Sigma- Aldrich and Fisher Scientific. Silica gel (SiliaFlash P60, 230-400 mesh, 40-63 μm) for flash column chromatography was purchased from Silicycle. C_{18}-Sep Pak cartridges were purchased from Waters. All deuterated solvents for NMR spectroscopy were purchased from Cambridge Isotope Laboratories. NMR spectra were recorded on a Bruker AM400 spectrometer and referenced to residual protons in the deuterated solvents. Chemical shifts are reported in parts per million (ppm). High resolution mass spectrometry (HRMS) was obtained by Dr. Phil Mortimer using fast atom bombardment ionization with a VG 7070SE mass spectrometer. ESI HRMS was performed using UPLC-MS on an Acquity UPLC H-Class/Xevo G2 QTof from Waters. DiQMPN$_2$, and DiQMPN$_3$ were synthesized by Dr. Mark Hutchinson as described previously.[45, 46] The succinimide-activated ester **13** was synthesized as previously described.[40] Oligonucleotides were synthesized by Integrated DNA Technologies (IDT) with standard desalting and used without further purification. γ- [^{32}P]-ATP was purchased from Perkin Elmer. T4 polynucleotide kinase and proteinase K were purchased from New England Biolabs. All aqueous solutions used water purified to a resistivity of greater than 17.8 MΩ. DNA concentrations were measured from their

absorption at 260 nm using an Agilent UV-Vis spectrophotometer and calculated using their ε_{260} values provided by IDT. Detection of radiolabeled oligonucleotides was carried out using a Typhoon 9410 phosphorimager and quantified using ImageQuant TL software.

2.4.2 Methods

2-(4-Hydroxy-3-(hydroxymethyl)phenoxy)acetic acid (2). 2-(4-Hydroxyphenoxy)acetic acid (**1**) (0.50 g, 2.97 mmol) was dissolved in 5 M aq. NaOH (1.37 mL), 1.3 mL of 37% aq. formaldehyde, and 15 mL of water. The solution was stirred at 55° C for 24 h. The solution was cooled to room temperature and the pH was adjusted to 2 with HCl. The product was extracted with ethyl acetate (3x50 mL). The organic phases were combined and washed with brine (2x50 mL), dried with $MgSO_4$, filtered, and concentrated under reduced pressure to yield **2** as a pink oil (0.54 g, 2.7 mmol, 92% yield). ^{1}H NMR (400 MHz, CD_3OD) δ ppm 4.51 (s, 2H), 4.57 (s, 2H), 6.65 (s, 2H), 6.87 (s, 1H). ^{13}C NMR (101 MHz, CD_3OD) δ ppm 59.0, 64.8, 113.5, 113.8, 114.7, 127.7, 148.6, 150.7, 171.3. FAB HRMS *m/z* Calcd for $C_9H_{10}O_5$ 198.0528, found 198.0531 ([M[+]]).

2-(4-(((*tert*-Butyldimethylsilyl)oxy)-3-(((*tert*-butyldimethylsilyl)oxy)-methyl)phenoxy)acetic acid (3). Compound **2** (0.54 g, 2.7 mmol) was dissolved in 25 mL anhydrous DMF. To the solution was added *tert*-butyldimethylchlorosilane (1.03 g, 6.81 mmol) and imidazole (0.930 g, 13.6 mmol). The reaction was stirred at room temperature under N_2 for 16 h. The reaction was quenched by the addition of 50 mL of H_2O and the product extracted with ethyl acetate (3x50 mL). The organic phases were pooled, washed with brine (2x50 mL), sat. ammonium chloride (2x50 mL), dried with $MgSO_4$, filtered and

concentrated under vacuum to yield compound **3** as a yellow oil (0.99 g, 2.32 mmol, 85% yield). ^{1}H NMR (400 MHz, CDCl$_3$) δ ppm 0.09 (s, 6H) 0.18 (s, 6H), 0.94 (s, 9H), 0.98 (s, 9H), 4.61 (s, 2H), 4.70 (s, 2H), 6.66 (t, $J = 3.50$ Hz, 2H), 7.07 (s, 1H). ^{13}C NMR (101 MHz, CDCl$_3$) δ ppm -5.60, -4.40, 18.0, 18.3, 25.5, 25.8, 60.3, 65.7, 113.0, 113.3, 118.4, 133.3, 146.5, 151.9, 174.6. FAB HRMS m/z Calcd for C$_{21}$H$_{38}$O$_5$Si$_2$ 426.2258, found 426.2249 ([M$^+$]).

2-(4-(((*tert*-Butyldimethylsilyl)oxy)-3-(((*tert*-butyldimethylsilyl)oxy)-methyl)phenoxy)ethan-1-ol (4). Borane/THF (1 M), (40 mL, 40 mmol) was added slowly to a solution of compound **3** (0.99 g, 2.3 mmol) in 20 mL of anhydrous THF while stirring under N$_2$. Stirring was continued for 2 h under N$_2$ and then the reaction was quenched by the addition of 50 mL of H$_2$O. The product was extracted with ethyl acetate (3x50 mL). The organic layers were pooled, washed with water (2x50 mL), brine (50 mL), dried with MgSO$_4$, filtered, and concentrated under reduced pressure to yield a pale yellow oil. The compound was purified using flash silica column chromatography with 4:1 hexanes:ethyl acetate to yield compound **4** as a clear viscous oil (0.48 g, 1.2 mmol, 52% yield). ^{1}H NMR (400 MHz, CDCl$_3$) δ ppm 0.10 (s, 6H), 0.18 (s, 6H), 0.95 (s, 9H), 0.99 (s, 9H), 3.93 (t, $J=$ 4.36 Hz, 2H), 4.03 (t, $J = 4.15$ Hz, 2H), 4.71 (s, 2H), 6.66 (d, $J = 1.77$ Hz, 2H), 7.06 (s, 1H). ^{13}C NMR (101 MHz, CDCl$_3$) δ ppm -5.80, -4.70, 17.8, 18.0, 25.3, 25.6, 60.1, 61.2, 69.2, 84.1, 112.6, 118.1, 132.8, 145.5, 152.7. FAB HRMS m/z Calcd for C$_{21}$H$_{40}$O$_4$Si$_2$ 412.2465, found 412.2462 ([M$^+$]).

2-(4-(((*tert*-Butyldimethylsilyl)oxy)-3-(((*tert*-butyldimethylsilyl)oxy)-methyl)phenoxy)ethyl methanesulfonate (5). Methanesulfonyl chloride (0.199 g, 1.74 mmol, 135 μL) was added dropwise to a solution of **4** (0.48 g, 1.2 mmol) in 15 mL of CH_2Cl_2 and triethylamine (243 μL, 1.74 mmol). The reaction was stirred for 2 h at room temperature. The reaction was quenched by the addition of 50 mL of H_2O and the product was extracted with CH_2Cl_2 (3x50 mL). The organic layers were pooled and washed with water (2x50 mL), dried with $MgSO_4$, filtered, and concentrated to yield **5** as an opaque viscous oil (0.47 g, 0.97 mmol, 83% yield). ^1H NMR (400 MHz, $CDCl_3$) δ ppm 0.10 (s, 6H), 0.18 (s, 6H), 0.95 (s, 9H), 0.99 (s, 9H), 3.08 (s, 3H), 4.19 (m, 2H), 4.56 (m, 2H), 4.71 (s, 2H), 6.65 (t, $J = 2.69$ Hz, 2H), 7.04 (d, $J = 3.27$ Hz, 1H). ^{13}C NMR (101 MHz, $CDCl_3$) δ ppm -5.30, -4.20, 18.3, 18.5, 25.8, 26.0, 37.9, 60.5, 66.4, 68.5, 113.2, 113.3, 118.6, 133.6, 146.4, 152.5. FAB HRMS *m/z* Calcd for $C_{22}H_{42}O_6SSi_2$ 490.2241, found 490.2247 ($[M^+]$).

N^1-(2-(4-(((*tert*-butyldimethylsilyl)oxy)-3-(((*tert*-butyldimethylsilyl)oxy) methyl)phenoxy)ethyl)-N^3-(3-((2-(4-(((*tert*-butyldimethylsilyl)oxy)-3-(((*tert*-butyldimethylsilyl)oxy)methyl)phenoxy)ethyl)(methyl)amino)propyl)-N^1,N^3-dimethylpropane-1,3-diamine (6). To a solution of **5** (0.47 g, 0.97 mmol) in 3 mL of CH_3CN and trimethylamine (134 μL, 0.97 mmol) was added N,N-bis[3-(methylamino)propyl] methylamine (97 μL, 0.48 mmol). The reaction was stirred at 75 °C for 16 hours. The solution was diluted with 150 mL ethyl acetate, washed with saturated aqueous $NaHCO_3$ (3x50 mL), dried with $MgSO_4$, filtered, and concentrated under vacuum to yield an orange oil. The compound was purified using flash silica column chromatography with 1:1 hexanes:ethyl acetate, followed by methanol/NEt_3 to yield **6** as an orange oil (0.38 g,

0.39 mmol, 82% yield). ^{1}H NMR (400 MHz, CDCl$_3$) δ ppm 0.08 (s, 12H), 0.15 (s, 12H), 0.93 (s, 18H), 0.97 (s, 18H), 1.79 (m, 4H), 2.32 (s, 6H), 2.41 (s, 3H), 2.51 (t, J = 7.64 Hz, 4H), 2.64 (q, J = 10.18 Hz, 4H), 2.77 (m, 4H), 4.00 (m, 4H), 4.69 (s, 4H), 6.62 (t, J = 1.38 Hz, 4H), 7.01 (s, 2H). ^{13}C NMR (101 MHz, CDCl$_3$) δ ppm -5.50, -4.40, 18.0, 18.3, 25.6, 25.8, 42.6, 55.5, 56.0, 56.1, 60.4, 66.2, 112.8, 112.9, 118.2, 132.8, 145.4, 153.1. FAB HRMS m/z Calcd for C$_{51}$H$_{99}$N$_3$O$_6$Si$_4$ 962.6689, found 962.6693 ([M$^+$]).

((((((Methylazanediyl)bis(propane-3,1-diyl))bis(methylazanediyl))bis(ethane-2,1-diyl))bis(oxy))bis(6-((*tert*-butyldimethylsilyl)oxy)-3,1-phenylene))dimethanol (7). *para*-Toluenesulfonic acid (0.239 g, 1.25 mmol) was added to a solution of **6** (0.378 g, 0.390 mmol) in 5 mL methanol and stirred for 1 h at room temperature. The product was diluted with 100 mL of ethyl acetate, washed with saturated aqueous NaHCO$_3$ (2x50 mL), dried with MgSO$_4$, filtered, and concentrated under reduced pressure. The crude product was dissolved in 2 mL methanol and washed with 5 mL hexane to remove residual TBDMS, and concentrated under reduced pressure to yield **7** as an orange oil (0.14 g, 0.19 mmol, 48% yield). ^{1}H NMR (400 MHz, CDCl$_3$) δ ppm 0.18 (s, 12H), 0.98 (s, 18H), 1.66 (m, 4H), 2.18 (s, 3H), 2.29 (s, 6H), 2.33 (m, 4H), 2.44 (m, 4H), 2.73 (m, 4H), 3.98 (m, 4H), 4.60 (s, 4H), 6.66 (q, J = 2.70 Hz, 4H), 6.91 (s, 2H). ^{13}C NMR (101 MHz, CDCl$_3$) δ ppm -3.70, 18.7, 26.3, 42.7, 43.5, 56.2, 56.4, 56.6, 58.9, 61.9, 67.0, 114.5, 115.0, 119.5, 133.1, 147.4, 153.7. FAB HRMS m/z Calcd for C$_{39}$H$_{71}$N$_3$O$_6$Si$_2$ 734.4960, found 734.4959 ([M$^+$]).

((((((Methylazanediyl)bis(propane-3,1-diyl))bis(methylazanediyl))bis(ethane-2,1-diyl))bis(oxy))bis(6-((*tert*-butyldimethylsilyl)oxy)-3,1-phenylene))bis(methylene)

diacetate (8). Acetyl chloride (0.37 g, 0.47 mmol, 34 μL) was added to a solution of **7** (0.138 g, 0.190 mmol) in 5 mL CH_2Cl_2 and triethylamine (66 μL, 0.47 mmol) and stirred at room temperature for 1 h. The reaction was diluted with 100 mL of CH_2Cl_2, washed with saturated aqueous $NaHCO_3$ (2x50 mL), dried with $MgSO_4$, filtered, and concentrated under reduced pressure to a yellow oil. The compound was purified using flash silica chromatography with methanol/triethylamine to yield **8** as a pale yellow oil (0.085 g, 0.10 mmol, 55% yield). ^1H NMR (400 MHz, $CDCl_3$) δ ppm 0.18 (s, 12H), 0.97 (s, 18H), 1.69 (m, 4H), 2.24 (s, 3H), 2.31 (s, 6H), 2.41 (m, 4H), 2.47 (m, 4H), 2.76 (t, J = 6.01 Hz, 4H), 3.99 (m, 4H), 5.05 (s, 4H), 6.71 (q, J = 2.61 Hz, 4H), 6.85 (s, 2H),. ^{13}C NMR (101 MHz, $CDCl_3$) δ ppm -4.90, 17.5, 20.4, 25.1, 34.1, 34.6, 42.2, 47.7, 55.0, 55.4, 55.7, 61.5, 65.9, 114.4, 115.5, 118.6, 126.5, 147.0, 152.3, 170.3. FAB HRMS *m/z* Calcd for $C_{43}H_{75}N_3O_8Si_2$ 818.5171, found 818.5177 ($[M^+]$).

tert-Butyl (3-aminopropyl)carbamate (16). To a solution of methanol (15 mL), 36% aqueous HCl (3.36 mL, 40.5 mmol) was added at 0 °C and stirred for 15 min. Stirring was continued at room temperature for an additional 15 min before adding **15** (3.38 mL, 3.00 g, 40.5 mmol) at 0 °C. The reaction mixture was then stirred at room temperature for 15 min. Water (10 mL) was added and the mixture was stirred for an additional 30 min at room temperature. To the reaction mixture was added Boc_2O (8.80 g, 40.5 mmol) in methanol (15 mL), and the mixture was stirred for 1 h. Organic solvents were removed under reduced pressure. The mixture was then washed with ether (2x100 mL) to remove unreacted 1,3-diaminopropane. The product was extracted from the aqueous phase with CH_2Cl_2 (2x100 mL), washed with brine (100 mL), dried with $MgSO_4$, filtered, and concentrated under

reduced pressure to yield **15** (3.40 g, 19.5 mmol, 49% yield) as a pale yellow oil. ^{1}H NMR

(400 MHz, CDCl$_3$) δ ppm 1.36 (s, 9H), 1.57 (quin, 2H, J = 12.11 Hz), 2.72 (t, 2H, J=10.09

Hz), 3.11 (t, 2H, J=10.09 Hz), 5.18 (s, 1H). ^{13}C NMR (101 MHz, CDCl$_3$) δ ppm 28.4, 32.7,

38.3, 39.4, 79.0, 156.1. FAB HRMS m/z Calcd for C$_8$H$_{18}$N$_2$O$_2$ 175.1402, found 175.1449

[M+H]$^+$.

2,5-Dioxopyrrolidin-1-yl quinoxaline-2-carboxylate (18). N-Hydroxysuccinimide

17 (0.346 g, 3.45 mmol) was added to an anhydrous DMF solution (10 mL) of **16** (0.300 g,

1.72 mmol). This mixture was cooled to 0 °C and combined with 1-ethyl-3-(3-

dimethylaminopropyl) carbodiimide (EDC, 0.660 g, 3.45 mmol). The mixture was then

stirred overnight under N$_2$ at room temperature. The reaction mixture was diluted with brine

(50 mL), and extracted with Et$_2$O (3x50 mL). The organic phases were pooled and washed

with sat. ammonium chloride (2x50 mL) and brine (50 mL), dried with MgSO$_4$, filtered, and

concentrated under reduced pressure to yield **18** (0.143 g, 0.530 mmol, 31% yield) as a

brown solid. ^{1}H NMR (400 MHz, CDCl$_3$) δ ppm 2.95 (s, 4H), 7.93 (m, 2H), 8.17 (dd, 1H,

J=1.59, 8.43 Hz), 8.26 (dd, 1H, J=1.59, 8.43 Hz), 9.52 (s, 1H). ^{13}C NMR (101 MHz, CDCl$_3$)

δ ppm 25.4, 25.6, 25.7, 129.4, 130.7, 131.6, 133.6, 138.8, 141.5, 144.1, 144.9, 159.7, 169.2.

tert-**Butyl (3-(quinoxaline-2-carboxamido)propyl)carbamate (19).** To a solution

of **18** (0.143 g, 0.530 mmol) in anhydrous CH$_3$CN (10 mL) was added **15** (0.111 g, 0.630

mmol) and triethylamine (176 µL, 1.26 mmol). The reaction was stirred under N$_2$ for 2 h and

then quenched with 50 mL of H$_2$O and 2 mL of acetic acid. The product was extracted with

ether (3x50 mL). The organic phases were pooled and washed with brine (2x50 mL) and sat.

NaHCO$_3$ (3x50 mL), dried with MgSO$_4$, filtered, and concentrated under reduced pressure to yield **19** (0.15 g, 0.45 mmol, 87% yield) as a light brown solid. ^{1}H NMR (400 MHz, CDCl$_3$) δ ppm1.83 (quin, 2H, *J*=6.64 Hz), 3.24 (q, 2H, *J*=6.64 Hz), 3.60 (q, 2H, *J*=6.57 Hz), 5.03 (s, 1H,), 8.10 (m, 2H), 8.16 (dd, 2H, *J*=1.90, 6.18 Hz), 8.19, (dd, 2H, *J*=1.90, 6.18 Hz), 8.24 (s, 1H), 9.65 (s, 1H). FAB HRMS m/z Calcd for C$_{17}$H$_{22}$N$_4$O$_3$ 331.1725, found 331.17677 [M+H]$^+$.

3-(Quinoxaline-2-carboxamido)propan-1-aminium 2,2,2-trifluoroacetate (20). To a solution of **19** (0.15 g, 0.45 mmol) in CH$_2$Cl$_2$ (5 mL) was added trifluoroacetic acid (5 mL). The reaction mixture was stirred for 30 min at room temperature. The product was concentrated under vacuum to yield **20** (0.15 g, 0.45 mmol) as a light brown solid that was used without further purification.

(2-((*tert*-Butyldimethylsilyl)oxy)-5-(3-oxo-3-((3-(quinoxaline-2-carboxamido)propyl)amino)propyl)-1,3-phenylene)bis(methylene) diacetate (21, BisQMPQuin1). To a solution of **14** (0.080 g, 0.19 mmol) in anhydrous CH$_3$CN (10 mL) was added **20** (0.79 g, 0.23 mmol) and triethylamine (210 μL, 1.50 mmol). The reaction was stirred for 2 h at room temperature under N$_2$ and then quenched by addition of 50 mL of H$_2$O and 2 mL of acetic acid. The product was extracted with Et$_2$O (3x50 mL). The organic phases were pooled and washed with brine (2x50 mL) and sat. NaHCO$_3$ (3x50 mL), dried with MgSO$_4$, filtered, and concentrated under reduced pressure to yield **21** (0.060 g, 0.09 mmol, 50% yield). ^{1}H NMR (400 MHz, CDCl$_3$) δ ppm 0.16 (s, 6H), 0.99 (s, 9H), 1.75 (q, 2H, J=6.32 Hz), 2.09 (s, 6H,), 2.57 (t, 2H, J=8.16 Hz), 2.95 (t, 2H, J=8.16 Hz), 3.31 (q, 2H,

J=6.52 Hz), 3.48 (q, 2H, J=6.52 Hz), 5.06 (s, 4H), 6.60 (s, 1H), 7.16 (s, 2H), 7.86 (m, 2H), 8.11 (d, 2H, J=8.36 Hz), 8.20, (d, 2H, J=8.36 Hz), 8.31 (s, 1H), 9.63 (s, 1H). ^{13}C NMR (101 MHz, CDCl$_3$) δ ppm -3.7, 1.0, 8.5, 18.6, 21.0, 25.9, 30.3, 36.1, 36.2, 38.4, 61.9, 125.5, 127.0, 130.1, 131.8, 134.0, 143.6, 149.8, 164.4, 170.9, 173.2. FAB HRMS m/z Calcd for C$_{33}$H$_{44}$N$_4$O$_7$Si 637.3013, found 637.3056 [M+H]$^+$.

N-benzyl-3-chloroquinoxalin-2-amine (23). To a solution of 2,3-dichloroquinoxaline **22** (1.0 g, 5.0 mmol) in ethanol (20 mL) was added dried benzylamine (1.1 mL, 10 mmol). The mixture was then heated under reflux for 6 h and the solvent was removed under reduced pressure. The resulting yellow residue was subjected to silica gel flash column chromatography (9:1 hexanes:ethyl acetate) to yield **23** as a yellow solid (0.95 g, 3.5 mmol, 70% yield). ^{1}H NMR (400 MHz, CDCl$_3$) δ ppm 4.80 (d, J = 5.7, 2H), 5.86 (br, 1H), 7.35 (m, 1H), 7.44 (m, 5H), 7.60 (m, 1H), 7.76 (dq, J = 0.60, 1H) 7.83 (dq, J = 0.60, 1H). ^{13}C NMR (101 MHz, CDCl$_3$) δ ppm 45.2, 124.8, 125.7, 127.3, 127.5, 128.4, 129.8, 136.3, 137.4, 137.8, 140.9, 147.5. FAB HRMS m/z Calcd for C$_{15}$H$_{12}$ClN$_3$ 270.0722, found 270.0774 [M+H]$^+$.

***tert*-Butyl (3-((3-(benzylamino)quinoxalin-2-yl)amino)propyl)carbamate (24).** To a solution of **23** (0.2 g, 0.7 mmol) in ethanol (15 mL) was added **16** (1.02 g, 5.90 mmol) and triethylamine (206 μL, 1.40 mmol). The mixture was then heated under reflux for 8 h. The solvent was removed under reduced pressure. The resulting yellow residue was subjected to silica gel flash column chromatography (3:1 hexanes:ethyl acetate) to yield **24** as a pale yellow solid (0.080 g, 0.19 mmol, 27% yield), in addition to unreacted starting materials. ^{1}H

NMR (400 MHz, CDCl$_3$) δ ppm 1.43 (s, 9H), 1.76 (q, J = 6.75, 2H), 3.19 (q, J = 6.75, 2H), 3.65 (q, J = 6.75, 2H), 4.79 (d, J = 5.0, 2H), 5.51 (br, 1H), 5.58 (br, 1H), 6.02 (br, 1H), 7.32 (m, 5H), 7.44 (d, J = 7.9, 2H), 7.66 (q, J = 3.5, 2H). ^{13}C NMR (101 MHz, CDCl$_3$) δ ppm 27.9, 29.1, 36.7, 36.9, 45.4, 79.3, 123.9, 124.1, 124.6, 125.1, 126.9, 128.1, 136.4, 136.6, 138.4, 143.6, 143.8, 156.7. FAB HRMS m/z Calcd for C$_{23}$H$_{29}$N$_5$O$_2$ 408.2355, found 408.2394 [M+H]$^+$.

3-((3-(Benzylamino)quinoxalin-2-yl)amino)propan-1-aminium 2,2,2-trifluoroacetate (25). To a solution of **24** (0.08 g, 0.19 mmol) in DCM (5 mL) was added trifluoroacetic acid (5 mL). The reaction mixture was stirred for 30 min at room temperature. The product was concentrated under vacuum to yield **25** (0.080 g, 0.19 mmol) as a yellow oil that was used without further purification.

(5-(3-((3-((3-(Benzylamino)quinoxalin-2-yl)amino)propyl)amino)-3-oxopropyl)-2-((tert-butyldimethylsilyl)oxy)-1,3-phenylene)bis(methylene) diacetate (26, BisQMPQuin2). To a solution of **14** (0.083 g, 0.16 mmol) in anhydrous CH$_3$CN (10 mL) was added **25** (0.080 g, 0.19 mmol) and triethylamine (179 μL, 1.30 mmol). The reaction was stirred for 2 h at room temperature under N$_2$. The reaction was then quenched by the addition of 40 mL of H$_2$O and 2 mL of acetic acid. The product was extracted with Et$_2$O (3x50 mL). The organic phases were pooled and washed with brine (2x50 mL) and sat. NaHCO$_3$ (3x50 mL), dried with MgSO$_4$, filtered, and concentrated under reduced pressure to yield **26** (0.060 g, 0.080 mmol, 53% yield). ^{1}H NMR (400 MHz, CDCl$_3$) δ ppm 0.16 (s, 6H), 1.00 (s, 9H), 1.70 (q, J = 6.5, 2H), 2.03 (s, 6H), 2.44 (t, J = 7.90, 2H), 2.81 (t, J = 7.90, 2H),

3.25 (q, J = 6.50, 2H), 3.49 (t, J = 6.50, 2H), 4.78 (s, 2H), 5.04 (s, 4H), 5.70 (br, 1H), 6.05 (br, 1H), 6.40 (br, 1H), 7.09 (s, 2H), 7.27 (m, 5H), 7.42 (d, J = 7.10, 2H), 7.50 (t, J = 5.40, 1H), 7.60 (t, J = 5.40, 1H). ^{13}C NMR (101 MHz, CDCl$_3$) δ ppm -3.6, 18.8, 21.1, 29.5, 30.4, 30.9, 36.4, 37.6, 38.5, 45.9, 70.0, 124.3, 124.5, 124.8, 125.7, 127.2, 127.4, 128.1, 128.4, 128.5, 128.6, 128.9, 130.0, 136.9, 139.1, 144.0, 144.4, 149.9, 171.1, 172.9. FAB HRMS m/z Calcd for C$_{39}$H$_{51}$N$_5$O$_6$Si 714.3642, found 714.3678 [M+H]$^+$.

tert-**Butyl (2-aminoethyl)carbamate (28).** To a solution of methanol (8 mL), 36% aqueous HCl (1.38 mL, 16.6 mmol) was added at 0 °C and stirred for 15 min. The reaction mixture was then stirred at room temperature for an additional 15 min before adding ethane-1,2-diamine **27** (1.11 mL, 1.00 g, 16.6 mmol) at 0 °C. The reaction mixture was then stirred at room temperature for 15 min. Water (5 mL) was added and stirred for an additional 30 min at room temperature. To the reaction mixture was added Boc$_2$O (3.6 g, 16.6 mmol) in methanol (15 mL), and the mixture was stirred for 1 h. The mixture was concentrated under reduced pressure, then washed with ether (2x50 mL) to remove unreacted ethane-1,2-diamine. The product was extracted from the aqueous phase with CH$_2$Cl$_2$ (2x50 mL), washed with brine (50 mL), dried with MgSO$_4$, filtered, and concentrated under reduced pressure to yield **28** (1.15 g, 7.20 mmol, 43% yield) as a yellow oil. ^{1}H NMR (400 MHz, CDCl$_3$) δ ppm 1.33 (s, 9H), 1.93 (br, 2H), 2.70 (t, J=5.82 Hz, 2H), 3.06 (q, J=5.98 Hz, 2H), 5.33 (br, 1H).

tert-**Butyl (2-(quinoxaline-2-carboxamido)ethyl)carbamate (29).** To a solution of **18** (0.133 g, 0.490 mmol) in anhydrous CH$_3$CN (10 mL) was added **28** (0.095 g, 0.59 mmol) and triethylamine (165 µL, 1.19 mmol). The reaction was stirred under N$_2$ for 2 h and then

quenched with 50 mL of H_2O and 2 mL of acetic acid. The product was extracted with ether

(3x50 mL). The organic phases were pooled, washed with brine (2x50 mL) and sat. $NaHCO_3$

(3x50 mL), dried with $MgSO_4$, filtered, and concentrated under reduced pressure to yield **29**

(0.064 g, 0.20 mmol, 42% yield) as a yellow solid. ^{1}H NMR (400 MHz, $CDCl_3$) δ ppm 1.42

(s, 9H), 3.46 (q, *J*=7.04 Hz, 2H), 3.67 (q, *J*=5.97 Hz, 2H), 5.16 (br, 1H), 7.81 (m, 2H), 8.06

(dd, *J*=1.94, 7.43 Hz, 1H), 8.16 (dd, *J*=1.94, 7.43 Hz, 1H), 8.37 (br, 1H), 9.64 (s, 1H). [13]C

NMR (101 MHz, $CDCl_3$) δ ppm 28.3, 40.3, 79.6, 129.4, 129.6, 130.8, 131.6, 140.2, 143.3,

143.7, 143.8, 156.5, 164.0.

2-(Quinoxaline-2-carboxamido)ethan-1-aminium 2,2,2-trifluoroacetate (30). To a

solution of **29** (0.064 g, 0.20 mmol) in CH_2Cl_2 (5 mL) was added trifluoroacetic acid (5 mL).

The reaction mixture was stirred for 30 mins at room temperature. The product was

concentrated under vacuum to yield **30** (0.067 g, 0.20 mmol) as a yellow oil that was used

without further purification.

(2-((*tert*-Butyldimethylsilyl)oxy)-5-(3-oxo-3-((2-(quinoxaline-2-

carboxamido)ethyl)amino)propyl)-1,3-phenylene)bis(methylene) diacetate (31,

BisQMPQuin3). To a solution of **14** (0.045 g, 0.086 mmol) in anhydrous CH_3CN (10 mL)

was added **30** (0.034 g, 0.10 mmol) and triethylamine (97 μL, 0.69 mmol). The reaction was

stirred for 2 h at room temperature under N_2. The reaction was then quenched by the

addition of 40 mL of H_2O and 2 mL of acetic acid. The product was extracted with Et_2O

(3x50 mL). The organic phases were pooled, washed with brine (2x50 mL) and sat. $NaHCO_3$

(3x50 mL), dried with $MgSO_4$, filtered, and concentrated under reduced pressure to yield **31**

(0.025 g, 0.040 mmol, 47% yield). ^{1}H NMR (400 MHz, CDCl$_3$) δ ppm 0.16 (s, 6H), 1.00 (s, 9H), 2.08 (s, 6H), 2.48 (t, J = 8.09, 2H), 2.89 (t, J = 8.09, 2H), 3.57 (q, J = 6.11, 2H), 3.66 (q, J = 6.11, 2H), 5.04 (s, 4H), 6.27 (br, 1H), 7.11 (s, 2H), 7.87 (m, 2H), 8.12 (dd, J = 2.20, 7.69, 1H), 8.17 (dd, J = 2.20, 7.69, 1H), 8.36 (br, 1H), 9.63 (s, 1H). ^{13}C NMR (101 MHz, CDCl$_3$) δ ppm -3.9, 21.1, 25.7, 30.2, 30.7, 34.1, 38.2, 40.1, 67.2, 125.4, 126.7, 129.4, 129.6, 129.9, 130.8, 131.6, 134.0, 140.1, 142.9, 143.5, 143.9, 149.6, 164.5, 170.8, 172.7. ESI HRMS m/z Calcd for C$_{32}$H$_{42}$N$_4$O$_7$Si 623.2856, found 623.2896 [M+H]$^+$.

tert-Butyl (2-((3-(benzylamino)quinoxalin-2-yl)amino)ethyl)carbamate (32). To a solution of **23** (0.20 g, 0.70 mmol) in ethanol (15 mL) was added **28** (0.480 g, 2.95 mmol) and triethylamine (621 μL, 4.20 mmol). The mixture was then heated under reflux for 16 h. The solvent was removed under reduced pressure. The resulting yellow residue was subjected to silica gel flash column chromatography (3:1 hexanes:ethyl acetate) to yield **32** as a yellow oil (0.170 g, 0.400 mmol, 58% yield) in addition to unreacted starting materials. ^{1}H NMR (400 MHz, CDCl$_3$) δ ppm 1.33 (s, 9H), 3.39 (q, J= 5.79 Hz, 2H), 3.62 (q, J= 5.41 Hz, 2H), 4.76 (s, 2H), 5.59 br, 1H), 7.30 (dd, J= 2.90, 6.98 Hz, 5H), 7.42 (d, J= 7.46 Hz, 2H), 7.61 (m, 2H) ^{13}C NMR (101 MHz, CDCl$_3$) δ ppm 28.2, 40.6, 43.1, 45.7, 80.0, 124.4, 124.5, 125.5, 127.2, 128.2, 128.4, 136.7, 138.6, 143.8, 144.0, 158.1. ESI HRMS m/z Calcd for C$_{22}$H$_{27}$N$_5$O$_2$ 394.2198, found 394.2243 [M+H]$^+$.

2-((3-(Benzylamino)quinoxalin-2-yl)amino)ethan-1-aminium 2,2,2-trifluoroacetate (33). To a solution of **32** (0.050 g, 0.13 mmol) in CH$_2$Cl$_2$ (5 mL) was added trifluoroacetic acid (5 mL). The reaction mixture was stirred for 30 mins at room

temperature. The product was concentrated under vacuum to yield **33** (0.050 g, 0.13 mmol) as a yellow solid that was used without further purification. ESI HRMS m/z Calcd for $C_{19}H_{20}F_3N_5O_2$ 407.1569, found 407.2321 [M^+].

(5-(3-((2-((3-(Benzylamino)quinoxalin-2-yl)amino)ethyl)amino)-3-oxopropyl)-2-((tert-butyldimethylsilyl)oxy)-1,3-phenylene)bis(methylene) diacetate (34, BisQMPQuin4). To a solution of **14** (0.053 g, 0.10 mmol) in anhydrous CH_3CN (10 mL) was added **33** (0.050 g, 0.12 mmol) and triethylamine (112 µL, 0.800 mmol). The reaction was stirred for 2 h at room temperature under N_2. The reaction was then quenched by the addition of 40 mL of H_2O and 2 mL of acetic acid. The product was extracted with Et_2O (3x50 mL). The organic phases were pooled, washed with brine (2x50 mL) and sat. $NaHCO_3$ (3x50 mL), dried with $MgSO_4$, filtered, and concentrated under reduced pressure to yield **34** (0.050 g, 0.070 mmol, 70% yield) as a yellow oil. ^1H NMR (400 MHz, CDCl$_3$) δ ppm 0.15 (s, 6H), 0.99 (s, 9H), 2.04 (s, 6H), 2.32 (t, J= 8.07 Hz, 2H), 2.69 (t, J= 7.99 Hz, 2H), 3.47 (q, J= 7.07 Hz, 2H), 3.66 (q, J= 5.53 Hz, 2H), 4.76 (s, 2H), 4.99 (s, 4H), 6.94 (s, 2H), 7.29 (m, 5H), 7.39 (d, J= 8.38 Hz, 2H), 7.43 (m, 1H), 7.50 (m, 1H). ^{13}C NMR (101 MHz, CDCl$_3$) δ ppm 3.9, 20.8, 25.7, 30.1, 30.5, 37.9, 41.1, 41.5, 45.5, 61.7, 124.3, 124.4, 125.5, 126.7, 127.1, 128.1, 128.2, 128.3, 129.9, 133.5, 136.9, 138.7, 149.7, 168.9, 170.8, 173.7. ESI HRMS m/z Calcd for $C_{38}H_{49}N_5O_6Si$ 700.3486, found 700.3508 [M+H]$^+$.

General Oligonucleotide Studies. Duplex DNA was annealed by heating the [^{32}P]-DNA (2.8 µM) with its complementary strand (3.0 µM) in MES (10 mM, pH 7) and NaF (10 mM) at 95 °C for 2 minutes followed by slow cooling to room temperature. Crosslinking

experiments involved the addition of the quinone methide precursor in acetonitrile to the above mixture, yielding a final reaction volume of 20 μL., containing a final concentration of 20% acetonitrile. Reactions were quenched by the addition of 2X formamide loading dye (0.05% bromophenol blue and 0.05% xylene cyanol in formamide) and frozen in liquid nitrogen. Samples were thawed for 5 min at room temperature, analyzed by 20% denaturing polyacrylamide gel electrophoresis (PAGE), and visualized by phosphorimagery. Samples were quantified using ImageQuant TL software by and yields were reported as the intensity of each band relative to the total signal intensity per lane.

Piperidine Cleavage of Alkylated Oligonucleotides. Frozen samples of DNA treated with QMs were lyophilized and dissolved in 10% piperidine (30 μL). The samples were heated at 90 ºC for 30 min and then lyophilized. To remove residual piperidine, samples were dissolved in water (30 μL) and lyophilized in three consecutive repetitions. Samples were dissolved in water (10 μL) and combined with formamide containing bromophenol blue and xylene cyanol (10 μL). Samples were analyzed by 20% denaturing PAGE, visualized, and quantified by phosphorimagery.

Ethanol Precipitation of DNA. To each sample was added NaOAc (0.3 M, pH 5.2) and 10 volumes of cold ethanol. The samples were incubated on dry ice for 30 min. The samples were centrifuged to pellet the DNA (13, 200 g, 15 min). The supernatant was carefully removed via pipette and the remaining pellet was lyophilized to dryness. The samples were resuspended in MES (10 mM, pH 7.0), NaF (10 mM), acetonitrile (20%), and water to a final volume of 20 μL.

Chapter 3: Effect of Nucleosome Assembly on BisQMAcr's Alkylation

3.1 Introduction

Many anticancer drugs, such as the electrophilic compounds temozolomide and the nitrogen mustard chlorambucil, damage cellular DNA and induce apotosis of the cancer cells.[9, 13] The effectiveness of DNA alkylating agents is often investigated *in vitro* using DNA that lacks the proteins associated with chromatin. However, this state of DNA does not reflect its *in vivo* environment and may not provide an accurate measure of the clinical efficacy of these compounds. Cellular DNA does not exist free in solution, but rather is wrapped around octamers containing two copies each of the four core histone proteins (H2A, H2B, H3, and H4) to form nucleosome core particles (NCPs).[69-71] Nucleosome assembly alters DNA's duplex geometry, solvent accessibility, and electrostatic environment. All of these factors may alter DNA's reactivity relative to that in its unpackaged state.[72] Therefore, investigating the potency of DNA alkylating agents within nucleosomes should more accurately reflect a compound's reactivity in a cellular environment and serve as a model system for understanding how DNA packaging into chromatin *in vivo* will affect DNA alkylation.

The assembly of DNA into the NCP has been shown to alter the profile of DNA alkylation of drugs and toxins relative to unpackaged DNA. Compounds that target the minor groove, such as mitomycin C and duocarmycin B_2 experience suppressed reaction with nucleosomal versus free DNA.[73, 74] However, this suppression is not observed in all minor groove alkylating agents, as yatakemycin's alkylation is unaffected by NCP assembly.[75] Reaction of compounds that alkylate the major groove is often suppressed as well. Alkylation

by nitrogen mustards[6] and aflatoxin B$_1$ was universally suppressed by the NCP across all dGN7s.[76] The deformation of groove structure and the steric block provided by the histones generally limit groove binding and intercalation. On the other hand, some intercalators, such as N-(2,3-epoxypropyl)-1,8-naphthalimide, can bind the nucleosomal DNA where the DNA helix stretches through the dyad axis.[77] The yield of DNA alkylation may also be limited by competition with the histone proteins for reaction. For instance, acrolein, an exogenous toxin found in the environment as a constituent of cigarette smoke, alkylates the histone proteins in addition to DNA.[78] Unlike most alkylating agents, not only does nucleosome assembly influence acrolein's alkylation, but also acrolein's alkylation modulates DNA packaging. Acrolein's alkylation of the histones influences nucleosome formation and maintenance by preventing histone acetylation and thereby disassembling the nucleosome.[79] The histones can also form DNA-protein crosslinks by reacting with bifunctional alkylating agents designed to crosslink DNA.[80]

The reactivity of QMs with nucleosomal DNA has yet to be investigated, despite the abundance of studies concerning QMs' dynamic alkylation of DNA. BisQMAcr has been demonstrated to dynamically alkylate DNA free in solution, but how this compound responds to DNA packaging has not yet been characterized. Here, we compare bisQMAcr's DNA alkylation profile in free and packaged DNA. Furthermore, how bisQMAcr responds to the presence of the histones will be characterized, since few studies have examined the ability of *ortho*-QMs to alkylate proteins. Thus, our work will assess how bisQMAcr may behave in a cellular environment by examining its ability to alkylate DNA and histones in the NCP.

3.2 Results and Discussion

3.2.1 Effect of Nucleosome Assembly on DNA Alkylation by BisQMAcr

A NCP generated from Widom's 601 sequence (Figure 3.1) and *Xenopus laevis*
histones H2A, H2B, H3, and H4 expressed in *E.coli* were chosen to provide a homogeneous
target for QM reaction. Widom's 601 sequence of DNA was identified for its ability to form
a stable NCP with uniform rotational and positional orientation.[81] Heterologous expression of
the histone proteins (a generous contribution from Dr. Kun Yang) avoids potential
contamination by natural histone variants and epigenetic modifications that are present in
NCPs isolated from endogenous sources.

Figure 3.1 Sequence of the Widom 601 DNA. The "top"
strand (black) is radiolabeled as indicated and the positions
of its guanines that are examined by piperidine-induced
fragmentation after alkylation are indicated relative to the
5'-terminus. The complementary strand is shown in gray.

To determine the effect of nucleosome assembly on DNA's reactivity with QMs,
DNA free in solution and assembled in NCPs were individually treated with increasing
concentrations of bisQMPAcr for 24 h. The resulting samples were then treated with
piperidine to induce fragmentation at sites of dGN7 alkylation, bisQMPAcr's primary target
(Figure 3.2A).[40] Full consumption of the parent duplex DNA occurred with 250 µM of
bisQMAcr for the free DNA. In contrast, only approximately 10% (based on the band

intensities of fragmented DNA relative to the total intensity of the lane) of the DNA

assembled in the NCP was consumed after treatment with 500 µM of bisQMAcr after 24 h.

The profile of alkylation at dGN7 did not differ significantly in the two different DNA

targets, as the relative distribution of fragments remained similar, as determined by

densitometry of the relative signals of the bands. Equivalent alkylation profiles were also
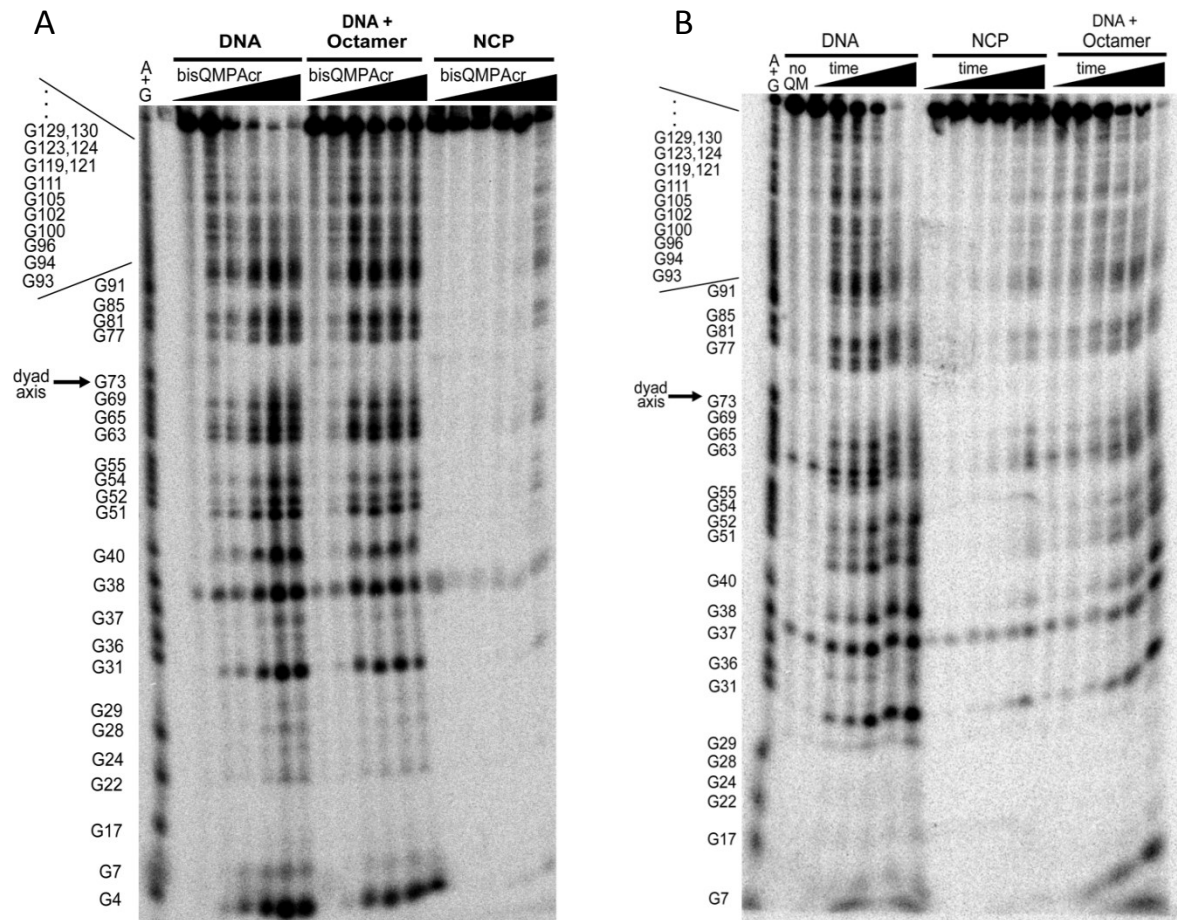
Figure 3.2 BisQMAcr alkyation of DNA in the absence and presence of histone octamer and after assembled into a NCP. A) Samples were treated with increasing concentrations of bisQMPAcr (0, 5, 50, 100, 250, 500 µM) at 4 ºC for 24 h and then treated with piperidine to identify sites of alkylation. B) Samples were treated with bisQMPAcr (500 µM) and quenched after 0, 2, 4, 8, and 24 h. The samples were then treated with piperidine to identify sites of alkylation.

maintained over the time of reaction (Figure 3.2B).

Diminished reaction with the NCP may result from weakened DNA binding affinity of bisQMAcr or inaccessibility of DNA's nucleophiles to bisQMAcr's electrophilic sites. DNA in the NCP experiences kinking and bending into the major and minor grooves, which impairs binding of other DNA targeting drugs.[82] BisQMAcr's alkylation at dGN7 was suppressed uniformly throughout the DNA sequence, suggesting that QM access to the DNA was not selectively blocked. A uniform suppression of binding to and reaction with DNA in the NCP also occurred for several other electrophiles, such as the nitrogen mustards, mitomycin C, and benzo[α]pyrene diol epoxide.[72, 73, 83, 84]

DNA distortion may disrupt the base stacking that permits intercalation of bisQMAcr's acridine ligand. The intercalators ethidium bromide and aflatoxin B_1 bind more weakly to the NCP than to unpackaged DNA due to changes in DNA's conformation.[72, 76, 85] Inability to effectively bind the NCP would suppress reaction of bisQMAcr because intercalation has been postulated to drive its reaction by positioning the electrophiles to react with DNA, especially at dGN7s.[40, 41] Thus, a weakened ability to intercalate with packaged DNA may lead to suppressed alkylation of DNA in the NCP. Despite diminished binding and reaction with the NCP, some intercalators accumulate at the nucleosome dyad axis, where base pair unstacking that arises from minor groove kinking induced by DNA stretching creates an opening in the otherwise compact NCP structure. The alkylating agent N-(2,3-epoxypropyl)-1,8-naphthalimide reacts strongly at the dyad due to increased accessibility for its intercalation.[77] However, the differences in binding and reactivity profiles of these various intercalators may reflect differences in the orientation of the electrophiles when bound to the

DNA in the NCP. Acridine may still bind the dyad axis, but in a conformation that precludes bisQMAcr's reaction with the DNA.

The reactivity of DNA with bisQMAcr was examined in the competing presence of the histone octamer when not assembled into the NCP to determine the contributions of DNA packaging and the added concentration of nucleophiles provided by the histones on bisQMAcr's diminished reactivity with DNA assembled in the NCP relative to DNA free in solution. The histones provide additional nucleophiles that can compete with the nucleophiles in DNA for reaction with bisQMAcr. Full consumption of the parent DNA after incubation with 500 µM of bisQMAcr for 24 h was not detected in the presence of the histone octamer. However, the yield of alkylation at dGN7s (~80%) compared more favorably to that observed with the unpackaged DNA than that with the NCP (Figure 3.2). Nonspecific association of the DNA and the histone octamer is possible in the absence of NCP reconstitution, but this did not significantly impact the reaction relative to DNA alone. Overall, the DNA packaging into the NCP, rather than competition with the histones, is responsible for significant suppression of DNA alkylation by bisQMAcr.

3.2.2 DNA- Protein Crosslink Formation with the NCP

BisQMAcr has the potential to form DNA- protein crosslinks with the NCP due to two electrophiles that can react with any pair of reactive nucleophiles. To investigate the efficiency of DNA-protein crosslinking, the NCP was treated with increasing concentrations of bisQMAcr for 24 h. A smear with low electrophoretic mobility appeared on the gel with as low as 50 µM of bisQMAcr, with the yield of low mobility products increasing to approximately 20% after treatment with 500 µM of bisQMAcr (Figure 3.3). The loss of the
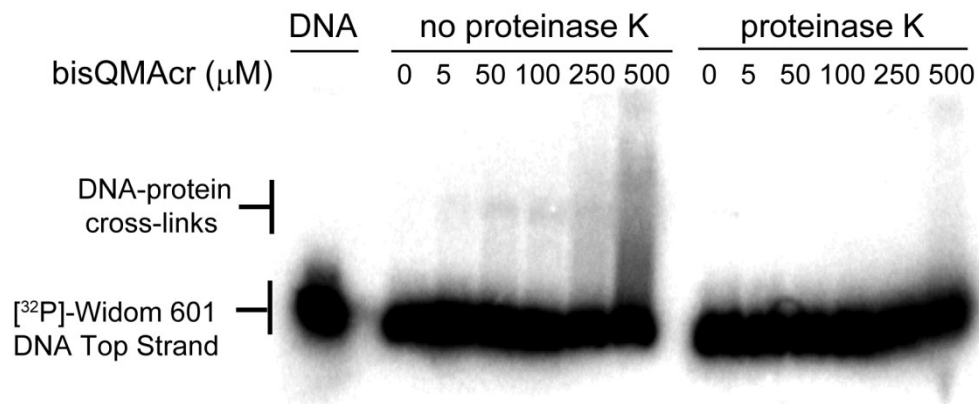
Figure 3.3 Formation of DNA-histone crosslinks with the NCP after treatment with bisQMAcr. Individual samples of the NCP were treated with the indicated concentrations of bisQMPAcr at 4 ° C and quenched after 24 h by freezing in liquid N_2. Samples were then thawed for 5 min at room temperature and divided into two sets. One set was analyzed directly, and the second set was treated with proteinase K (2 µL, 1.6 U) for 15 min at room temperature. All samples were then combined with loading dye, separated by 10% SDS-PAGE, and visualized by phosphorimagery.

products after treatment with proteinase K confirmed their identity as DNA-protein crosslinks. The heterogeneity of products suggests an equally heterogeneous array of DNA-protein crosslinks.

Other electrophiles have also been reported to form DNA- protein crosslinks, albeit in lower yields than that of bisQMAcr. The nitrogen mustards react with over 130 proteins in cells to form DNA-protein crosslinks, but few contained the histone proteins.[86] Similarly, cis-platin generated DNA-protein crosslinks with 250 proteins in vivo, but only sparse reaction with the histones was observed.[87] The limited formation of DNA-histone crosslinks by bisQMAcr and other electrophiles is likely to be beneficial, as an abundance of DNA-protein crosslinks could impair cellular functions.

BisQMAcr most likely generates DNA-protein crosslinks in the NCP by direct nucleophilic addition to both of its electrophiles. However, recent studies have demonstrated

that DNA-protein crosslinks can result from nucleophilic reaction of lysines from the histone tails with abasic sites that may be generated by depurination of alkylated dGN7s.[88] Nucleosome assembly significantly suppresses depurination of alkylated dGN7s relative to that in free DNA.[89] Thus, the crosslinks that we observe most likely result from bisQMAcr's bifunctional alkylation.

3.2.3 Alkylation of the Histones by MonoQMAcr and BisQMAcr

Table 3.1 QM-peptide adducts observed from alkylation of histone octamer and NCP.

Entry	Peptide-QM Adduct	Adduct Position	Reaction with	Experimental Mass (Da)	Calculated Mass (Da)	Observed with the NCP?	Observed after Transfer?
I	TESSK	H2A 121-125	MonoQM	948.3704	948.4460	Yes	Yes
II	RR	Either/and H2B 30-31, H3 53-54, H3 129-130, H4 46-47, H4 50-51	MonoQM	728.2477	728.3990	No	No
III	IAGEASR	H2B 74-80	MonoQM	1100.3669	1100.5522	No	Yes
IV	SAK	H2A 126-128	BisQM	715.1870	715.3615	No	Yes
V	DIQLAR	H3 124-129	BisQM	1126.3824	1126.3734	No	No

monoQMPAcr
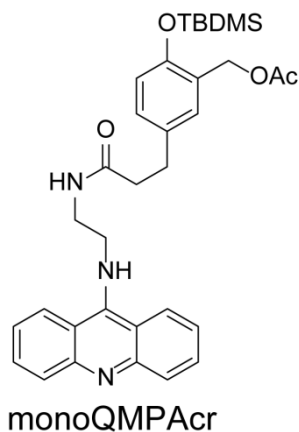
Scheme 3.1. Structure of the *tert*-butyl dimethylsilyl-protected precursor to monoQMAcr.

73

The formation of DNA-protein crosslinks by bisQMAcr with the NCP indicates that bisQMAcr alkylates the histone proteins. To determine where and which residues bisQMAcr alkylates, we examined QM-treated histones by UPLC-MS. However, monoQMAcr (Scheme 3.1), the monofunctional analogue of bisQMAcr, was initially used to identify the possible sites of QM modification of the histones without the complications of bifunctional alkylation.

Histone Octamer

No QM coverage: 68.9 %   Combined coverage: 71.7%   QM coverage: 70.9%
No QM unique coverage: 16.6 %   Common coverage: 68.1%   QM unique coverage: 29.3%

Histone H2A
1- 50   MSGRGKQGGK TRAKAKTRSS RAGLQFPVGR VHRLLRKGNY AERVGAGAPV
51- 100 YLAAVLEYLT AEILELAGNA ARDNKKTRII PRHLQLAVRN DEELNKLLGR
101- 130 VTIAQGGVLP NIQSVLLPKK TESSKSAKSK

Histone H2B
1- 50   MPDPAKSAPA AKKGSKKAVT KTQKDGKKR RKSRKESYAI YVYKVLKQVH
51- 100 PDTGISSKAM SIMNSFVNDV FERIAGEASR LAHYNKRSTI TSREIQTAVR
101- 126 LLLPGELAKH AVSEGTKAVT KYTSAK

Histone H3
1- 50   MARTKQTARK STGGKAPRKQ LATKAARKSA PATGGVKKPH RYRPGTVALR
51- 100 EIRRYQKSTE LLIRKLPFQR LVREIAQDFK TDLRFQSSAV MALQEASEAY
101- 136 LVGLFEDTNL CGIHAKRVTI MPKDIQLARR IRGERA

Histone H4
1- 50   MSGRGKGGKG LGKGGAKRHR KVLRDNIQGI TKPAIRRLAR RGGVKRISGL
51- 100 IYEETRGVLK VFLENVIRDA VTYTEHAKRK TVTAMDVVYA LKRQGRTLYG
101-103 FGG

Figure 3.4 Peptides detected by UPLC-MS after trypsin digestion of the histone octamer. Sequences highlighted in yellow represent peptides that were detected prior to bisQMAcr treatment and underlined sequences represent peptides that were detected after treatment with bisQMAcr. Spacing indicates the fragments expected from trypsin digestion.

The histone octamer, rather than the NCP, was initially used to identify the total number of

sites of histone alkylation. The histone octamer was treated with monoQMAcr (500 µM) for

24 h, before the histones were digested with trypsin. Six new species were observed by

UPLC-MS analysis following treatment with monoQMAcr when compared with the digested

histones in the absence of monoQMAcr treatment (Figure 3.4, 3.5A, and Table 3.1). The

Figure 3.5 Peptide-monoQMAcr adducts formed with the histone octamer. A) Total ion count was monitored during elution of the peptides before (black) and after (red) reaction with monoQMAcr. Signals unique to the alkylated samples are labeled according to Table 3.1. Signals labeled with "0" do not contain $[M+H]^+$ values that correspond to a QM adduct or peptide fragment. Peptide coverage by this analysis is summarized in Figure 3.4. B) MS^2 spectrum of the adduct formed between monoQMAcr and TESSK of histone H2A (Table 3.1, entry I). C) MS^2 spectrum of the adduct formed between monQMAcr and RR (Table 3.1, entry II). D) MS^2 spectrum of the adduct formed between monoQMAcr and IAGEASR of histone H2B (Table 3.1, entry III).

QM-H$_2$O adduct formed by quenching of monoQMAcr by solvent. The two products labeled "0" were observed in the presence, but not absence of monoQMAcr, but did not correspond to histone adducts. The remaining products, labeled "I-III", represent alkylated peptides with parent ions that correspond to the combined mass of monoQMAcr and the amino acid sequence corresponding to a histone peptide. Signals corresponding to alkylated peptides were recognized by the presence of secondary ions in the mass spectra that corresponded to monoQMAcr, as well as a characteristic fragment of 9-aminoacridine. MonoQMAcr alkylated TESSK and IAGEASR, which are unique to histones H2A and H2B, respectively (Figure 3.5B, D, and Table 3.1, entries I and III). The third adduct contains RR, and may be derived from multiple sites in histones H2B, H3, and H4 (Figure 3.5C and Table 3.1, entry II).

The analogous experiment was then performed with bisQMAcr to determine its sites of alkylation on the histone octamer. BisQMAcr is capable of reacting with one histone nucleophile and water, or with two histone nucleophiles. Two products were identified that contain peptides and bisQMAcr (Figure 3.6A). BisQMAcr alkylated SAK and DIQLAR from histones H2A and H3, respectively (Table 3.1, entries IV and V and Figure 3.6B, C). Interestingly, these sites are not identical to the sites of reaction observed for monoQMAcr. The lack of common sites of reaction between monoQMAcr and bisQMAcr may indicate sensitivity to the orientation of the reactants. Our data indicated reaction of bisQMAcr with individual peptides at one of the benzylic positions. The species that reacted at the second benzylic position was likely lost during the mass spectrometry ionization process.
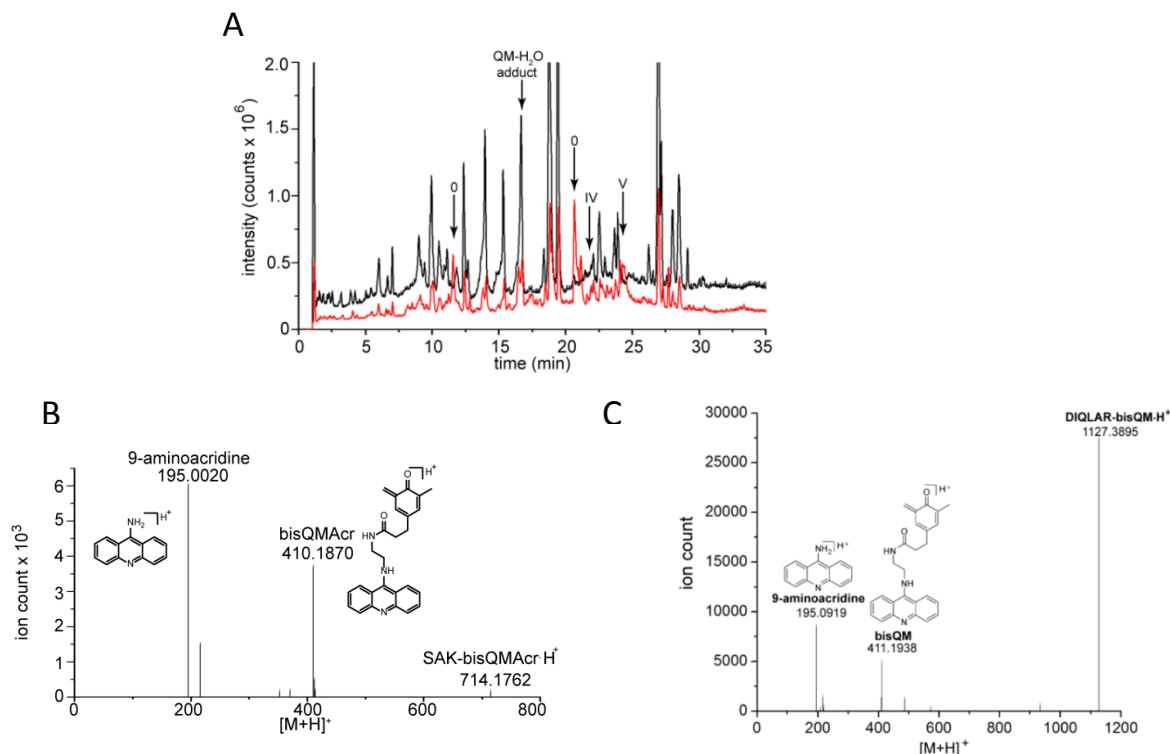
Figure 3.6 Peptide-bisQMAcr adducts formed with the histone octamer. A) Total ion count was monitored during elution of the peptides before (black) and after (red) reaction with bisQMAcr. Signals unique to the alkylated samples are labeled according to Table 3.1. Signals labeled with "0" do not contain $[M+H]^+$ values that correspond to a QM adduct or peptide fragment. Peptide coverage by this analysis is summarized in Figure 3.4. B) MS^2 spectrum of the adduct formed between bisQMAcr and SAK of histone H2A (Table 3.1, entry IV). C) MS^2 spectrum of the adduct formed between bisQMAcr and DIQLAR of histone H3 (Table 3.1, entry V).

Both QMs formed few adducts with the histones, with monoQMAcr generating slightly more adducts than bisQMAcr. Previous reports have demonstrated that both *para*- and *ortho*-QMs react favorably with cysteine's highly nucleophilic thiol side chain.[90, 91] However, the presence of only a single cysteine in the NCP and its general inaccessibility may explain why no reaction between cysteine and monoQMAcr and bisQMAcr was

observed. The next most reactive side chain, lysine's side chain amine, was an expected target for QM alkylation, especially in the lysine-rich N-terminal histone tails. Adducts with lysine may be too labile for detection by UPLC-MS conditions, as has been noted for previous studies of *para*-QMs.[92] We were not able to assign the exact residue of QM alkylation within an identified peptide due to the loss of the QM during MS^2 analysis. The most nucleophilic site within the peptides from products I, III, and IV is serine, while the only possible side chain in product II is arginine. Both amino acids are weakly nucleophilic under physiological conditions, and do not seem likely targets of QM alkylation. The carboxylate side chain in product V presents the only possible nucleophile for alkylation, but QM-carboxylate adducts are typically quite labile. The QM could alkylate lysines and arginines at the C-termini of the identified peptides, but alkylation at these sites is expected to prevent cleavage by trypsin. However, exceptions have been reported that demonstrate cleavage by trypsin at glycinylglycinyl-lysines due to the presence of a positive charge that affords recognition by trypsin.[93]

Despite the abundance of both enzymatic and nonenzymatic electrophilic modifications reported to occur on the histone tails, monoQMAcr and bisQMAcr were not observed to react with residues on the tails, but rather with residues that are in both surface and interior regions of the histone octamer core (Figure 3.7). This site preference likely results from association of acridine to these hydrophobic regions of the protein.

To determine the effect of nucleosome assembly on protein alkylation, the reconstituted NCP was first treated with monoQMAcr for 24 h, followed by digestion with trypsin. Only the adduct at TESSK on histone H2A was observed (Figure 3.8A and Table 3.1, entry I). Treatment of the NCP with bisQMAcr revealed a similar trend in the alkylation profile, no identifiable protein adducts were observed (Figure 3.8B). Specific sites of histone reaction are suppressed in the NCP relative to that with the unassembled histone proteins. Hence, both DNA and protein reaction with QMs are affected by nucleosome assembly.
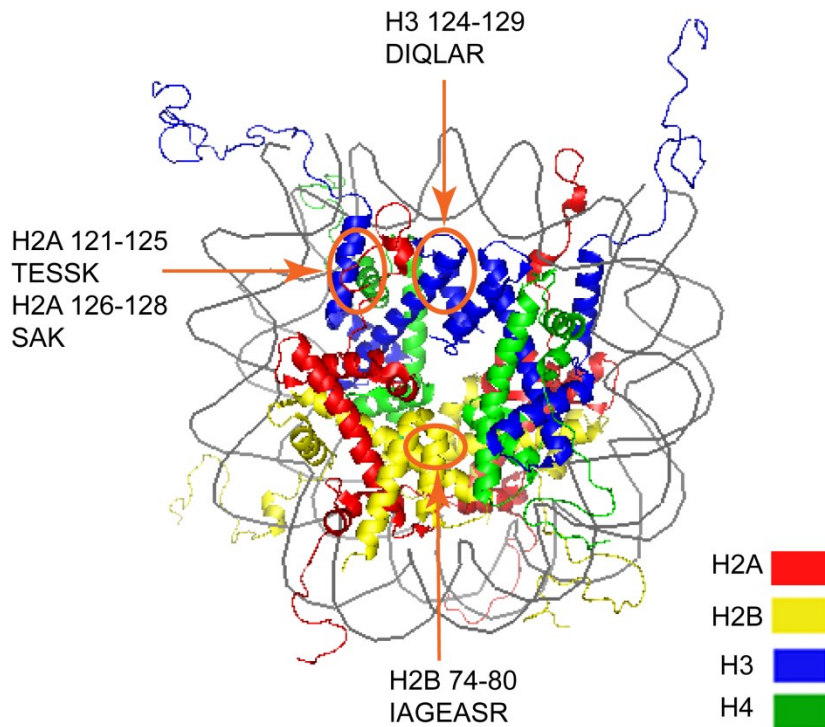
Figure 3.7 Location of protein adducts formed in the NCP (PDB: 1KX5) from alkylation by monoQMAcr and bisQMAcr.
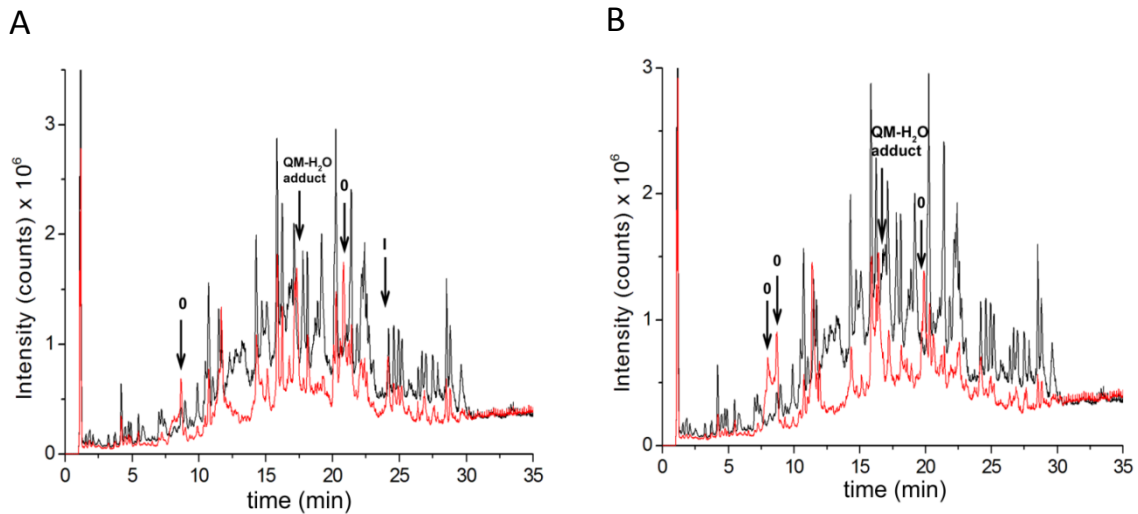
Figure 3.8 Peptide-QM adducts formed with the NCP after treatment with A) monoQMAcr or B) bisQMAcr. Total ion count was monitored during UPLC-MS separation and analysis of NCP treated alternatively with each QM under conditions equivalent to those used to modify the histone octamer. DNA was degraded prior to trypsin treatment by digestion with benzonase. Untreated samples are indicated in black and those treated with QM are indicated in red. Signals corresponding to peptide-QM adducts are labeled according to Table 1. Signals labeled with "0" are only evident after QM exposure, but their $[M+H]^+$ values do not correspond to a QM adduct or peptide fragment. All unlabeled signals represent tryptic peptides from the histones.

3.2.4 Nucleosome Assembly After Exposure to BisQMAcr.

Nucleosome assembly is a dynamic process that has the potential to expose both DNA and the histones to electrophilic modification. To determine whether bisQMAcr's DNA alkylation affects NCP assembly, the unpackaged DNA was first treated with bisQMAcr (250 µM) for 24 h. Excess bisQMAcr was removed via gel filtration chromatography before subjection to reconstitution with the histone octamer. The NCP was assembled in 25% yield, while 75% of the DNA remained in its unpackaged state, as determined by quantification of the radiolabeled DNA by phosphorimagery (Figure 3.9A). In contrast, reconstitution of the NCP using unmodified DNA occurs in greater than 95% yield (Appendix C, Figure C.1). Assembly of the NCP with DNA that has been incubated with bisQMPAcr in the absence of

fluoride results in similarly high yields of NCP formation (Figure 3.9B). Thus, bisQMAcr's

covalent modification of DNA, rather than acridine's intercalation, significantly impairs its

reconstitution to form the NCP.

BisQMAcr's ability to impair nucleosome assembly may stem from distortions of the

DNA helical structure after alkylation that prevent wrapping of the DNA around the histones.

Other bulky forms of DNA damage, such as pyrimidine photodimers caused by UV

irradiation, impair reconstitution of the NCP by unwinding the DNA double helix.[94] DNA

that is unwound may be more susceptible to modification by bisQMAcr. Alkylation of

unpackaged DNA by bisQMAcr will then hamper its ability to assemble into nucleosomes,

which may alter regulation and expression of the genome.
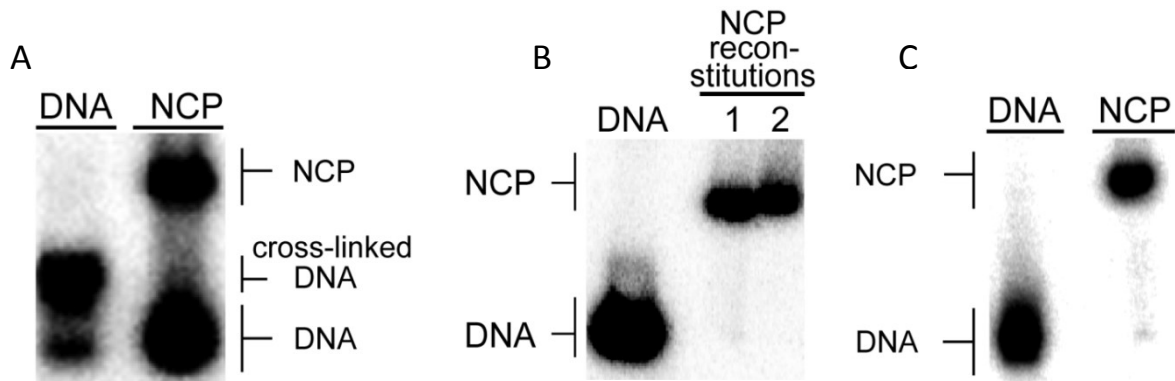
Figure 3.9 Reconstitution of the NCP after alternative treatment of the Widom 601 DNA with bisQMPAcr in the A) presence or B) absence of sodium fluoride, and the C) histone octamer with bisQMAcr. Lanes labeled as DNA contain DNA prior to reconstitution and lanes labeled NCP contain the products generated after reconstitution with the histone octamer. The relative distribution of species separated by native PAGE (6%) was measured by phosphorimaging the [^{32}P]-labeled DNA.

To determine whether alkylation at specific DNA sites may reconstitute preferentially over others, the alkylated DNA used to reconstitute the NCP was separated by native PAGE. The samples were then treated with piperdine to detect sites of alkylation at dGN7. The data revealed a decreased yield of DNA alkylation in both of the samples that were incubated for over 8 h during reconstitution and gel separation relative to the sample that was immediately treated with piperidine (Figure 3.10). This difference in yield likely results from the reversibility of alkylation at dGN7, which permits transfer and quenching of the bisQMAcr

Figure 3.10 Profile of piperidine-induced fragmentation of DNA after NCP reconstitution. The NCP was reconstituted under standard conditions using DNA treated with bisQMAcr for 24 h. DNA free in solution and reconstituted in the NCP were separated by and extracted from native PAGE (6%). The treated DNA prior to reconstitution (lane 1), the free DNA after reconstitution (lane 2), and the reconstituted DNA after proteinase K treatment (lane 3) were treated with piperidine. The resulting fragments were separated by denaturing PAGE (10%) and visualized by phosphorimagery.

adduct with water during reconstitution. A lower yield of alkylation was observed for the sample that reconstituted than for the sample that remained unpackaged, which may indicate that a mixture of unmodified DNA and some of the alkylated DNA assembled, while the remaining alkylated DNA remained unassembled. In addition, no preferential tolerance for alkylation at specific sites along the NCP was apparent from the similarities in sites of alkylation between the two samples.

To compare the effect of DNA alkylation on NCP assembly with that of histone alkylation, the histone octamer was incubated with bisQMAcr (500 µM) for 24 h before removal of excess QM and reconstitution with unmodified Widom 601 duplex DNA. Reconstitution was not impeded, as the NCP was assembled in a comparable yield to that of assembly of unmodified DNA and histone octamer (Figure 3.9C). Hence, only DNA, but not protein, alkylation by bisQMAcr affects the assembly of the NCP.

3.2.5 Transfer of QM Alkylation from DNA to Histone Octamer.

BisQMAcr's reversible alkylation of dGN7 permits the QM to transfer to alkylate water or other nucleobases within DNA.[42, 43] The nucleophiles within the histones have the potential to capture the QM once released from its initial adduct with dGN7. To determine if QMs can transfer their alkylation between DNA and the histones, unpackaged Widom 601 duplex DNA was treated with monoQMAcr (500 µM) for 24 h, followed by incubation with the histone octamer for an additional 24 h. The histones were then digested with trypsin and analyzed by UPLC-MS (Scheme 2). The monoQMAcr adducts of TESSK and IAGEASR (Table 3.1, entries I, III), but not RR (Table 1, entry II) were detected (Figure 3.11A). The experiment was then performed with bisQMAcr, which revealed a similar trend to that of
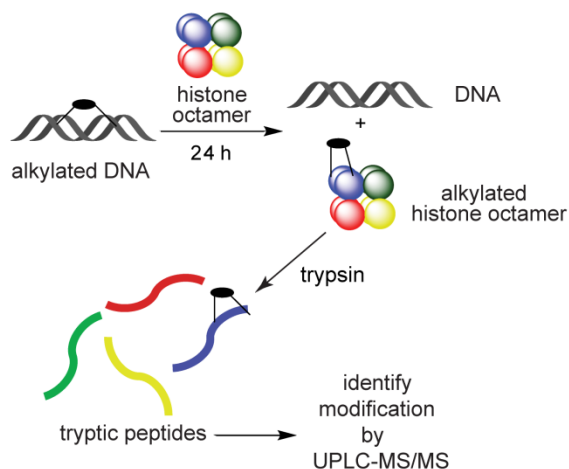
Scheme 3.2. QM transfer from DNA to the histone octamer.

monoQMAcr. BisQMAcr transferred to alkylate SAK (Table 3.1, entry IV), but not

DIQLAR (Figure 3.11B and Table 3.1, entry V). In addition, water competed with the

histones to quench both QMs upon their release from the DNA, as evidenced by detection of

the QM-H_2O adduct.

The transfer of QM adducts from DNA to the histones may suggest a sacrificial role

for the histone proteins as terminal acceptors of the QM's alkylation to essentially repair the

DNA adducts. Our results indicated that bisQMAcr's modification of the histone octamer did

not impair its ability to form NCPs. Thus, the modified histones would likely support NCP

assembly, with little impact on downstream DNA processing and gene expression.
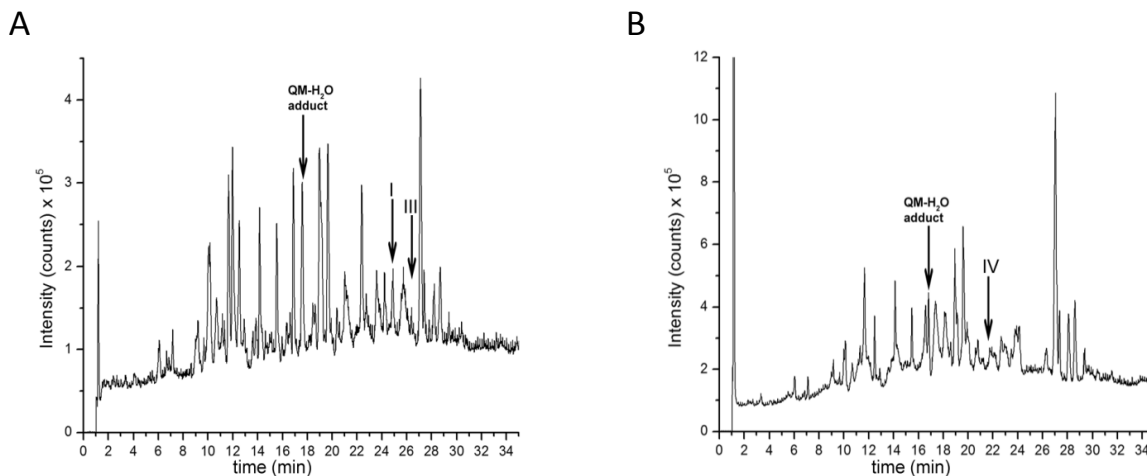
Figure 3.11 Transfer of A) monoQMAcr and B) bisQMAcr from DNA to the histone octamer. Widom 601 duplex DNA (0.030 µM) and salmon sperm DNA (2.47 µM) were treated alternatively with each QM (500 µM) for 24 h at room temperature. Excess QM and its low molecular weight products were removed from the DNA by using a Bio-Rad P6 spin column. The isolated DNA was then added to the histone octamer (2.5 µM) and incubated for 24 h at 4 °C. Samples were subsequently digested with benzonase and trypsin and analyzed by UPLC-MS. Signals corresponding to peptide-QM adducts are labeled according to Table 3.1.

3.3 Summary

We have characterized the response of bisQMAcr to DNA packaging and the presence of the histone proteins by investigating its reactivity with the NCP. The NCP provides a protective function against DNA modification by bisQMAcr since bisQMAcr's alkylation was significantly suppressed with the NCP compared with DNA free in solution. DNA packaging, rather than competing nucleophiles provided by the histones, resulted in bisQMAcr's suppressed DNA alkylation. The NCP also fosters protection against QM-induced DNA damage by using the histones as sacrificial terminal acceptors of QM intermediates that are released from the DNA. This phenomenon essentially functions to repair the QM-DNA adducts. Our data suggests that the subsequent modification of the histone octamer by the QMs will likely not affect its ability to assemble into NCPs. On the

other hand, bisQMAcr's alkylation of unpackaged duplex DNA significantly impeded nucleosome assembly, as only 25% of the alkylated DNA reconstituted with the histone octamer to form NCPs. BisQMAcr's preferential alkylation of unpackaged DNA may impair its assembly into nucleosomes *in vivo*. The NCP was also shown to foster toxicity by reacting with bisQMAcr to form DNA-histone crosslinks. DNA-histone crosslinks may interfere with cellular functions, and result in QM-induced toxicity to cells. This is the first report of bisQMAcr's reactivity with proteins, as the compound was developed as a DNA crosslinking agent. Our data suggests that the acridine ligand, originally designed to increase bisQMAcr's affinity for DNA, may also direct its reaction with proteins by binding to hydrophobic surfaces. Overall, our characterization of bisQMAcr's reactivity with the nucleosome core particle suggests that the greatest impact of QMs on chromatin will likely occur in the linker regions of DNA that are free from the protection afforded by the NCP.

3.4 Materials and Methods

3.4.1 Materials

Oligonucleotides were synthesized by Integrated DNA Technologies with standard desalting and were purified by 20% denaturing PAGE prior to use. BisQMPAcr was prepared as described previously.[40] MonoQMPAcr was provided by Dr. Blessing Deeyaa. The Widom 601 DNA was ligated from 30- 35 base pair oligonucleotides and the top strand was radiolabeled at its 5'- end with [^{32}P] as described previously.[81, 95] The core histone proteins (*Xenopus laevis*) were expressed in *Escherichia coli* and assembled *in vitro* into the native histone octamer under standard conditions by Dr. Kun Yang from Prof. Marc Greenberg's lab.[96] T4 polynucleotide kinase, T4 DNA ligase, and proteinase K were obtained

from New England Biolabs. Benzonase and trypsin (powder, Bovine pancreas) were purchased from Sigma. γ- ^{32}P-ATP was purchased from Perkin Elmer. C_{18}-Sep Pak cartridges were purchased from Waters Corp. Salmon sperm DNA (10 mg/mL) was purchased from Invitrogen. Amicon Ultra centrifugal filters with a 10,000 molecular weight cutoff were purchased from Millipore.

3.4.2 Methods

General Procedures. All reactions and digestions were conducted in siliconized tubes that were purchased from Bio Plas Incorporated. Radiolabeled oligonucleotides were detected and quantified using a Typhoon 9400 phosphorimager and ImageQuant TL software. Oligonucleotide concentrations were calculated from their absorption at 260 nm and extinction coefficients that were provided by the manufacturer. Histone concentrations were determined directly by their absorbance at 276 nm.[96]

Ligation of the 601 Sequence DNA for Reconstitution of the Nucleosome Core Particle.[95] Oligonucleotides (1.5 nmol each) (Appendix C, Figure C.2) were enzymatically phosphorylated at their 5'- termini, each in separate 50 µL reactions containing 1x T4 DNA ligase buffer (50 mM Tris-HCl pH 7.5, 10 mM MgCl$_2$, 10 mM DTT, 1 mM ATP) and 5 µL of T4 polynucleotide kinase (50 U) at 37° C for 1 h. The solution was then heated at 65°C for 20 min to inactivate the enzyme. The phosphorylated oligonucleotides were mixed with the unphosphorylated 5'- end oligonucleotides (1.5 nmol) and 2 nmol of the corresponding scaffold strands. Hybridization was carried out by heating the resulting mixture at 95° C for 2 min followed by slow cooling to room temperature. 3 µL of T4 DNA ligase (1200 U) and 5

µL of 10x T4 DNA ligase buffer were added to the solution containing the hybridized strands (200 µL total volume). The ligation was incubated at 16°C overnight. The DNA in the ligation reaction was extracted with phenol (equal volume) and precipitated from 0.3 M NaOAc pH 5.2. The ligated products were purified by 8% denaturing PAGE and the desired bands were excised from the gel. The DNA was eluted from the gel in 1 mL of elution buffer (0.2 M NaCl and 1 mM EDTA) overnight. The slurry was filtered, concentrated to approximately 75 µL, and washed two times with 400 µL of water. The concentration of the ligated products was determined by their absorption at 260 nm.

5'- [^{32}P] Radiolabeling and Hydridization of the Widom 601 Duplex DNA. The Widom 601 DNA top strand was 5′- ^{32}P-labeled in a 50 µL reaction mixture containing 20 pmol of Widom 601 DNA "top" strand, 1 x T4 polynucleotide kinase buffer (70 mM Tris-HCl pH 7.6, 10 mM MgCl2, 5 mM DTT), 40 µCi of γ- [^{32}P]-ATP, and 50 U of T4 Polynucleotide Kinase (5 µL) at 37 °C for 4 h. Unincorporated γ-[^{32}P]- ATP was removed by passing the reaction mixture through a Bio-Rad P6 spin column prewashed with water (1000 g, 4 min). To the mixture was added the complementary strand of Widom 601 DNA (30 pmol), NaCl (0.1 M), and potassium phosphate buffer (10 mM, pH 7.2) to yield a total volume of 80 µL. This mixture was heated at 95 °C for 2 minutes and slowly cooled to room temperature (2- 3 h).

Reconstitution of the Nucleosome Core Particle.[95] The preassembled histone octamer (84 pmol) in 2 M NaCl (1 µL) was added to a solution of salmon sperm DNA (84 pmol) and 5'-[^{32}P]-radiolabeled Widom 601 duplex DNA (~1 pmol) in 2 M NaCl, 10 mM HEPES pH 7.8, and 1 mM EDTA (10 µL) with 1 mg/mL BSA. The mixture was then incubated for 1 h at

room temperature before serial dilution with nucleosome reconstitution buffer (10 mM

HEPES pH 7.5, 1 mM EDTA, and 1 mg/mL BSA) as indicated below and incubated for the

designated time. Dilutions were as follows (dilution number: volume of buffer added in μL,

incubation time in min): 1:12, 60; 2:6, 60; 3:6, 60; 4:10, 30; 5:10, 30; 6:20, 30; 7:50, 30;

8:100, 30. After the final dilution (224 μL total volume), a small aliquot (5 μL) was removed

and analyzed by native gel electrophoresis (6% acrylamide/bis(acrylamide), 59:1, 0.6 x TBE)

to determine the reconstitution efficiency. The final solution was stored at 4 ºC until use.

Treatment with BisQMAcr. 5'-[^{32}P]-radiolabeled Widom 601 duplex DNA (0.08 pmol) in

the alternative presence and absence of the histone octamer (5.6 pmol) was added to a

solution of salmon sperm DNA (5.6 pmol) in 10 mM MES, 10 mM NaF, 7.5 mM HEPES,

0.75 mM EDTA, 0.75 mg/mL BSA and 67 mM NaCl at pH 7.0. An equivalent concentration

of reconstituted NCP was supplemented with 10 mM MES pH 7.0 and 10 mM NaF to

maintain similar solvent conditions. BisQMPAcr, in acetonitrile, was added to the three

individual samples above to generate a constant 20% solution. Samples (20 μL) were

incubated at 4 ºC for 24 h. Samples were treated with proteinase K (1.6 U) for 15 min at

room temperature just prior to quenching by freezing in liquid nitrogen.

Piperidine Treatment of Alkylated DNA. Frozen samples treated with bisQMP above were

lyophilized and dissolved in 5% piperidine (10 μL). The solutions were heated at 90 ºC for

30 min and then lyophilized. To remove residual piperidine, samples were dissolved in water

(30 μL) and lyophilized in three consecutive repetitions. Samples were dissolved in water

(10 μL) and formamide containing bromophenol blue and xylene cyanol (10 μL). Samples

were analyzed by 10% denaturing PAGE using 42 x 20 x 1 cm gel plates that were run at 65

W until the bromophenol blue dye migrated three-quarters of the gel length.

Protein Adducts Detected by Liquid Chromatography-Mass Spectrometry. Equal

concentrations of the histone octamer and reconstituted NCP in 10 mM HEPES, 1 mM

EDTA, 1 mg/mL BSA, and 89 mM NaCl were individually combined with of 10 mM MES

pH 7.0 and 10 mM NaF. The mixtures were treated alternatively with monoQMPAcr or

bisQMPAcr (500 µM) in acetonitrile to a final volume of 20 µL with 20% acetonitrile, and

incubated at 4 ºC for 24 h. Samples containing the NCP were subsequently treated with

benzonase (250 U) for 30 min at 37 ºC. All samples were then lyophilized, resuspended in

3.6 M guanidine-HCl, 50 mM Tris-HCl pH 7.2, and 2 mM DTT to a final volume of 20 µL,

and heated at 65 °C for 45 min to denature the protein. Samples were subsequently diluted

with 1 mM $CaCl_2$ and 50 mM Tris-HCl pH 7.2 to a final volume of 75 µL. Trypsin (in 111

mM potassium phosphate buffer pH 7.4) was added to generate a final trypsin to histone ratio

of 1:20 and incubated at 37 °C for 24 h. The resulting peptides were desalted using a C_{18}-

Sep Pak and eluted with 50% aqueous CH_3CN and 0.1% formic acid and analyzed by UPLC-

MS on an Acquity UPLC H-Class/Xevo G2 QTof from Waters equipped with a 2.1 mm x

100 mm HSST3-C18 column (1.7 µm pore size). Sample separation was accomplished with

an initial 5% aqueous CH_3CN solution with 0.1% formic acid for 1 min, followed by a linear

gradient to 40% aqueous CH_3CN over 36 min, and then to 95% aqueous CH_3CN for 3 min

with a flow rate of 0.3 mL/min. Mass spectra were acquired in the ESI positive ion mode

with MS^E using a capillary voltage of 3 kV, a sample cone voltage of 30 V, and an extraction

cone voltage of 4 V. The cone gas flow was set up to 30 L/h and desolvation gas flow was

800 L/h. Desolvation temperature and source temperature were set to 400 °C and 150 °C, respectively. The scan acquisition rate was 10 Hz over a range of m/z 100-3000. MassLynx and BioPharmaLynx software were used to analyze the resulting data.

Reconstitution of the Nucleosome Core Particle with Alkylated DNA. 5'-[^{32}P]-radiolabeled Widom 601 duplex DNA (1 pmol) and salmon sperm DNA (84 pmol) were incubated with bisQMPAcr (250 µM) in 10 mM MES pH 7.0 and 10 mM NaF for 24 h at room temperature. Excess bisQMPAcr and its low molecular weight products were removed by passing the reaction mixture through a Bio-Rad P6 spin column prewashed with water (1000 g, 4 min). The eluant was lyophilized, resuspended in 5 µL of H$_2$O, and used for nucleosome reconstitution as described above for the parent unmodified DNA.

Reconstitution of the Nucleosome Core Particle with Alkylated Histone Octamer. BisQMPAcr (250 µM) was incubated with the histone octamer (84 pmol) in 2 M NaCl, 10 mM MES pH 7.0, and 10 mM NaF for 24 h at 4 °C. The reconstitution was then performed as described above for the alkylated DNA.

Distribution of Alkylated DNA after NCP Reconstitution. Solutions of NCP reconstituted with alkylated DNA described above were concentrated to 30 µL at 4 °C using a 0.5 mL Amicon Ultra centrifigal filter with a molecular weight cutoff of 10,000 Da. DNA associated with reconstituted NCP and the remaining free DNA were separated by native PAGE (6%, acrylamide/(bis)acrylamide, 59:1, 0.6 × TBE buffer) using a running buffer of 0.2 x TBE and 200 V (1 h, 4 ºC). The DNA species were detected by phosphorimagery and extracted from

the gels by excision, maceration, and finally immersion in 2 mL of elution buffer (0.2 M NaCl, 1 mM EDTA) overnight at 4°C. Solid material was removed by passage through a Bio-Rad Poly-Prep column and the eluant was lyophilized. The isolated DNA was treated with proteinase K (1.6 U) for 15 min at room temperature, heated with piperidine for cleavage at sites of guanine N7 alkylation, and analyzed as described above.

Transfer of MonoQMAcr and BisQMAcr from DNA to the Histones. MonoQMPAcr and bisQMPAcr (500 µM) were alternatively incubated for 24 h at room temperature with duplex 601 DNA (0.03 µM) and salmon sperm DNA (2.47 µM) in 10 mM MES pH 7.0 and 10 mM NaF. Excess QM and its low molecular weight products were removed from the DNA by passage through a Bio-Rad P6 spin column prewashed with water (1000 g, 4 min). Histone octamer (2.5 µM) in 10 mM HEPES pH 7.8, 1 mM EDTA, 1 mg/mL BSA, and 89 mM NaCl was added to the resulting DNA and incubated at 4 ºC for 24 h. Samples were then digested with benzonase and trypsin and analyzed as described above to identify peptide adducts by UPLC-MS.

Chapter 4: Effect of QM-DNA Crosslinks on Primer Extension by DNA Polymerases

4.1 Introduction

DNA ICLs are commonly considered absolute blocks to DNA replication. ICLs prevent the necessary separation of DNA's strands by helicases and polymerases during DNA replication. Thus, ICLs inhibit DNA replication by preventing the action of the enzymes that move along DNA to transmit its genetic information. Further, ICLs also block the activity of RNA polymerases, which impairs gene expression. However, reversible DNA ICLs may not be resistant to the action of the enzymes involved in replication, since these enzymes generate mechanical force while moving along DNA. Determining whether bisQMAcr's DNA crosslinks block the action of DNA replication enzymes will address the potential toxicity of a reversible ICL on cells by elucidating the effect of the ICL on DNA replication.

DNA polymerases process DNA during both replication and repair to ensure the integrity of the genome. Polymerases must balance fidelity with processivity to synthesize DNA both quickly and with the correct sequence.[97, 98] Several DNA polymerases across different forms of life, such as DNA polymerase I from *E.coli*, φ29 DNA polymerase from bacteriophage φ29, and DNA polymerase ε from eukaryotes, possess exonuclease activity in addition to DNA synthesis activity.[99] Exonuclease activity functions as a proofreading mechanism by allowing the polymerases to excise misincorporated bases before synthesizing the correct DNA sequence using their polymerase activity (Figure 4.1). Proofreading
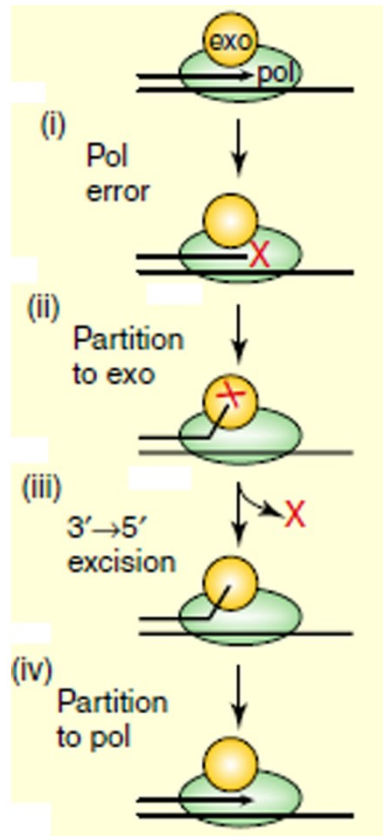
Figure 4.1 Partitioning between DNA polymerase and exonuclease activities. When DNA polymerases incorporate an incorrect nucleotide (red X), the polymerase changes conformation to allow its exonuclease active site to remove the incorrect base, before DNA synthesis continues using the polymerase active site. The image was copied from Albertson *et al.*[98]

improves fidelity by correcting mistakes that may arise due to the quick speed of replication required to permit sufficient processivity. Misincorporation rates for replicative polymerases are as low as 10^{-9}-10^{-12} errors/base pair replicated, which is a testament to the delicate balance of processivity and quality of replication that is achieved by polymerases.[100] The mechanism of DNA and dNTP binding to DNA polymerases is tightly coordinated to ensure faithful replication in a quick manner. The enzyme first binds a single-stranded DNA primer before then binding the incoming dNTP.[1] Fidelity of dNTP binding is ensured by shape complementarity and hydrogen-bonding interactions of the dNTP with the polymerase-DNA primer/template complex.[101, 102] Furthermore, amino acid residues in the active site serve as a

steric gate to exclude incorrect dNTPs from binding. The Klenow polymerase, a fragment of DNA polymerase I that lacks 5'-3' exonuclease activity, but still possesses polymerase and 3'-5' exonuclease activities, contains a glutamate in its active site that precludes incorrect dNTPs from binding.[103] The steric gate not only precludes mismatched dNTPs, but may prevent synthesis of DNA containing bases with bulky lesions. The phosphoric acid anhydride bonds of the incoming dNTP must then be hydrolyzed to incorporate the dNMP, with the energy produced from release of the pyrophosphate aiding the polymerase's movement along DNA to the next nucleotide.

DNA polymerases will encounter DNA lesions if damage is not repaired prior to replication.[104] The DNA will either be replicated successfully, mutated, or not replicated, depending on the interactions of the lesion with the polymerase. In addition, different polymerases process DNA lesions differently.[105-107] For example, DNA adducts formed by the enediyne neocarzinostatin block full primer extension by the Klenow, T4, and herpes simplex virus DNA polymerases.[108] However, each polymerase processes the lesion uniquely, as Klenow polymerase stops synthesis one base before the adduct, while the Klenow Exo⁻ polymerase synthesizes an additional nucleotide at the site of the adduct. Other lesions, such as deaminated nucleobases or abasic sites, do not always impair DNA polymerases and may facilitate incorporation of a new nucleotide. However, the fidelity of incorporation often suffers. For instance, the translesion synthesis polymerase, DNA Polymerase η, bypasses O^2-alkylthymidine lesions, but misincorporates deoxycytidine upon encountering the lesions.[109]

Despite the diversity of DNA lesions whose effects on DNA synthesis by polymerases have been investigated, few investigations concerning reversible DNA lesions

have been conducted. However, reversible acrolein adducts on guanine and adenosine prevent DNA synthesis beyond the adducts by the replicative eukaryotic polymerase Pol δ and Pol ε, but do not inhibit adduct bypass by the translesion synthesis (TLS) polymerases Rev1, Pol κ, and Pol γ.[110] Acrolein's DNA adducts do not cause mutagenicity in mouse and human cells as a result of their bypass by TLS polymerases.[111] BisQMAcr's reversible chemistry may also permit bypass of its lesions by DNA polymerases, especially if the QM regenerates from its DNA adducts upon encountering the polymerase. Previous studies demonstrated that an N-methylquinolium QM's DNA lesions caused extensive stops in primer extension by the T7 DNA polymerase.[112] However, the QM's adducts were irreversible adducts with dGN2.[113] Reversible QM-DNA adducts may affect the polymerase differently than irreversible QM-dGN2 adducts. Reversible adducts may not only permit polymerase bypass, but they may also be subject to polymerase-mediated migration along DNA. A polymerase may stall at the lesion until the QM regenerates. If so, the polymerase may continue its activity along the DNA sequence and cause the QM to alkylate the DNA further downstream. Otherwise, the polymerase may promote hydrolysis of the QM to break its DNA adducts.

The Klenow fragment of DNA polymerase I has seen widespread use in primer extension synthesis of damaged and undamaged DNA templates due to its high fidelity and processivity, as well as its ease of handling.[113-116] In addition, mutations to its exonuclease active site generate a mutant lacking all exonuclease activities, but retaining polymerase activity (Klenow Exo⁻).[117, 118] Thus, the Klenow Exo⁻ polymerase may be an ideal candidate enzyme to facilitate bisQMAcr's migration along DNA, since it cannot excise QM-DNA adducts through its proofreading mechanism.

The φ29 DNA polymerase may also facilitate bisQMAcr's migration since it functions as a pseudo polymerase-helicase. The φ29 polymerase possesses strand displacement activity in addition to polymerase and exonuclease activities.[115] Helicase activity may facilitate dissociation of DNA ICLs more easily than with a polymerase that lacks this capability. However, a reversible DNA ICL formed between an abasic site (AP) and the N6 position of adenine (dAN6) remained stable in the presence of the φ29 polymerase and blocked primer extension beyond the lesion. The AP-dAN6 ICL is nominally reversible, as its half-life is 84 h within duplex DNA.[119] Thus, the reversibility of this ICL may be too slow to permit its modulation by the φ29 polymerase. BisQMAcr's adducts with GN7 regenerate with a half-life of 2 h with dG nucleosides, and may regenerate even more quickly within duplex DNA.[37] BisQMAcr's DNA ICLs may be reversible on a time scale that is similar to that of φ29 polymerase's action along DNA, since bisQMAcr transfers it adducts between complementary DNA strands in as few as 4 h.[41]

BisQMAcr's greatest impact on a biological system will likely occur on DNA that is free from the histones, since nucleosome assembly significantly suppressed its DNA alkylation.[120] DNA replication presents a scenario during which cellular DNA is free from the protective function of nucleosomes and may be a more efficient target for bisQMAcr's alkylation. How DNA polymerases respond to reversible bisQM DNA ICLs and the effect of the polymerase's action on the ICLs, as described below, begins to address the potential effects of QMs on DNA replication.

4.2 Results and Discussion

4.2.1 Primer Extension by the Klenow Exo⁻ and φ29 DNA Polymerases in the Presence of a BisQMAcr DNA Crosslink

To determine whether a DNA polymerase will modulate migration of bisQMAcr's crosslink along DNA, the integrity of bisQMAcr's DNA ICL was assessed following primer extension by the Klenow Exo⁻ polymerase to determine whether the ICL was broken apart due to hydrolysis of the QM. BisQMAcr's crosslink was formed through transfer of its intra-strand crosslink to an inter-strand crosslink in order to localize the adducts to the 5'-end of the template strand (Scheme 2.1A) .[41] This localization of the crosslink provides a stretch of nucleotides between the adduct and the 3'-end of the primer for the polymerase to begin DNA synthesis. Furthermore, intra- to inter-strand transfer ensures a high yield of DNA crosslinks rather than monoadducts, since bisQMAcr was reported to form 4 monoadducts for every one crosslink of duplex DNA.[40] BisQMAcr's adducts were initially trapped by reacting with the G-rich sequence OD11 for 24 h. Excess QM was removed via a gel filtration spin column before addition of the complementary sequence [^{32}P]-OD12 for an additional 24 h. A ternary complex was formed by addition of the primer OD10, followed by initiation of primer extension via addition of dNTPs and the polymerase (Figure 4.2A). The crosslink did not dissociate and remained intact over 8 h of incubation with the polymerase (Figure 4.2B). The Klenow Exo⁻ polymerase has also been reported to fail to extend primers beyond oxidized abasic sites and dG-C8-(acetylamino)fluorene lesions.[116, 121]The precedent for aborted primer extension suggests that the polymerase may also abort synthesis in the presence of bisQMAcr ICLs, which likely distort the DNA more than dG-C8-(acetylamino)fluorine monoadducts.
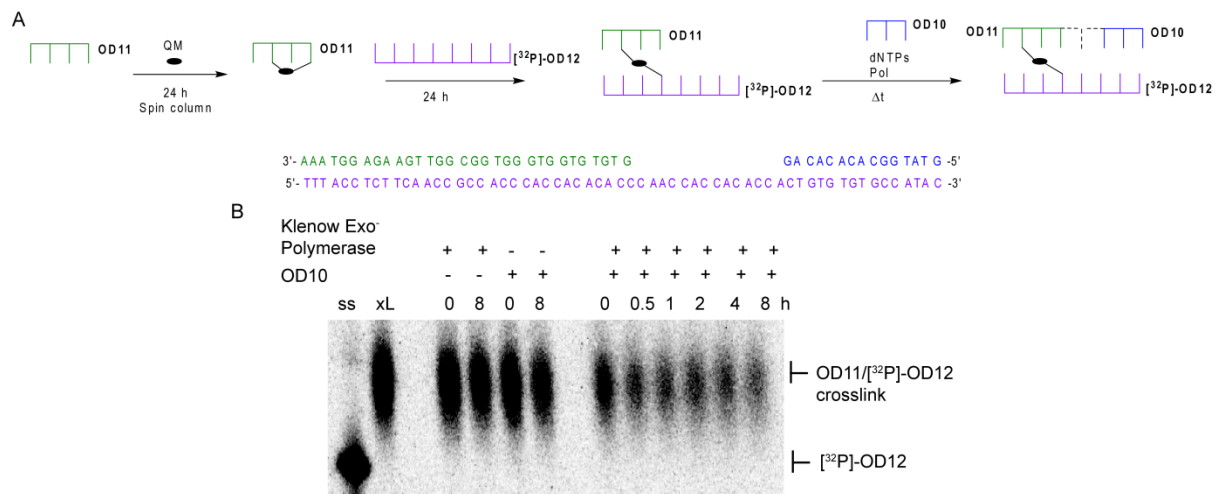
Figure 4.2 Persistence of bisQMAcr's DNA crosslink during primer extension by the Klenow Exo⁻ DNA polymerase. A) Scheme depicting the experimental setup. B) Crosslinked OD11/[^{32}P]-OD12 was prepared by first treating OD11 (3 µM) with monoQMPAcr or bisQMPAcr (500 µM) for 24 h in MES (10 mM, pH 7) and NaF (10 mM), followed by removal of excess QM with a P6 spin column. OD12 (3 µM) was then added for an additional 24 h. The crosslinked OD11/[^{32}P]-OD12 (200 nM) was added to a mixture of OD10 (240 nM) and dNTPs (100 µM) in Klenow polymerase reaction buffer. The primer/template complexes were incubated with the DNA polymerase (60 nM) for 0-8 h. Products were separated by denaturing PAGE (10%) and detected by phosphorimagery.

The ability of the polymerase to extend a primer in the presence of bisQMAcr's DNA crosslink was determined to further characterize Klenow Exo⁻'s response to crosslinks. BisQMAcr crosslinked OD11/OD12 was prepared as described above, followed by initiation of primer extension via addition of [^{32}P]-OD10, dNTPs, and the polymerase (Figure 4.3A). Additionally, monoQMAcr DNA adducts were prepared analogously to those for bisQMAcr in order to compare the effect of monoQMAcr adducts with bisQMAcr ICLs on primer extension (Schemes 2.2 and 3.1). Both monoQMAcr and bisQMAcr adducts stalled Klenow Exo⁻ at several sites up to the crosslink, while also inhibiting the polymerase's ability to extend the primer relative to the reaction with no QM present (Figure 4.3B). Major products were evident at sites 2, 5, 13, and 14 nucleotides away from OD11 on its 5'-end.
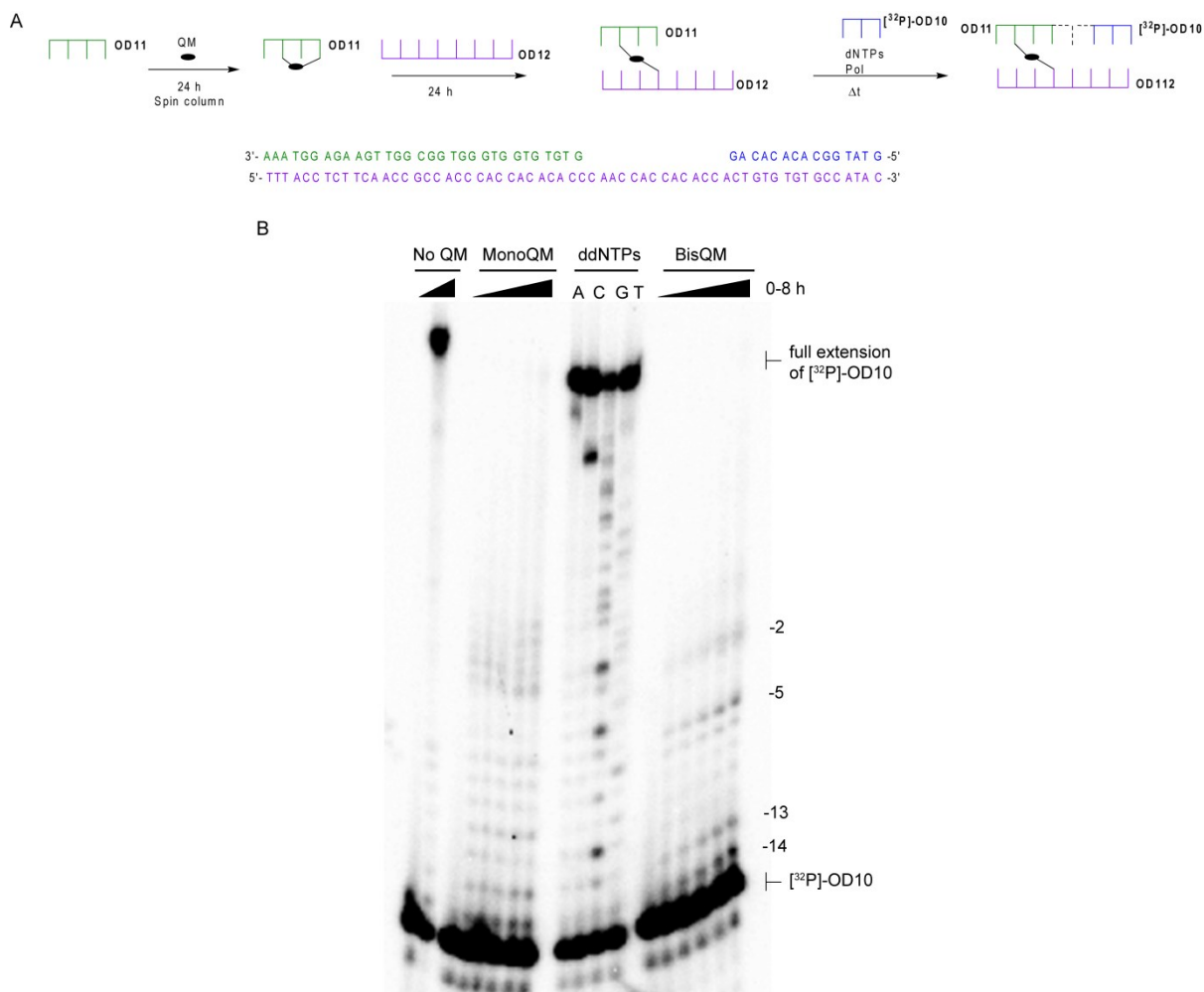
Figure 4.3 Primer extension by Klenow Exo⁻ DNA polymerase in the presence of a bisQMAcr DNA crosslink. A) Scheme depicting the experimental setup. B) OD12 (3 µM) was then added for an additional 24 h. Alkylated OD11/OD12 was prepared by first treating OD11(3 µM) with monoQMPAcr or bisQMPAcr (500 µM) for 24 h in MES (10 mM, pH 7) and NaF (10 mM), followed by removal of excess QM with a P6 spin column. OD12 (3 µM) was then added for an additional 24 h. Alkylated OD11/OD12 (200 nM) was added to a mixture of OD10 (240 nM), [³²P]-OD10 (5 nM) and dNTPs (100 µM) in Klenow polymerase reaction buffer. The primer/template complexes were incubated with the DNA polymerase (60 nM) for 0-8 h. Products were separated by denaturing PAGE (20%) and detected by phosphorimagery.

Klenow Exo⁻ aborts synthesis prior to reaching OD11 and the bisQMAcr crosslinks. Klenow Exo⁻ also failed to extend a primer at positions distant from dG-C8-(acetylamino)fluorene lesions, indicating that DNA damage at positions distant from the site of dNTP incorporation affects Klenow Exo⁻'s function.[121] Klenow's products of primer extension in the presence of

a bisQMAcr ICL are aborted synthesis products and unextended primer. Thus, Klenow Exo⁻

fails to dissociate bisQMAcr's crosslinks because it aborts primer extension before reaching

the site of the crosslinks.

The φ29 DNA polymerase was then utilized to determine whether its additional

strand displacement activity may result in dissociation or migration of bisQMAcr's crosslink.

As was the case for the Klenow Exo⁻ polymerase, the φ29 polymerase did not break apart

bisQMAcr's DNA ICLs (Figure 4.4). Furthermore, primer extension produced fewer

products than those for Klenow Exo⁻, as φ29 produced only one minor aborted product

before the site of OD11 (Figure 4.5). Additionally, φ29's exonuclease activity predominated,
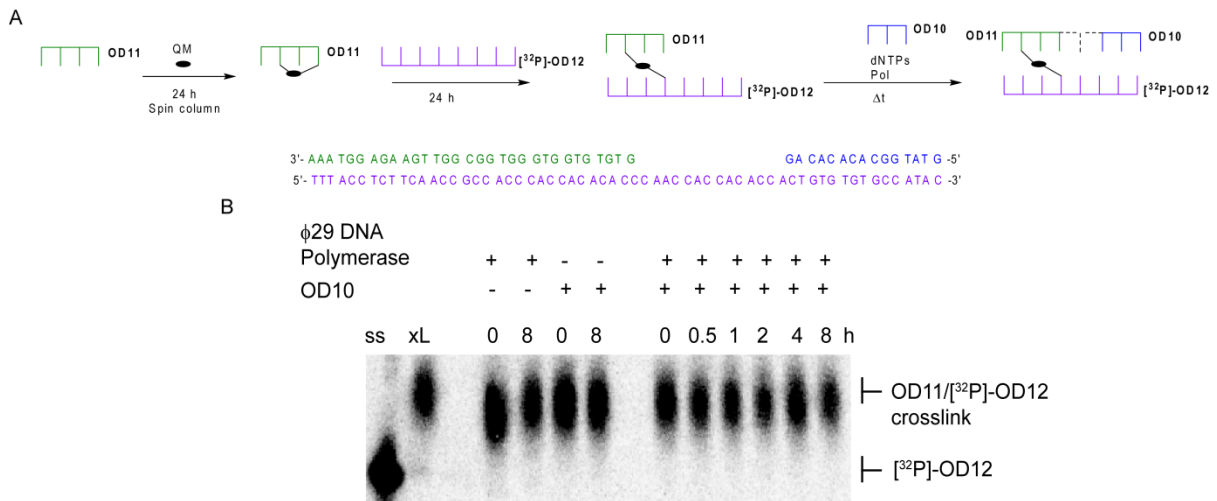
Figure 4.4 Persistence of bisQMAcr's DNA crosslink during primer extension by the φ29 DNA polymerase. A) Scheme depicting the experimental setup. B) Crosslinked OD11/[^{32}P]-OD12 was prepared by first treating OD11(3 μM) with monoQMPAcr or bisQMPAcr (500 μM) for 24 h in MES (10 mM, pH 7) and NaF (10 mM), followed by removal of excess QM with a P6 spin column. OD12 (3 μM) was then added for an additional 24 h. The crosslinked OD11/[^{32}P]-OD12 (200 nM) was added to a mixture of OD10 (240 nM) and dNTPs (100 μM) in φ29 polymerase reaction buffer. The primer/template complexes were incubated with the DNA polymerase (12 nM) for 0-8 h. Products were separated by denaturing PAGE (10%) and detected by phosphorimagery.

as the major products produced during synthesis were fragments of the primer. The presence of exonuclease degradation products indicates that φ29 does recognize and bind the primer template complex, despite its failure to extend the primer. Distant lesions may affect φ29's polymerase activity in a similar manner as they did for Klenow Exo⁻, while also triggering its exonuclease activity.

DNA polymerases may dissociate from the DNA once they stall at a lesion and aborts primer extension. This dissociation may allow a polymerase to find a primer/template complex that will provide productive and complete DNA synthesis. The polymerases' detachment from the DNA likely occurs within minutes, whereas bisQMAcr's reversible chemistry with DNA requires hours, since the half-life of QM-dGN7 adducts is approximately 2 hand the time frame required for bisQMAcr to traverse 10 base pairs is 7 days. As such, a polymerase will not have an opportunity to affect bisQMAcr's migration along DNA. Thus, bisQMAc's crosslink will likely be deleterious to cells due to its potential to block DNA replication by inhibiting the action of DNA polymerases if it is not repaired by DNA repair enzymes. Although the crosslink does prevent the polymerases from initiating synthesis and exonuclease degradation on the primer/template complex, it may distort the DNA in such a manner that prevents translocation of the polymerase along the DNA.
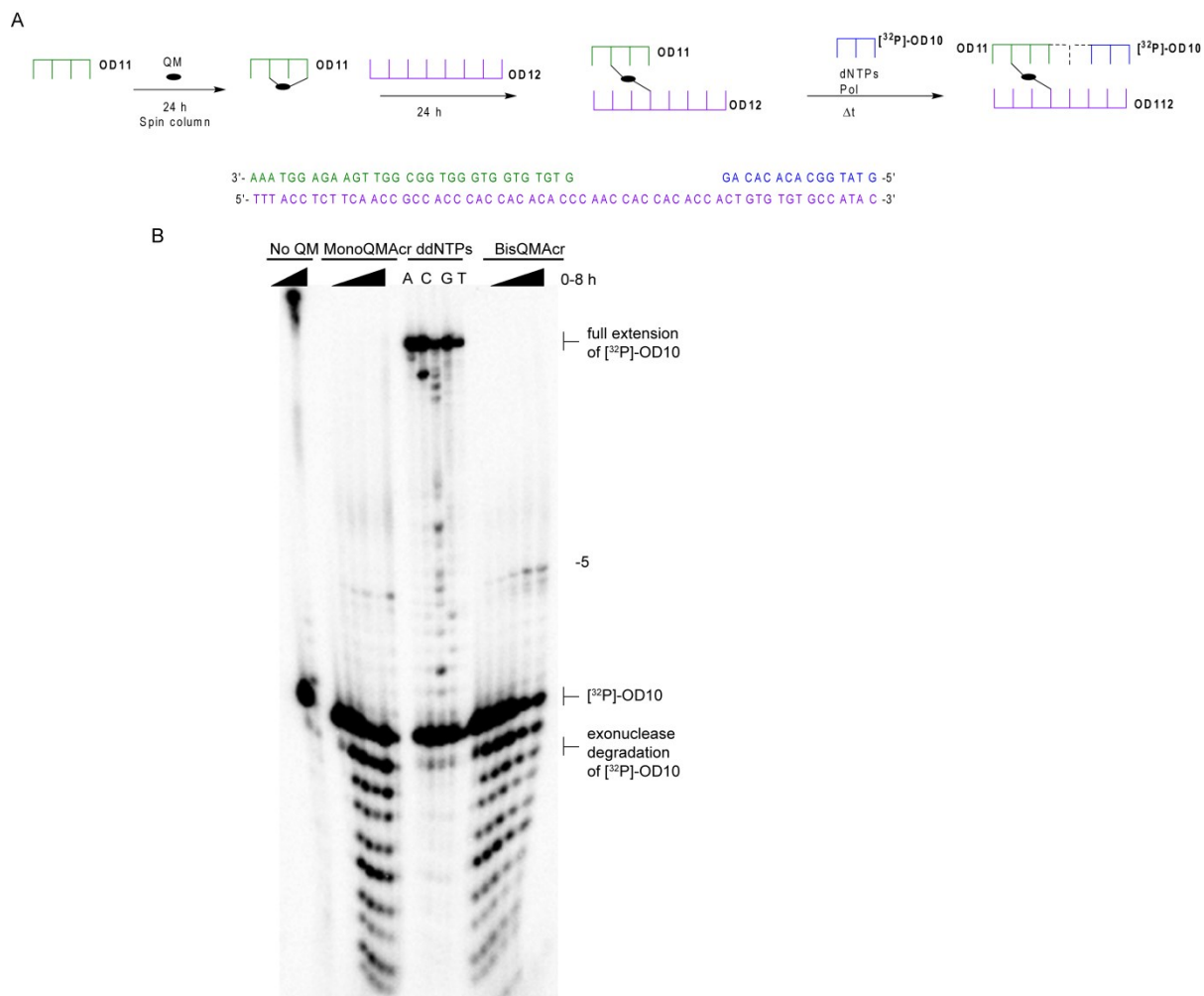
Figure 4.5 Primer extension by φ29 DNA polymerase in the presence of a bisQMAcr DNA crosslink. A) Scheme depicting the experimental setup. B) OD12 (3 µM) was then added for an additional 24 h. Alkylated OD11/OD12 was prepared by first treating OD11(3 µM) with monoQMPAcr or bisQMPAcr (500 µM) for 24 h in MES (10 mM, pH 7) and NaF (10 mM), followed by removal of excess QM with a P6 spin column. OD12 (3 µM) was then added for an additional 24 h. Alkylated OD11/OD12 (200 nM) was added to a mixture of OD10 (240 nM), [^{32}P]-OD10 (5 nM) and dNTPs (100 µM) in φ29 polymerase reaction buffer. The primer/template complexes were incubated with the DNA polymerase (12 nM) for 0-8 h. Products were separated by denaturing PAGE (20%) and detected by phosphorimagery.

4.2.2 Stalling of DNA Polymerases at QM-DNA Adducts

The abortion of primer extension and stalling of polymerases at QM-DNA lesions

may explain the inability of the polymerases induce separation of bisQMAcr's ICLs. The

template strand OD12 was treated alternatively with monoQMAcr and bisQMAcr to determine whether the polymerases stall at QM lesions and abort synthesis. The template strand OD12 was treated with a 1.3-fold stoichiometric excess of either monoQMAcr or bisQMAcr to produce a range of stalled products and prevent over-alkylation of the DNA by ensuring that each DNA duplex contains one bisQMAcr adduct at most. Over-alkylation may inhibit annealing of the primer or result in an inability of the polymerase to extend the primer. The primer-template complex was formed by addition of [^{32}P]-OD10, followed by initiation of the reaction with dNTPs and the indicated polymerase for up to 8 h (Figure 4.6A). Primer extension by both the Klenow Exo⁻ and φ29 polymerases was impaired relative to that of unmodified DNA (Figure 4.6B, C). Both polymerases stalled at a few sites, primarily within the first 8 nucleotides extended. A couple of stall sites at Cs farther downstream from the primer start site appear between 4 and 8 h of incubation with the Klenow Exo⁻, but not φ29 polymerase (Figure 4.6B). The φ29 polymerase stalls at fewer sites than Klenow Exo⁻, since its exonuclease activity is also activated while it processes the alkylated DNA. The exonuclease degradation of the primer increases in a time-dependent manner, and to a greater extent than extension of the primer (Figure 4.6C). The presence of aborted synthesis products suggests that the polymerases may stall on the alkylated template DNA.

The difficulty of both polymerases to extend the DNA primer may result from the homogeneity of the template strand. The template sequence is A-C rich, while the newly synthesized sequence will be G-T rich. Polymerases face difficulty replicating G-C-rich sequences, as well as those that contain several dinucleotide repeats.[122] Both polymerases may produce few aborted synthesis products with alkylated template DNA due to the
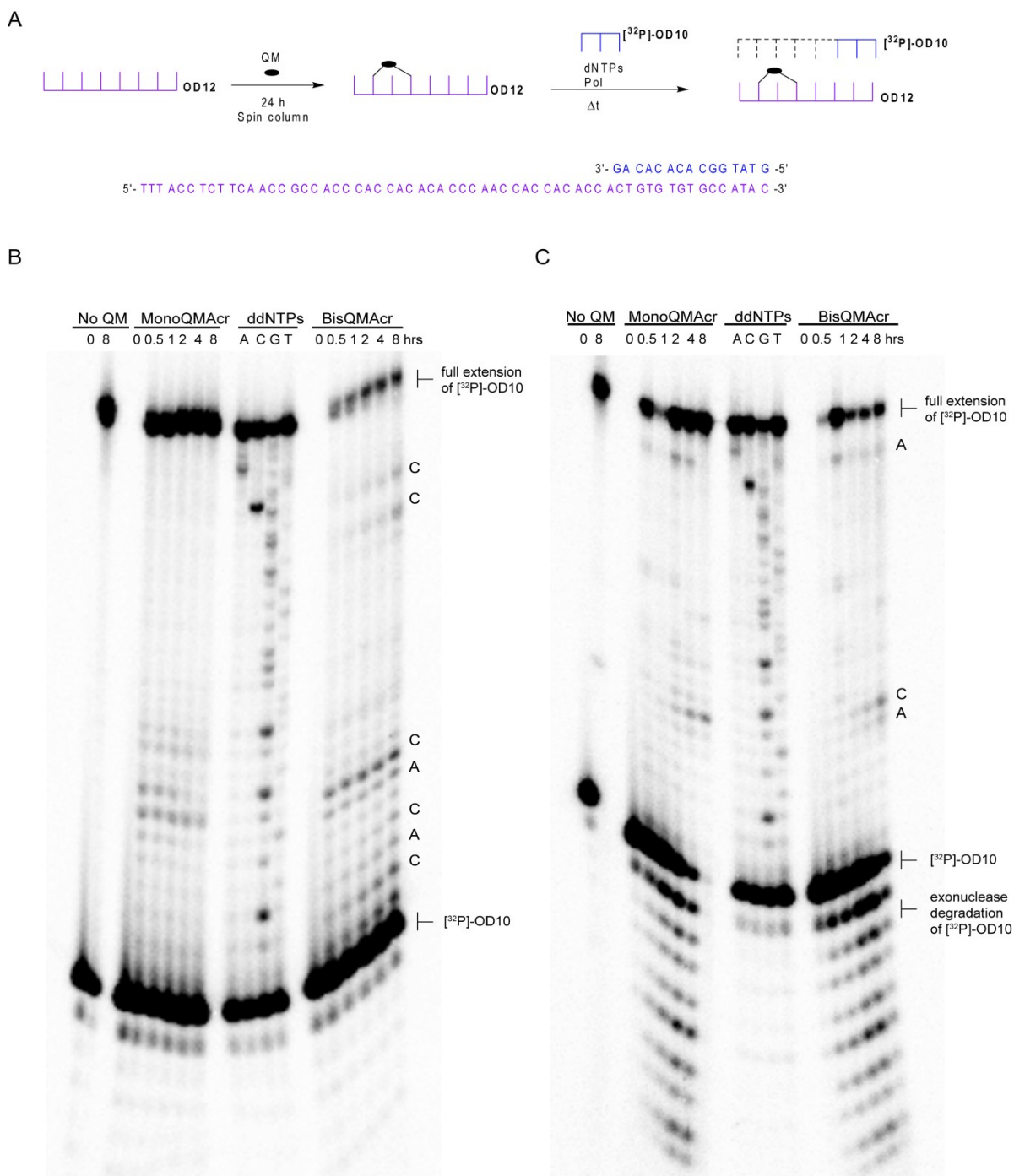
Figure 4.6 Primer extension of a template strand alkylated with monoQMAcr and bisQMAcr. A) Scheme depicting the experimental setup. B) OD12 (3 µM) was treated with monoQMPAcr or bisQMPAcr (4 µM) in in MES (10 mM, pH 7) and NaF (10 mM) for 24 h, followed by removal of excess QM using a P6 spin column (1000 g, 4 min). Alkylated OD12 (200 nM) was added to a mixture of OD10 (240 nM), [^{32}P]-OD10 (5 nM) and dNTPs (100 µM) in the appropriate polymerase reaction buffer. The primer/template complexes were incubated with the B) Klenow Exo$^-$ (60 nM) or C) φ29 DNA polymerase (12 nM) for 0-60 min. Products were separated by denaturing PAGE (20%) and detected by phosphorimagery.

sequence homogeneity and A-C-rich character of OD12. Use of a heterogeneous template sequence may provide a more extensive profile of stall sites when analyzing primer extension of an alkylated DNA.

The heterogeneous sequence OD2 was used as the template strand to induce a greater degree of products of aborted synthesis than those generated using OD12 as a template, since a heterogeneous DNA sequence may facilitate greater processivity of the polymerases (Figure 4.7A). A shorter incubation time (60 min) was used for the heterogeneous template sequence because the polymerases were quicker to process it than the homogeneous A-C-rich OD12 sequence. Both polymerases stalled at a wider variety of nucleotides located along the entire length of the DNA (Figure 4.7B, C). The Klenow Exo⁻ polymerase did not exhibit much time dependence for its activity, as it had completed synthesis by 1 min, and failed to overcome the lesions that resulted in aborted synthesis. No new products of primer extension were evident after 1 min. Meanwhile, the φ29 polymerase was slower to extend the primer, but stalled at many of the same sites as Klenow Exo⁻. The φ29 polymerase did not significantly degrade the primer, as it did with OD12. This suggests a more facile extension of the primer with OD2 than with OD12.
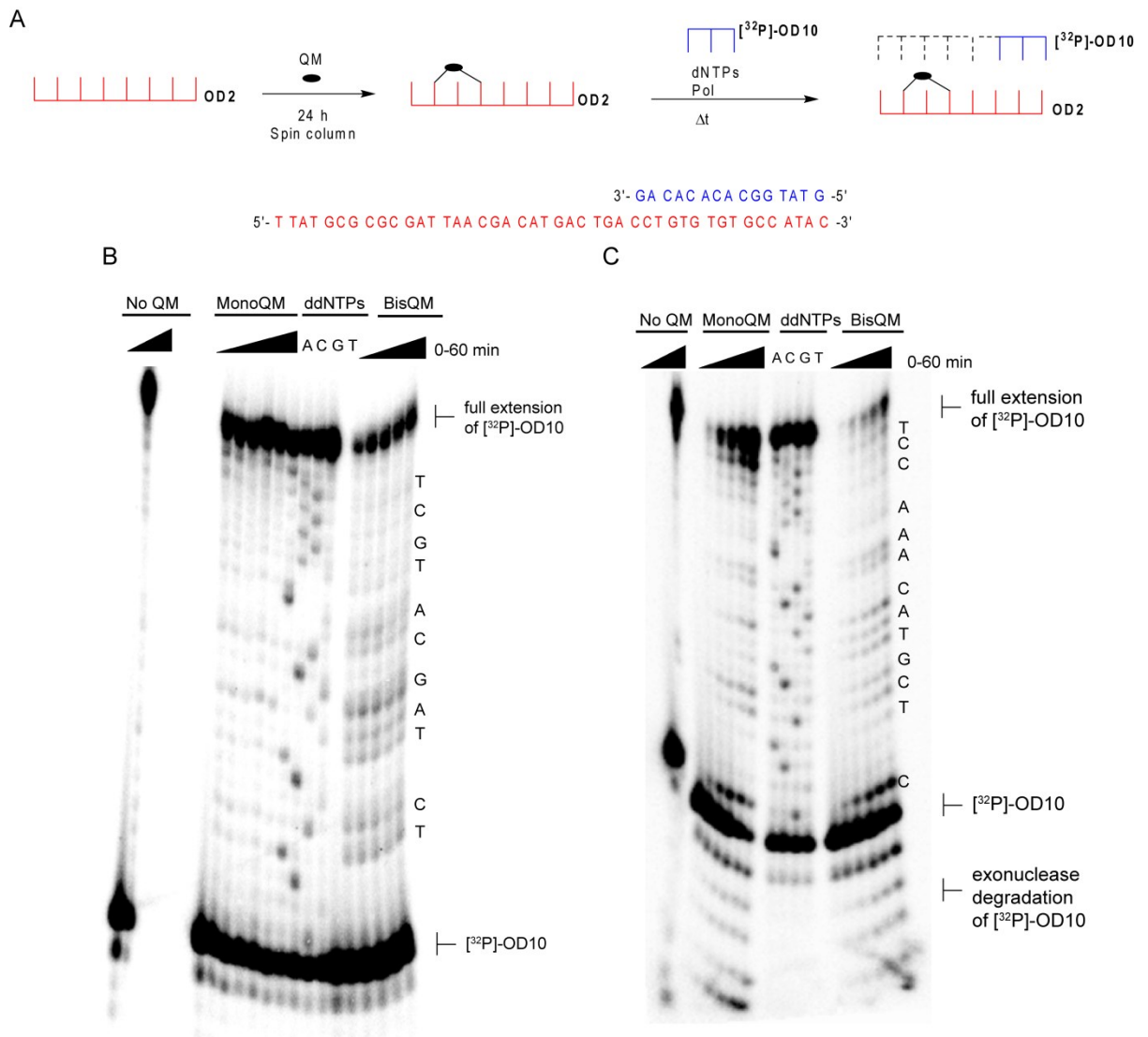
Figure 4.7 Primer extension of a heterogeneous template strand alkylated with monoQMAcr and bisQMAcr. A) Scheme depicting the experimental setup. B) OD2 (3 µM) was treated with monoQMPAcr or bisQMPAcr (4 µM) in in MES (10 mM, pH 7) and NaF (10 mM) for 24 h, followed by removal of excess QM using a P6 spin column (1000 g, 4 min). Alkylated OD2 (200 nM) was added to a mixture of OD10 (240 nM), [^{32}P]-OD10 (5 nM) and dNTPs (100 µM) in the appropriate polymerase reaction buffer. The primer/template complexes were incubated with B) Klenow Exo$^-$ (60 nM) or C) φ29 DNA polymerase (12 nM) for 0-60 min. Products were separated by denaturing PAGE (20%) and detected by phosphorimagery.

Little difference in sites of aborted synthesis occurred between the template DNA

treated with monoQMAcr and bisQMAcr. However, OD2 treated with monoQMAcr

supported a greater degree of full-length extension of the primer than when treated with

bisQMAcr. MonoQMAcr alkylates DNA with a lower yield than bisQMAcr, and forms fewer adducts than bisQMAcr since it contains one, rather than two electrophiles.[53] In both cases, some full-length extension is observed, since not every DNA molecule is alkylated with QM. Generally, a 20-30-fold stoichiometric excess of bisQMPAcr is required to achieve alkylation of every DNA molecule in solution.

The presence of an assortment of aborted synthesis products supports the hypothesis that QM-lesions on the template strand induce polymerase stalling, preventing full-length extension of the primer. Thus, DNA polymerases will not be modulate bisQMAcr's migration along DNA, since its lesions halt their polymerase activity. Furthermore, like most DNA ICLS, bisQMAcr's intra- and inter-strand crosslinks will likely pose as blocks to DNA replication *in vivo*, by preventing primer extension by DNA polymerases.[123]

4.2.3 Primer Extension of DNA Containing Crosslinks from Ammonium-Linked BisQMs

BisQMs linked to polyammonium ligands associate to DNA via electrostatic interactions with the phosphodiester backbone and form a significant yield of irreversible QM-DNA adducts.[45, 124] Furthermore, acridine's intercalation may distort the DNA in such a way that prevents the initiation of primer extension. Comparing primer extension in the presence of $bisQMN_2$ and $bisQMN_3$ lesions with that for bisQMAcr lesions will address how the binding mode affects polymerase activity. Thus, these bisQMs may impact the polymerases' primer extension of alkylated DNA differently than bisQMAc did.

The preference for ammonium-linked bisQMs to form irreversible DNA adducts suggests that polymerases likely will not induce dissociation of their ICLs. To confirm the

resistance of these ICLs to the action of DNA polymerases, bisQMN$_2$ and bisQMN$_3$

crosslinks were generated with OD10 and [^{32}P]-OD12 (Figure 4.8A). The G-T-rich OD10

and its complementary A-C-rich OD12 sequence were used to ensure crosslink formation via

isomerization from an intra- to inter-strand crosslink. This isomerization does not occur when

using the heterogeneous OD1, 2, and 4 sequences. The primer/template complex was formed,

and reaction was initiated via addition of dNTPs and the indicated polymerase. As

hypothesized, the Klenow Exo$^-$ polymerase failed to alter the integrity of both bisQMN$_2$ and

bisQMN$_3$'s DNA ICLs (Figure 4.8B, C).
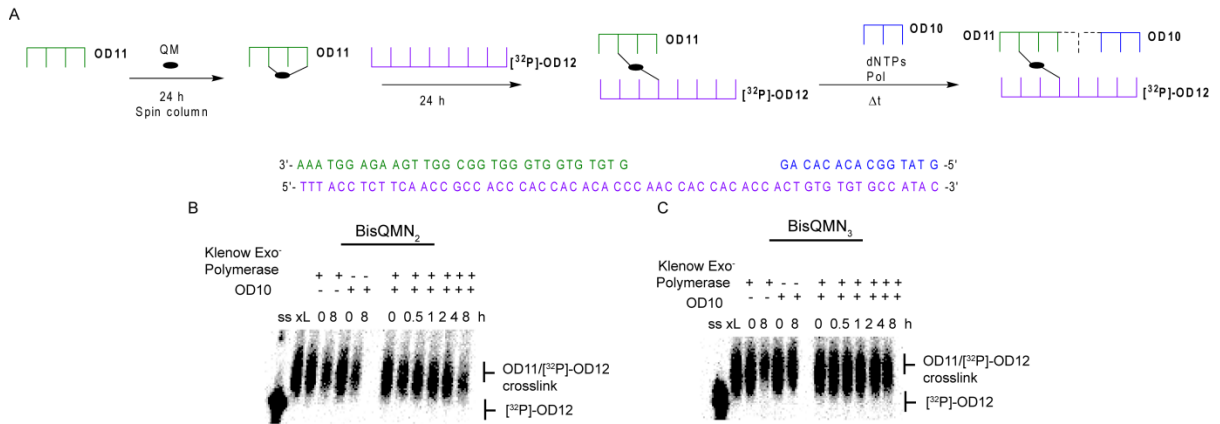
Figure 4.8 Persistence of bisQMN$_2$ and bisQMN$_3$ DNA crosslink during primer extension by the Klenow Exo$^-$ DNA polymerase. A) Scheme depicting the experimental setup. B) Crosslinked OD11/[^{32}P]-OD12 was prepared by first treating OD11(3 µM) with B) bisQMPN$_2$ or C) bisQMPN$_3$ (500 µM) for 24 h in MES (10 mM, pH 7) and NaF (10 mM), followed by removal of excess QM with a P6 spin column. OD12 (3 µM) was then added for an additional 24 h. The crosslinked OD11/[^{32}P]-OD12 (200 nM) was added to a mixture of OD10 (240 nM) and dNTPs (100 µM) in the polymerase reaction buffer. The primer/template complexes were incubated with the Klenow Exo$^-$ polymerase (60 nM) for 0-8 h. Products were separated by denaturing PAGE (20%) and detected by phosphorimagery.

To determine whether the ammonium-conjugated bisQM's also impair primer

extension of an alkylated template strand, OD2 was alkylated alternatively with each bisQM

for 24 h, before the primer-template complex was formed and extension was initiated with

dNTPs and each polymerase (Figure 4.9A). Primer extension resulted in a pattern of multiple
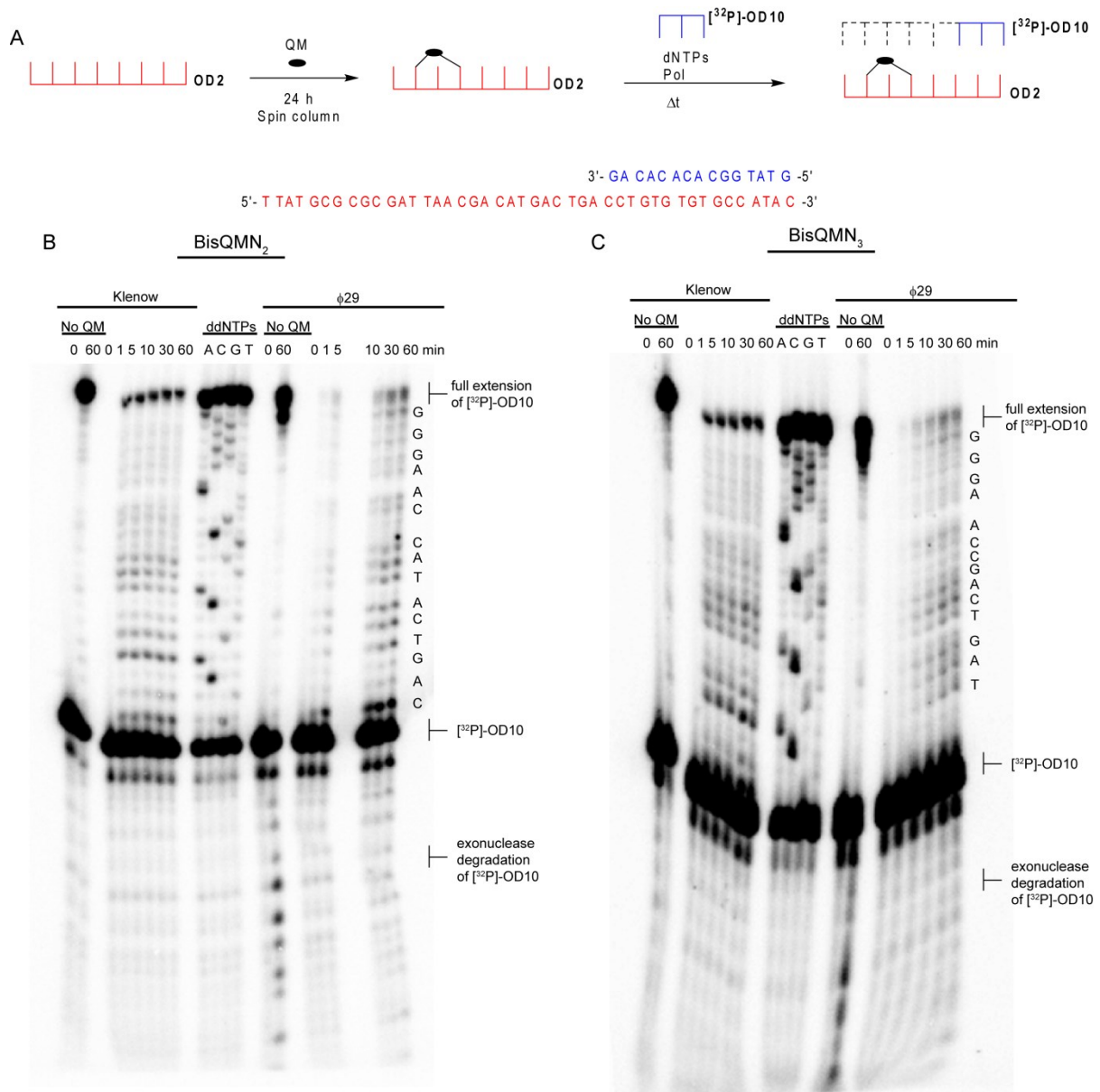
Figure 4.9 Primer extension by Klenow Exo⁻ and φ9 DNA polymerases of a heterogeneous template strand alkylated with bisQMN$_2$ or bisQMN$_3$. A) Scheme depicting the experimental setup. B) OD2 (3 µM) was treated with B) bisQMPN$_2$ or C) bisQMPN$_3$ (4 µM) in MES (10 mM, pH 7) and NaF (10 mM) for 24 h, followed by removal of excess QM using a Bio-Rad P6 spin column (1000 g, 4 min). Alkylated OD2 (200 nM) was added to a mixture of OD10 (240 nM), [^{32}P]-OD10 (5 nM) and dNTPs (100 µM) in the appropriate polymerase reaction buffer. The primer/template complexes were incubated with the DNA polymerase for 0-60 min. Products were separated by denaturing PAGE (20%) and detected by phosphorimagery.

stall sites at a wider variety of nucleotides than that of bisQMAcr (Figure 4.9B, C). BisQMAcr primarily stalled the polymerases at C's and T's, while $bisQMN_2$ and $bisQMN_3$ stalled the polymerases at all four bases. Both $bisQMN_2$ and $bisQMN_3$ affect the polymerases to the same extent and produce a similar primer extension profile. Little difference occurs when increasing the charge of the linker on the polymerases' processing of the damaged DNA. But, the binding mode of the ligand conjugated to the bisQM changes the identities of the aborted synthesis products. This likely occurs due to the differences in sites of reaction that result from each binding ligand directing the bisQM to react with different nucleophiles within DNA. Thus, the differences in aborted products of primer extension between bisQMAcr and $bisQMN_2$ and $bisQMN_3$ also support the differences in sites of reactivity that became apparent in previous work (refer to Chapter 2).[45]

4.2.4 Effect of DNA Binding Ligands on Primer Extension by the Klenow Exo⁻ and φ29 DNA Polymerases

Although the bisQMs impair primer extension by the Klenow Exo⁻ and φ29 DNA polymerase, whether ligand binding or covalent QM reaction causes the aborted synthesis products is not known. To determine whether and to what extent ligand binding impedes the primer extension of OD2 template DNA treated with the bisQMs, OD2 was treated with 9-aminoacridine, the diammonium linker, or the triammonium linker, rather than bisQMAcr, $bisQMN_2$, or $bisQMN_3$, respectively (Schemes 2.2 and 2.3). The template DNA was passed through a spin column after ligand treatment to maintain equivalent conditions to those used for experiments involving the bisQMs (Figure 4.10A). However, it is possible that ligand binding to OD2 may be disrupted during chromatography, since binding is non-covalent.
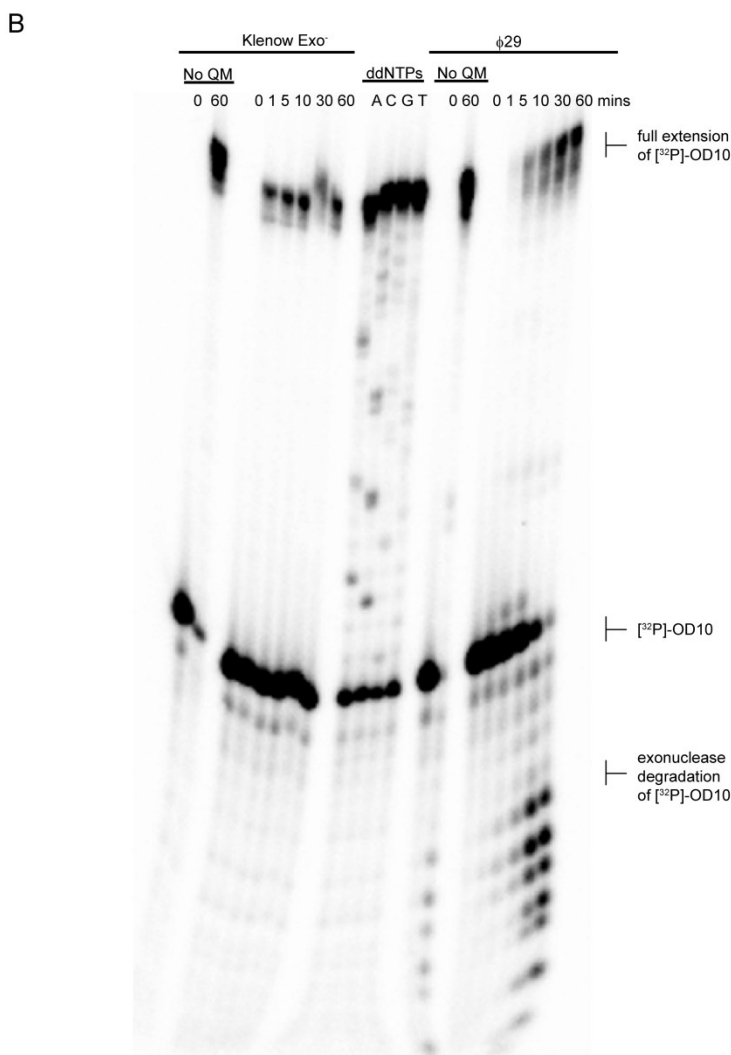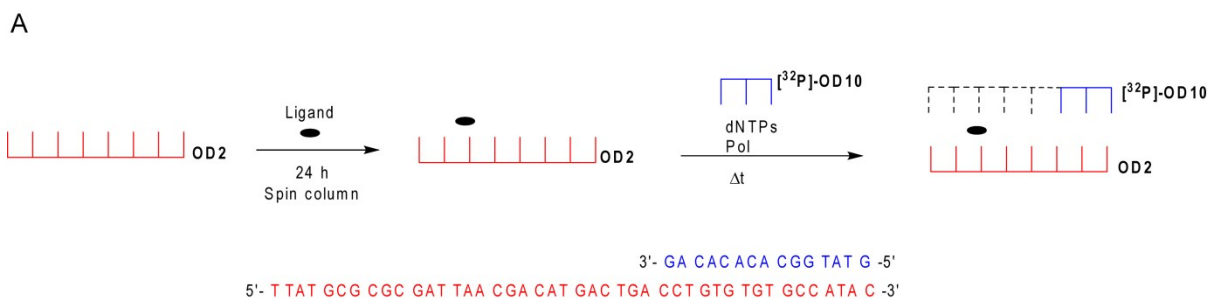
Figure 4.10 Primer extension of a heterogeneous template strand treated with 9-aminoacridine using either the Klenow Exo⁻ or φ29 DNA polymerases. A) Scheme depicting the experimental setup. B) OD2 (3 µM) was treated with 9-aminoacridine (4 µM) in MES (10 mM, pH 7) and NaF (10 mM) for 24 h, followed by removal of excess ligand using a P6 spin column (1000 g, 4 min). Alkylated OD2 (200 nM) was added to a mixture of OD10 (240 nM), [³²P]-OD10 (5 nM) and dNTPs (100 µM) in the appropriate polymerase reaction buffer. The primer/template complexes were incubated with the indicated DNA polymerase for 0-60 min. Products were separated by denaturing PAGE (20%) and detected by phosphorimagery.

Treatment with 9-aminoacridine resulted in suppressed primer extension relative to parent OD2 (Figure 4.10B). The level of inhibition of the polymerases' primer extension activity is similar to that of bisQMAcr, with the major difference being that 9-aminoacridine does not cause the polymerase to stall, as bisQMAcr does. Rather, the polymerase either extends the primer fully or not at all. Abortion of primer extension likely results from covalent QM-DNA adducts. Regardless, intercalation by acridine contributes to bisQMAcr's impairment of the primer extension activity of the two DNA polymerases.

Both ammonium linkers also did not lead to stalling of the polymerase during extension of the primer with OD2 template DNA (Figure 4.11). Like 9-aminoacridine, the linkers suppressed the yield of full extension of the primer relative to OD2 in the absence of ligand, but did not inhibit the polymerases extending the primer. Thus, bisQMN$_2$'s and bisQMN$_3$'s suppression of the polymerases' primer extension activity also likely derives from both covalent reaction of the QMs and binding of the ammonium linkers to DNA. Association to DNA may suppress the yield of primer extension, while QMs' covalent reactions contribute to the polymerases' stalling and inability to extend a primer.

4.3 Summary

DNA polymerases were initially considered as candidate enzymes that may modulate bisQMAcr's migration along DNA. Polymerases act as biological machines, proceeding quickly along DNA with their motion coupled to energy expenditure from dNTP incorporation. This activity may affect reversible reactions with DNA by either hastening the chemistry of the DNA adduct or modulating the direction of migration of reversible adducts. However, the Klenow Exo$^-$ and φ29 DNA polymerases did not cause separation of

bisQMAcr's DNA ICLs during primer extension. Crosslinks did not dissociate upon

incubation with the polymerases, but rather impaired the polymerases' ability to extend a
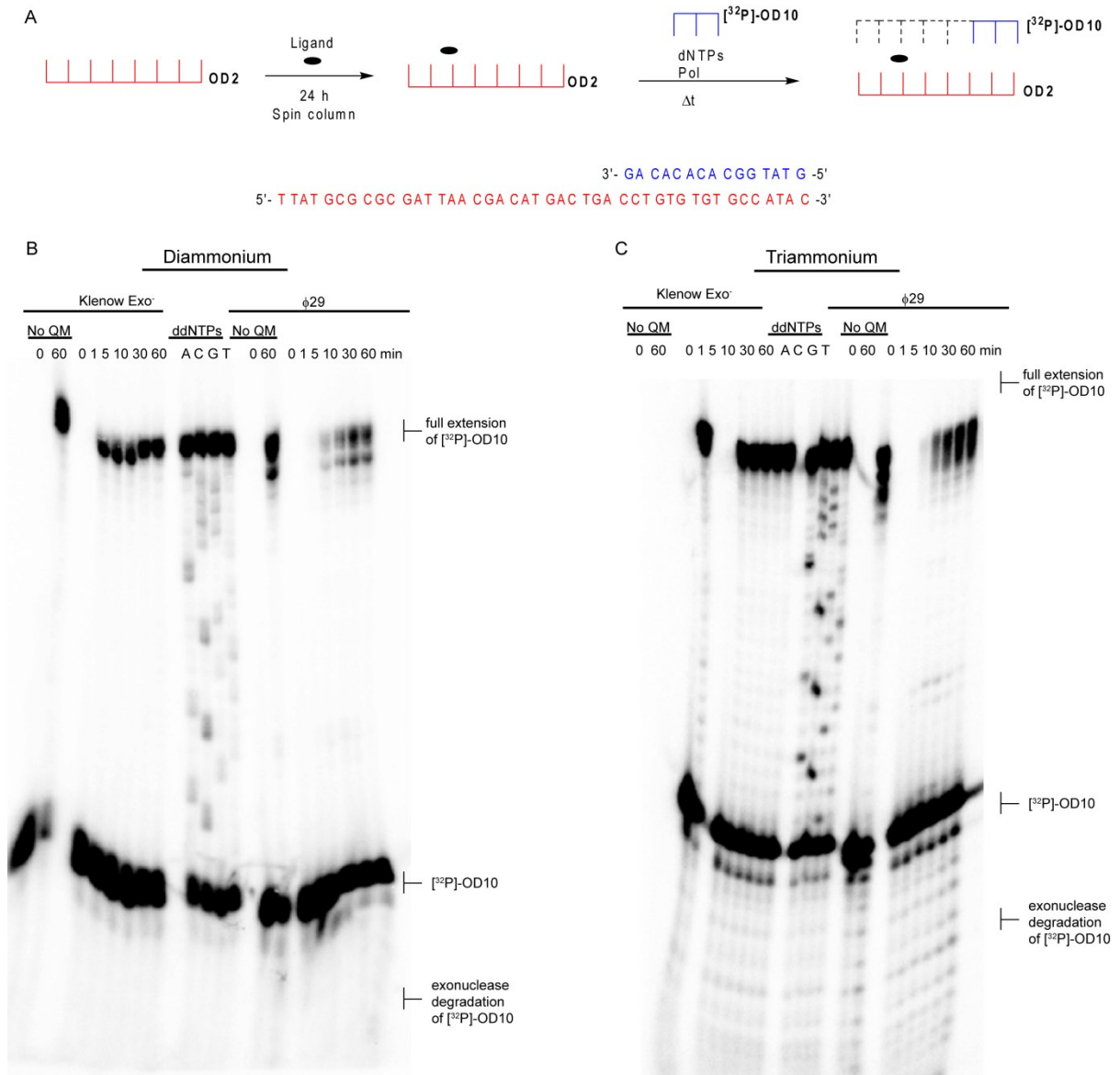
Figure 4.11 Primer extension by Klenow Exo⁻ and φ9 DNA polymerases of a heterogeneous template strand treated with the diammonium or triammonium linker. A) Scheme depicting the experimental setup. B) OD2 (3 µM) was treated with the B) diammonium or C) triammonium linker (4 µM) in MES (10 mM, pH 7) and NaF (10 mM) for 24 h, followed by removal of excess ligand using a P6 spin column (1000 g, 4 min). Alkylated OD2 (200 nM) was added to a mixture of OD10 (240 nM), [32P]-OD10 (5 nM) and dNTPs (100 µM) in the appropriate polymerase reaction buffer. The primer/template complexes were incubated with the DNA polymerase for 0-60 min. Products were separated by denaturing PAGE (20%) and detected by phosphorimagery.

primer, and triggered φ29's exonuclease activity. The generation of products representing aborted synthesis during extension of a primer in the presence of alkylated template DNA and premature termination of extension suggests that the polymerases may stall at QM lesions and dissociate from the DNA. Dissociation likely occurs within minutes while bisQMAcr's reversible chemistry requires hours, preventing the polymerase from affecting bisQMAcr's migration along DNA.

Comparison of the polymerases' primer extension activity between DNA treated with bisQMAcr and the ammonium-linked bisQMs highlights the differences in sites of reaction that the ligands direct the bisQMs to. BisQMN$_2$ and bisQMN$_3$ also suppressed primer extension, but led to the formation of terminated synthesis products at different nucleotide sites than those detected for DNA treated with bisQMAcr. Overall, our data suggests that bisQMs will impair DNA replication *in vivo* by suppressing DNA polymerases. This effect may be significant, unless the DNA is properly repaired, since its transcription and translation to express the encoded gene will be prevented. However, polymerase switching to a TLS polymerase would likely occur in a cell.[104] The TLS polymerase Pol ν has been demonstrated to bypass DNA ICLs, and thus may either bypass bisQMAcr lesions or modulate their migration along DNA.[125, 126] Investigation of whether Pol ν bypasses bisQMAcr's crosslink would determine whether bisQMAcr would act as an absolute replication block in cells, or only pose a hindrance to replicative polymerases.

Furthermore, DNA helicases may be a more processive class of enzymes than DNA polymerases to investigate the interactions that may result from bisQMAcr's reversible chemistry. Helicases are quite processive, possess strong strand displacement activity, and interact with DNA during replication before polymerases. As will be discussed in Chapter 5,

helicases do not dissociate from DNA containing lesions as quickly as polymerases do, providing a greater likelihood of affecting bisQMAcr's reversible DNA adducts.

4.4 Materials and Methods

4.4.1 Materials

T4 polynucleotide kinase, Klenow Exo⁻ polymerase, φ29 DNA polymerase, and an equimolar solution containing 10 mM of the four dNTPs were purchased from New England Biolabs. γ- [^{32}P]-ATP was purchased from Perkin Elmer. The four individual ddNTPs were purchased from Sigma. Oligonucleotides were purchased from Integrated DNA Technologies with standard desalting and were purified by denaturing PAGE. BisQMPAcr was synthesized as described previously.[40] MonoQMPAcr was provided by Dr. Blessing Deeyaa. BisQMPN$_2$ and bisQMPN$_3$ were provided by Dr. Mark Hutchinson. 9-Aminoacridine was synthesized as described previously.[127]

4.4.2 Methods

General Oligonucleotide Studies. Oligonucleotides were labeled at their 5'-terminus with γ-[^{32}P]- ATP using T4 polynucleotide kinase according to the manufacturer's protocol. Duplex DNA was annealed by heating the [^{32}P]- DNA (3 μM) with its complementary strand (3 μM) in MES (10 mM, pH 7) and NaF (10 mM) at 95 °C for 2 min followed by slow cooling to room temperature over 2-3 h.

DNA Alkylation with QMs. The indicated QMP in acetonitrile was added to the preannealed duplex DNA in MES (10 mM, pH 7) and NaF (10 mM) to yield a final reaction

volume of 20 µL with 20% acetonitrile. Reactions were quenched by the addition of 2X

formamide loading dye (0.05% bromophenol blue and 0.05% xylene cyanol in formamide)

and analyzed by 20% denaturing polyacrylamide gel electrophoresis. Alternatively, samples

were subjected to piperidine cleavage as described previously and analyzed by 20%

denaturing PAGE. Products were detected by phosphorimagery using a Typhoon 9410

phosphorimager and quantified with ImageQuant software to determine the reaction yields

(% product band relative to total material).

Persistence of BisQMs' DNA Crosslink Following Primer Extension by DNA

Polymerases. OD11 (3 µM) in MES (10 mM, pH 7) and NaF (10 mM) was treated with the

indicated BisQMP (500 µM, in CH_3CN) for 24 h at ambient temperature in a solution with a

final concentration of 20% acetonitrile. OD12 (2.8 µM) and $[^{32}P]$- OD12 (0.2 µM) were

added to the reaction mixture to bring the final volume to 20 µL, and incubated for an

additional 24 h at ambient temperature. Excess QM was removed via gel filtration

chromatography by passing the reaction mixture through a Bio-Rad P6 spin column (1000 g,

4 min). The crosslinked DNA was added to a solution of OD10 (0.24 µM), dNTPs (100 µM),

and 1x polymerase buffer. The indicated polymerase was added to the reaction mixture to

bring the final volume to 20 µL. Reactions were quenched at the indicated times with 20 µL

of formamide loading dye that contained 25 mM EDTA. The products were analyzed by

denaturing PAGE (20%) and detected by phosphorimagery.

Primer Extension Using Klenow Exo- Polymerase. The 1x reaction buffer used for the

Klenow Exo⁻ polymerase contains NaCl (50 mM), Tris-HCl (10 mM, pH 7.9), and $MgCl_2$ (10

mM). Klenow Exo⁻ (60 nM) in storage buffer (25 mM Tris-HCl, pH 7.4, 1 mM DTT, 0.1 mM EDTA, and 50% glycerol) was added to the reaction mixture described above at ambient temperature.

Primer Extension Using φ29 DNA Polymerase. The 1x reaction buffer used for the φ29 DNA polymerase contains Tris-HCl (50 mM, pH 7.5), $MgCl_2$ (10 mM), and $(NH_4)_2SO_4$ (10 mM). The reaction mixture described above was supplemented with BSA (10 mg/mL) before addition of φ29 DNA polymerase (12 nM) in storage buffer (10 mM Tris-HCl, pH 7.4, 100 mM KCl, 1 mM DTT, 0.1 mM EDTA, 50% glycerol, 0.5% Tween 20, and 0.5% IGEPAL CA-630) at ambient temperature.

Primer Extension by DNA Polymerases in the Presence of a bisQM DNA Inter-Strand Crosslink. OD11 (3 µM) in MES (10 mM, pH 7) and NaF (10 mM) was treated with the indicated BisQMP (500 µM, in CH_3CN) for 24 h in a solution that contained 20% acetonitrile. OD12 (3 µM) was added to the reaction mixture to bring the final volume to 20 µL, and incubated for an additional 24 h. Excess QM was removed via gel filtration chromatography by passing the reaction mixture through a Bio-Rad P6 spin column (1000 g, 4 min). The crosslinked DNA was added to a solution of OD10 (0.24 µM), [^{32}P]-OD10 (0.005 µM), dNTPs (100 µM), and 1x polymerase buffer. The indicated polymerase was added to the reaction mixture to bring the final volume to 20 µL. Reactions were quenched at various times with 20 µL of formamide loading dye that contained 25 mM EDTA. The products were analyzed by denaturing PAGE (20%) and detected by phosphorimagery.

Dideoxynucleotide DNA Sequencing. The indicated DNA template strand (0.2 µM) was added to a solution of OD10 (0.24 µM), dNTPs (20 µM), and 1x Klenow Exo⁻ polymerase buffer (50 mM NaCl, 10 mM Tris-HCl, 10 mM MgCl$_2$, 1 mM DTT, pH 7.9). Each ddNTP (600 µM) was added individually to separate reactions before addition of the Klenow Exo⁻ Polymerase (0.06 µM) to bring the final reaction volume to 20 µL. Reactions were incubated for 1 h at ambient temperature before quenching by the addition of 20 µL of formamide loading dye containing 25 mM EDTA. The products were analyzed by 20% denaturing PAGE and detected by phosphorimagery.

Alkylation and Extension of Template Strand by DNA Polymerases. The indicated DNA template strand (3 µM) in MES (10 mM, pH 7) and NaF (10 mM) was treated with the indicated bisQMP (500 µM, in CH$_3$CN) for 24 h to bring the final volume to 20 µL and the final acetonitrile concentration to 20% at ambient temperature. Excess QM was removed via gel filtration chromatography by passing the reaction mixture through a Bio-Rad P6 spin column (1000 g, 4 min). The alkylated DNA (0.2 µM) was added to a solution of OD10 (0.24 µM), [^{32}P]-OD10 (0.005 µM), dNTPs (100 µM), and 1x polymerase buffer. The indicated polymerase was added to the reaction mixture to bring the final volume to 20 µL and reactions were quenched at the indicated times with 20 µL of formamide loading dye that contained 25 mM EDTA. The products were analyzed by 20% denaturing PAGE and detected by phosphorimagery.

Chapter 5: Unwinding of DNA Containing BisQMAcr Crosslinks by the T7 Bacteriophage Gene 4 Protein Helicase

5.1 Introduction

The failure of the Klenow Exo⁻ and φ29 DNA polymerases to extend a primer in the presence of bisQMAcr's ICLs suggests that bisQMAcr's ICLs may pose a replication block. However, helicases must first unwind duplex DNA before DNA polymerases can synthesize a new daughter strand, and would encounter DNA damage before a polymerase.[128] Helicases hydrolyze dNTPs to generate power that promotes their processive translocation along DNA and concurrent unwinding of the duplex (Scheme 5.1). To determine the full impact of a reversible DNA ICL on replication, the ability of a helicase to unwind DNA containing ICLs should be evaluated. A reversible ICL may not pose a replication block for helicases, as irreversible ICLs may, if the time frame for reversible chemistry aligns with that of the helicase's action. Helicases may stall at lesions without dissociating from the DNA,
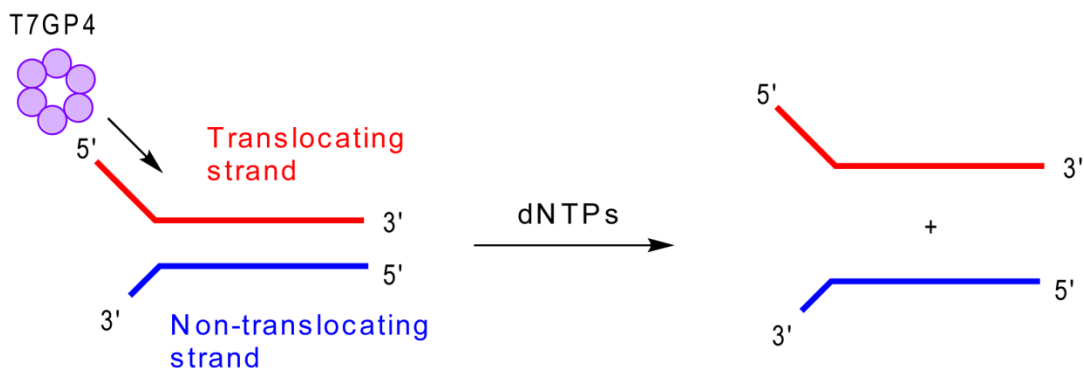
Scheme 5.1 General depiction of translocation and concurrent unwinding of duplex DNA by hexameric DNA helicases.

providing enough time for the reversible chemistry to occur. Once regenerated, the reactive species could dissociate from the DNA, re-alkylate a different site on the DNA, or alkylate the helicase. Precedent exists for helicase stalling at DNA lesions, especially during nucleotide excision repair. For example, the XPD helicase serves as a means of damage recognition by stalling at DNA lesions to recruit the relevant repair proteins.[129, 130] Reversible ICLs may not prevent the action of helicases if they stall at the lesion long enough for the adduct to release the electrophile and restore the unmodified DNA.

Several DNA helicases have been reported to be inhibited by monoadducts and DNA-protein crosslinks on the strand upon which the helicase translocates. For example, cyclopyrimidine dimers and cisplatin DNA adducts inhibit translocation by Rad3, the *Saccharomyces cerevisiae* homolog of XPD.[131, 132] However, only adducts on the translocating DNA strand, but not complementary strand, prevent DNA unwinding by Rad3.[132] The Werner syndrome (WRN) helicase cannot unwind DNA containing benzo[c]phenanthrene (BcPh)-dA adducts on the translocating strand.[4] However, BcPh adducts on the non-translocating strand only impaired helicase activity when the adduct was spatially oriented towards the advancing helicase.[131, 133] The pendant alcohols on the BcPh adduct can face towards the 3'-end of the DNA or the 5'-end. When oriented towards the 5'-end, the BcPh's alcohols face towards the helicase as it translocates from the 5'-end to the 3'-end of the DNA. The effect of orientation of BcPh adducts on the translocation of the WRN helicase highlights the effect of adduct positioning on facilitating or preventing DNA unwinding. Hexameric, replicative helicases from T7 bacteriophage, *E.coli*, and humans are also inhibited by bulky lesions on the translocating strand. DNA-protein crosslinks on the

translocating strand prevent DNA unwinding by the T7 bacteriophage Gene 4 Protein (T7GP4), DnaB, and Mcm467 helicases.[134]

All lesions that have been examined for their ability to hinder the activity of DNA helicases form irreversibly. How reversible bisQMAcr DNA ICLs respond to the action of a DNA helicase may address the question of whether reversible DNA alkylation mitigates the potency of an alkylating agent. Regeneration of the reactive species may release the unmodified DNA, essentially affording repair of the adduct. However, the regenerated alkylating agent may also re-alkylate the DNA at a new site or may alkylate the helicase. These latter two possibilities would likely enhance the alkylating agent's toxicity to cells by preventing DNA replication and repair. Helicases have been suggested as catalysts for the migration of reversible DNA adducts along DNA.[25] However, to our knowledge, the possibility of this phenomenon has never been investigated. Here, we hypothesize that a DNA helicase may modulate bisQMAcr's migration along DNA, either by causing its crosslinks to dissociate or by controlling its direction and speed of migration.

We chose to utilize the 56 kDa fragment of the T7GP4 helicase for our studies. The full-length T7GP4 protein possesses both helicase and primase activities, but the 56 kDa fragment contains an N-terminal truncation that abolishes primase activity.[135, 136] T7GP4 has been demonstrated to stall at benzo[α]pyrene adducts on the translocating strand.[137] These lesions inhibit T7GP4's forward progression along DNA and sequester the helicase with bound dTTP.[137, 138] T7GP4 hydrolyzes dTTP to dTDP to facilitate its translocation along DNA, but fails to hydrolyze the bound dTTP when sequestered by the benzo[α]pyrene lesion.[137, 139, 140] However, removal of the lesion may permit reinitiation of T7GP4's translocation along DNA, since it still has bound dTTP. A reversible lesion, such as

bisQMAcr's DNA ICL, may permit lesion bypass by T7GP4 if the QM of bisQMAcr regenerates from its DNA adduct and releases the unmodified DNA. Here, we investigated T7GP4's ability to affect bisQMAcr's reversible DNA-adducts. Helicase-catalyzed migration of QM adducts could represent a means by which reversible DNA-adducts afford their own repair if the helicase can dissociate a reversible DNA ICL.

5.2 Results and Discussion

5.2.1 Unwinding DNA Crosslinks by T7GP4

The 56 kDa fragment of the T7GP4 helicase was expressed and purified as described previously (Appendix D, Figure D.1).[141, 142] A mini-replication fork containing a 5'-single-stranded region on OD13 and a 3'-single-stranded region on OD14 was utilized to determine the efficiency of DNA unwinding by T7GP4 with unmodified DNA, as T7GP4 requires single-stranded DNA as a model replication fork to initiate its translocation.[143] The OD13/OD14 sequences were chosen for DNA unwinding by T7GP4 due prior reports of its ability to be unwound rapidly and for the single strands to be detected by native PAGE.[140, 144] T7GP4 unwound OD13/OD14 in a concentration-dependent manner within 10 min (Appendix D, Figure D.2).

To determine how bisQMAcr's DNA ICL responds to DNA unwinding by T7GP4, OD13/[^{32}P]-OD14 duplex DNA was crosslinked with bisQMAcr and used as a substrate for unwinding by T7GP4. The duplex DNA was treated with bisQMPAcr in the presence of NaF for 2 h, before removal of excess bisQMAcr using a P6 spin column. A 2 h treatment of the DNA with bisQMPAcr was chosen in order to ensure a high yield of DNA ICLs, while preventing more than one bisQMAcr adduct per duplex DNA molecule (Figure 5.1B). Over-

123

Figure 5.1 Kinetics of unwinding of OD13/[^{32}P]-OD14 duplex DNA containing bisQMAcr crosslinks by T7GP4. A) Scheme depicting the experimental setup. B) Crosslinked OD13/[^{32}P]-OD14 (10 nM) was incubated with dTTP (1 mM) and T7GP4 (55 nM monomer concentration) at 37 ℃ and samples were quenched after 0, 1, 5, 10, 20, and 30 min with EDTA (40 mM). Samples were separated by 10% denaturing PAGE and visualized by phosphorimagery. C) The time-dependent unwinding of crosslinked OD13/[^{32}P]-OD14 depicted in (B) was quantified and the amount of crosslink remaining was plotted over time. The amount of crosslink (%) was expressed relative to the total signal of DNA on the gel. Data from three separate trials of the experiment are reported, with bars representing the average of the data from the three independent experiments.

alkylation of the duplex DNA may prevent helicase unwinding due to the presence of

multiple lesions that must be overcome by T7GP4. In addition, the presence of Ts in the

single-stranded regions of the DNA guarantee that no bisQMAcr adducts will form that may

interfere with helicase loading and translocation, since bisQMAcr does not react with Ts.[37]

The crosslinked OD13/[^{32}P]-OD14 duplex DNA was incubated with dTTP and T7GP4 and

products were separated by denaturing PAGE to determine whether the ICLs are broken over

time (Figure 5.1A). A monomer concentration of 55 nM of T7GP4 was chosen to ensure a

high yield of duplex DNA unwinding within 10 min, while maintaining a stoichiometric ratio of hexameric T7GP4 to duplex DNA (Appendix D, Figure D.2). OD13/[^{32}P]-OD14 containing bisQMAcr crosslinks was unwound by T7GP4 in as quick as 1 min, with the yield of unwound DNA increasing to approximately 40% over 30 min (Figure 5.1B, C). Unwinding of bisQMAcr's ICLs requires T7GP4 and dTTP, thus confirming that T7GP4's translocase activity results in ICL unwinding. The observation of single-stranded DNA by PAGE that migrate more quickly than crosslinked OD13/[^{32}P]-OD14 suggests that unwinding by T7GP4 causes the ICLs to dissociate, albeit only 40% of the ICLs are consumed.

To determine whether crosslink unwinding is sequence independent, the analogous experiment was conducted using OD15/[^{32}P]-OD16 duplex DNA, rather than OD13/[^{32}P]-OD14 (Figure 5.2A). OD15 and OD16 include the sequences that were used to demonstrate ebisQMAcr's migration along DNA, with the addition of a single-stranded poly-T sequences.[41] OD16 contains many guanines that provide sites of reversible QM-DNA adduct formation at dGN7, which may facilitate helicase-catalyzed migration of bisQMAcr's aducts along DNA. OD15/OD16 represents a G-rich DNA duplex, while OD13/OD14 contains a heterogeneous sequence of nucleotides. BisQMAcr's DNA ICLs in OD15/[^{32}P]-OD16 dissociated with similar kinetics and yield as those in the heterogeneous OD13/[^{32}P]-OD14 sequences (Figure 5.2B, C). T7GP4 unwinds bisQMAcr ICLs with similar efficiencies in two different DNA sequences, suggesting that crosslink unwinding occurs regardless of the DNA sequence. Again, approximately 40% of the ICLs are broken, while the remaining 60% of ICLs remain intact in both DNA duplexes. There is an initially burst of crosslink dissociation

Figure 5.2 Kinetics of unwinding of OD15/[^{32}P]-OD16 duplex DNA containing bisQMAcr crosslinks by T7GP4. A) Scheme depicting the experimental setup. B) Crosslinked OD15/[^{32}P]-OD16 (10 nM) was incubated with dTTP (1 mM) and T7GP4 (55 nM monomer concentration) at 37 ºC and samples were quenched after 0, 1, 5, 10, 20, and 30 min with EDTA (40 mM). Samples were separated by 10% denaturing PAGE and visualized by phosphorimagery. C) The time-dependent unwinding of crosslinked OD15/[^{32}P]-OD16 depicted in (B) was quantified and the amount of crosslink remaining was plotted over time. The amount of crosslink (%) was expressed relative to the total signal of DNA on the gel. Data from three separate trials of the experiment are reported, with bars representing the average of the data from the three independent experiments.

in both sequences within the first 10 min of incubation, followed by a plateau in the yield of crosslinks unwound between 10-30 min of incubation with T7GP4.

To ensure that unwinding of bisQMAcr DNA ICLs occurs on both the translocating and nontranslocating strands, the translocating, rather than nontranslocating strand was radiolabeled, crosslinked to its complementary strand with bisQMAcr, and incubated with T7GP4 and dTTP (Figure 5.3A). Crosslinks in both the heterogeneous [^{32}P]-OD13/OD14 and G-rich [^{32}P]-OD15/OD16 duplex DNA sequences were unwound with the same kinetics and

126

Figure 5.3 Kinetics of unwinding of DNA containing bisQMAcr crosslinks by T7GP4 using radiolabeled translocating strand. A) Scheme depicting the experimental setup. B) Crosslinked [^{32}P]-OD13/OD14 (10 nM) was incubated with dTTP (1 mM) and T7GP4 (55 nM monomer concentration) at 37 ºC and samples were quenched after 0, 1, 5, 10, 20, and 30 min with EDTA (40 mM). Samples were separated by 10% denaturing PAGE and visualized by phosphorimagery. C) The time-dependent unwinding of crosslinked [^{32}P]-OD13/OD14 depicted in (B) was quantified and the amount of crosslink remaining was plotted over time. The amount of crosslink (%) was expressed relative to the total signal of DNA on the gel. Data from three separate trials of the experiment are reported, with bars representing the average of the data from the three independent experiments. D) The analogous experiment to that conducted in (B) was performed using crosslinked [^{32}P]-OD15/OD16. D) The data from (D) was quantified and plotted as described in (C).

127

yield as the non-translocating strand (Figure 5.3B, C, D). Radiolabeling either the non-translocating strand or the translocating strand does not alter the percent of crosslink dissociation observed after DNA unwinding by T7GP4.

BisQMAcr's 9-aminoacridine ligand may inhibit duplex DNA unwinding if its intercalation blocks the action of T7GP4. To address whether intercalation of 9-aminoacridine limits the yield of unwinding of bisQMAcr's DNA ICLs by T7GP4, OD13/[^{32}P]-OD14 was first treated with 9-aminoacridine for 2 h before excess ligand was removed with a P6 spin column. The DNA was then incubated with T7GP4 and dTTP and the products were separated by native PAGE to quantify the loss of duplex DNA over time (Figure 5.4A). The heterogeneous OD13/[^{32}P]-OD14 sequence was used because the G-rich OD15/[^{32}P]-OD16 duplex DNA reanneals during native PAGE. 9-Aminoacridine did not suppress the rate or yield of duplex DNA unwinding by T7GP4 relative to that of unmodified duplex DNA (Figure 5.4B, C). Thus, intercalation by acridine likely does not contribute to the lack of a 100% yield of DNA unwinding that is observed following incubation of bisQMAcr ICLs with T7GP4.

The unwinding of DNA containing bisQMAcr ICLs by T7GP4 is, to our knowledge, the first direct example of a DNA ICL that is dissociated by a helicase *in vitro*. The Fanconi anemia translocase complex FANCM/MHF promoted replication bypass of psoralen DNA ICLs *in vivo*.[145] The FANCM/MHF translocase complex is not hexameric like T7GP4, as FANCM binds to a tetramer of MHF before initiating its progression along DNA.[146] However, FANCM/MHF's bypass of psoralen ICLs merely proves that DNA replication occurs despite the presence of the ICLs. No data was provided about the stability of the ICLs following helicase treatment. Thus, FANCM/MHF may bypass psoralen ICLs to facilitate

Figure 5.4 Time-dependent unwinding of OD13/[^{32}P]-OD14 duplex DNA by T7GP4 in the presence and absence of 9-aminoacridine. A) Scheme depicting the experimental setup. B) OD13/[^{32}P]-OD14 in MES (10 mM) and NaF (50 mM) was incubated with 9-aminoacridine (250 µM) for 2 h. Excess 9-aminoacridine was then removed with a P6 Micro-spin column. OD13/[^{32}P]-OD14 (10 nM) with or without 9-aminoacridine treatment was incubated in buffer (40 mM Tris-HCl pH 7.5, 10 mM MgCl$_2$, and 50 mM potassium glutamate) with dTTP (1 mM) and T7GP4 (55 nM monomer concentration) at 37 ºC and samples were quenched after 0, 1, 5, and 10 min with EDTA (40 mM). Samples were separated by 10% native PAGE and visualized by phosphorimagery. C) The data depicted in (B) were quantified and the amount of duplex DNA remaining was plotted over time. The amount of duplex DNA (%) was expressed relative to the total signal of DNA on the gel. Data from three separate trials of the experiment are reported, with bars representing the average of the data from the three independent experiments

replication, but the ICLs remain intact and will require repair post-replication. Although

Huang *et al* propose that not all ICLs may pose as absolute blocks to DNA replication, our

data not only supports this notion but extends it by suggesting that at least the

T7GP4 helicase mediates dissociation of reversible bisQMAcr ICLs.[145] BisQMAcr ICLs should not pose an absolute block to DNA replication, since they will not remain intact following T7GP4's translocation along DNA, unlike the psoralen ICLs. Nevertheless, T7GP4 only dissociates 40% of bisQMAcr's DNA ICLs, leaving 60% of the ICLs intact. The lack of full consumption of bisQMAcr's ICLs by T7GP4's unwinding of DNA will still result in blocked DNA replication.

5.2.2 Correlation of T7GP4's dTTPase Activity with its Translocation along DNA

T7GP4's translocation along DNA has been suggested to be coupled to its ability to hydrolyze dTTP.[137, 147] T7GP4's dTTPase activity may correlate with its inability to unwind 100% of bisQMAcr's DNA ICLs. T7GP4 hydrolyzes low levels of dTTP in the absence of DNA, thus necessitating a determination of its background dTTPase activity before investigating its activity with DNA.[135] Incubation of T7GP4 with α-[^{32}P]-dTTP and separation of α-[^{32}P]-dTDP and pyrophosphate by thin layer chromatography (TLC) with polyethylenimine-cellulose (PEI) coated TLC plates revealed an approximately 10% yield of dTTP hydrolysis to dTDP in the absence of DNA after 30 min (Figure 5.5A).[140] Single-stranded DNA has been reported to stimulate T7GP4's dTTPase activity by 100-fold relative to that in the absence of DNA.[135, 148] Reports in the literature utilize long, circular, single-stranded DNA from the M13 phage to stimulate T7GP4's dTTPase activity.[149] T7GP4 was incubated with M13 DNA and the products of dTTP hydrolysis were separated by PEI-cellulose TLC to determine the maximum yield of T7GP4's dTTPase activity. M13 DNA stimulated T7GP4 to hydrolyze 5-fold more dTTP than in the absence of DNA (Figure 5.5B,
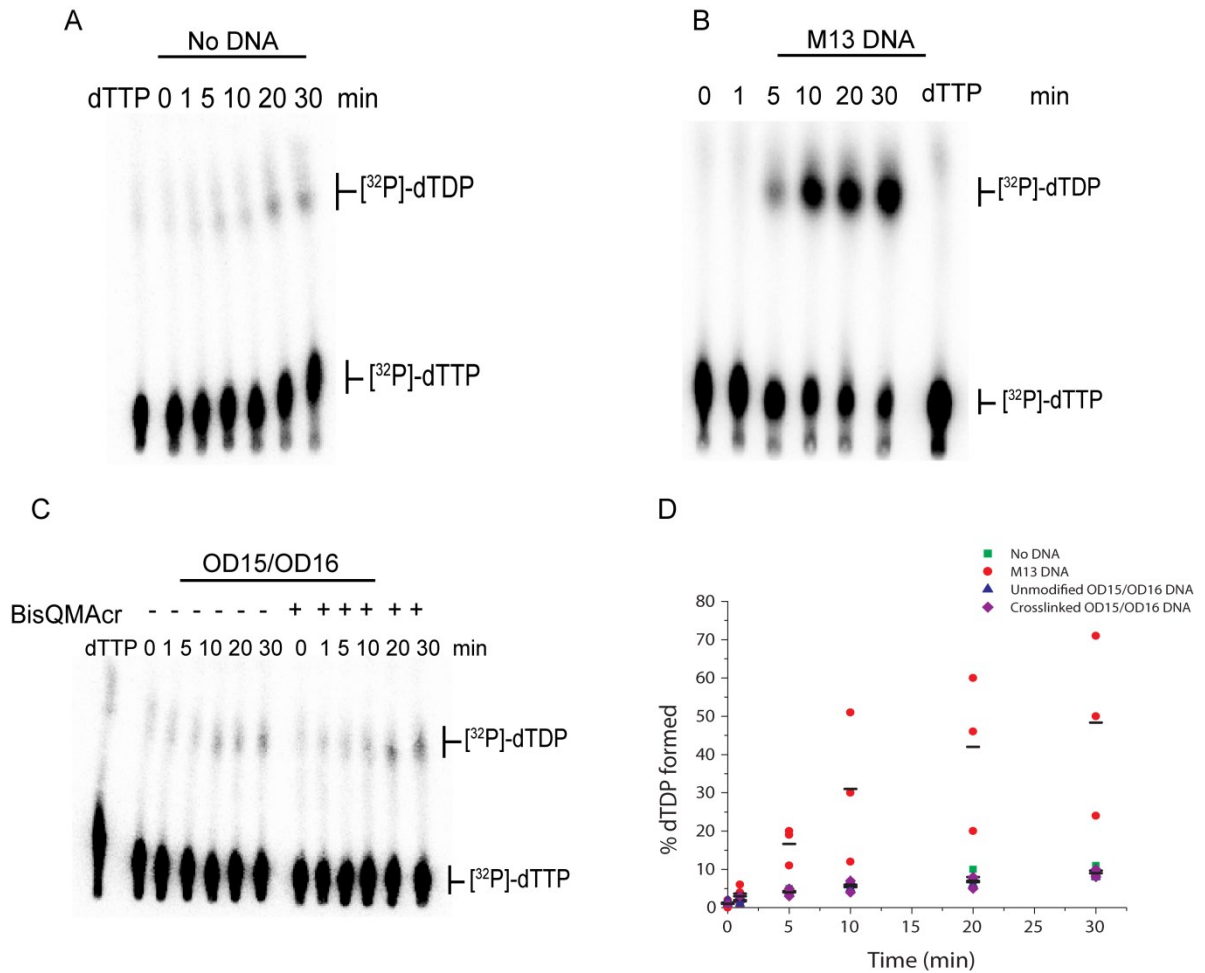
Figure 5.5 dTTP hydrolysis by T7GP4 with A) no DNA present, B) M13 single-stranded circular DNA or C) unmodified and bisQMAcr crosslinked OD15/OD16 duplex DNA. OD15/OD16, or water for the case of no DNA, in MES (10 mM, pH 7) and NaF (50 mM) was incubated with or without bisQMPAcr (250 μM) for 2 h at ambient temperature. Excess bisQMAcr and its low molecular weight products were removed with a P6 Micro Bio-spin column. α-[^{32}P]-dTTP (1 mM) was incubated with T7GP4 (55 nM monomer concentration) and the relevant DNA (10 nM) in buffer (40 mM Tris-HCl pH 7.5, 10 mM MgCl$_2$, and 50 mM potassium glutamate) at 37 °C and reactions were quenched after 0, 1, 5, 10, 20, and 30 min with an equal volume of 10% formic acid. Samples were separated by PEI-cellulose thin layer chromatography using 0.5 M formic acid and 0.5 M LiCl, and visualized by phosphorimagery. D) The data depicted in (A), (B), and (C) were quantified and the amount of dTDP formed (%) was plotted against time. The bars represent the average of three individual experiments.

D). T7GP4's dTTPase activity in the presence and absence of bisQMAcr ICLs in OD15/O16 duplex DNA was determined, now that upper and lower limits of T7GP4's dTTPase activity have been established. Incubation of OD15/O16 duplex DNA, with and without bisQMAcr

treatment, with T7GP4 and [^{32}P]-dTTP generated a 10% yield of dTDP formation over 30 min (Figure 5.5C). T7GP4's dTTPase activity was not stimulated beyond background levels with the OD15/OD16 duplex containing relatively short 65mer and 85mer oligonucleotides, regardless of whether the DNA was modified with bisQMAcr ICLs or not (Figure 5.5D). As such, no conclusion can be made concerning the question of whether translocation correlates with dTTP hydrolysis for T7GP4's unwinding of DNA containing bisQMAcr ICLs. Only long, single-stranded DNA activates T7GP4's dTTPase activity. Thus, dTTP hydrolysis by T7GP4 is not always a direct measure of its translocation along DNA and cannot provide information about whether T7GP4 is impaired in its traverse of DNA containing bisQMAcr ICLs.

5.2.3 Heterogeneous Response to Crosslinked DNA by T7GP4

Although T7GP4 unwinds DNA containing bisQMAcr ICLs, only 40% of the ICLs dissociate, while the remaining ICLs stay intact. However, the question lingers of why 100% of bisQMAcr's DNA ICLs aren't unwound by T7GP4. The possibility that the reaction components required for unwinding to occur, such as dTTP, T7GP4, and incubation time, may limit the yield of unwinding was investigated. The amount of dTTP could limit unwinding if the initial aliquot of dTTP were hydrolyzed within incubation period, while T7GP4 could limit unwinding if the enzyme became inactive within 30 min. BisQMAcr DNA ICLs in OD15/[^{32}P]-OD16 were incubated with T7GP4 and dTTP for 30 min, before an additional aliquot of either dTTP or T7GP4 was added to the mixture (Figure 5.6A). Neither additional dTTP nor T7GP4 increased the observed 40% yield of unwound ICLs (Figure 5.6B, C). Crosslink unwinding is not limited by the amount of dTTP present or by

the loss of activity of T7GP4 over time. There may then be a mixture of bisQMAcr-DNA

adducts, some of which facilitate rapid DNA unwinding, and others that either resist

unwinding or require a longer incubation time with T7GP4 in order to allow DNA

unwinding.

Figure 5.6 Determination of whether dTTP or T7GP4 limit unwinding of DNA containing bisQMAcr crosslinks. A) Scheme depicting the experimental setup. B) Crosslinked OD15/[^{32}P]-OD16 (10 nM) was incubated with dTTP (1 mM) and T7GP4 (55 nM monomer concentration) for 30 min at 37 ºC. Samples were divided into three sets. To one set was added buffer, to the second was added a fresh aliquot of dTTP, and to the third was added a fresh aliquot of T7GP4. Samples (10 µL) were incubated at 37 ºC and quenched at 0, 1, 5, 10, 20, and 30 min with EDTA (40 mM). Samples were separated by 10% denaturing PAGE and visualized by phosphorimagery. C) The data from three individual experiments were quantified and plotted against time. The amount of crosslinked DNA (%) was expressed relative to the total signal of DNA on the gel. Data from three separate trials of the experiment are reported, with bars representing the average of the data from the three independent experiments.

While T7GP4 unwinds a stoichiometric concentration of unmodified duplex DNA within 10 min, complete unwinding of bisQMAcr's crosslinks may require a longer incubation time since the ICLs may present an obstacle for T7GP4. BisQMAcr may react with a variety of DNA nucleobases to form some lesions that present less of a challenge than others for T7GP4 to unwind. To determine if a longer incubation time increases the yield of bisQMAcr ICLs that T7GP4 unwinds, OD15/[^{32}P]-OD16 containing bisQMAcr ICLs was incubated with T7GP4 and dTTP for 4 h rather than 30 min, as before (Figure 5.7A). The

Figure 5.7 Extended time course of T7GP4 unwinding of OD15/[^{32}P]-OD16 containing bisQMAcr crosslinks. A) Scheme depicting the experimental setup. B) Crosslinked OD15/[^{32}P]-OD16 (10 nM) was incubated with dTTP (1 mM) and T7GP4 (55 nM monomer concentration) at 37 °C and samples were quenched after 0, 1, 5, 10, 20, 30, 60, 120, and 240 min with EDTA (40 mM). Samples were separated by 10% denaturing PAGE and visualized by phosphorimagery. C) The data in (B) were quantified and the amount of crosslink remaining was plotted over time. The amount of crosslink (%) was expressed relative to the total signal of DNA on the gel. Data from three separate trials of the experiment are reported, with bars representing the average of the data from the three independent experiments.

yield of crosslink dissociation again plateaued after the first 30 min, and remained constant from 30 min to 4 h of incubation with T7GP4 (Figure 5.7B, C). The amount of time provided for unwinding to occur does not appear to limit the yield of crosslinks that T7GP4 dissociates.

The failure of the reaction components (dTTP and T7GP4) and the incubation time to limit the yield of bisQMAcr ICL dissociation by T7GP4 suggests that the helicase may be inhibited or sequestered by bisQMAcr DNA ICLs. Benzo[α]pyrene lesions have been reported to inhibit T7GP4's translocation along DNA.[137, 138] A complex consisting of T7GP4 and bound dTTP was isolated, suggesting that the adducts sequestered T7GP4 with dTTP and was unable to be hydrolyzed to allow translocation along the DNA.[137] To determine whether bisQMAcr's ICLs inhibit T7GP4, non-radiolabeled bisQMAcr-treated OD15/OD16 was incubated with T7GP4 and dTTP for 10 min before addition of radiolabeled bisQMAcr-treated OD15/[^{32}P]-OD16 for 30 min (Figure 5.8A). T7GP4 unwound DNA containing bisQMAcr's ICLs in a time-dependent manner (Figure 5.8B, C). Crosslink unwinding proceeded with a yield of approximately 80% of the ICLs remaining intact, as opposed to 60% remaining intact in previous experiments (Figure 5.2B, C). Prior work has established that T7GP4 unwinds duplex DNA in a concentration-dependent manner.[141, 148] To confirm that the lower yield of crosslink hydrolysis results from an increased concentration of substrate DNA present in the preincubation experiment, T7GP4 and dTTP were incubated with 20 nM of bisQMAcr-treated OD15/[^{32}P]-OD16, compared with 10 nM in previous experiments (Figure 5.9A). T7GP4 unwound approximately 20% of the ICLs, with the remaining 80% of ICLs staying intact (Figure 5.9B, C). Thus, the increased concentration of substrate DNA accounts for the lower yield of ICLs unwound by T7GP4.

Figure 5.8 Preincubation of T7GP4 with OD15/[^{32}P]-OD16 containing bisQMAcr crosslinks in the presence and absence of dTTP. A) Scheme depicting the experimental setup. B) Unlabeled, preannealed OD15/OD16 (300 nM) in MES (10 mM, pH 7) and NaF (50 mM) was treated with bisQMAcr (250 μM) for 2 h at ambient temperature. Excess bisQMAcr and its low molecular weight products were removed with a P6 Micro-spin column. The unlabeled crosslinked OD15/OD16 (10 nM) that was recovered from the spin column was incubated in buffer (40 mM Tris-HCl pH 7.5, 10 mM MgCl$_2$, and 50 mM potassium glutamate) with T7GP4 (55 nM monomer concentration) at 37 ºC for 10 min in the presence or absence of dTTP (1 mM). dTTP (1 mM) was added to the sample that lacked dTTP during the preincubation and radiolabeled crosslinked OD15/[^{32}P]-OD16 (10 nM) was then added to all samples and samples were quenched after 0, 1, 5, 10, 20, and 30 min with EDTA (40 mM). Samples were separated by 10% denaturing PAGE and visualized by phosphorimagery. C) The data depicted in (B) were quantified and the amount of crosslink remaining was plotted over time. The amount of crosslink (%) was expressed relative to the total signal of DNA on the gel. Data from three separate trials of the experiment are reported, with bars representing the average of the data from the three independent experiments.

T7GP4 was not inhibited by bisQMAcr's crosslinks, since further unwinding occurred after the initial 10 min preincubation period. To rule out the possibility that T7GP4 is sequestered in a complex with bisQMAcr's ICL, T7GP4 was incubated with the unlabeled DNA in the presence or absence of dTTP for the initial 10 min preincubation period (Figure 5.8A). T7GP4 requires dTTP for its loading onto and translocation through single-stranded

Figure 5.9. Unwinding of 20 nM of DNA containing bisQMAcr crosslinks by T7GP4. A) Scheme depicting the experimental setup. B) Crosslinked OD15/[^{32}P]-OD16 (20 nM) was incubated with dTTP (1 mM) and T7GP4 (55 nM monomer concentration) at 37 ºC and samples were quenched after 0, 1, 5, 10, 20, and 30 min with EDTA (40 mM). Samples were separated by 10% denaturing PAGE and visualized by phosphorimagery. C) The data depicted in (B) were quantified and the amount of crosslink remaining was plotted over time. The amount of crosslink (%) was expressed relative to the total signal of DNA on the gel. Data from three separate trials of the experiment are reported, with bars representing the average of the data from the three independent experiments.

DNA.[149, 150] Comparing differences in ICL unwinding in the presence and absence of dTTP

in the preincubation may determine whether or not T7GP4 is sequestered as a complex with

the ICL. Preincubation in the absence of dTTP will prevent loading of T7GP4 onto the DNA

containing ICLs, while preincubation in the presence of dTTP will permit T7GP4's loading

onto the DNA. T7GP4 unwound 40% of bisQMAcr's ICLs in OD15/[^{32}P]-OD16 in both the

presence and absence of dTTP during the initial preincubation (Figure 5.8B, C). These data

suggest that T7GP4 is not sequestered since unwinding occurs with the same yield regardless of whether T7GP4 was loaded onto the unlabeled OD15/OD16 bisQMAcr ICLs or not.

Our data rule out limitations resulting from dTTP, enzyme, and incubation time as causes for the dissociation of only 40% of bisQMAcr's ICLs by T7GP4's unwinding of duplex DNA. Additionally, T7GP4 is not inhibited or sequestered by the ICLs. Thus, there are likely multiple subpopulations of DNA containing bisQMAcr ICLs, some of which resist unwinding by T7GP4, while others permit unwinding. BisQMAcr displays a strong preference for alkylating reversibly at dGN7s, but may form a mixture of both reversible and irreversible DNA adducts.[37, 41] The subpopulations that permit unwinding may be bisQMAcr's reversible DNA adducts, while those that resist unwinding may be irreversible adducts. BisQMAcr may form irreversible adducts by reacting with dAN6, dGN1, or dGN2 (refer to Chapter 1, Scheme 1.4). BisQMAcr may either immediately form a mixture of reversible and irreversible adducts upon reacting with the DNA, or its reversible adducts may regenerate and evolve in a time-dependent manner to form irreversible adducts.[37] A possibility is that T7GP4 may promote the migration of reversible to irreversible adducts, which could prevent their helicase-mediated dissociation,. Although it is possible for bisQMAcr to react immediately to form a mixture of irreversible and reversible DNA adducts, bisQMAcr has been demonstrated to display a preference for forming adducts with dGN7.[41]

5.2.4 Failure to Unwind DNA Containing Irreversible Mechlorethamine Crosslinks by T7GP4

Based on the data obtained so far, we hypothesize that T7GP4 is able to unwind only bisQMAcr's reversible ICLs, but not its irreversible ICLs. To confirm that T7GP4 fails to separate irreversible ICLs, DNA containing irreversible ICLs was used as a substrate for T7GP4's unwinidng. The nitrogen mustard mechlorethamine (HN2) crosslinks DNA irreversibly by reacting at dGN7s.[152] OD15/[^{32}P]-OD16 was treated with HN2 before
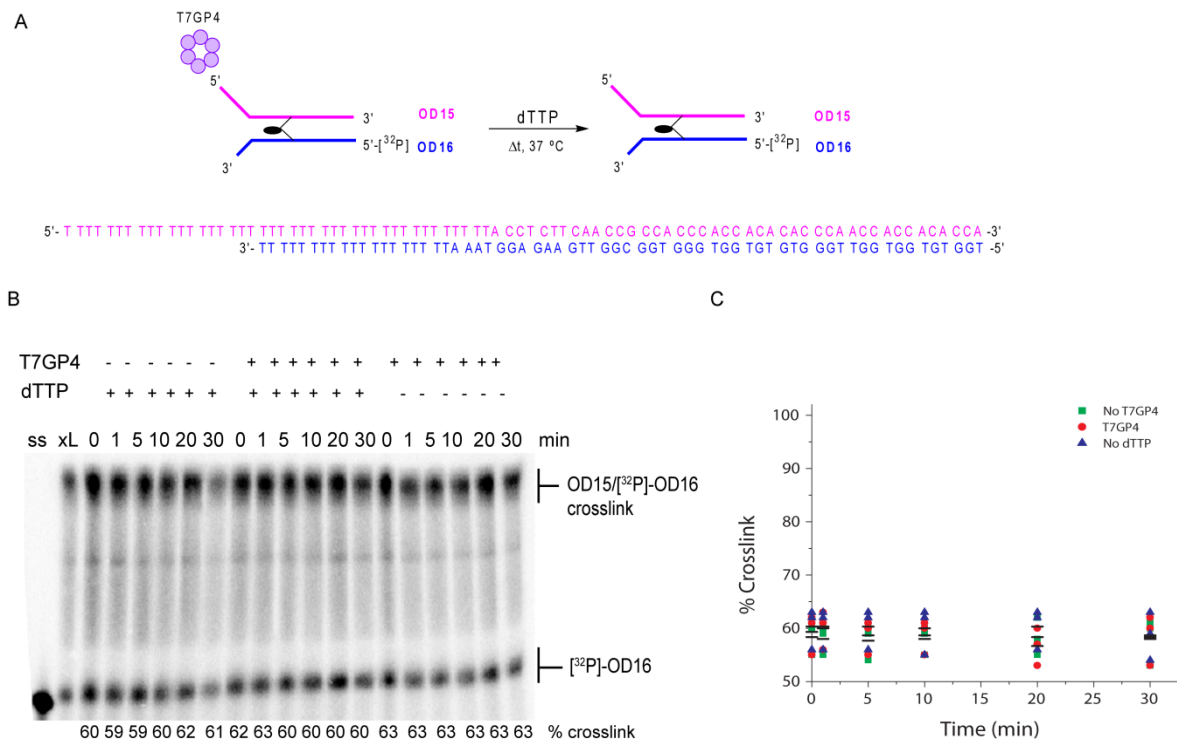
Figure 5.10 T7GP4 does not unwind DNA containing mechlorethamine crosslinks. A) Scheme depicting the experimental setup. B) Pre-annealed OD15/[^{32}P]-OD16 (300 nM) in potassium phosphate buffer (40 mM, pH 8) and NaCl (10 mM) was treated with mechlorethamine (5 mM) for 3 h at 37 °C. Excess mechlorethamine was removed with a P6 Micro-spin column. The resulting mixture containing duplex and crosslinked OD15/[^{32}P]-OD16 (10 nM) was incubated in buffer (40 mM Tris-HCl pH 7.5, 10 mM MgCl$_2$, and 50 mM potassium glutamate) with dTTP (1 mM) and T7GP4 (55 nM monomer concentration) at 37 °C and samples were quenched after 0, 1, 5, 10, 20, and 30 min with EDTA (40 mM). Samples were separated by 10% denaturing PAGE and visualized by phosphorimagery. C) The data depicted in (B) were quantified and the amount of crosslink remaining was plotted over time. The amount of crosslink (%) was expressed relative to the total signal of DNA on the gel. Data from three separate trials of the experiment are reported, with bars representing the average of the data from the three independent experiments.

incubation with T7GP4 and dTTP to determine whether T7GP4 unwinds DNA containing irreversible ICLs (Figure 5.10A). HN2 crosslinks OD15/[^{32}P]-OD16 less efficiently than bisQMAcr, generating a 60% yield of ICLs as opposed to the 100% yield formed with bisQMAcr (Figure 5.10B). Incubation with T7GP4 and dTTP did not change the yield of HN2's DNA ICLs over time (Figure 5.10B, C). T7GP4 fails to unwind DNA containing irreversible ICLs induced by HN2, as the ICLs do not dissociate to form single-stranded DNA after incubation with T7GP4. T7GP4 is only able to unwind reversible bisQMAcr DNA ICLs, but not irreversible HN2 ICLs. This result could be extrapolated to suggest that the subpopulations of bisQMAcr ICLs that are not unwound by T7GP4 constitute irreversible DNA ICLs formed by bisQMAcr.

Several irreversible DNA ICLs have been demonstrated to block DNA replication by preventing DNA synthesis by polymerases, while little evidence exists of the effect of reversible ICLs on the ability of helicases to unwind DNA. HN2 and psoralen's potency as chemotherapeutics is thought to arise from their capacity to block replication through their irreversible covalent chemistry with DNA.[153, 154] The specific contributions of helicases and polymerase *in vitro* to ICL's ability to inhibit replication have not been extensively developed. Our results suggest that ICLs prevent the action of helicases to unwind DNA during its replication, but only if the ICLs are irreversible. BisQMAcr's reversible chemistry likely permits dissociation of its crosslinks to single-stranded DNA by T7GP4 since we and reports in the literature have demonstrated the inability of helicases to separate irreversible ICLs. Neither supplementing DNA unwinding reactions with dTTP or T7GP4 nor increasing the incubation time permit consumption of the 60% of bisQMAcr's ICLs that resist unwinding. BisQMAcr's ICLs also do not inhibit T7GP4's ability to dissociate from DNA

containing irreversible ICLs and unwind other duplex DNA molecules. Our data suggest that bisQMAcr's ICLs that resist DNA unwinding are irreversible, since other possibilities have been ruled out as to why 60% of the ICLs remain intact. If bisQMAcr's irreversible ICLs do not dissociate to single-stranded DNA upon incubation with T7GP4, then it is likely that bisQMAcr's ICLs that do hydrolyze represent reversible DNA adducts.

5.2.5 Mechanism of Crosslink Dissociation

The mechanism for how T7GP4 achieves ICL dissociation remains to be uncovered. One mechanism of ICL dissociation could be hydrolysis of bisQMAcr's ICL from one DNA strand, while the other strand maintains a bisQMAcr adduct. The translocating and nontranslocating DNA strands were alternatively radiolabeled and treated with piperidine after incubation with T7GP4 to examine whether a loss of adducts is evident on either DNA strand (Scheme 5.11A). The heterogeneous OD13/OD14 sequences were utilized instead of OD15/OD16 because OD15 contains only a single G, which would at most lead to a single fragment following piperidine treatment. Furthermore, the DNA was treated with 50 μM, rather than 250 μM of bisQMAcr in order to minimize over-alkylation of the DNA. More than one adduct per DNA strand would complicate analysis of individual adducts after treatment with piperidine. No loss of fragments was evident using either radiolabeled OD13 or OD14 (Figure 5.11B, C). This result is inconsistent with the dissociation of ICLs that is evident from denaturing PAGE analysis that revealed distinct species corresponding to the ICL and single-stranded DNA (Figure 5.1B) This result would imply that bisQMAcr's dGN7 adducts are not lost from either the translocating or non-translocating DNA strands. Further,

the relative quantities of fragmentation at individual dGN7s did not change over time. However, comparison of the data to the background fragmentation that resulted from piperidine cleavage of DNA that was not treated with bisQMAcr indicates that the signal to noise ratio was too low properly to evaluate the data (Figure 5.11B, C).

As an alternate approach to determine how T7GP4 induces hydrolysis of BisQMAcr's ICLs, T7GP4's ability to cause the loss of monoQMAcr-DNA adducts was investigated. Loss of monoQMAcr adducts would indicate that T7GP4 causes QM adducts to dissociate from the DNA. A loss of monoQMAcr adducts from DNA will assess whether or not T7GP4 hydrolyzes QM-DNA adducts from a single strand of DNA, just as the experiment detailed in Figure 5.11A would have. However, the ease of detecting adducts is easier in this case due to a greater signal to noise ratio. Piperidine cleavage can occur if an abasic site is present in the DNA, resulting in high levels of background fragmentation. DNA containing monoQMAcr adducts migrates distinctly on denaturing PAGE from unmodified single-stranded DNA. Comparison of the profile of adducts evident on denaturing PAGE following incubation with T7GP4 can provide direct evidence of a loss of QM adducts from a particular DNA strand. $[^{32}P]$-OD15/OD16 was treated with monoQMAcr before incubation with T7GP4 and dTTP for 30 min to determine whether adducts are lost from the translocating strand (Figure 5.12A). Approximately 50% of monoQMAcr's DNA adducts were lost following incubation with T7GP4, as evidenced by the time-dependent disappearance of the more slowly migrating species and appearance of the more quickly migrating species corresponding to unmodified $[^{32}P]$-OD15 (Figure 5.12B, C). Alternatively, OD15/$[^{32}P]$-OD16 was treated with monoQMAcr before incubation with T7GP4 and dTTP for 30 min to determine whether adducts are also lost from the non-translocating strand.

A

5'- TT TTT TTT TTT TTT TTT TTT TTT TTT TTT TTT TTT TTT TTT TGG CAT GTC ACG ACG TTG TAA AAC GAC GGC CAG TGA ATT CGA GCT CGG TAC CCG GCG -3'
3'- TTT TTT TTT TTT TTT TTT TCC GTA CAG TGC TGC AAC ATT TTG CTG CCG GTC ACT TAA GCT CGA GCC ATG GGC CGC -5'

B

C

Figure 5.11 Piperidine cleavage of OD13/[^{32}P]-OD14 or [^{32}P]-OD13/OD14 containing bisQMAcr crosslinks after unwinding by T7GP4. A) Scheme depicting the experimental setup. Either B) OD13/[^{32}P]-OD14 (300 nM) or C) [^{32}P]-OD13/OD14 in MES (10 mM, pH 7.0) and NaF (10 mM) was treated with bisQMPAcr (50 μM) for 30 min, before excess QM was removed with a P6 spin column (1000 g, 4 min). Crosslinked OD13/OD14 (10 nM) was incubated in buffer (40 mM Tris-HCl pH 7.5, 10 mM MgCl$_2$, and 50 mM potassium glutamate) with dTTP (1 mM) and T7GP4 (55 nM monomer concentration) at 37 ºC and samples were quenched after 0, 1, 5, 10, 20, and 30 min with EDTA (40 mM). Samples were then treated with hot piperidine, separated by denaturing PAGE, and visualized by phosphorimagery.

T7GP4's unwinding of duplex DNA not only causes the loss of monoQMAcr adducts on the translocating strand, but also on the non-translocating strand (Figure 5.12D, E).

T7GP4's translocation along DNA affects the stability of monoQMAcr adducts on both strands of the duplex. T7GP4 translocates along a single strand of DNA by passing the DNA through a central channel formed by its 6 monomers that assemble into a ring-like hexamer.[155] Passage of the DNA containing monoQMAcr adducts through the central channel may assist in hydrolysis of the QM from its DNA-adducts by providing a mechanical force that facilitates bond cleavage. The adducts may not fit within the steric constraints of the channel, which may contribute to bond cleavage that hydrolyzes the QM from the DNA. T7GP4 also interacts with the non-translocating strand through hydrophobic interactions with a phenylalanine residue that exclude the strand from entering the central channel.[18, 25] The dynamic hydrophobic DNA-protein interactions that occur with the phenylalanine on the non-translocating strand during T7GP4's translocation may contribute to the loss of monoQMAcr adducts on the non-translocating strand.

The loss of monoQMAcr adducts on both DNA strands suggests a potential mechanism for how T7GP4 mediates dissociation of bisQMAcr's DNA ICLs (Scheme 5.2). T7GP4 binds a 5'-single-stranded DNA tail and translocates along the DNA until encountering a bisQMAcr ICL. T7GP4's translocation likely leads to loss of the QM-DNA adduct from the translocating strand by cleavage of the bond between the QM and dGN7. The regenerated QM intermediate likely then reacts with a water molecule, before dissociation QM-DNA adduct from the non-translocating strand and subsequent reaction with water. T7GP4 can complete its translocation along the DNA to fully unwind the duplex DNA, resulting in two single-strands of DNA and the bisQMAcr-H_2O adduct. Meanwhile,

Figure 5.12 Loss of monoQMAcr-DNA adducts induced by T7GP4. A) Scheme depicting the experimental setup. B) Alkylated [^{32}P]-OD15/OD16 (10 nM) was incubated with dTTP (1 mM) and T7GP4 (55 nM monomer concentration) at 37 ºC and samples were quenched after 0, 1, 5, 10, 20, and 30 min with EDTA. Samples were separated by 10% denaturing PAGE and visualized by phosphorimagery. C) The time-dependent unwinding of alkylated [^{32}P]-OD15/OD16 depicted in (B) was quantified and the amount of alkylated DNA remaining was plotted over time. The amount of alkylated DNA (%) was expressed relative to the total signal of DNA on the gel. Data from three separate trials of the experiment are reported, with bars representing the average of the three independent experiments. D) Time-dependent unwinding of monoQMAcr alkylated OD15/[^{32}P]-OD16 was performed analogously to the experiment described in (B). E) Quantification of the data from Figure (C) was performed analogously to that described in (C).

T7GP4 likely dissociates from the duplex DNA upon encountering an irreversible QM-DNA adduct, as its translocation along the DNA will not be able to dissociate an irreversible ICL. Ongoing experiments seek to confirm the loss of the QM from the DNA and the formation of the QM-H_2O adduct by quantifying the time-dependent generation of the QM-H_2O adduct via UPLC-MS. Achieving this result would provide further support for our proposed mechanism of crosslink dissociation.
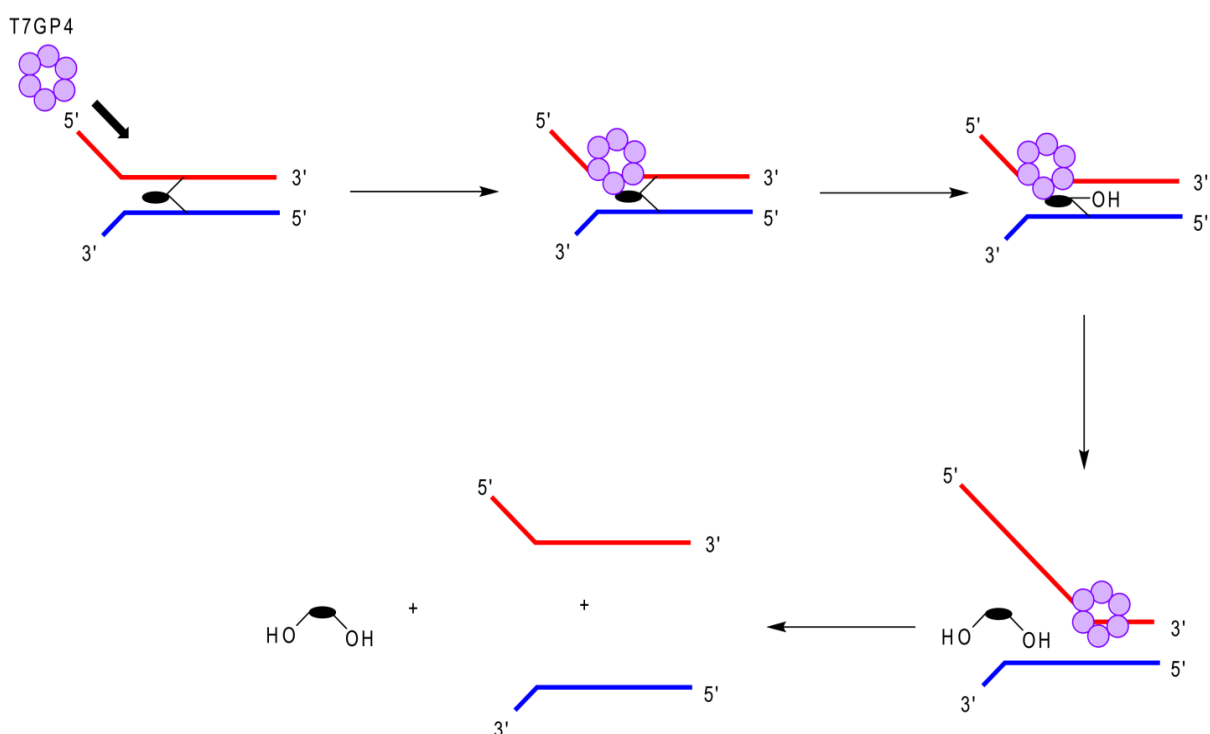
Scheme 5.2 A proposed mechanism for T7GP4's dissociation of bisQMAcr's DNA ICLs.

5.3 Summary

T7GP4 causes some of bisQMAcr's DNA ICLs to dissociate when it unwinds duplex DNA that contains bisQMAcr ICLs. Crosslink hydrolysis by T7GP4 depends on the presence

of dTTP, which suggests T7GP4's translocation along DNA results in ICL dissociation. There does not appear to be sequence dependence for crosslink consumption by T7GP4, as incubation with T7GP4 led to the dissociation of bisQMAcr ICLs in two different DNA sequences. However, only 40% of bisQMAcr's ICLs separated into single-stranded DNA, while the other 60% of the ICLs remained intact and resisted unwinding by T7GP4. Multiple subpopulations of DNA containing bisQMAcr ICLs likely exist because neither increasing the concentrations of dTTP or T7GP4 nor increasing the incubation time improved the yield of ICL unwinding. Furthermore, T7GP4 was not sequestered by bisQMAcr's DNA ICL, as preincubation with unlabeled DNA containing bisQMAcr's ICL did not affect T7GP4's unwinding activity. BisQMAcr likely forms a mixture of reversible and irreversible DNA ICLs, where the reversible ICLs permit unwinding and the irreversible ICLs resist unwinding. T7GP4 is unable to unwind DNA containing irreversible ICLs formed by the nitrogen mustard mechlorethamine, which lends support to the notion that irreversible bisQMAcr ICLs may resist unwinding.

T7GP4 likely causes bisQMAcr's ICLs to dissociate by first removing the adduct from the translocating strand by facilitating regeneration of one of bisQMAcr's electrophile. The QM likely reacts with a water molecule before the lesion on the non-translocating strand is removed. This would then allow T7GP4 to complete its translocation along the DNA, while generating the bisQMAcr-H_2O adduct. Our results suggest that reversible DNA ICLs may not pose a replication block, at least for DNA helicases. Helicase unwinding of reversible ICLs may represent a means by which reversible DNA lesions can be repaired without relying on specific DNA repair enzymes to process the damaged DNA. QMs generated from the metabolism of toxins may pose little damage to cells if helicases can

remove their reversible lesions from DNA. It remains to be seen whether all hexameric helicases can dissociate bisQMAcr's ICLs, or whether T7GP4 is unique in that respect.

5.4 Materials and Methods

5.4.1 Materials

General Materials. Oligonucleotides (desalted) were synthesized by Integrated DNA Technologies (IDT) and PAGE purified prior to use. BisQMPAcr was prepared as described previously,[40] and monoQMPAcr was a gift from Blessing Deeyaa. [53] Oligonucleotides were radiolabeled on their 5'-terminus as described in Chapter 2. M13mp18 single-stranded DNA (250 µg/mL) and NiCo21(DE3) competent cells were purchased from New England Biolabs. γ-^{32}P-ATP and α-^{32}P-dTTP were purchased from Perkin Elmer. PEI-cellulose coated TLC plates (20 x 20 cm, 100 µm layer thickness), 5'-ATP agarose resin (catalog number A2767), and dTTP (sodium salt solution, PCR grade) were purchased from Sigma-Aldrich. P6 Micro Bio-Spin columns and Bradford reagent were purchased from Bio-Rad. HisPur™ Ni-NTA resin was purchased from ThermoFisher Scientific. Amicon Ultra centrifugal filters with a 10,000 molecular weight cutoff were purchased from Millipore. The plasmid harboring the gene for the 56 kDa fragment of T7GP4 was a gift from Prof. Charles Richardson. Dr. Seung-Joo Lee from the Richardson Lab provided helpful suggestions to troubleshoot the purification of T7GP4.

5.4.2 Methods

General Methods. Detection and quantification of radiolabeled oligonucleotides was carried out using a Typhoon 9410 phosphorimager equipped with ImageQuant TL software.

Products were quantified and yields were reported (%) relative to total labeled DNA. The concentrations of all oligonucleotides were calculated from their absorption at 260 nm and their extinction coefficients that were provided by the manufacturer. Protein concentration was determined by its absorbance at 595 nm after the addition of Bradford reagent. DNA was treated with hot piperidine as described in Chapter 2.

Overexpression and purification of T7GP4. Overexpression and purification was adapted from a previous protocol.[15] The plasmid pET19-56-Kan) containing a gene fusion of His_{10} and the 56 kDa fragment of T7GP4 was described previously.[142] The plasmid was transformed into *E.Coli* NiCo21(DE3) chemically competent cells on media supplemented with kanamycin (50 µg/mL). Cultures were grown in LB media (1 L) supplemented with kanamycin (50 µg/mL) at 37 ºC with vigorous shaking (220 rpm) until they reached an OD_{600} of ~ 1. Expression of T7GP4 was induced with isopropyl-β-D-thiogalactopyranoside at a final concentration of 1 mM at 37 ºC for 3 h with vigorous shaking (220 rpm). Cells were harvested by centrifugation (5000 rpm for 15 min, 4 ºC), flash frozen in liquid N_2, and stored at -80 ºC until use.

Frozen cell pellets were thawed on ice and resuspended in 20 mL of Ni-NTA wash buffer 1 (50 mM potassium phosphate pH 8, 500 mM NaCl, 10 mM imidazole). Lysozyme was added to a final concentration of 100 µg/mL and the cells were incubated on ice for 1 h. Cells were lysed by three rounds of flash freezing in liquid nitrogen and thawing on ice. Cell debris was removed by centrifugation (35,000 g for 1 h, 4 ºC) and the resulting supernatant was applied by gravity to a column containing 1 mL of HisPur™ nickel-nitroloacetic acid resin. The column was washed with 30 mL of Ni-NTA wash buffer 1 followed by 20 mL of

Ni-NTA wash buffer 2 (50 mM potassium phosphate pH 8, 500 mM NaCl, 100 mM imidazole). The protein was then eluted with Ni-NTA elution buffer (50 mM potassium phosphate pH 8, 500 mM NaCl, 500 mM imidazole). The protein was desalted to remove imidazole using a GE PD-10 spin column (1000 g, 2 min, 4 ºC) equilibrated with ATP-agarose wash buffer (20 mM potassium phosphate pH 6.8, 0.5 mM DTT, 10% glycerol, 500 mM KCl, and 10 mM MgCl$_2$.

The desalted protein was applied by gravity to a column containing 0.5 mL of ATP-agarose resin.[139] The column was washed with 10 mL of ATP-agarose wash buffer. Impurities resulting from proteolytic cleavage at the linker connecting the primase and helicase domains were eluted first with ATP-agarose elution buffer (20 mM potassium phosphate pH 6.8, 0.5 mM DTT, 20 mM EDTA, 10% glycerol, and 500 mM KCl). Pure T7GP4 was eluted by increasing the concentration of KCl to 1 M. Protein was concentrated to 200 µL with an Amicon Ultra-centrifugal filter with molecule weight cut-off of 10,000 kDa. The protein was washed three times with 500 µL of H$_2$O in the filter to dilute the salt concentration, and then further diluted with glycerol and potassium phosphate pH 7.5 to a final concentration of 50% glycerol and 20 mM potassium phosphate. Protein purity was determined by SDS-PAGE analysis and staining with Coomassie Blue.

Crosslinking of Preannealed Duplex DNA with BisQMAcr. Duplex DNA was annealed by combining a labeled 5'-[^{32}P]-oligonucleotide (300 nM) and its complement (300 nM) in MES (10 mM, pH 7) and NaF (50 mM), heating the solution at 95 ºC for 2 min and subsequently cooling slowly to ambient temperature. BisQMPAcr in acetonitrile was then added to the mixture above to generate a final solution of 20 µL that contained 20%

acetonitrile and 250 µM of bisQMPAcr. The reaction was incubated at ambient temperature for 2 h. Excess bisQMAcr and its low molecular weight products were removed from the DNA with a Bio-Rad P6 Micro Bio-Spin column prewashed with water (1000 g, 4 min). The eluent was stored at -20 ºC until use.

Unwinding of Unmodified Duplex DNA by T7GP4.[14] A duplex DNA substrate containing noncomplementary single-stranded tails was prepared by annealing 5'-^{32}P-labeled DNA to its complement, as described above. The indicated amounts of T7GP4 (in 50% glycerol, 20 mM potassium phosphate, pH 7.5) were added to the DNA substrate (10 nM) in a buffer containing 40 mM Tris-HCl pH 7.5, 10 mM $MgCl_2$, 50 mM potassium glutamate, and 1 mM dTTP. Samples (10 µL) were incubated at 37 ºC for 10 min. The reaction was terminated by the addition of EDTA to a final concentration of 40 mM (1 µL) and 30% glycerol loading buffer containing bromophenol blue and xylene cyanol (4 µL). Aliquots of each sample (4 µL) were loaded onto a gel (10 x 8 x 0.15 cm) and separated by 10% nondenaturing PAGE (0.5 x TBE, 60 V, 2.5 h).

Unwinding of Crosslinked DNA by T7GP4. The experiment was conducted as described above, but using crosslinked DNA. Samples were combined with bromophenol blue and xylene cyanol in formamide (10 µL) for separation by 10% denaturing PAGE.

Crosslinking of Preannealed Duplex DNA with HN2. Duplex DNA was annealed by combining a labeled 5'-[^{32}P]-oligonucleotide (300 nM) and its complement (300 nM) in potassium phosphate (40 mM, pH 8) and NaCl (10 mM), heating the solution at 95 ºC for 2 min and subsequently cooling slowly to ambient temperature. HN2 (from a fresh solution in

40 mM potassium phosphate buffer, pH 8) was then added to the mixture above to a final

concentration of 5 mM. The reaction was incubated at 37 ºC for 3 h. Excess HN2 and its low

molecular weight products were removed from the DNA with a Bio-Rad P6 Micro Bio-Spin

column prewashed with water (1000 g, 4 min). The eluent was stored at -20 ºC until use.

Hydrolysis of dTTP by T7GP4.[140] T7GP4 (55 nM monomer concentration, 2 µL, in 50%

glycerol, 20 mM Tris-HCl pH 7.5) was added to crosslinked OD1-39T/ OD4L-19T (10 nM)

in a buffer containing 40 mM Tris-HCl pH 7.5, 10 mM $MgCl_2$, 50 mM potassium glutamate,

and 1 mM [α-^{32}P]-dTTP (0.1 µCi). Samples (10 µL) were incubated at 37 ºC and quenched at

the indicated times by the addition of 10% formic acid (10 µL). Aliquots (1 µL) of each

sample were spotted onto a PEI-cellulose TLC plate for separation. The TLC plate was

developed with a solution containing 0.5 M formic acid and 0.5 M LiCl for 1.5 h. The plate

was dried, exposed to a phosporimaging cassette for 1 h, and visualized by phosphorimagery.

Chapter 6: Conclusions

The environment contains numerous compounds that generate electrophiles upon metabolic activation. Pollutants, food additives, products of combustion, and drugs can alkylate DNA's nucleobases following their activation from metabolism. The lesions produced by these alkylating agents may prevent replication of DNA and suppress gene expression. Accumulation of adducts within DNA may also result in DNA mutations and initiate the progression of cancer. Achieving an understanding of the toxicology of naturally occurring alkylating agents is necessary to determine the role of environmental electrophiles in mutagenesis and disease progression. However, not all alkylating agents react irreversibly with DNA, as some agents form lesions that are intrinsically reversible. Reversible lesions may not necessarily exhibit the same toxicity as irreversible adducts, since their intrinsic chemistry may afford spontaneous repair of their own adducts. This dissertation investigated QMs as a model for reversible DNA alkylation to evaluate the consequences of this dynamic system in biology.

BisQMAcr had previously been demonstrated to migrate along DNA, albeit too slowly to be effective *in vivo*. DiQMs linked to alkylammonium chains and bisQMs conjugated to quinoxlines were synthesized in order to enhance the rate of QM migration along DNA to be relevant under physiological conditions. Neither diQMN$_3$ nor bisQMQuins1-4 migrated along DNA, as their binding precluded dynamic DNA alkylation. Polyammonium groups directed diQMN$_3$ to bind in the minor groove and react with the accessible nucleophiles that form irreversible QM-DNA adducts, while the quinoxalines may have bound DNA too weakly to afford significant yields of ICLs. DiQMs possessed

increased conformational flexibility relative to bisQMs and predominantly formed monoadducts rather than ICLs with DNA. The conformational flexibility of diQMs may be well-suited for future evaluation as DNA-protein crosslinking agents, since coupling to bouth targets may require conformational freedom. A delicate balance between strong binding to DNA and reaction with nucleophiles that form reversible adducts must be achieved to successfully design a bifunctional QM capable of quickly migrating along duplex DNA. DiQMN$_3$ likely bound DNA in the minor groove where it predominantly formed irreversible DNA-adducts. On the other hand, the bisQMQuins likely bound in a conformation that delivered the QMs to the major groove where they could react reversibly with DNA. However, the bisQMQuins may have bound too weakly to afford high yields of crosslinks. BisQMAcr binds strongly enough and in the major groove to produce high yields of reversible DNA ICLs, but still manages to dissociate from the DNA in order to traverse the duplex DNA. BisQMAcr represents the best QM to investigate the biological consequences of dynamic alkylation even though it required 7 days to migrate.

Although BisQMAcr's dynamic DNA alkylation was demonstrated using DNA free in solution, this does not represent DNA as is found in cells. DNA is packaged around an octamer of the four core histone proteins to form nucleosomes in order to fit the constraints of a cell. The true potency of a DNA alkylating agent in a cell should include evaluation by determining its efficiency of alkylation with DNA packaged in the NCP. BisQMAcr's potency for alkylation decreases by 90% with the DNA in the NCP relative to DNA free in solution, illustrating a protective function of NCP assembly. NCPs further protect against QM-DNA damage by serving as terminal acceptors of bisQMAcr's DNA adducts, restoring the DNA to its unmodified state once bisQMAcr spontaneously releases from the DNA.

BisQMAcr adducts on the histones do not prevent formation of nucleosomes as bisQMAcr's histone adducts do not impair assembly of the NCP. This effect differs from suppressed NCP formation that occurs using alkylated DNA. Consequently, QMs formed from metabolic activation in the body may not significantly affect regulation of the genome, at least at the level of DNA packaging, since few DNA adducts will form in the NCP and histone adducts will not impair formation of new nucleosomes. The greatest yield of bisQMAcr's alkylation *in vivo* will likely occur on histone-free DNA, either in the linker DNA connecting nucleosomes or during DNA replication. Even if bisQMAcr alkylates histone-free DNA, the DNA can be repaired by transfer of the QM's adducts to nearby histone proteins. BisQMAcr previously appeared to represent a promising example of a potential strategy for designing new chemotherapeutic alkylating agents based on its efficiency of dynamic alkylation of DNA free in solution. However, the significant suppression of its DNA alkylation with DNA in the NCP discounts its efficacy as a potential drug. Rather, our results suggest that QMs that form naturally as toxins may not cause as much harm as once thought, since their DNA adducts can be captured by the histone proteins. Whether this phenomenon extends to other reversible alkylating agents remains to be determined.

The significant suppression of bisQMAcr's DNA alkylation with DNA packaged in the NCP relative to DNA free in solution suggests that bisQMAcr may have a pronounced effect on histone-free DNA. DNA is free from the protective functions of the nucleosome during its replication. BisQMAcr's DNA crosslinks may affect the activity of the processive proteins that function to replicate DNA, namely polymerases and helicases. Polymerases and helicases were postulated to hasten bisQMAcr's migration through DNA based on a mechanical force applied to reversible bisQMAcr-DNA adducts. The T7GP4 DNA helicase,

but not the Klenow Exo⁻ and φ29 DNA polymerases, induced dissociation of bisQMAcr's DNA ICLs during its translocation along DNA. The polymerases likely stalled at sites near bisQMAcr's adducts and dissociated from the DNA upon failure to bypass the lesions. BisQMAcr's DNA ICLs may pose a roadblock to the primer extension activity of DNA polymerases and prevent DNA replication.

Interestingly, DNA helicases unwind DNA before polymerases initiate synthesis, and will likely break reversible QM-DNA ICLs before the polymerase initiates its activity. Thus, the evolutionary role of helicases acting on DNA before polymerases may facilitate DNA replication in the presence of reversible DNA ICLs. Dissociation of reversible DNA ICLs by helicases represents a second mechanism by which the reversibility of bisQMAcr's chemistry with DNA enables repair of its adducts. Furthermore, our observation that DNA helicases dissociate bisQMAcr's reversible DNA ICLs challenges the paradigm that the severe toxicity of DNA ICLs to cells derives from their ability to block DNA replication. Our data, while specific to bisQMAcr and T7GP4, suggests that reversible DNA adducts, unlike irreversible adducts, may not inhibit DNA replication by preventing separation of DNA's strands.

The work presented in this dissertation uncovered several mechanisms by which reversible QM-DNA adducts are repaired during the packaging and processing of DNA by the histone proteins and DNA helicases. Reversible QMs may lead to reduced toxicity for cells than irreversible alkylating agents due to the reduction in their potency of DNA alkylation that results from their reversible chemistry. QMs formed as undesired byproducts of metabolism, such as the QM formed from oxidation of BHT, may not induce toxicity to cells, since their adducts should not resist unwinding by DNA helicases and will not preclude DNA replication. Future efforts can be directed towards understanding the properties that

permit DNA helicases to break apart bisQMAcr's reversible DNA ICLs. Presumably, the force generated by helicases during their translocation may facilitate cleavage of the bond formed between bisQMAcr and dGN7, but would need to be verified experimentally. Additionally, the generality of bisQMAcr's ICL dissociation by helicases could be established by examining whether other hexameric helicases, such as DnaB from *E.coli*, are also able to break reversible ICLs. T7GP4 belongs to helicase superfamily 4, but helicases from the other five superfamilies could be evaluated for their ability to break apart bisQMAcr's revesible ICLs to further generalize the phenomenon of crosslink unwinding. Helicases across different superfamilies differ in their sequence motifs, polarity of translocation, ring structure, and preference for translocating along duplex or single-stranded DNA. How the characteristics of helicases in each superfamily affect their ability to break apart bisQMAcr's ICLs could be evaluated more comprehensively to understand the mechanistic basis of how T7GP4 dissociates reversible bisQMAcr ICLs. Our work has provided a glimpse into how QM's reversible alkylation will affect biochemical processes within the cell. However, determining the consequences of bisQMAcr's alkylation in vivo and its potential effect on cellular fitness represents the next step towards elucidating the toxicology of QMs and whether their adducts contribute to carcinogenesis.

References

1. Barnes, J. L.; Zubair, M.; John, K.; Poirier, M. C.; Martin, F. L., Carcinogens and DNA damage. *Biochem. Soc. Trans.* **2018,** 46, 1213-1224.
2. Perera, F.; Tang, D.; Whyatt, R.; Lederman, S. A., DNA Damage from Polycyclic Aromatic Hydrocarbons Measured by Benzo[α]pyrene-DNA Adducts in Mothers and Newborns from Northern Manhattan , The World Trade Center Area , Poland , and China. *Cancer Epidemiology, Biomarkers & Prevention* **2005,** 14, 709-714.
3. Ewa, B.; Danuta, M.-S., Polycyclic aromatic hydrocarbons and PAH-related DNA adducts. *J Appl Genetics* **2017,** 58, 321-330.
4. Sinha, R. P.; Häder, D.-P., UV-induced DNA damage and repair: a review. *Photochem. Photobiol. Sci.* **2002,** 1, 225-236.
5. Sachs, R. K.; Chen, P.-L.; Hahnfeldt, P. J.; Hlatky, L. R., DNA Damage Caused by Ionizing Radiation. *Mathematical Biosciences* **1992,** 112, 271-303.
6. Lomax, M. E.; Folkes, L. K.; Neill, P. O., Biological Consequences of Radiation-induced DNA Damage: Relevance to Radiotherapy Statement of Search Strategies Used and Sources of Information Why Radiation Damage is More Effective than Endogenous Damage at Killing Cells Ionising Radiation-induced Double-strand. *Clinical Oncology* **2013,** 25, 578-585.
7. Zhang, J.; Stevens, M. F. G.; Bradshaw, T. D., Temozolomide : Mechanisms of Action , Repair and Resistance. *Curr. Mol. Pharm.* **2012,** 5, 102-114.
8. Yoon, J.-H.; Lee, C.-S., Sequence Specificity for DNA Interstrand Cross-linking Induced by Anticancer Drug Chiorambucil. *Arch. Pharm. Res.* **1997,** 20, 550-554.
9. Shrivastav, N.; Li, D.; Essigmann, J. M., Chemical biology of mutagenesis and DNA repair: Cellular responses to DNA alkylation. *Carcinogenesis* **2009,** 31, 59-70.
10. Schroeder, G. K.; Lad, C.; Wyman, P.; Williams, N. H.; Wolfenden, R., The time required for water attack at the phosphorus atom of simple phosphodiesters and of DNA. *Proc. Natl. Acad. Sci. USA* **2006,** 103, 4052-4055.
11. Cheng, K. C.; Cahill, D. S.; Kasai, H.; Nishimura, S.; Loeb, L. A., 8-Hydroxyguanine, an Abundant Form of Oxidative DNA Damage, Causes G → T and A → C Substitutions. *J. Biol. Chem.* **1992,** 267, 166-172.
12. Deans, A. J.; West, S. C., DNA interstrand crosslink repair and cancer. *Nat. Rev. Cancer* **2011,** 11, 467-480.
13. Rajski, S. R.; Williams, R. M., DNA Cross-Linking Agents as Antitumor Drugs. *Chem. Rev.* **1998,** 98, 2723-2796.
14. Kreutzer, D. A.; Essigmann, J. M., Oxidized , deaminated cytosines are a source of C to T transitions in vivo. *Proc. Natl. Acad. Sci. USA* **1998,** 95, 3578-3582.
15. Ignatov, A. V.; Bondarenko, K. A.; Makarova, A. V., Non-bulky Lesions in Human DNA: The Ways of Formation, Repair, and Replication. *Acta Naturae* **2017,** 9, 12-26.
16. Mishina, Y.; Duguid, E. M.; He, C., Direct Reversal of DNA Alkylation Damage. *Chem. Rev.* **2006,** 106, 215-232.
17. Stivers, J. T.; Jiang, Y. L., A Mechanistic Perspective on the Chemistry of DNA Repair Glycosylases. *Chem. Rev.* **2003,** 103, 2729-2759.

18. Kisker, C.; Kuper, J.; Houten, B. V., Prokaryotic Nucleotide Excision Repair. *Cold Spring Harb. Perspect. Biol.* **2013,** 5, a012591.

19. Noll, D. M.; McGregor Mason, T.; Miller, P. S., Formation and repair of interstrand cross-links in DNA. *Chem. Rev.* **2006,** 106, 277-301.

20. Clauson, C.; Schärer, O. D.; Niedernhofer, L., Advances in understanding the complex mechanisms of DNA interstrand cross-link repair. *Cold Spring Harb. Perspect. Biol.* **2013,** 5, a012732.

21. Stingele, J.; Bellelli, R.; Boulton, S. J., Mechanisms of DNA–protein crosslink repair. *Nat. Rev. Mol. Cell Biol.* **2017,** 18, 563-573.

22. Rink, S. M.; Solomon, M. S.; Taylor, M. J.; Rajur, S. B.; Mclaughlin, L. W.; Hopkins, P. B., Covalent structure of a nitrogen mustard-induced DNA interstrand cross-link: An N7 to N7 linkage of deoxyguanosine residues at the duplex sequence 5'-d(GNC). *J. Am. Chem. Soc.* **1993,** 115, 2551-2557.

23. Tomasz, M., Mitomycin C: small, fast and deadly (but very selective). *Chem. Biol.* **1995,** 2, 575-579.

24. Tomasz, M.; Chawla, A. K.; Lipman, R., Mechanism of monofunctional and bifunctional alkylation of DNA by mitomycin C. *Biochemistry* **1988,** 27, 3182-3187.

25. Zewail-Foote, M.; Hurley, L. H., Differential rates of reversibility of Ecteinascidin 743 - DNA covalent adducts from different sequences lead to migration to favored bonding sites. *J. Am. Chem. Soc.* **2001,** 123, 6485-6495.

26. Kozekov, I. D.; Nechev, L. V.; Sanchez, A.; Harris, C. M.; Lloyd, R. S.; Harris, T. M., Interchain cross-linking of DNA mediated by the principal adduct of acrolein. *Chem. Res. Toxicol.* **2001,** 12, 1482-1485.

27. Stevens, J. F.; Maier, C. S., Acrolein: Sources, metabolism, and biomolecular interactions relevant to human health and disease. *Mol. Nutr. Food Res.* **2008,** 52, 7-25.

28. Pawłowicz, A. J.; Munter, T.; Zhao, Y.; Kronberg, L., Formation of acrolein adducts with 2′ -deoxyadenosine in calf thymus DNA. *Chem. Res. Toxicol.* **2006,** 19, 571-576.

29. Wang, H. T.; Hu, Y.; Tong, D.; Huang, J.; Gu, L.; Wu, X. R.; Chung, F. L.; Li, G. M.; Tang, M. S., Effect of carcinogenic acrolein on DNA repair and mutagenic susceptibility. *J. Biol. Chem.* **2012**, 287, 12379-12386.

30. Tang, M. S.; Wang, H. T.; Hu, Y.; Chen, W. S.; Akao, M.; Feng, Z.; Hu, W., Acrolein induced DNA damage, mutagenicity and effect on DNA repair. *Mol. Nutr. Food Res.* **2011,** 55, 1291-1300.

31. *Quinone Methides* (Rokita, S.E., Ed.) **2009**. John Wiley & Sons, Inc., Hoboken, NJ.

32. Marques, M. M.; Beland, F. A., Identification of tamoxifen-DNA adducts formed by 4-hydroxytamoxifen quinone methide. *Carcinogenesis* **1997,** 18, 1949-1954.

33. Hulsman, N.; Medema, J. P.; Bos, C.; Jongejan, A.; Leurs, R.; Smit, M. J.; Esch, I. J. P. D.; Richel, D.; Wijtmans, M., Chemical insights in the concept of hybrid drugs : the antitumor effect of nitric oxide-donating aspirin involves a quinone methide but not nitric oxide nor Aspirin. *Chem. Res. Toxicol.* **2007,** 50, 2424-2431.

34. Takahashi, O.; Hiraga, K., The role of 2,6-di-tert-butyl-4-methylene-2,5-cyclohexadienone (BHT quinone methide) in the metabolism of butylated hydroxytoluene. *Food Chem. Toxicol.* **1983,** 21, 279-283.

35. Bolton, J. L.; Sevestre, H.; Ibe, B. O.; Thompson, J. A., Formation and reactivity of alternative quinone methides from butylated hydroxytoluene : possible explanation for species-specific pneumotoxicity. *Chem. Res. Toxicol.***1990,** 3, 65-70.

36. Percivalle, C.; Doria, F.; Freccero, M., Quinone Methides as DNA Alkylating Agents: An Overview on Efficient Activation Protocols for Enhanced Target Selectivity. *Curr. Org. Chem.* **2014,** 18, 19-43.

37. Weinert, E. E.; Frankenfield, K. N.; Rokita, S. E., Time-dependent evolution of adducts formed between deoxynucleosides and a model quinone methide. *Chem. Res. Toxicol.* **2005,** 18, 1364-1370.

38. Weinert, E. E. Quinone Methide Alkylation of DNA: Understanding Reactivity through Reversibility, Trapping, and Substituent Effects. University of Maryland, College Park, MD, 2006.

39. Zeng, Q.; Rokita, S. E., Tandem quinone methide generation for cross-linking DNA. *J. Org. Chem.* **1996,** 61, 9080-9081.

40. Veldhuyzen, W. F.; Pande, P.; Rokita, S. E., A transient product of DNA alkylation can be stabilized by binding localization. *J. Am. Chem. Soc.* **2003,** 125, 14005-14013.

41. Fakhari, F.; Rokita, S. E., A walk along DNA using bipedal migration of a dynamic and covalent crosslinker. *Nat. Commun.* **2014,** 5, 5591.

42. Wang, H.; Wahi, M. S.; Rokita, S. E., Immortalizing a transient electrophile for DNA cross-linking. *Angew. Chem. Int. Ed.* **2008,** 47, 1291-1293.

43. Wang, H.; Rokita, S. E., Dynamic cross-linking is retained in duplex DNA after multiple exchanges of strands. *Angew. Chem. Int. Ed.* **2010,** 49, (34), 5957-5960.

44. Weinert, E. E.; Dondi, R.; Colloredo-melz, S.; Frankenfield, K. N.; Charles, H.; Freccero, M.; Rokita, S. E., Quinone Methide Substituents Strongly Modulate the Formation and Stability of Its Nucleophilic Adducts. *J. Am. Chem. Soc.* **2006,** 128, 11940-11947.

45. Hutchinson, M. A.; Development of Bifunctional Alkylating Agents for Association and Migration along DNA. Johns Hopkins University, Baltimore, MD, 2016.

46. Hutchinson, M.A.; Deeyaa, B.; Byrne, S.R.; Williams, S.; Rokita, S.E.; Directing Quinone Methide-Dependent Alkylation and Cross-Linking of Nucleic Acids with Quaternary Amines. *In Preparation*.

47. Gold, B.; Marky, L. M.; Stone, M. P.; Williams, L. D., A Review of the Role of the Sequence-Dependent Electrostatic Landscape in DNA Alkylation Patterns. *Chem. Res. Toxicol.* **2006,** 19, 1402-1414.

48. Song, Z.; Weng, X.; Weng, L.; Huang, J.; Wang, X.; Bai, M.; Zhou, Y.; Yang, G.; Zhou, X., Synthesis and oxidation-induced DNA cross-linking capabilities of bis(catechol) quaternary ammonium derivatives. *Chem. Eur. J.* **2008,** 14, 5751-5754.

49. Bai, M.; Huang, J.; Zheng, X.; Song, Z.; Tang, M., Highly Selective Suppression of Melanoma Cells by Inducible DNA Cross-Linking Agents: Bis (catechol) Derivatives. *J. Am. Chem. Soc.* **2010,** 132, 15321-15327.

50. Wang, P.; Liu, R.; Wu, X.; Ma, H.; Cao, X.; Zhou, P.; Zhang, J.; Weng, X.; Zhang, X.-l.; Qi, J.; Zhou, X.; Weng, L., A Potent , Water-Soluble and Photoinducible DNA Cross-Linking Agent. *J. Am. Chem. Soc.* **2003,** 125, 1116-1117.

51. Squire, C. J.; Clark, G. R.; Denny, W. A., Minor groove binding of a bis-quaternary ammonium compound: The crystal structure of SN 7167 bound to d(CGCGAATTCGCG)2. *Nuc. Acids Res.* **1997,** 25, 4072-4078.

52. Hud, N. V.; Sklenář, V.; Feigon, J., Localization of ammonium ions in the minor groove of DNA duplexes in solution and the origin of DNA A-tract bending. *J. Mol. Biol.* **1999,** 286, 651-660.

53. Deeyaa, B.; Conjugation of Monofunctional Quinone Methides to DNA Ligands for the Promotion of Reversible Alkylation. Johns Hopkins University, Baltimore, MD, 2017.

54. Deeyaa, B.; Rokita, S.E.; *In Preparation*.

55. Nagata, W.; Okada, K.; Aoki, T., Ortho-specific a-Hydroxyalkylation of Phenols with Aldehydes. An Efficient Synthesis of Saligenol Derivatives. *Synthesis* **1979,** 5, 365-368.

56. Li, H.-J.; Wu, Y.-Y.; Wu, Q.-X.; Wang, R.; Dai, C.-Y.; Shen, Z.-L.; Xie, C.-L.; Wu, Y.-C.; Water-promoted ortho-selective monohydroxymethylation of phenols in the NaBO2 system. *Organic & Biomolecular Chemistry* **2014,** 12, 3100-3107.

57. Albrecht, S.; Defoin, A.; Tarnus, C., Simple Preparation of O-Substituted Hydroxylamines from Alcohols. *Synthesis* **2006,** 10, 1635-1638.

58. Izzo, I.; De Caro, S.; De Riccardis, F.; Spinella, A., Synthesis of Alkylphenols and Alkylcatechols from the marine mullusc Hamineoa Callidegenita. *Tet. Lett.* **2000,** 41, 3975-3978.

59. Lamoureux, G.; Agüero, C., A comparison of several modern alkylating agents. *Arkivoc* **2009,** i, 251-264.

60. Atkinson, B. N.; Williams, J. M. J., Dimethylsulfoxide as an N-Methylation Reagent for Amines and Aromatic Nitro Compounds. *ChemCatChem* **2014,** 6, 1860-1862.

61. Jiang, X.; Wang, C.; Wei, Y.; Xue, D.; Liu, Z.; Xiao, J., A General Method for N-Methylation of Amines and Nitro Compounds with Dimethylsulfoxide. *Chem. Eur. J.* **2014,** 20, 58-63.

62. Kashima, C.; Harada, K.; Omote, Y., The influence of a base on the methylation of aminoalcohols. *Can. J. Chem.* **1985,** 63, 288-290.

63. Mahata, T.; Kanungo, A.; Ganguly, S.; Modugula, E. K.; Choudhury, S.; Pal, S. K.; Basu, G.; Dutta, S., The Benzyl Moiety in a Quinoxaline-Based Scaffold Acts as a DNA Intercalation Switch. *Angew. Chem. Int. Ed.* **2016,** 55, 7733-7736.

64. Ammar, Y. A.; Al-Sehemi, A. G.; El-Sharief, A. M. S.; El-Gaby, M. S. A., Chemistry of 2,3-Dichloroquinoxalines. *Phosphorus Sulfur* **2009,** 184, 660-698.

65. Lee, D. W.; Ha, H. J.; Lee, W. K., Selective Mono-BOC Protection of Diamines. *Synth. Commun.* **2007,** 37, 737-742.

66. Keivanloo, A.; Bakherad, M.; Rahimi, A.; Taheri, S. A. N., One-pot synthesis of 1,2-disubstituted pyrrolo[2,3-b]quinoxalines via palladium-catalyzed heteroannulation in water. *Tet. Lett.* **2010,** 51, 2409-2412.

67. Kanungo, A.; Patra, D.; Mukherjee, S.; Mahata, T.; Maulik, P. R.; Dutta, S., Synthesis of a visibly emissive 9-nitro-2,3-dihydro-1H-pyrimido[1,2-a]quinoxalin-5-amine scaffold with large stokes shift and live cell imaging. *RSC Adv.* **2015,** 5, 70958-70967.

68. Waring, M. J.; Ben-Hadda, T.; Kotchevar, A. T.; Ramdani, A.; Touzani, R.; Elkadiri, S.; Hakkou, A.; Bouakka, M.; Ellis, T., 2,3-Bifunctionalized quinoxalines: Synthesis, DNA interactions and evaluation of anticancer, anti-tuberculosis and antifungal activity. *Molecules* **2002,** 7, 641-656.

69. Luger, K.; Rechsteiner, T. J.; Flaus, A. J.; Waye, M. M.; Richmond, T. J., Characterization of nucleosome core particles containing histone proteins made in bacteria. *J. Mol. Biol.* 1997, 301-311.

70. McGinty, R. K.; Tan, S., Nucleosome structure and function. *Chem. Rev.* **2015,** 115, 2255-2273.

71. Arents, G.; Burlingame, R.W.; Wang, B-C.; Love, W.E.; Moudrianakis, E.N.; The nucleosomal core histone octamer at 3.1 A resolution: A tripartite protein assembly and a left-handed superhelix. *Proc. Natl. Acad. Sci. USA* **1991**, 88, 10148-10152.

72. Millard, J. T., DNA modifying agents as tools for studying chromatin structure. *Biochimie* **1996,** 78, 803-806.

73. Millard, J. T.; Spencer, R. J.; Hopkins, P. B., Effect of nucleosome structure on DNA intrastrand cross-linking reactions. *Biochemistry* **1998,** 37, 5211-5219.

74. Zou, T.; Kizaki, S.; Pandian, G. N.; Sugiyama, H., Nucleosome assembly alters the accessibility of the antitumor agent duocarmycin B2 to duplex DNA. *Chem. Eur. J.* **2016,** 22, 8756-8758.

75. Trzupek, J. D.; Gottesfeld, J. M.; Boger, D. L., Alkylation of duplex DNA in nucleosome core particles by duocarmycin SA and yatakemycin. *Nat. Chem. Biol.* **2006,** 2, 79-82.

76. Moyer, R.; Marien, K.; Van Holde, K.; Bailey, G., Site-specific aflatoxin B1 adduction of sequence-positioned nucleosome core particles. *J. Biol. Chem.* **1989,** 264, 12226-12231.

77. Davey, G. E.; Wu, B.; Dong, Y.; Surana, U.; Davey, C. A., DNA stretching in the nucleosome facilitates alkylation by an intercalating antitumour agent. *Nuc. Acids Res.* **2010,** 38, 2081-2088.

78. Chen, D.; Fang, L.; Li, H.; Tang, M. S.; Jin, C., Cigarette smoke component acrolein modulates chromatin assembly by inhibiting histone acetylation. *J. Biol. Chem.* **2013,** 288, 21678-21687.

79. Galligan, J. J.; Marnett, L. J., Histone adduction and its functional impact on epigenetics. *Chem. Res. Toxicol.* **2017,** 30, 376-387.

80. Gherezghiher, T. B.; Ming, X.; Villalta, P. W.; Campbell, C.; Tretyakova, N. Y., 1,2,3,4-Diepoxybutane-Induced DNA−Protein Cross-Linking in Human Fibrosarcoma (HT1080) Cells. *J. Proteome Res.* **2013,** 12, 2151-2164.

81. Lowary, P. T.; Widom, J., New DNA sequence rules for high affinity binding to histone octamer and sequence-directed nucleosome positioning. *J. Mol. Biol.* **1998,** 276, 19-42.

82. Richmond, T. J.; Davey, C. A., The structure of DNA in the nucleosome core. *Nature* **2003,** 423, 145-150.

83. Smith, B. L.; Macleod, M. C., Covalent Binding of the Carcinogen BenzoCulpyrene Diol Epoxide to Xenopus laevis 5S DNA Reconstituted into Nucleosomes. *J. Biol. Chem.* **1993,** 268, 20620-20629.

84. Thrall, B. D.; Mann, D. B.; Smerdon, M. J.; Springer, D. L., Nucleosome Structure Modulates Benzo[a]pyrenediol Epoxide Adduct Formation. *Biochemistry* **1994,** 33, 2210-2216.

85. McMurray, C. T.; van Holde, K. E., Binding of Ethidium to the Nucleosome Core Particle. 1. Binding and Dissociation Reactions. *Biochemistry* **1991,** 30, 5631-5643.

86. Groehler, A.; Villalta, P. W.; Campbell, C.; Tretyakova, N., Covalent DNA-Protein Cross-Linking by Phosphoramide Mustard and Nornitrogen Mustard in Human Cells. *Chem. Res. Toxicol.* **2016,** 29, 190-202.

87. Ming, X.; Groehler, A.; Michaelson-Richie, E. D.; Villalta, P. W.; Campbell, C.; Tretyakova, N. Y., Mass Spectrometry Based Proteomics Study of Cisplatin-Induced DNA-Protein Cross-Linking in Human Fibrosarcoma (HT1080) Cells. *Chem. Res. Toxicol.* **2017,** 30, 980-995.

88. Sczepanski, J. T.; Wong, R. S.; McKnight, J. N.; Bowman, G. D.; Greenberg, M. M., Rapid DNA-protein cross-linking and strand scission by an abasic site in a nucleosome core particle. *Proc. Natl. Acad. Sci. USA* **2010,** 107, 22475-22480.

89. Yang, K.; Park, D.; Tretyakova, N. Y.; Greenberg, M. M., Histone tails decrease N7-methyl-2′-deoxyguanosine depurination and yield DNA – protein cross-links in nucleosome core particles and cells. *Proc. Natl. Acad. Sci. USA* **2018,** 115, (48), 11212-11220.

90. Bolton, J. L.; Turnipseed, S. B.; Thompson, J. A., Influence of quinone methide reactivity on the alkylation of thiol and amino groups in proteins: Studies utilizing amino acid and peptide models. *Chem.-Biol. Int.* **1997,** 107, 185-200.

91. Modica, E.; Zanaletti, R.; Freccero, M.; Mella, M., Alkylation of amino acids and glutathione in water by o-Quinone methide. Reactivity and selectivity. *J. Org. Chem.* **2001,** 66, 41-52.

92. Meier, B. W.; Gomez, J. D.; Zhou, A.; Thompson, J. A., Immunochemical and proteomic analysis of covalent adducts formed by quinone methide tumor promoters in mouse lung epithelial cell lines. *Chem. Res. Toxicol.* **2005,** 18, 1575-1585.

93. Burke, M. C.; Wang, Y.; Lee, A. E.; Dixon, E. K.; Castaneda, C. A.; Fushman, D.; Fenselau, C., Unexpected Trypsin Cleavage at Ubiquitinated Lysines. *Anal. Chem.* **2015,** 87, 8144-8148.

94. Mann, D. B., DNA damage can alter the stability of nucleosomes: Effects are dependent on damage type. *Proc. Natl. Acad. Sci. USA* **1997,** 94, 2215-2220.

95. Banerjee, S.; Chakraborty, S.; Jacinto, M. P.; Paul, M. D.; Balster, M. V.; Greenberg, M. M., Probing enhanced double-strand break formation at abasic sites within clustered lesions in nucleosome core particles. *Biochemistry* **2017,** 56, (1), 14-21.

96. Luger, K.; Mader, A. W.; Richmond, R. K.; Sargent, D. F.; Richmond, T. J., Crystal structure of the nucleosome core particle at 2 .8 A. *Nature* **1997,** 7, 251-260.

97. Berdis, A. J.; Fidelity, G., Mechanisms of DNA Polymerases. *Chem. Rev.* **2009,** 109, 2862-2879.

98. Albertson, T. M.; Preston, B. D., DNA Replication Fidelity: Proofreading in Trans. *Curr. Biol.* **2006,** 16, 209-211.

99. Pursell, Z. F.; Kunkel, T. A., DNA Polymerase ε. A Polymerase of Unusual Size (and Complexity). *Prog. Nuc. Acid Res. Mol. Biol.* **2008,** 82, 101-145.

100. Carroll, S. S.; Benkovic, S. J., Mechanistic Aspects of DNA Polymerases: *Escherichia coli* DNA Polymerase I (Klenow Fragment) as a Paradigm. *Chem. Rev.* **1990,** 90, 1291-1307.

101. Dzantiev, L.; Alekseyev, Y. O.; Morales, J. C.; Kool, E. T.; Romano, L. J., Significance of nucleobase shape complementarity and hydrogen bonding in the formation and stability of the closed polymerase - DNA complex. *Biochemistry* **2001,** 40, 3215-3221.

102. Ganai, R. A.; Johansson, E., DNA Replication-A Matter of Fidelity. *Mol. Cell* **2016,** 62, (5), 745-755.

103. Minnick, D. T.; Liu, L.; Grindley, N. D. F.; Kunkel, T. A.; Joyce, C. M., Discrimination against purine-pyrimidine mispairs in the polymerase active site of DNA polymerase I: A structural explanation. *Proc. Natl. Acad. Sci. USA* **2002,** 99, 1194-1199.

104. Trakselis, M. A.; Cranford, M. T.; Chu, A. M., Coordination and Substitution of DNA Polymerases in Response to Genomic Obstacles. *Chem. Res. Toxicol.* **2017,** 30, 1956-1971.

105. Eckert, K. A.; Opresko, P. L., DNA polymerase mutagenic bypass and proofreading of endogenous DNA lesions. *Mutat. Res.-Fund. Mol. M.* **1999,** 424, 221-236.

106. Wu, W.-J.; Yang, W.; Tsai, M.-D., How DNA polymerases catalyse replication and repair with contrasting fidelity. *Nat. Rev. Chem.* **2017,** 1, 0068.

107. Latham, G. J.; Harris, C. M.; Harris, T. M.; Lloyd, R. S., The Efficiency of Translesion Synthesis Past Single Styrene Oxide DNA Adducts In Vitro Is Polymerase-Specific. *Chem. Res. Toxicol.* **1995,** 8, 422-430.

108. Kappen, L. S.; Goldberg, I. H., Replication block by an enediyne drug - DNA deoxyribose adduct. *Biochemistry* **1999,** 38, 235-242.

109. Williams, N. L.; Wang, P.; Wang, Y., Replicative Bypass of O2-Alkylthymidine Lesions *in Vitro*. *Chem. Res. Toxicol.* **2016,** 29, 1755-1761.

110. Kasiviswanathan, R.; Minko, I. G.; Lloyd, R. S.; Copeland, W. C., Translesion synthesis past acrolein-derived DNA adducts by human mitochondrial DNA polymerase γ. *J. Biol. Chem.* **2013,** 288, (20), 14247-14255.

111. Kim, S. I.; Pfeifer, G. P.; Besaratinia, A., Lack of mutagenicity of acrolein-induced DNA adducts in mouse and human cells. *Cancer Res.* **2007,** 67, (24), 11640-11647.

112. Zhou, Q.; Qu, Y.; Mangrum, J. B.; Wang, X., DNA alkylation with N-methylquinolinium quinone methide to N2-dG adducts resulting in extensive stops in primer extension with DNA polymerases and subsequent suppression of GFP expression in A549 cells. *Chem. Res. Toxicol.* **2011,** 24, 402-411.

113. Klenow, H.; Henningsen, I., Selective elimination of the exonuclease activity of the deoxyribonucleic acid polymerase from Escherichia coli B by limited proteolysis. *Proc. Natl. Acad. Sci. USA* **1970,** 65, 168-175.

114. Bebenek, K.; Joyce, C. M.; Fitzgerald, M. P.; Kunkel, T. A., The fidelity of DNA synthesis catalyzed by derivatives of Escherichia coli DNA polymerase I. *J. Biol. Chem.* **1990,** 265, 13878-13887.

115. Sanger, F.; Nicklen, S.; Coulson, R., DNA Sequencing with chain-terminating inhibitors. *Proc Natl Acad Sci USA* **1977,** 74, 5463-5467.

116. Greenberg, M. M.; Weledji, Y. N.; Kroeger, K. M.; Kim, J.; Goodman, M. F., In Vitro Effects of a C4'-Oxidized Abasic Site on DNA Polymerases. *Biochemistry* **2004,** 43, 2656-2663.

117. Derbyshire, V.; Freemont, P. S.; Sanderson, M. R.; Beese, L.; Friedman, J. M.; Joyce, C. M.; Steitz, T. A.; Derbyshire, V.; Freemont, P. S.; Sanderson, M. R.; Beese, L.; Friedman, J. M.; Joyce, C. M.; Steitz, T. A., Genetic and Crystallographic Studies of the 3'-5' Exonucleolytic Site of DNA Polymerase I. *Science* **1988,** 240, 199-201.

118. Blanco, L.; Bernad, A.; Lázaro, J. M.; Martín, G.; Garmendia, C.; Salas, M.; Bernads, A.; Lharo, J. M.; Martins, G., Highly Efficient DNA Synthesis by the Phage 429 DNA Polymerase. *J. Biol. Chem.* **1989,** 264, 8935-8940.

119. Price, N.E.; Catalano, M.J.; Liu, S.; Wang, Y.; Gates, K.S.; Chemical and structural characterization of interstrand cross-links formed between abasic sites and adenine residues in duplex DNA. *Nuc. Acid. Res.* **2015**, 43, 3434-3441.

120. Byrne, S. R.; Yang, K.; Rokita, S. E., Effect of Nucleosome Assembly on Alkylation by a Dynamic Electrophile. *Chem. Res. Toxicol.* **2019,** 32, 917-925.

121. Miller, H.; Grollman, A. P., Kinetics of DNA polymerase I (Klenow fragment exo-) activity on damaged dna templates: Effect of proximal and distal template damage on DNA synthesis. *Biochemistry* **1997,** 36, (49), 15336-15342.

122. Zhu, X. J.; Sun, S.; Xie, B.; Hu, X.; Zhang, Z.; Qiu, M.; Dai, Z. M., Guanine-rich sequences inhibit proofreading DNA polymerases. *Sci. Rep.* **2016,** 6, 1-8.

123. Deans, A. J.; West, S. C., DNA interstrand crosslink repair and cancer. *Nat. Rev. Cancer* **2011,** 11, 467-480.

124. Kabir, A.; Suresh Kumar, G., Binding of the Biogenic Polyamines to Deoxyribonucleic Acids of Varying Base Composition: Base Specificity and the Associated Energetics of the Interaction. *PLoS One* **2013,** 8, e70510.

125. Yamanaka, K.; Minko, I. G.; Takata, K.-i.; Kolbanovskiy, A.; Kozekov, I. D.; Wood, R. D.; Rizzo, C. J.; Lloyd, R. S.; Station, B.; V, V. U.; Nash, V., Novel Enzymatic Function of DNA Polymerase ν in Translesion DNA Synthesis Past Major Groove DNA -Peptide and DNA-DNA Cross-Links. *Chem. Res. Toxicol.* **2010,** 23, 689-695.

126. Gowda, A. S. P.; Spratt, T. E., DNA Polymerase ν Rapidly Bypasses O6- Methyl-dG but Not O6-[4-(3-Pyridyl)-4-oxobutyl-dG and O2 -Alkyl-dTs. *Chem. Res. Toxicol.* **2016**, 29, 1894-1900.

127. Zeng, Q. Development of Inducible DNA Crosslinking Agents. State University of New York at Stony Brook, Stony Brook, NY, 1995.

128. Villani, G.; Le Gac, N. T., Interactions of DNA helicases with damaged DNA: Possible biological consequences. *J. Biol. Chem.* **2000,** 275, 33185-33188.

129. Batty, D. P.; Wood, R. D., Damage recognition in nucleotide excision repair of DNA. *Gene* **2000,** 241, 193-204.

130. Sugasawa, K., Mechanism and regulation of DNA damage recognition in mammalian nucleotide excision repair. *Genes and Environ.* **2019,** 41, 1-6.

131. Khan, I.; Sommers, J. A.; Brosh, R.M., Close encounters for the first time: Helicase interactions with DNA damage. *DNA Repair* **2015,** 33, 43-59.

132. Naegeli, H.; Modrich, P.; Friedberg, E. C., The DNA helicase activities of Rad3 protein of Saccharomyces cerevisiae and helicase II of Escherichia coli are differentially inhibited by covalent and noncovalent DNA modifications. *J. Biol. Chem.* **1993,** 268, 10386-10392.

133. Driscoll, H. C.; Matson, S. W.; Sayer, J. M.; Kroth, H.; Jerina, D. M.; Brosh, R. M., Inhibition of Werner Syndrome Helicase Activity by Benzo[c]phenanthrene Diol Epoxide dA Adducts in DNA Is Both Strand- and Stereoisomer-dependent. *J. Biol. Chem.* **2003,** 278, 41126-41135.

134. Nakano, T.; Miyamoto-Matsubara, M.; Shoulkamy, M. I.; Salem, A. M. H.; Pack, S. P.; Ishimi, Y.; Ide, H., Translocation and stability of replicative DNA helicases upon encountering DNA-protein cross-links. *J. Biol. Chem.* **2013,** 288, 4649-4658.

135. Bernstein, J. A.; Richardson, C. C., Purification of the 56-kDa Component of the Bacteriophage T7 Primase / Helicase and Characterization of Its Nucleoside. *J. Biol. Chem.* **1988,** 263, 14891-14899.

136. Bernstein, J. A.; Richardson, C. C., A 7-kDa region of the bacteriophage T7 gene 4 protein is required for primase but not helicase activity. *Proc Natl Acad Sci USA* **1988,** 85, 396-400.

137. Brown, W. C.; Romano, L. J., Benzo[α]pyrene-DNA Adducts Inhibit Translocation by the Gene 4 Protein of Bacteriophage T7. *J. Biol. Chem.* **1989,** 264, 6748-6754.

138. Yong, Y.; Romano, L. J., Benzo[a]pyrene - DNA Adducts Inhibit the DNA Helicase Activity of the Bacteriophage T7 Gene 4 Protein. *Chem. Res. Toxicol.* **1996,** 9, 179-187.

139. Lee, S. J.; Richardson, C. C., Acidic residues in the nucleotide-binding site of the bacteriophage T7 DNA primase. *J. Biol. Chem.* **2005,** 280, 26984-26991.

140. Satapathy, A. K.; Crampton, D. J.; Beauchamp, B. B.; Richardson, C. C., Promiscuous Usage of Nucleotides by the DNA Helicase of Bacteriophage T7. *J. Biol. Chem.* **2009,** 284, 14286-14295.

141. Zhu, B.; Lee, S.-j.; Richardson, C. C., An in Trans Interaction at the Interface of the Helicase and Primase Domains of the Hexameric Gene 4 Protein of Bacteriophage T7 Modulates Their Activities. *J. Biol. Chem.* **2009,** 284, 23842-23851.

142. Guo, S.; Tabor, S.; Richardson, C. C., The Linker Region between the Helicase and Primase Domains of the Bacteriophage T7 Gene 4 Protein Is Critical for Hexamer Formation. *J. Biol. Chem.* **1999,** 274, 30303-30309.

143. Lechner, R. L.; Engler, M. J.; Richardson, C. C., Characterization of strand displacement synthesis catalyzed by bacteriophage T7 DNA polymerase. *J. Biol. Chem.* **1983,** 258, 11174-11184.

144. Ahnert, P.; Patel, S. S., Asymmetric Interactions of Hexameric Bacteriophage T7 DNA Helicase with the 5' - and 3' -Tails of the Forked DNA Substrate. *J. Biol. Chem.* **1997,** 272, 32267-32273.

145. Huang, J.; Liu, S.; Bellani, M. A.; Thazhathveetil, A.; Ling, C.; deWinter, J. P.; Wang, Y.; Wang, W.; Seidman, M. M., The DNA Translocase FANCM/MHF Promotes Replication Traverse of DNA Interstrand Crosslinks. *Mol. Cell* **2013,** 52, 434-446.

146. Tao, Y.; Jin, C.; Li, X.; Qi, S.; Chu, L.; Niu, L.; Yao, X.; Teng, M., The structure of the FANCM/MHF complex reveals physical features for functional assembly. *Nat. Commun.* **2012,** 3:782.

147. Matson, S. W.; Tabor, S.; Richardson, C. C., The gene 4 protein of bacteriophage T7. Characterization of helicase activity. *J. Biol. Chem.* **1983,** 258, 14017-14024.

148. Satapathy, A. K.; Kochaniak, A. B.; Mukherjee, S.; Crampton, D. J.; Oijen, A. V.; Richardson, C. C., Residues in the central β -hairpin of the DNA helicase of bacteriophage T7 are important in DNA unwinding. *Proc Natl Acad Sci USA* **2010,** 107, 3-8.

149. Satapathy, A. K.; Kulczyk, A. W.; Ghosh, S.; Oijen, A. M. V.; Richardson, C. C., Coupling dTTP Hydrolysis with DNA Unwinding by the DNA Helicase of Bacteriophage T7. *J. Biol. Chem.* **2011,** 286, 34468-34478.

150. Liao, J.-C.; Jeong, Y.-J.; Kim, D.-E.; Patel, S. S.; Oster, G., Mechanochemistry of T7 DNA Helicase. *J. Mol. Biol.* **2005,** 1, 452-475.

151. Crampton, D. J.; Ohi, M.; Qimron, U.; Walz, T.; Richardson, C. C., Oligomeric States of Bacteriophage T7 Gene 4 Primase/Helicase. *J. Mol. Biol.* **2006,** 360, 667-677.

152. Rink, S. M.; Solomon, M. S.; Taylor, M. J.; Rajur, S. B.; Mclaughlin, L. W.; Hopkins, P. B., Covalent Structure of a Nitrogen Mustard-Induced DNA Interstrand Cross-Link: An N7 to N7 Linkage of Deoxyguanosine Residues at the Duplex Sequence 5'-d(GNC). *J. Am. Chem.* **1993,** 115, 2551-2557.

153. Rycenga, H. B.; Long, D. T., The evolving role of DNA inter-strand crosslinks in chemotherapy. *Curr. Opin. Pharm.* **2018,** 41, 20-26.

154. Vare, D.; Groth, P.; Carlsson, R.; Johansson, F.; Erixon, K.; Jenssen, D., DNA interstrand crosslinks induce a potent replication block followed by formation and repair of double strand breaks in intact mammalian cells. *DNA Repair* **2012,** 11, 976-985.

155. Egelman, E. H.; Yu, X.; Wild, R.; Hingorani, M.; Patel, S. S., Bacteriophage T7 helicase/primase proteins form rings around single-stranded DNA that suggest a general structure for hexameric helicases. *Proc Natl Acad Sci USA* **1995,** 92, 3869-3873.

Appendix A: List of Oligonucleotides Used Throughout this Dissertation

Table A.1 Sequences of oligonucleotides used throughout this dissertation.

Oligo-nucleotide	Sequence (5' to 3')
OD1	GTA TGG CAC ACA CAG GTC AGT CAT GTC GTT AAT CGC GCG CAT AA
OD2	TTA TGC GCG CGA TTA ACG ACA TGA CTG ACC TGT GTG TGC CAT AC
OD3	ATG TCG TTA ATC GCG CGC ATA A
OD4	GTA TGG CAC ACA CAG GTC AGT C
OD5	GTC GTT AAT CGC GCG CAT AA
OD6	TTA TGC GCG CGA TTA ACG ACA TGA C
OD7	TGA CCT GTG TGT GCC ATA CT
OD8	AGT ATG GCA CAC ACA GGT CAG TCA T
OD9	TTA TGC GCG CTT GAT TAA CGA CAT GAC TGA CCT GTG TGT GCC ATA C
Widom 601 Top Strand	ATC GAT GTA TAT ATC TGA CAC GTG CCT GGA GAC TAG GGA GTA ATC CCC TTG GCG GTT AAA ACG CGG GGG ACA GCG CGT ACG TGC GTT AAG CGG TGC TA GAG CTG TCT ACG ACC AAT TGA GCG GCC TCG GCA CCG GGA TTC TGA T
Widom 601 Bottom Strand	ATC AGA ATC CCG GTG CCG AGG CCG CTC AAT TGG TCG TAG ACA GCT CTA GCA CCG CTT AAA CGC ACG TAC GCG CTG TCC CCC GCG TTT TAA CCG CCA AGG GGA TTA CTC CCT AGT CTC CAG GCA CGT GTC AGA TAT ATA CAT CGA T
OD10	GTA TGG CAC ACA CAG
OD11	GTG TGT GGT GGG TGG CGG TTG AAG AGG TAA A
OD12	TTT ACC TCT TCA ACC GCC ACC CAC CAC ACA CCC AAC CAC CAC ACC ACT GTG TGT GCC ATA C
OD13	TTT TTT TTT TTT TTT TTT TTT TTT TTT TTT TTT TTT GGC ATG TCA CGA CGT TGT AAA ACG ACG GCC AGT GAA TTC GAG CTC GGT ACC CGG CG
OD14	CGC CGG TAC CGA GCT CGA ATT CAC TGC CGT CGT TTA CAA CGT CGT GAC ATG CCT TTT TTT TTT TTT TTT TTT
OD15	TTT TTT TTT TTT TTT TTT TTT TTT TTT TTT TTT TTT TTT ACC TCT TCA ACC GCC ACC CAC CAC ACA CCC AAC CAC CAC ACC A
OD16	TGG TGT GGT GGT TGG GTG TGT GGT GGG TGG CGG TTG AAG AGG TAA ATT TTT TTT TTT TTT TTT TT

Appendix B: Supporting Information for Chapter 2
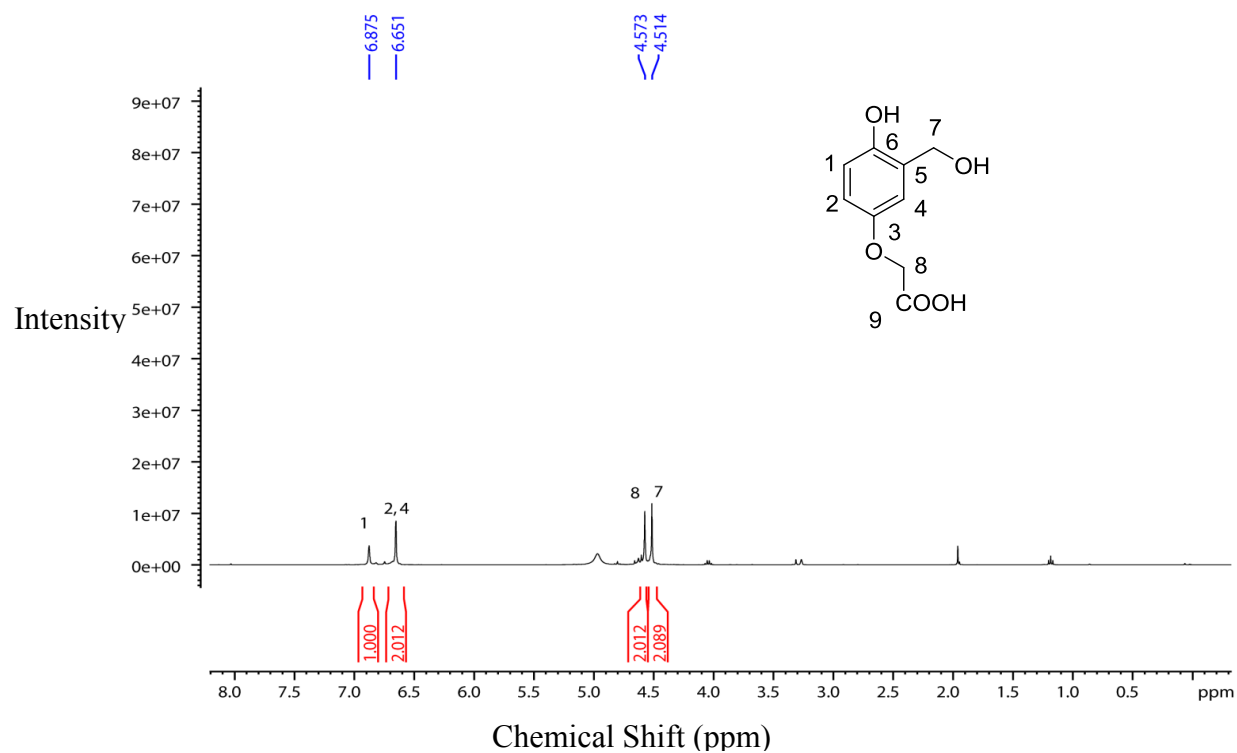
Figure B.1 ^{1}H NMR of **2** in CD₃OD at 400 MHz
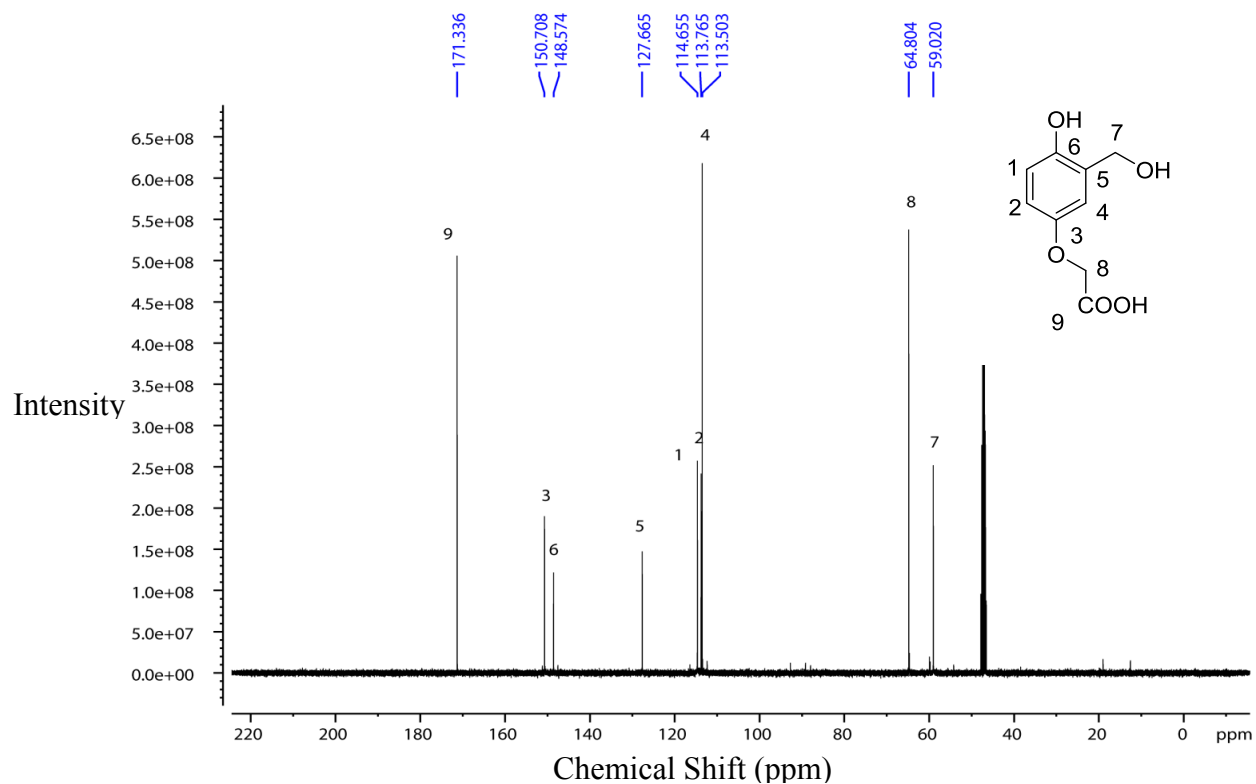
Figure B.2 ^{13}C NMR of **2** in CD₃OD at 101 MHz
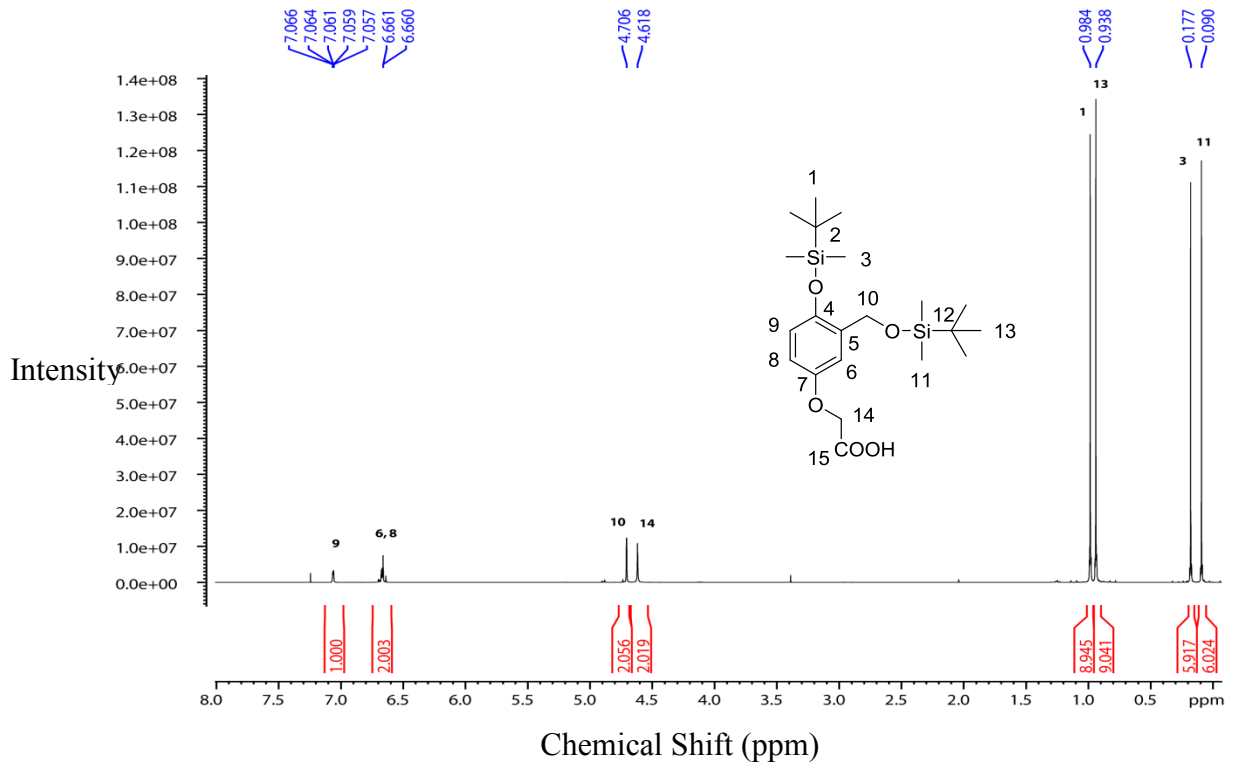
Figure B.3 ^{1}H NMR of **3** in CDCl$_3$ at 400 MHz.
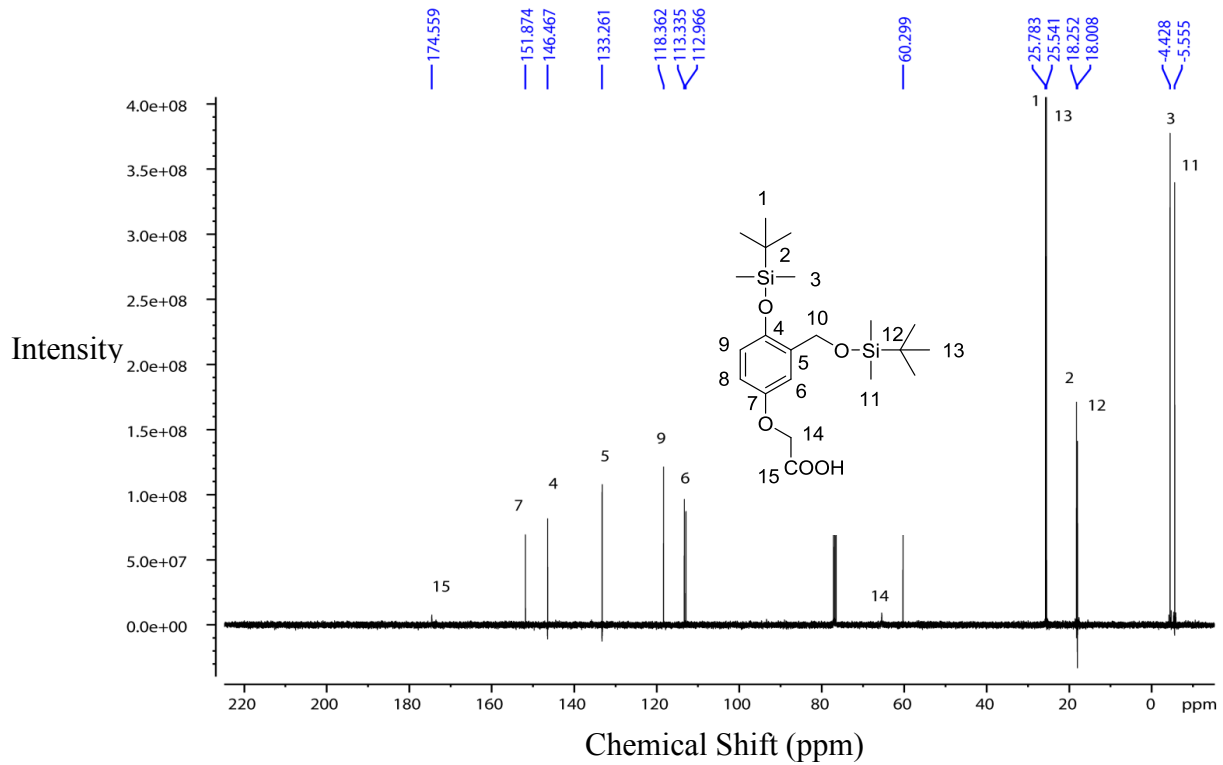
Figure B.4 ^{13}C NMR of **3** in CDCl$_3$ at 101 MHz

169
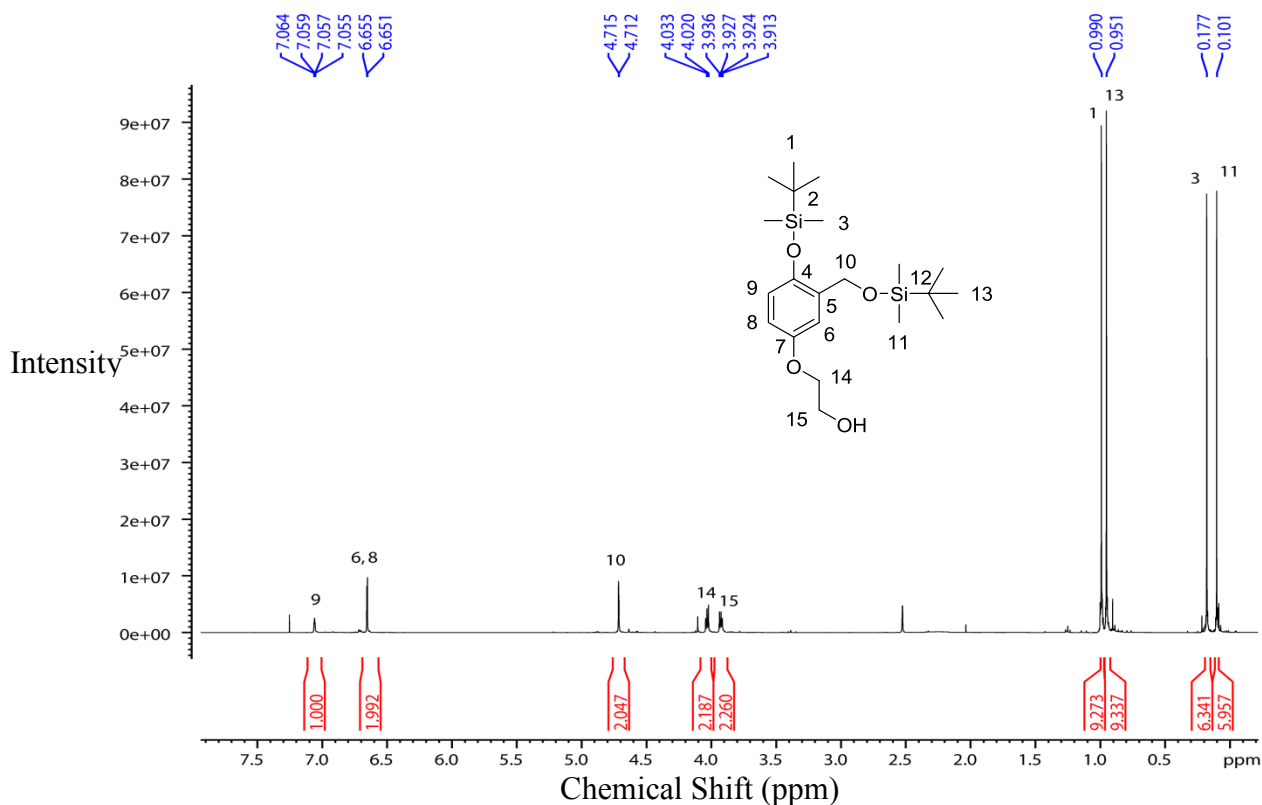
Figure B.5 ^{1}H NMR of **4** in CDCl$_3$ at 400 MHz
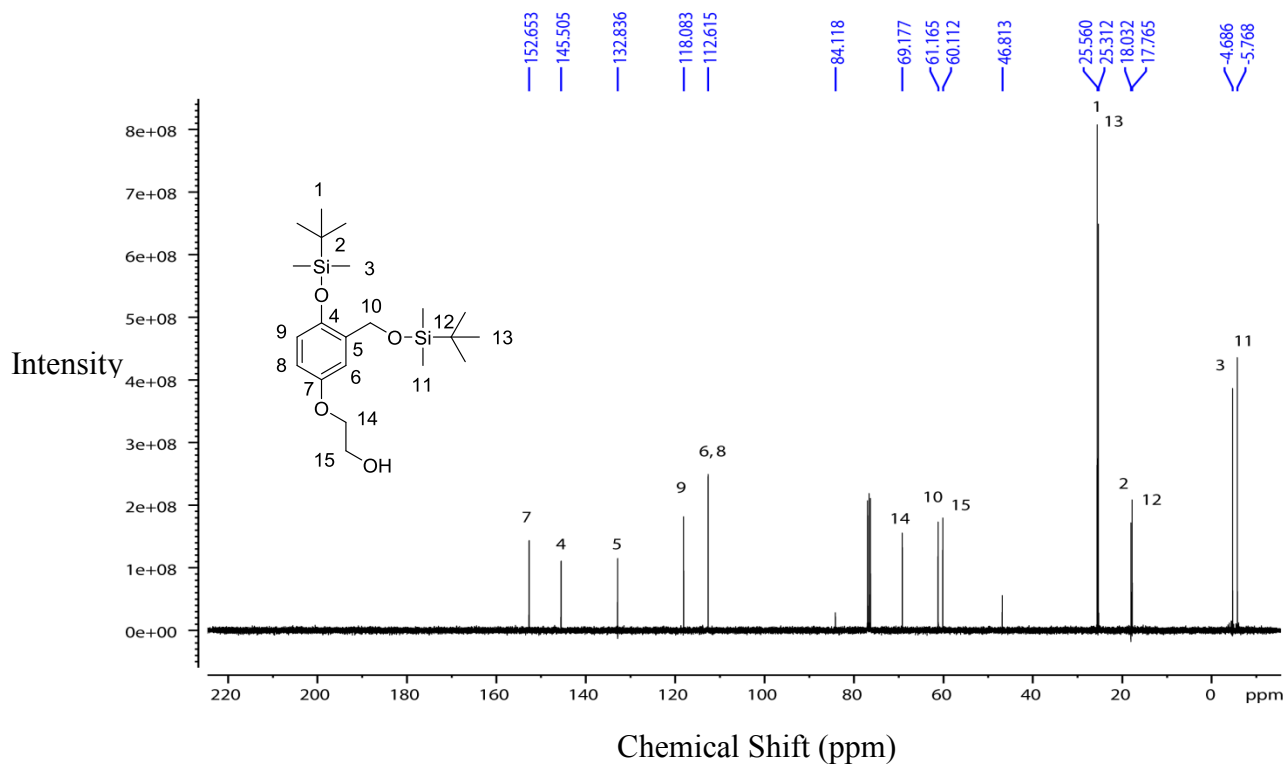
Figure B.6 ^{13}C NMR of **4** in CDCl$_3$ at 101 MHz
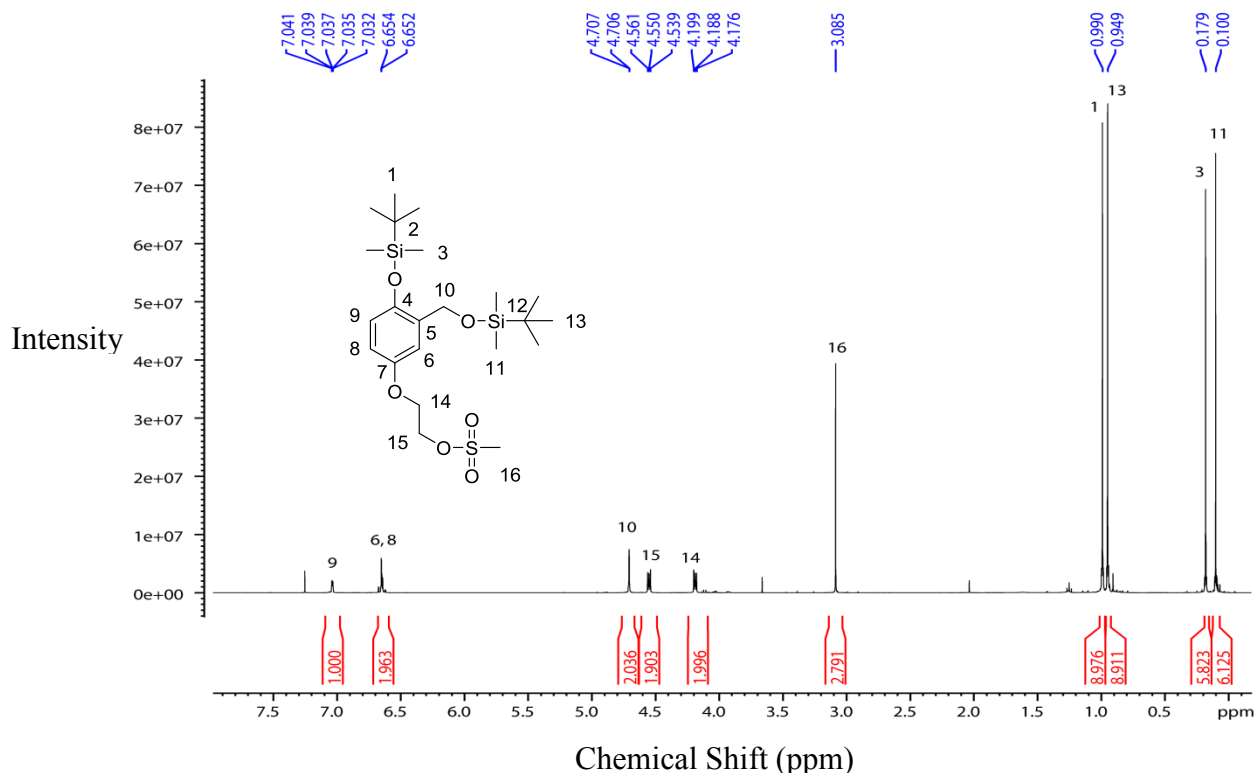
Figure B.7 ^{1}H NMR of **5** in CDCl$_3$ at 400 MHz
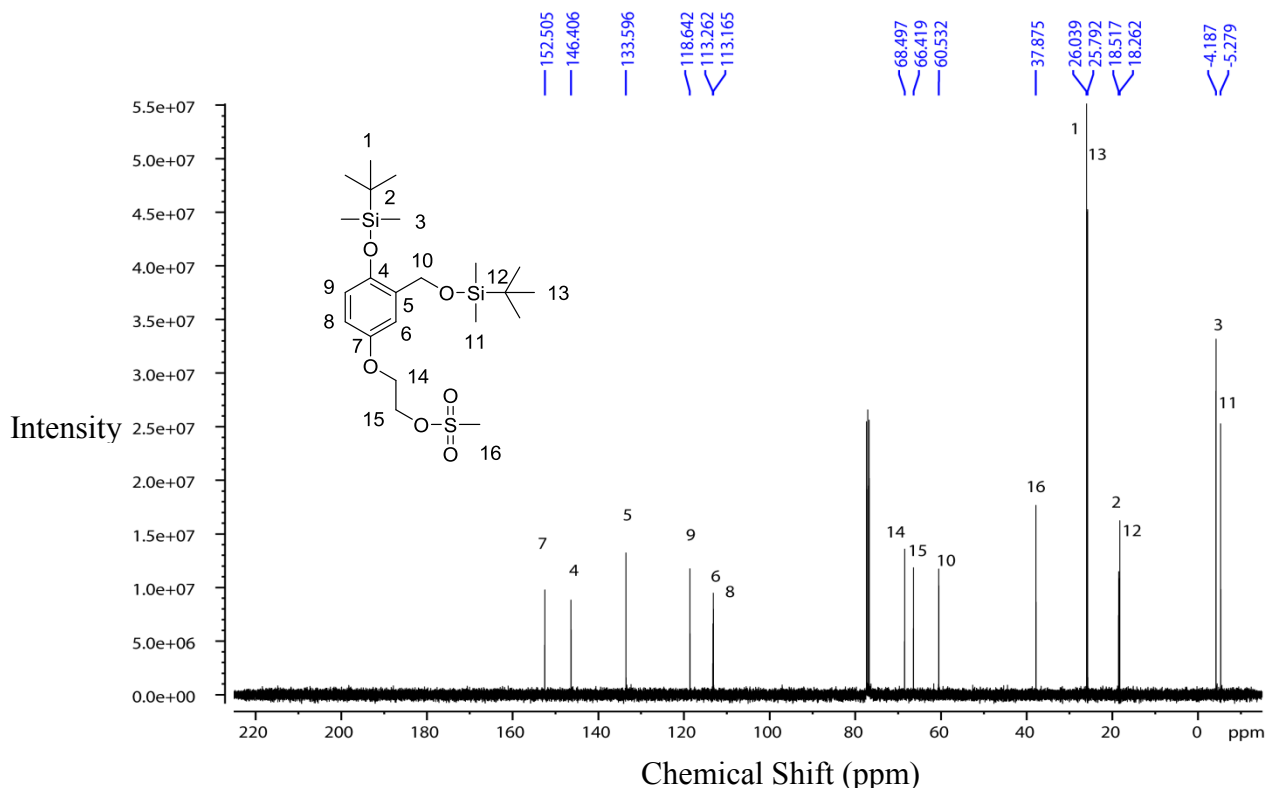
Figure B.8 ^{13}C NMR of **5** in CDCl$_3$ at 101 MHz

Figure B.9 ^{1}H NMR of **6** in CDCl$_3$ at 400 MHz

Figure B.10 ^{13}C NMR of **6** in CDCl$_3$ at 101 MHz

Figure B.11 ^{1}H NMR of **7** in CDCl$_3$ at 400 MHz

Figure B.12 ^{13}C NMR of **7** in CDCl$_3$ at 101 MHz
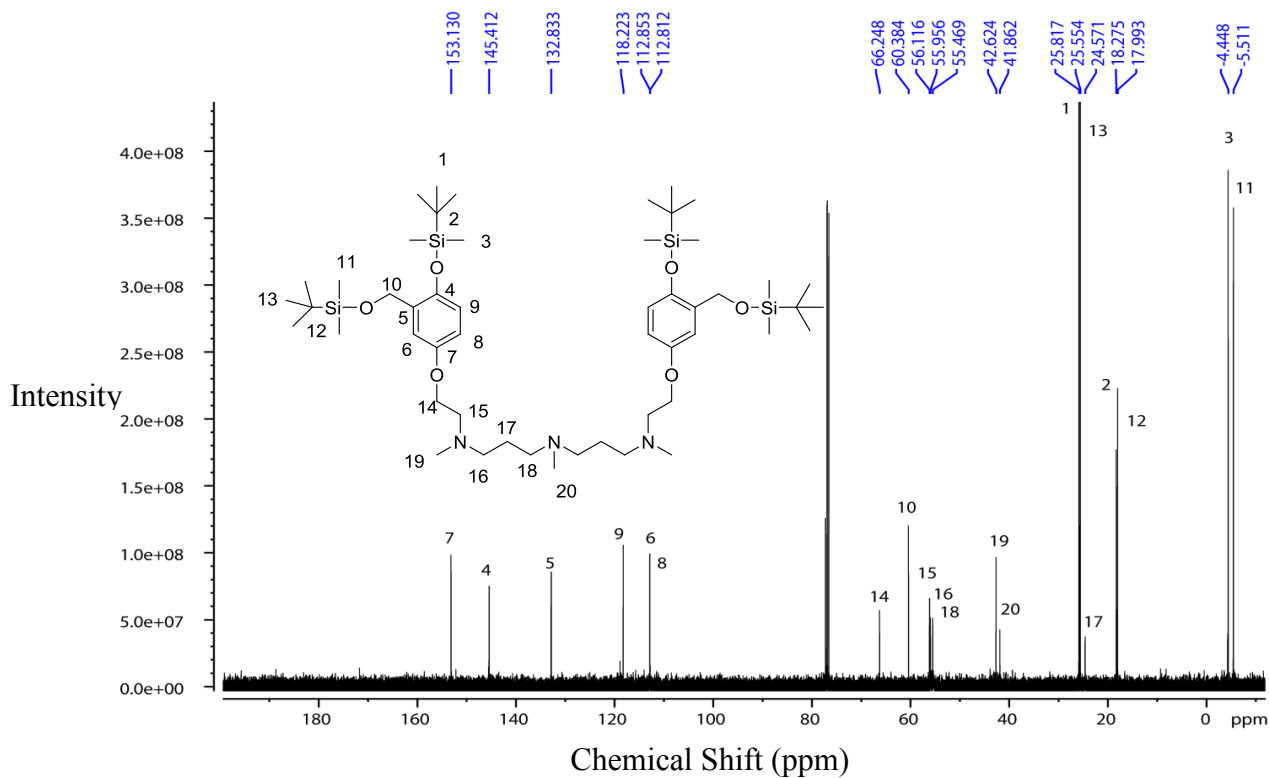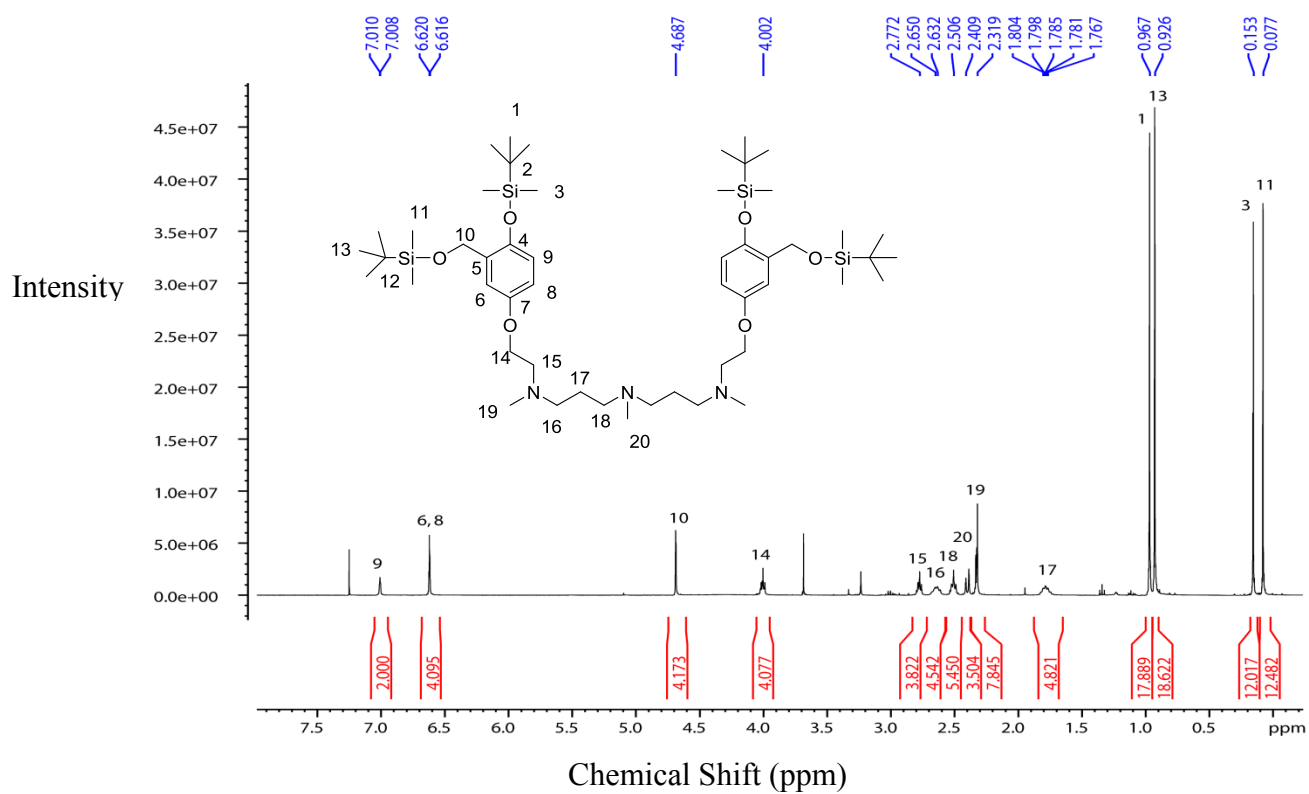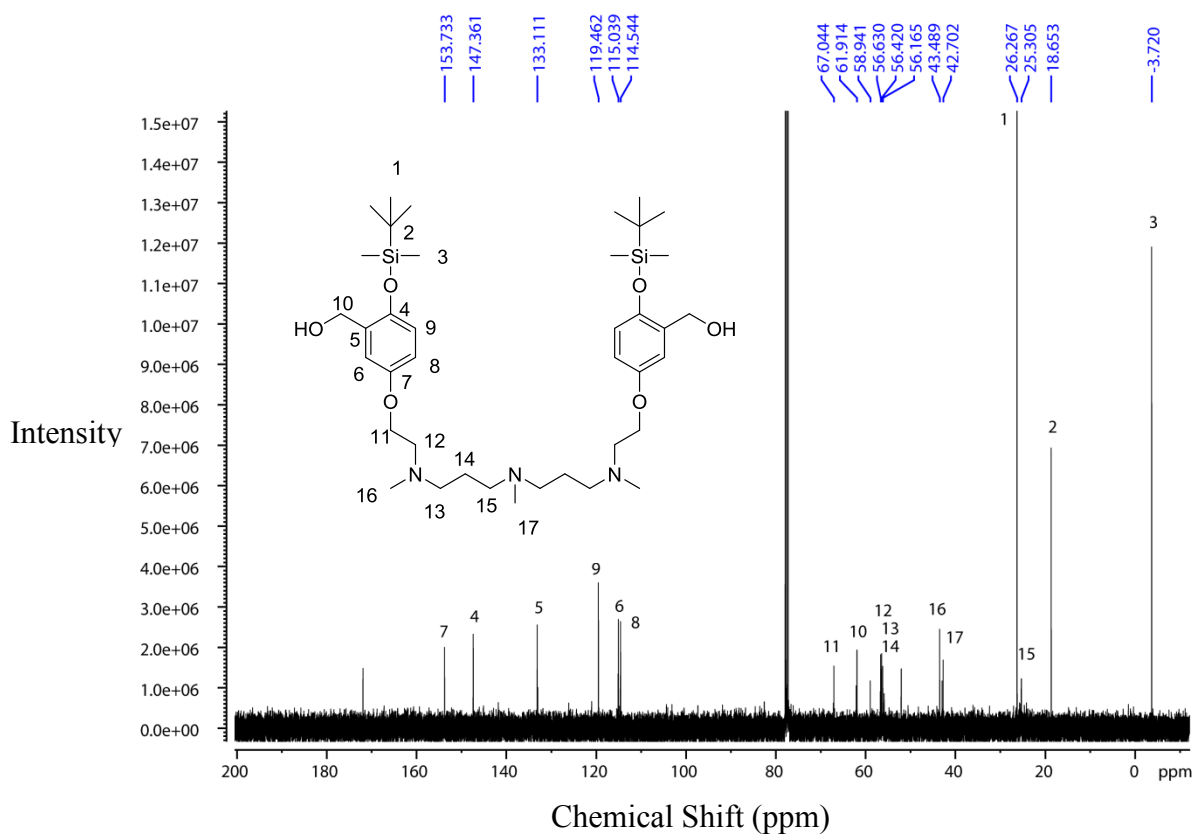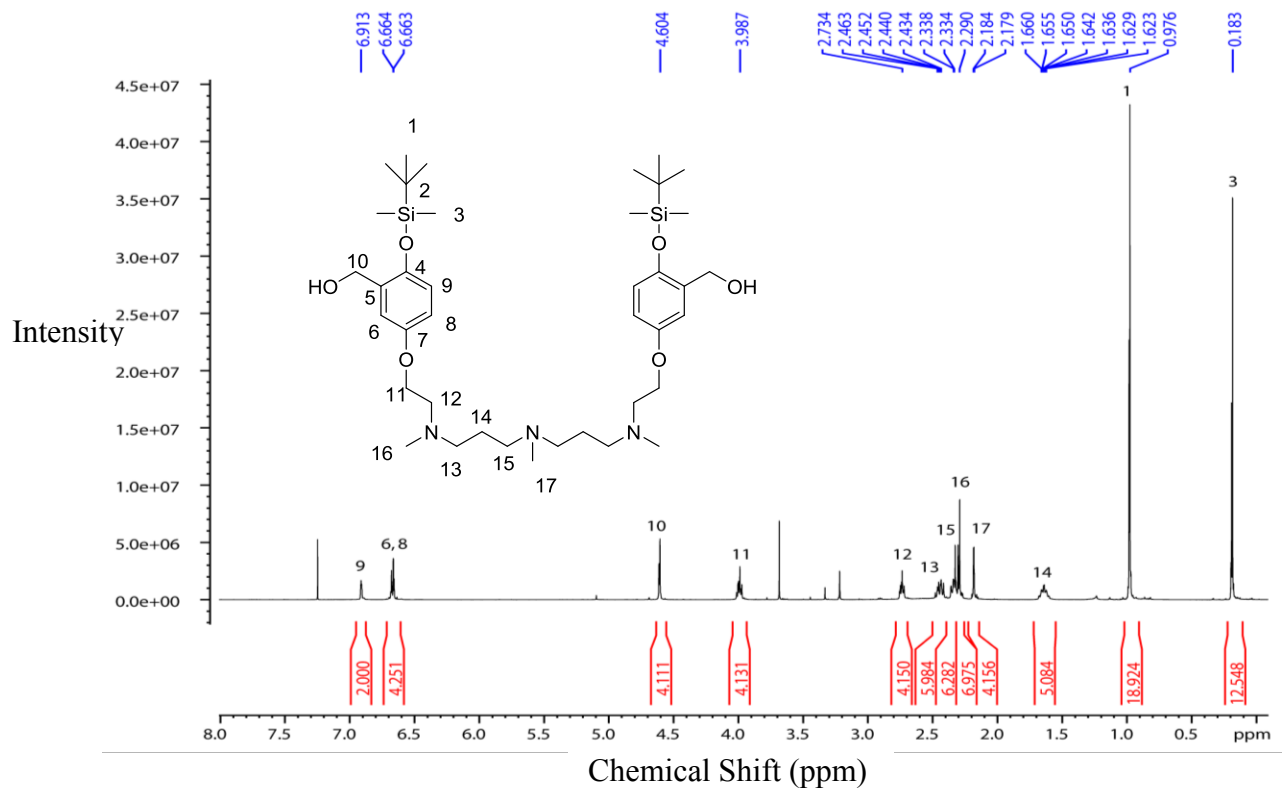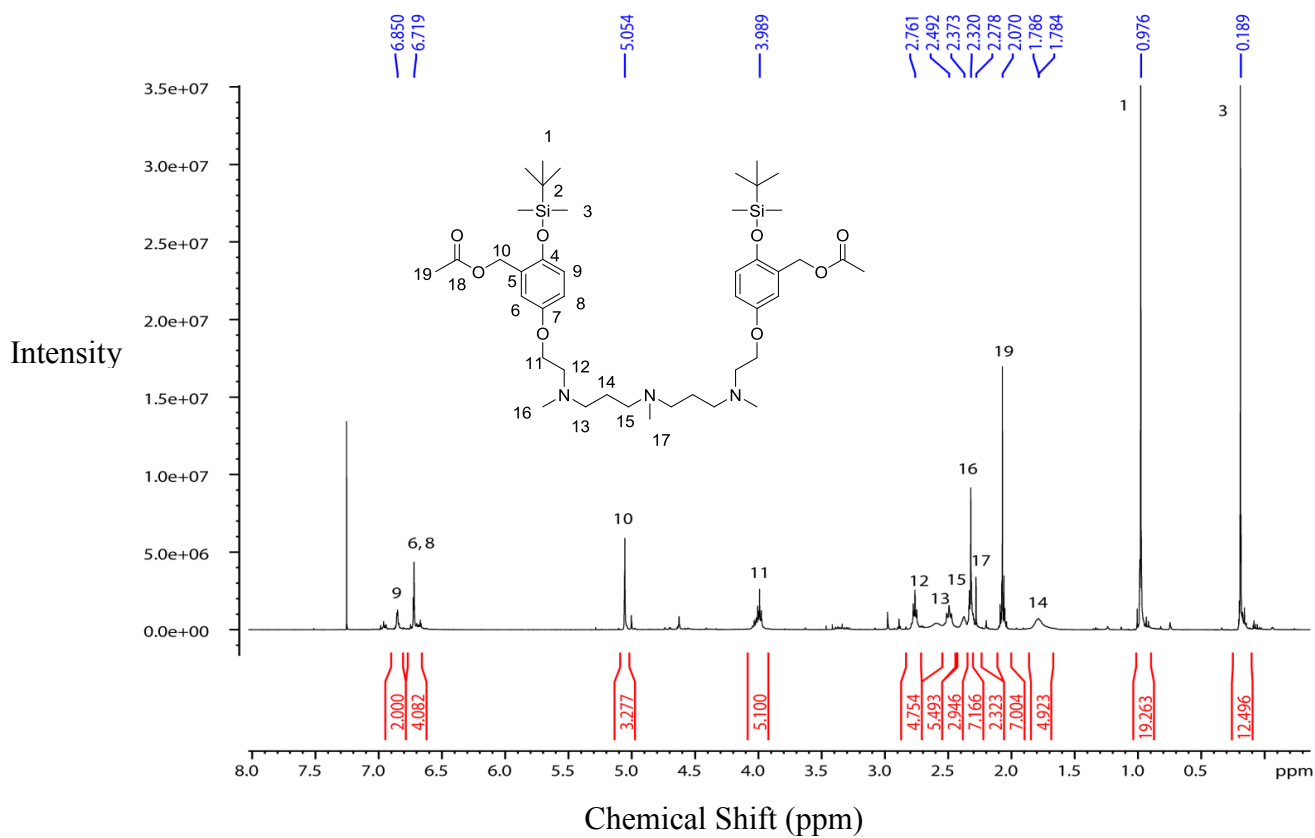
Figure B.13 ^{1}H NMR of **8** in CDCl$_3$ at 400 MHz
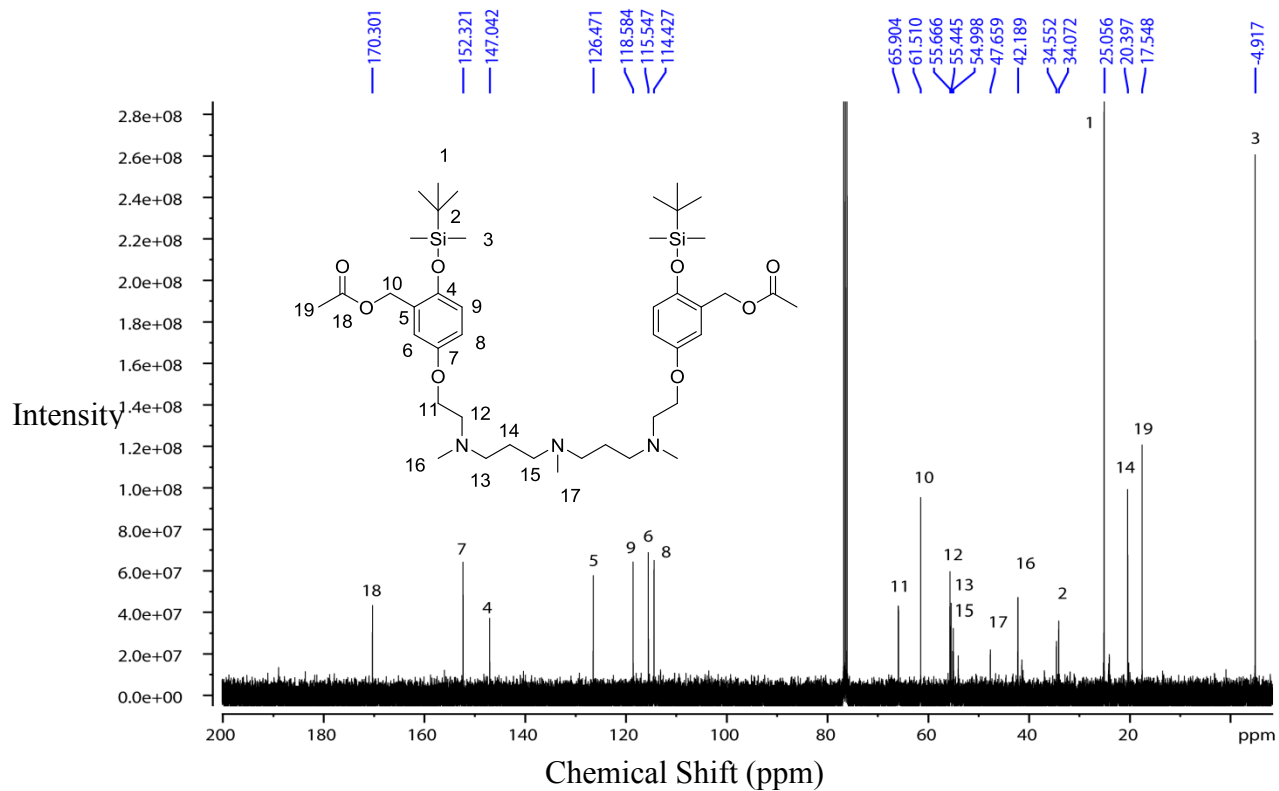
Figure B.14 ^{13}C NMR of **8** in CDCl$_3$ at 101 MHz

174

Chemical Shift (ppm)
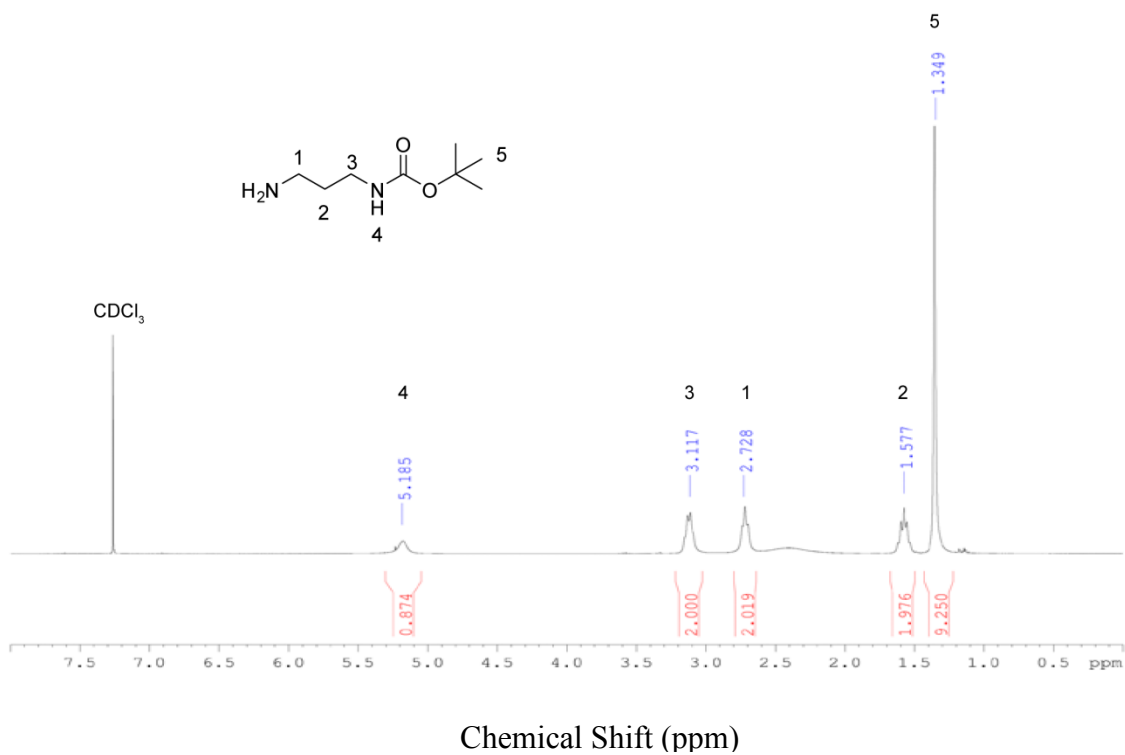
Figure B.15 ^{1}H NMR of **16** in CDCl$_3$ at 400 MHz

Chemical Shift (ppm)
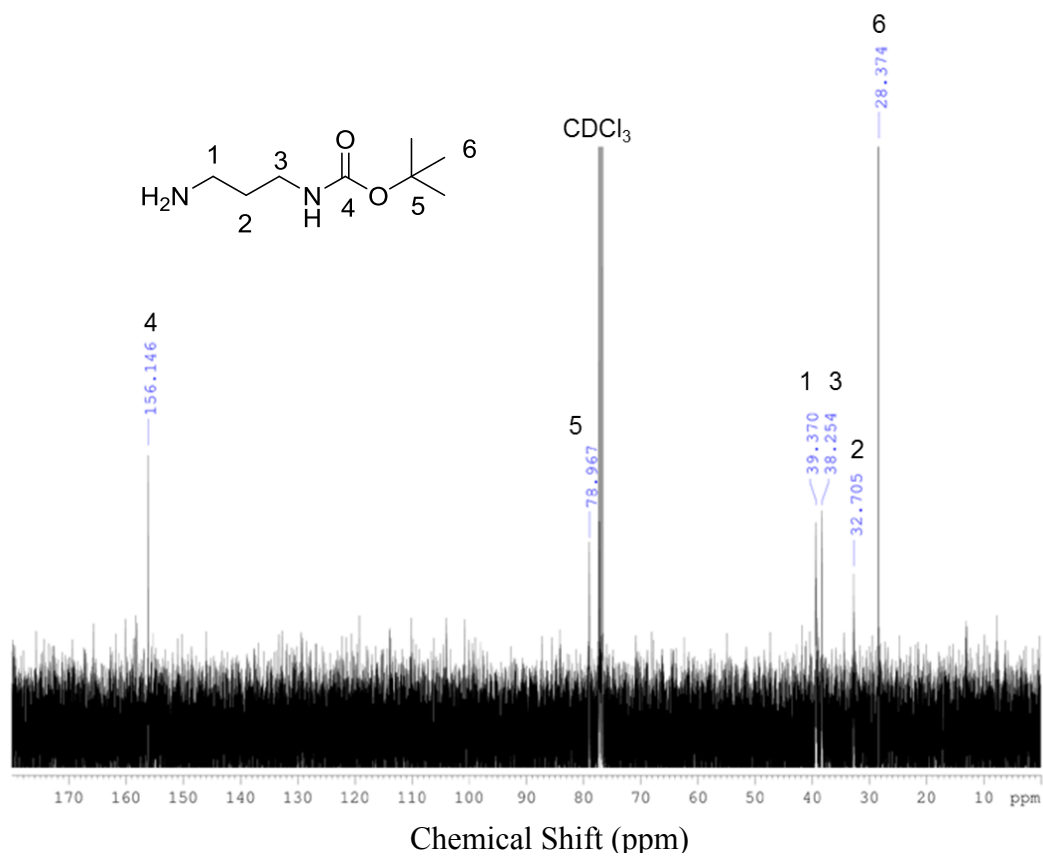
Figure B.16 ^{13}C NMR of **16** in CDCl$_3$ at 101 MHz
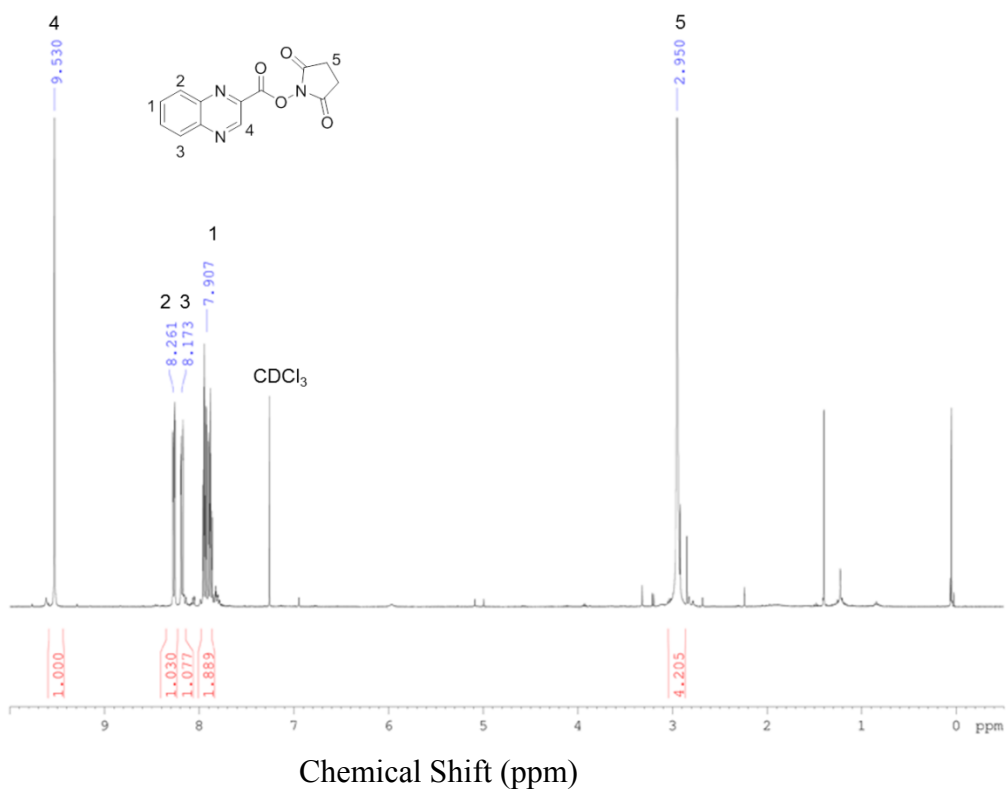
Figure B.17 ^{1}H NMR of **18** in CDCl$_3$ at 400 MHz
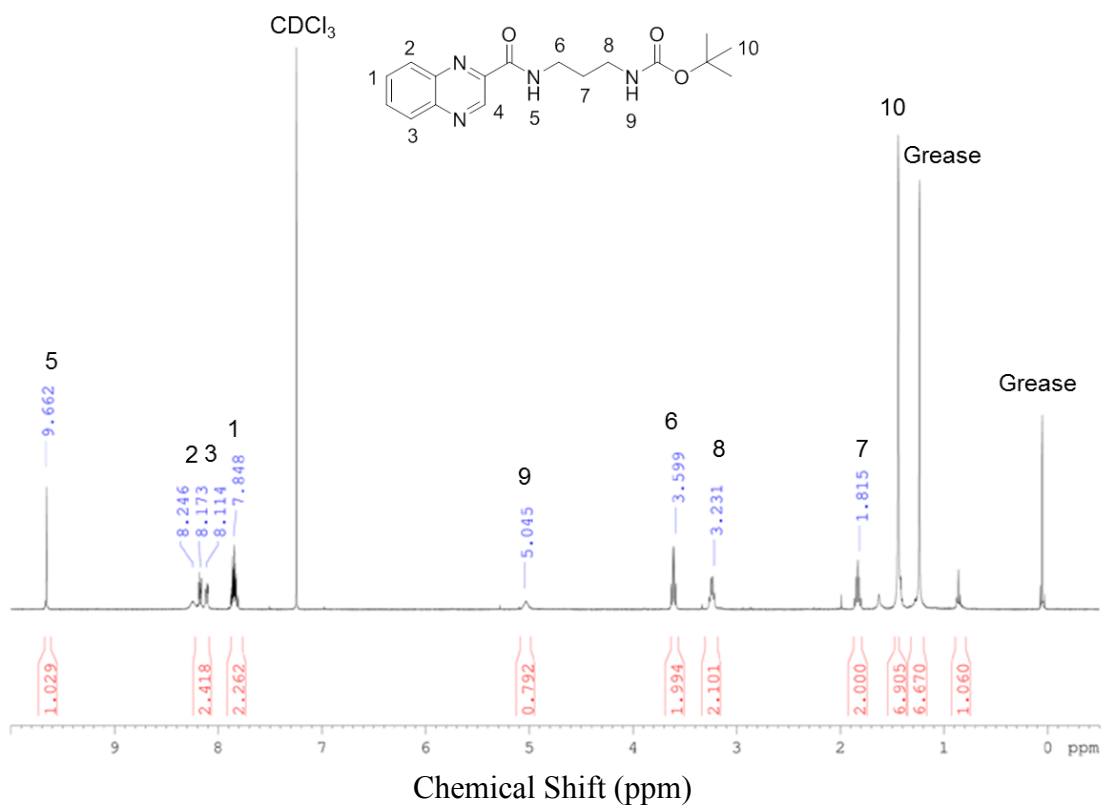
Figure B.18 ^{1}H NMR of **19** in CDCl$_3$ at 400 MHz
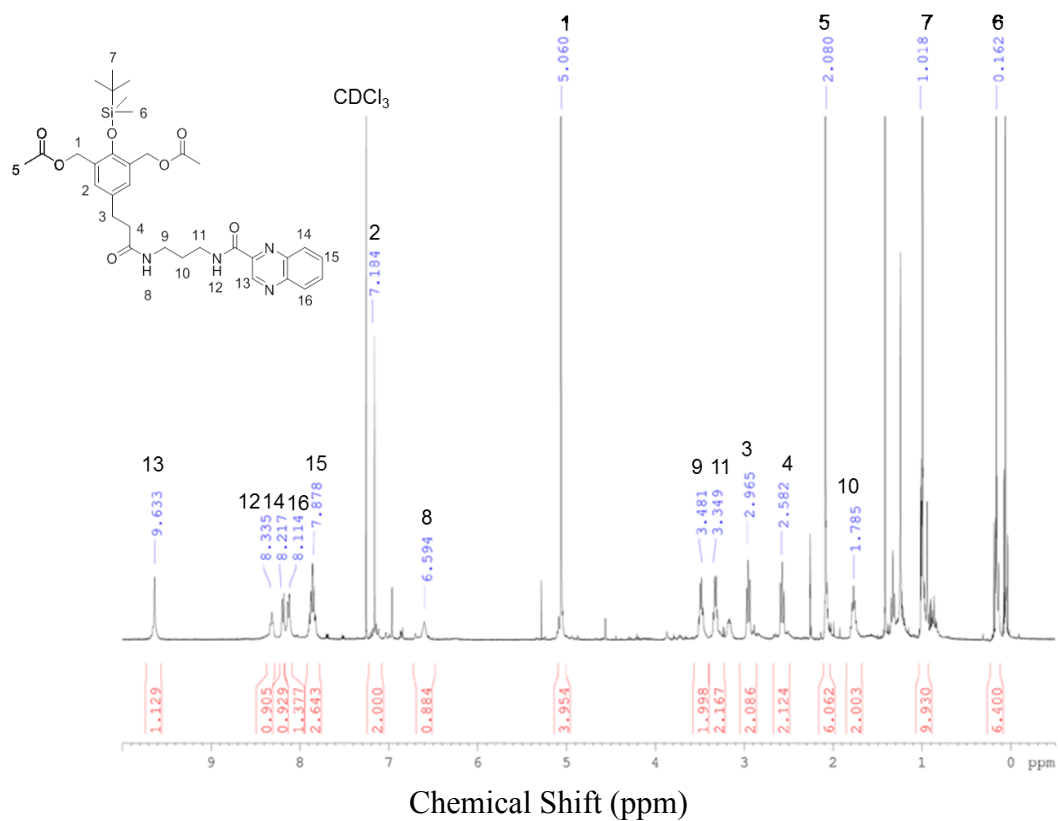
Figure B.19 ^{1}H NMR of **21** in CDCl$_3$ at 400 MHz
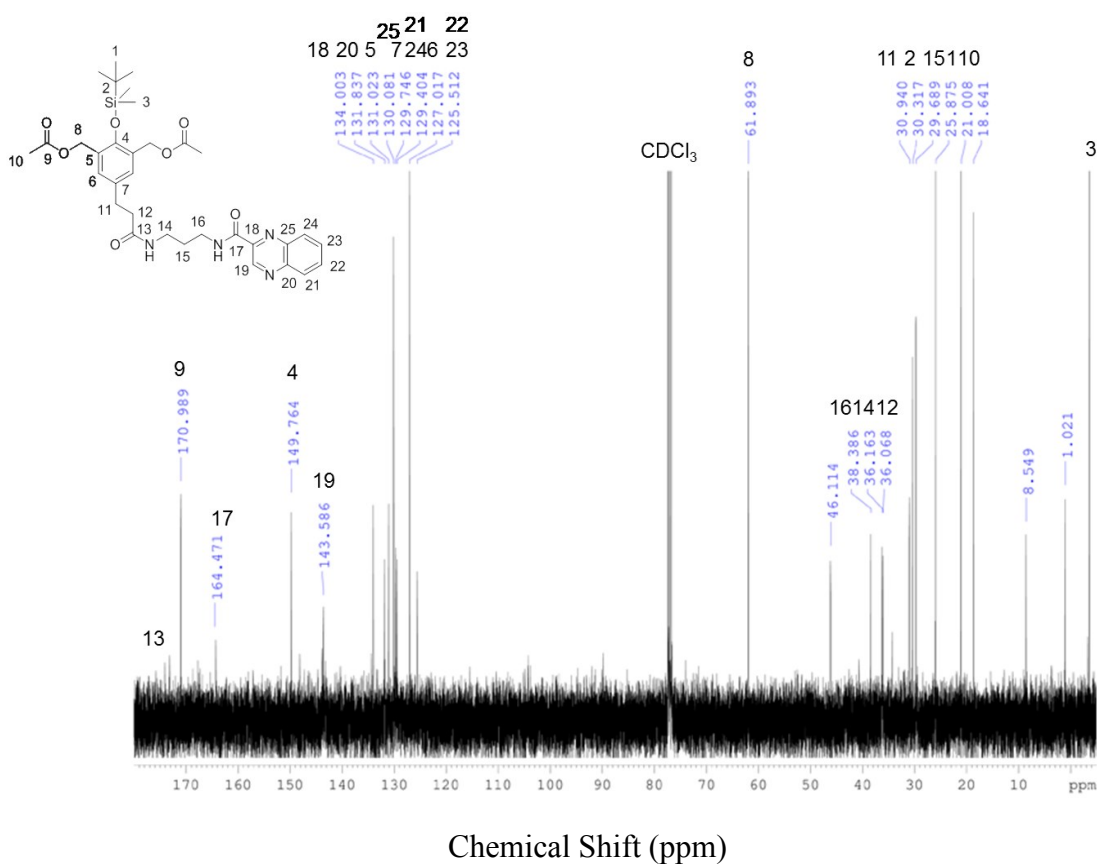
Figure B.20 ^{13}C NMR of **21** in CDCl$_3$ at 101 MHz

177
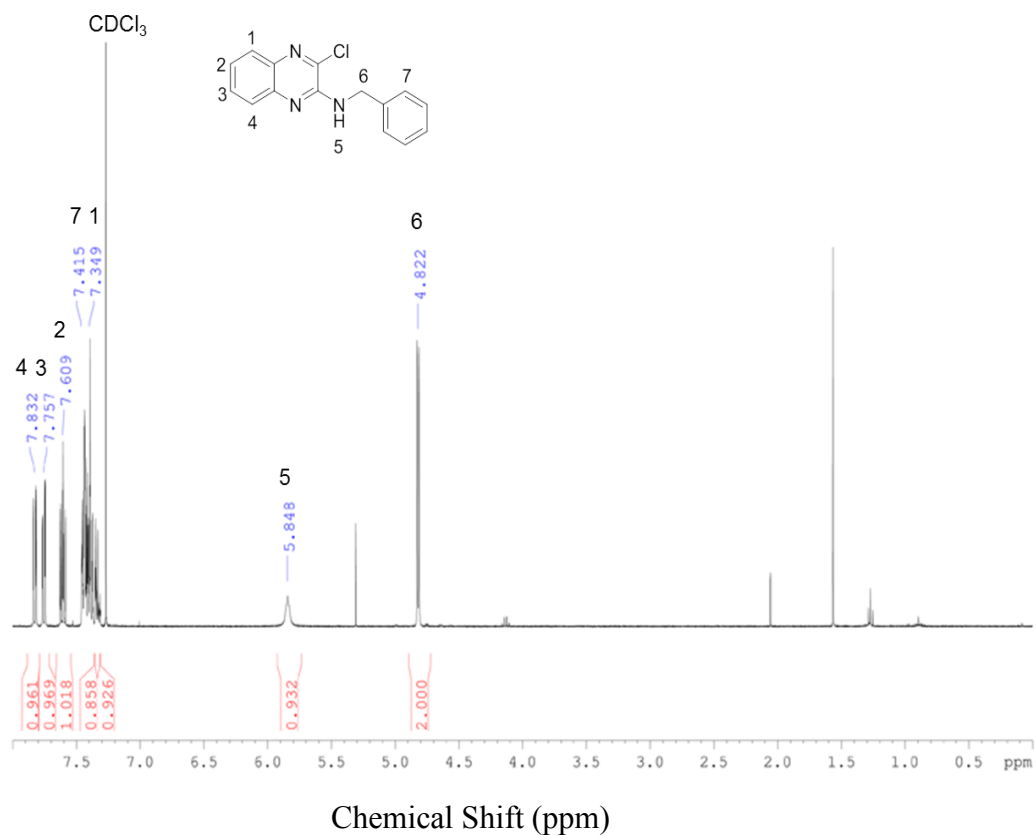
Figure B.21 ^{1}H NMR of **23** in CDCl$_3$ at 400 MHz
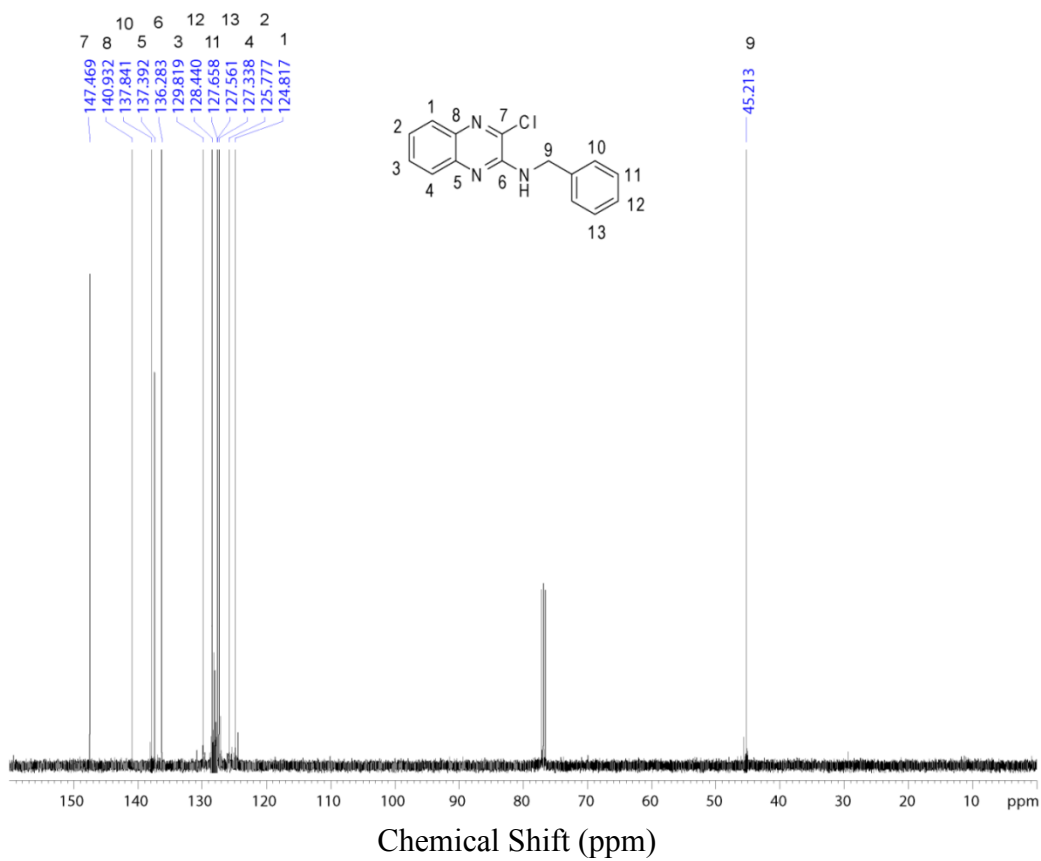
Figure B.22 ^{13}C NMR of **23** in CDCl$_3$ at 101 MHz

178
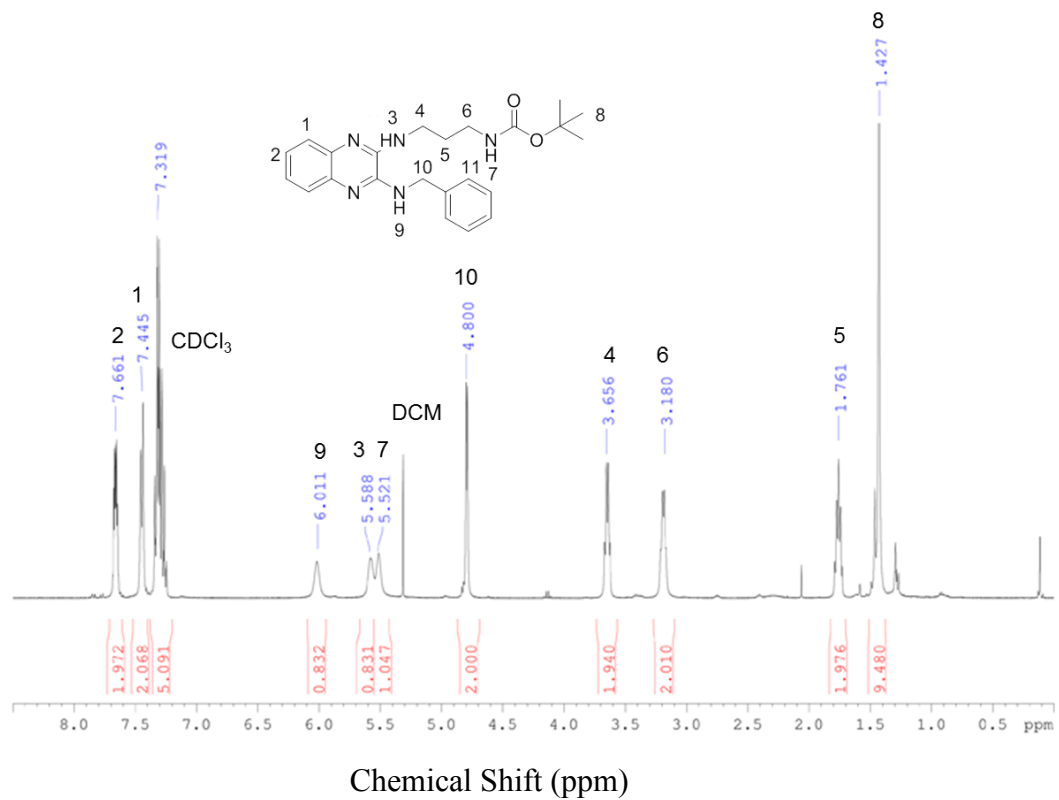
Figure B.23 ^{1}H NMR of 24 in CDCl$_3$ at 400 MHz
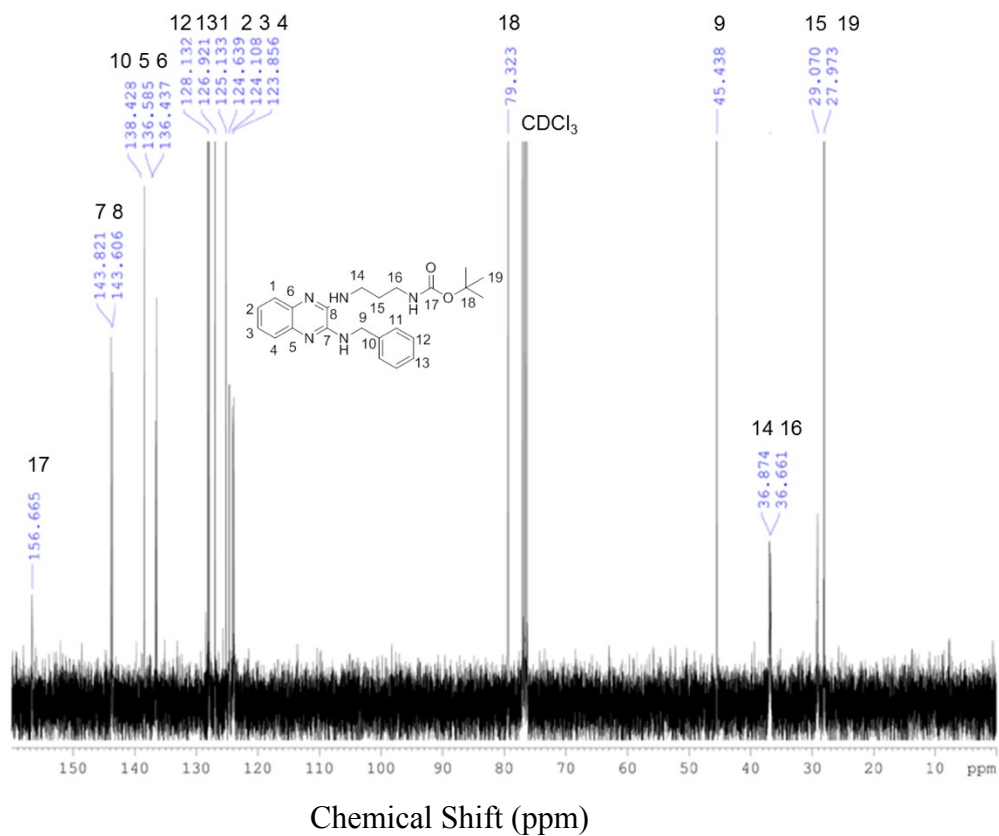
Figure B.24 ^{13}C NMR of 24 in CDCl$_3$ at 101 MHz
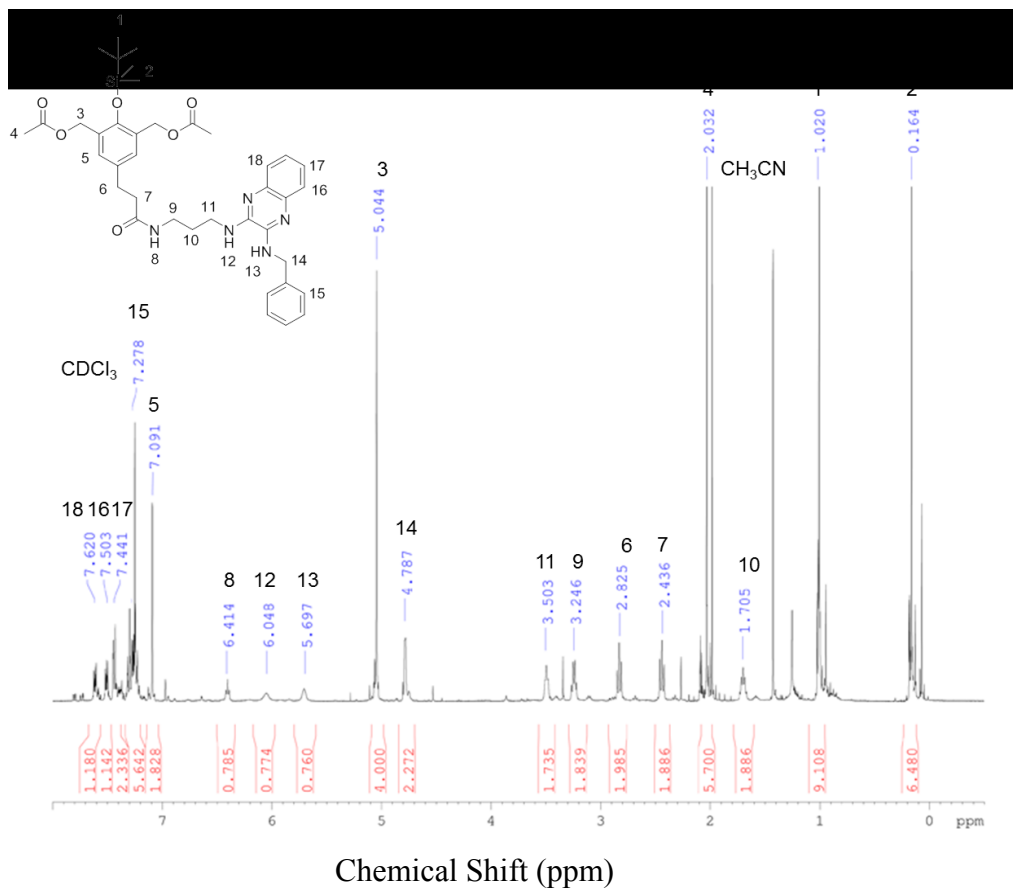
Figure B.25 ^{1}H NMR of **26** in CDCl$_3$ at 400 MHz
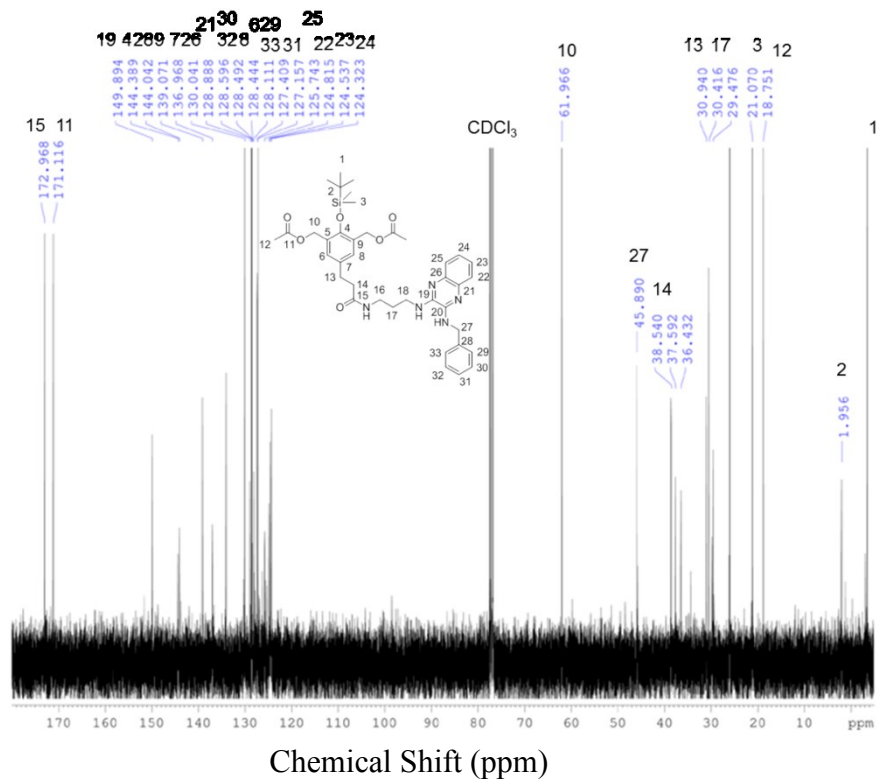
Figure B.26 ^{13}C NMR of **26** in CDCl$_3$ at 101 MHz
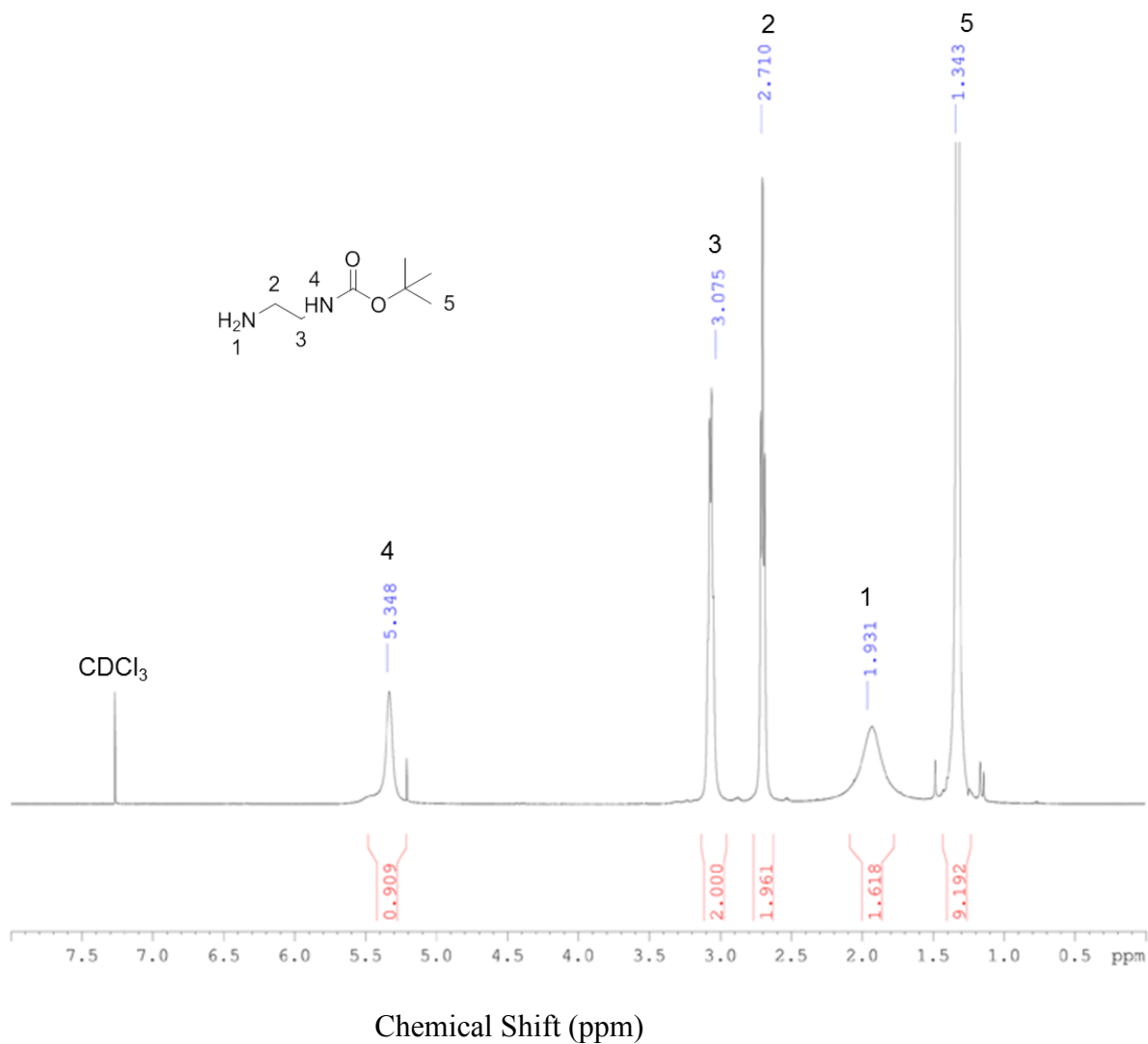
Figure B.27 ^{1}H NMR of 28 in CDCl$_3$ at 400 MHz
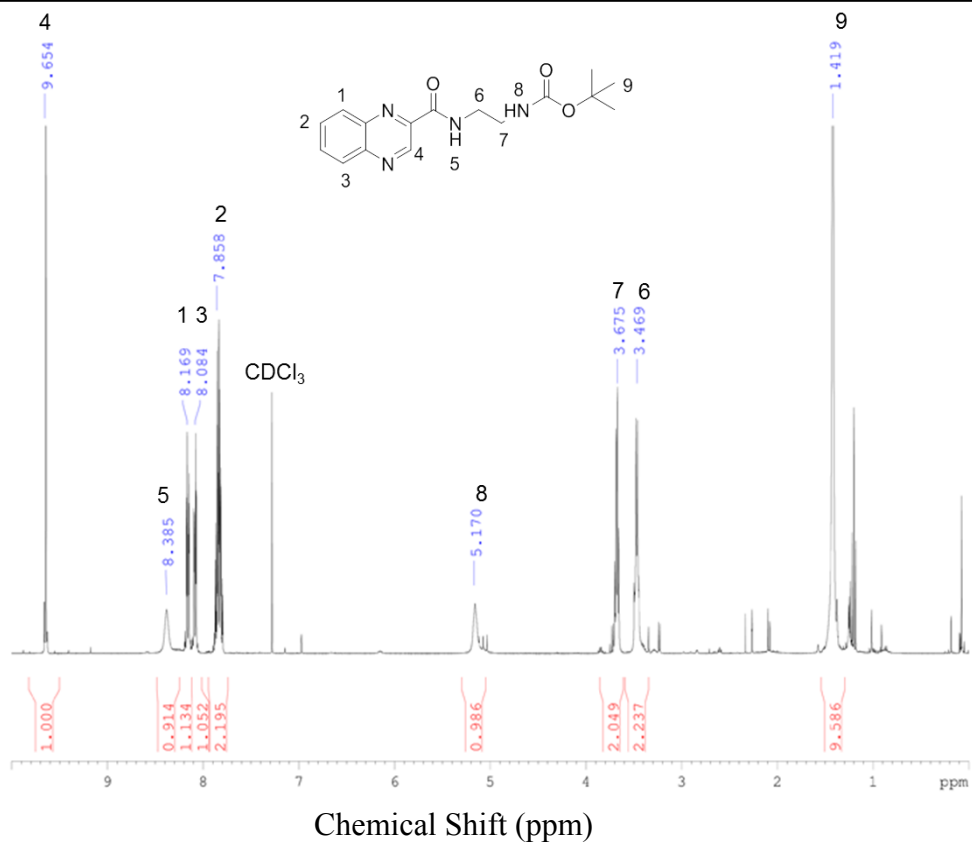
Figure B.28 ^{1}H NMR of **29** in CDCl$_3$ at 400 MHz
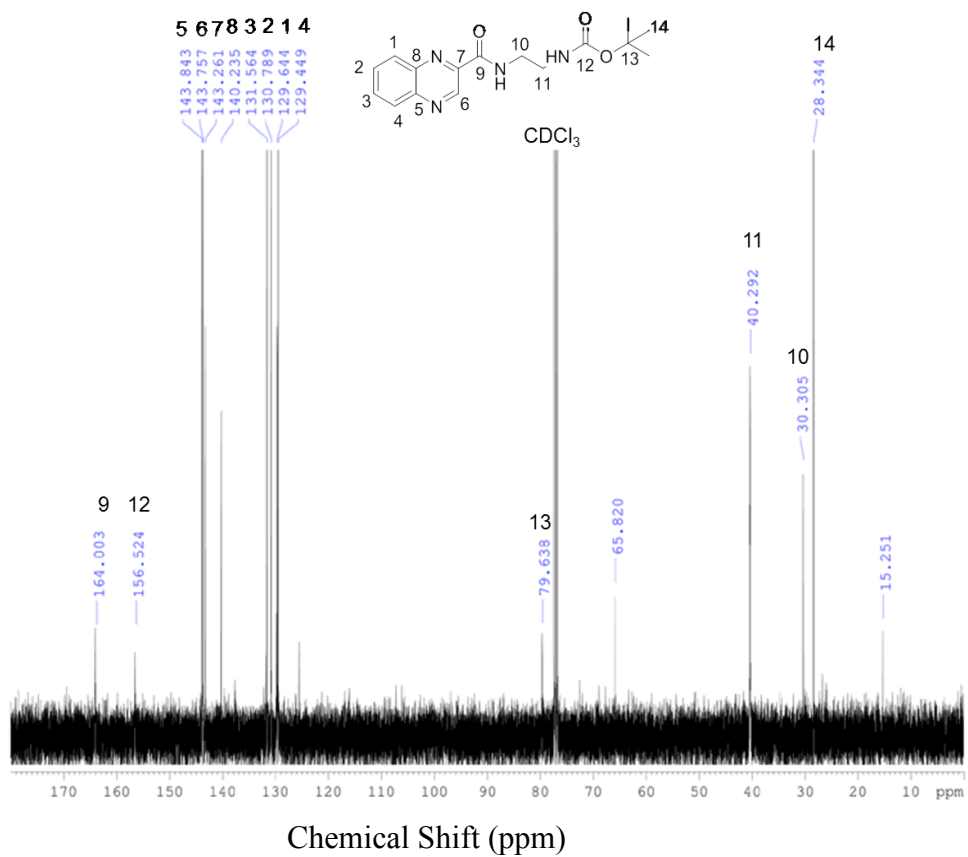
Figure B.29 ^{13}C NMR of **29** in CDCl$_3$ at 101 MHz
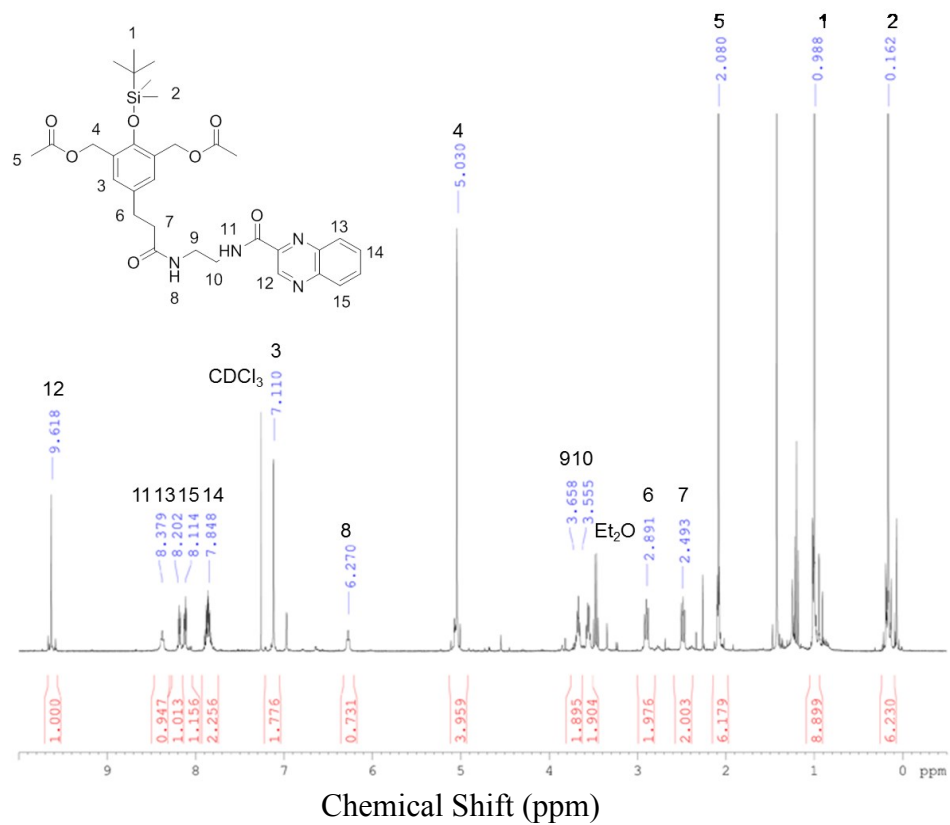
Figure B.30 ^{1}H NMR of **31** in CDCl$_3$ at 400 MHz
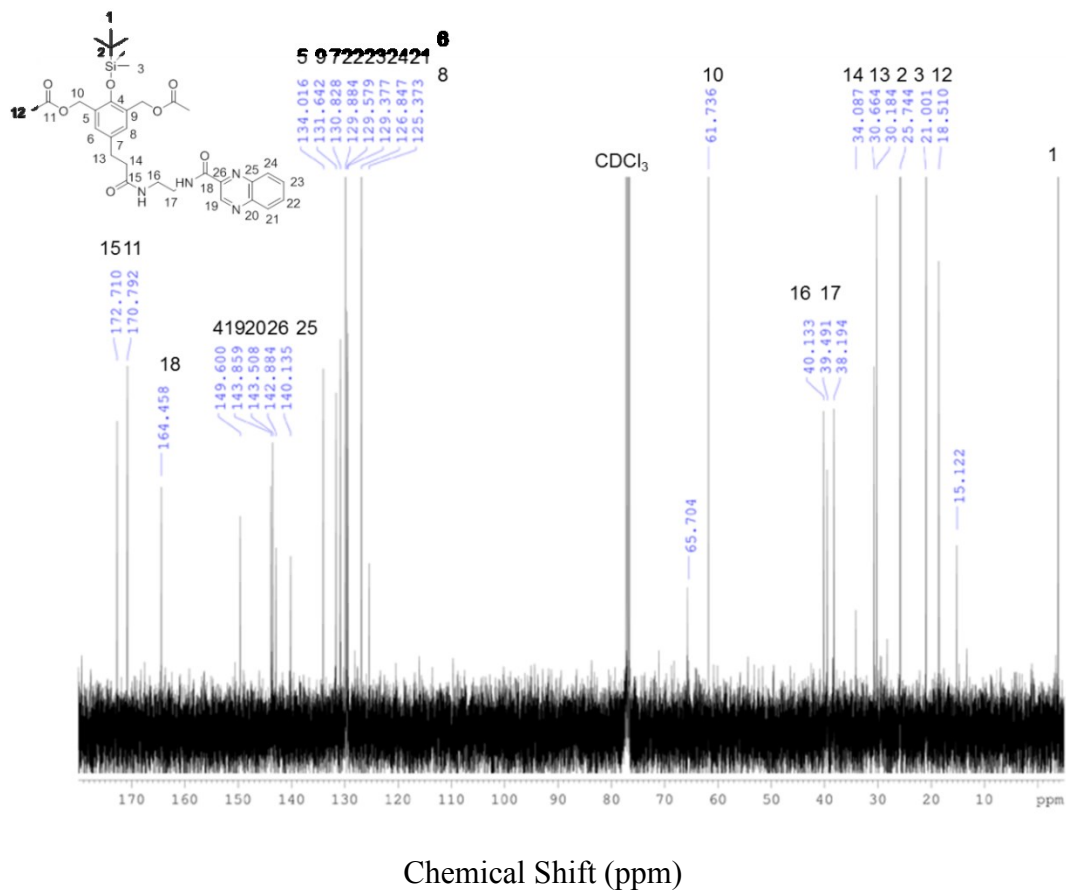
Figure B.31 ^{13}C NMR of **31** in CDCl$_3$ at 101 MHz
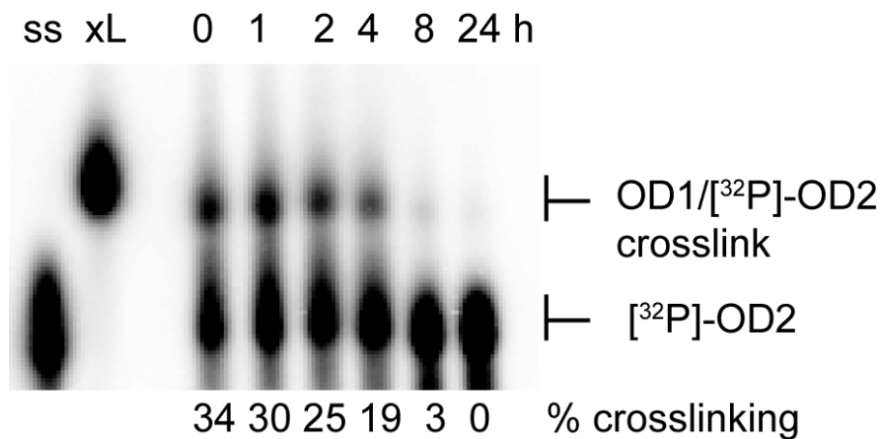
Figure B.32 Quenching of bisQMQuin3 by water. BisQMPQuin3 (500 μM) was incubated in MES (10 mM, pH 7), NaF (10 mM) and 20% acetonitrile for 0-24 h. At each time point, duplex DNA OD1/[^{32}P]-OD2 (3 μM) was added and allowed to react for 24 hours. Samples were frozen in liquid nitrogen and separated by 20% denaturing PAGE.
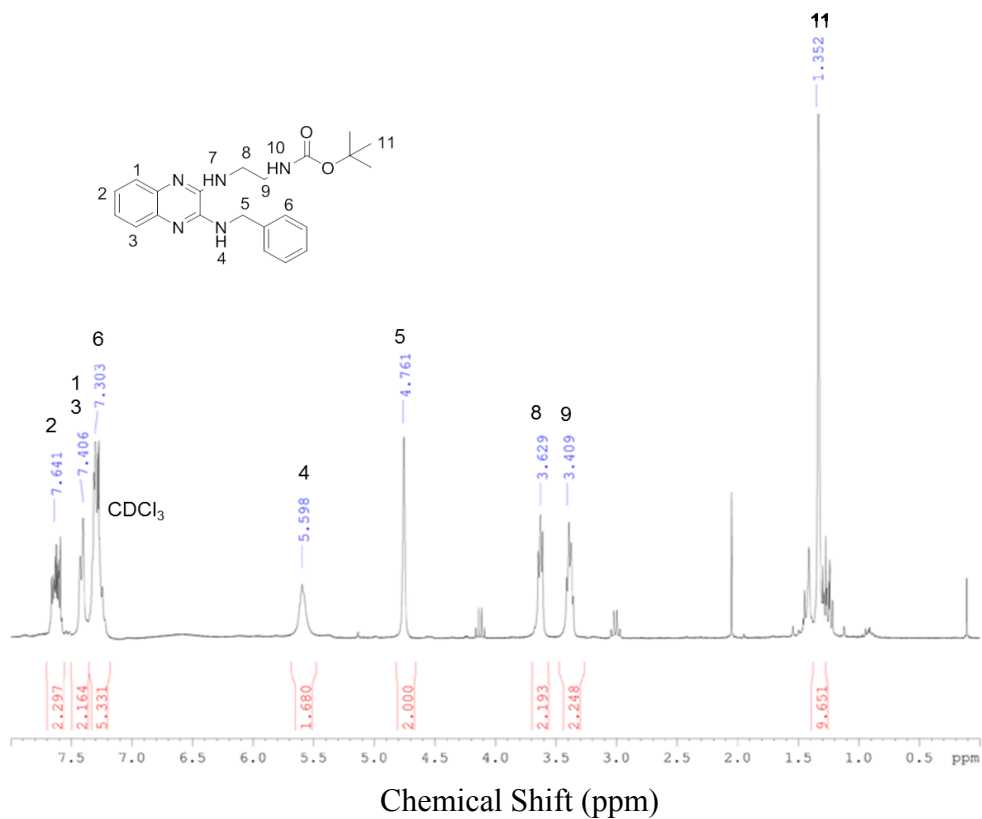
Figure B.33 ^{1}H NMR of **32** in CDCl$_3$ at 400 MHz
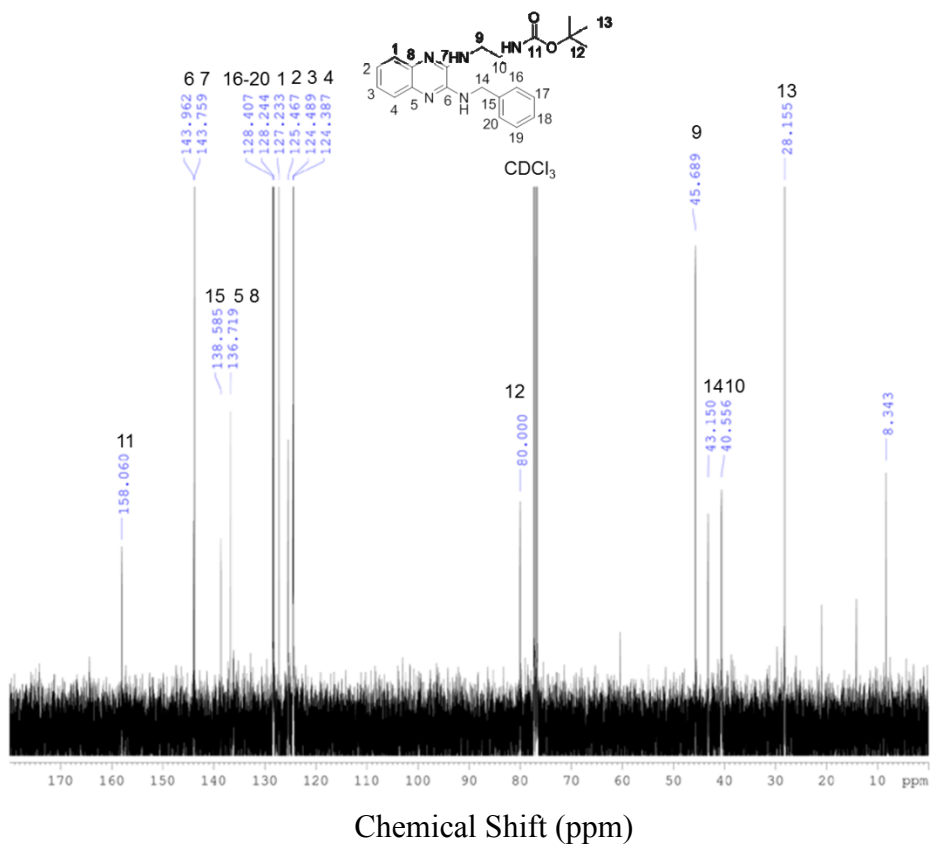
Figure B.34 ^{13}C NMR of **32** in CDCl$_3$ at 101 MHz

Chemical Shift (ppm)
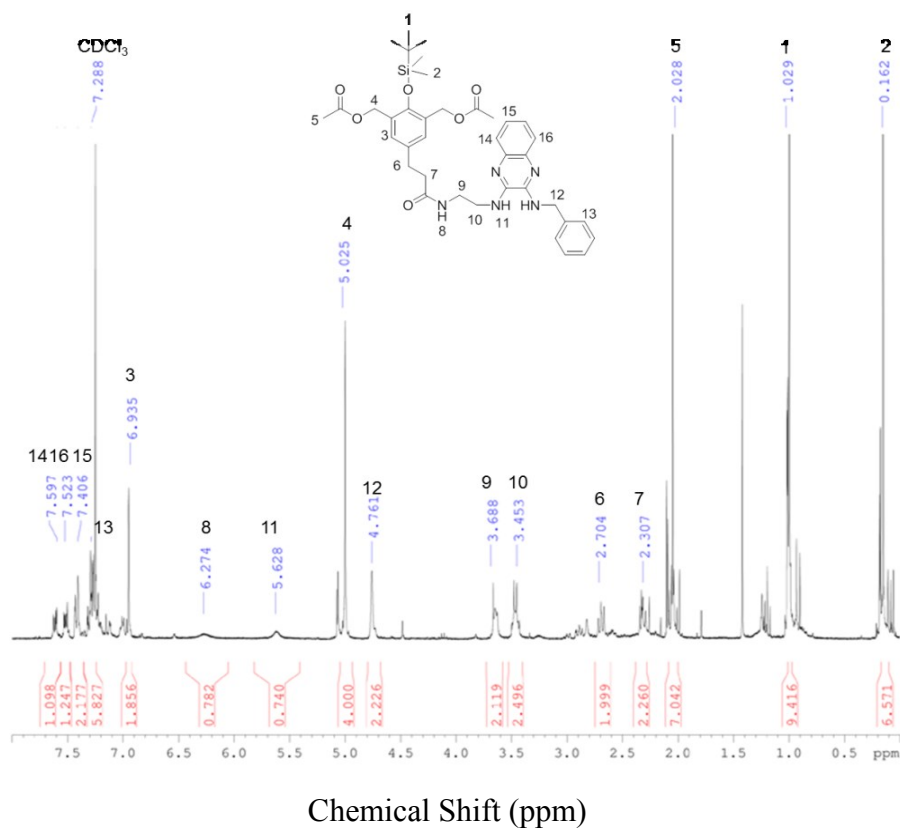
Figure B.35 ^{1}H NMR of **34** in CDCl$_3$ at 400 MHz

Chemical Shift (ppm)
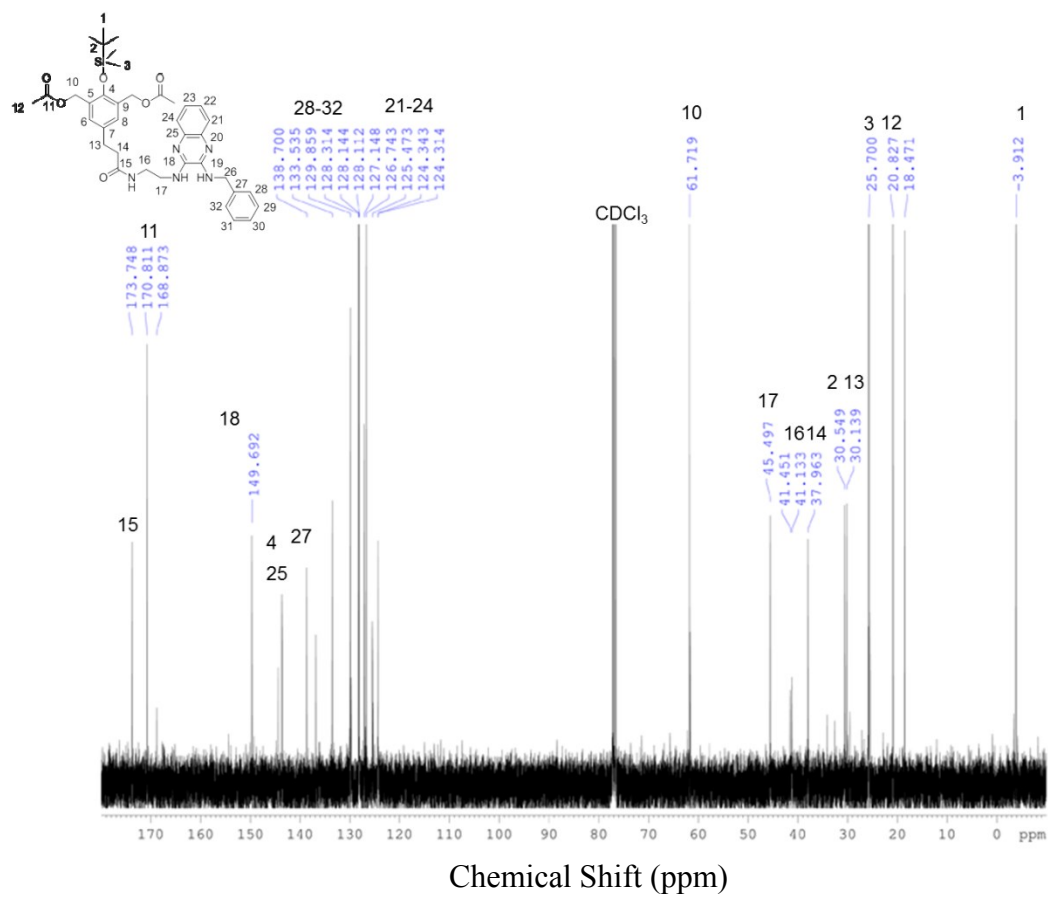
Figure B.36 ^{13}C NMR of **34** in CDCl$_3$ at 101 MHz

Appendix C: Supporting Information for Chapter 3
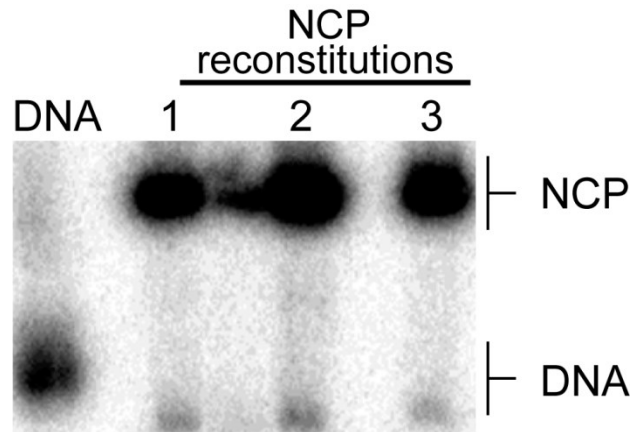
Figure C.1 Reconstitution of the nucleosome core particle. [^{32}P]-labeled Widom 601 duplex DNA (~1 pmol) and salmon sperm DNA (84 pmol) in NaCl (2 M) and BSA (1 mg/mL) were combined with the histone octamer (84 pmol) in 2 M NaCl, 10 mM HEPES pH 7.8, and 1 mM EDTA (1 µL). The samples were incubated under ambient conditions for 1 h before standard serial dilution with nucleosome reconstitution buffer (10 mM HEPES pH 7.5, 1 mM EDTA, and 1 mg/mL BSA). Each lane (1-3) represents independent reconstitution experiments that were analyzed by native PAGE (6%) and visualized by phosphorimagery.

601 Upper Strand (Ligation of 4 oligos)

I (30mer)   II (35mer)   III (35mer)   IV (45mer)

5' ▬▬▬▬▬ ▬▬▬▬▬ ▬▬▬▬▬ ▬▬▬▬▬▬

       ▬▬▬   ▬▬▬   ▬▬▬ 5'

V (20mer)   VI (20mer)   VII (20mer)
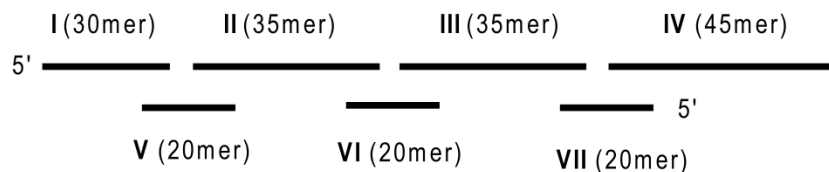
I: 5'- A_1TC GAT GTA TAT ATC TGA CAC GTG CCT GGA_{30} -3'

II: 5'- G_{31}AC TAG GGA GTA ATC CCC TTG GCG GTT AAA ACG CG_{65} -3'

III: 5'- G_{66}GG GAC AGC GCG TAC GTG CGT TTA AGC GGT GCT AG_{100} -3'

IV: 5'- A_{101}GC TGT CTA CGA CCA ATT GAG CGG CCT CGG CAC CGG GAT TCT GAT_{145} -3'

V: 5'- C_{251}TC CCT AGT CTC CAG GCA CG_{270} -3'

VI: 5'- C_{216}GC TGT CCC CCG CGT TTT AA_{235} -3'

VII: 5'- G_{181}TA GAC AGC TCT AGC ACC GC_{200} -3'

601 Bottom Strand (Ligation of 4 oligos)

VIII (35mer)   IX (30mer)   X (35mer)   XI (45mer)

5' ▬▬▬▬▬ ▬▬▬▬▬ ▬▬▬▬▬ ▬▬▬▬▬▬

       ▬▬▬   ▬▬▬▬▬   ▬▬▬ 5'

XII (20mer)   III (35mer)   XIII (20mer)
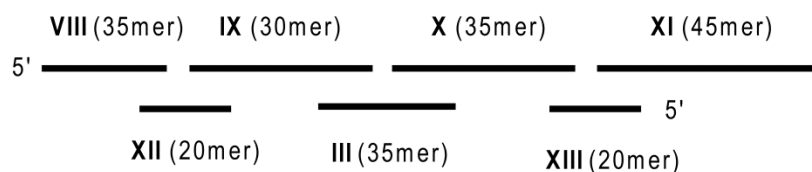
VIII: 5'- A_{146}TC AGA ATC CCG GTG CCG AGG CCG CTC AAT TGG TC_{180} -3'

IX: 5'- G_{181}TA GAC AGC TCT AGC ACC GCT TAA ACG CAC_{210} -3'

X: 5'- G_{211}TA CGC GCT GTC CCC CGC GTT TTA ACC GCC AAG GG_{245} -3'

XI: 5'- G_{246}AT TAC TCC CTA GTC TCC AGG CAC GTG TCA GAT ATA TAC ATC GAT_{290} -3'

XII: 5'- A_{101}GC TGT CTA CGA CCA ATT GA_{120} -3'

XIII: 5'- G_{36}GG AGT AAT CCC CTT GGC GG_{55} -3'

Figure C.2 Oligonucleotides used to ligate the Widom 601 duplex DNA.

188

Appendix D: Supporting Information for Chapter 5

A

1= uninduced cells
2= induced cells
3= clarified lysate
4= flowthrough column load
5= 10 mM imidazole wash
6= 100 mM imidazole wash
7-14 = 500 mM imidazole elution fractions

B

1= Ni-NTA pool
2= column wash
3-8 = ATP-agarose elution fractions 0.5 M KCl
9-14 = ATP-agarose elution fractions 1 M KCl
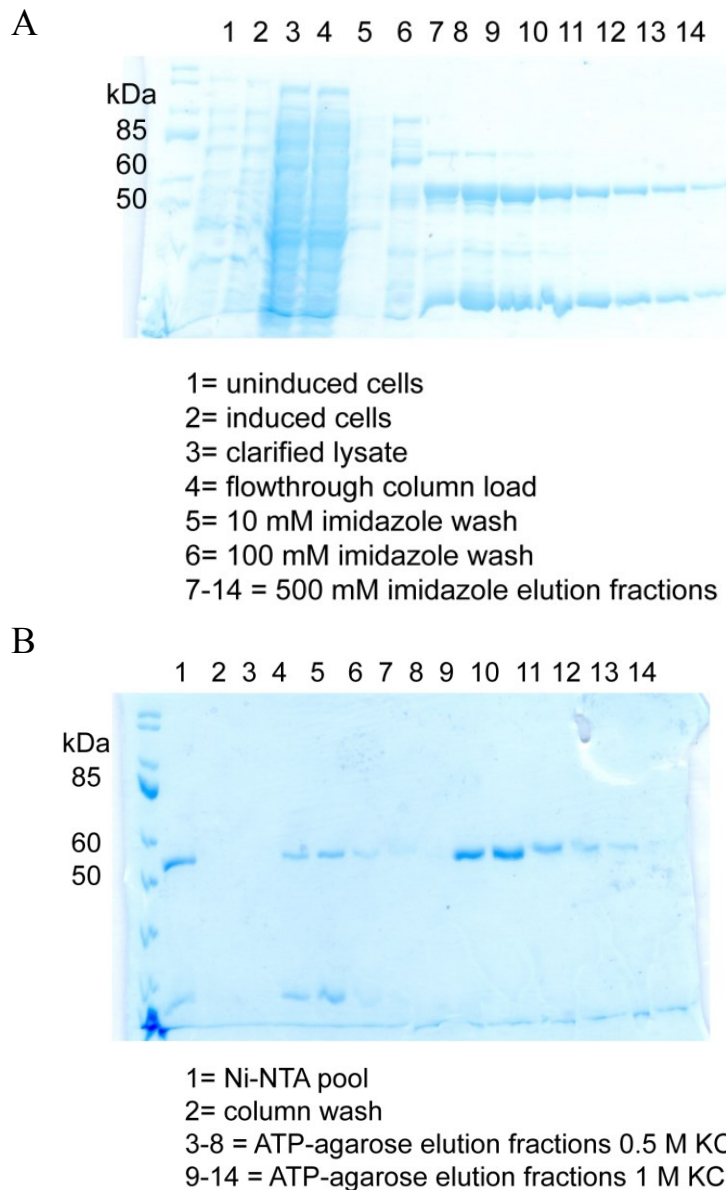
Figure D.1 Expression and purification of T7GP4. A) T7GP4 containing a His_{10}-tag was purified by affinity chromatography using a Ni-NTA column. Impurities were removed by washing with a gradient of 10-100 mM imidazole followed by elution with 500 mM imidazole. Fractions were collected, separated by 10% SDS-PAGE, and visualized by staining with Coomassie Blue. B) T7GP4 was further purified via affinity chromatography using an ATP-agarose column. The crude protein was loaded onto the column in buffer containing 10 mM Mg^{2+}, and impurities were removed by washing with buffer. Pure T7GP4 was eluted from the column using a buffer containing 20 mM EDTA and a gradient of 0.5-1 M KCl. Fractions were collected, separated by 10% SDS-PAGE, and visualized by staining with Coomassie Blue.
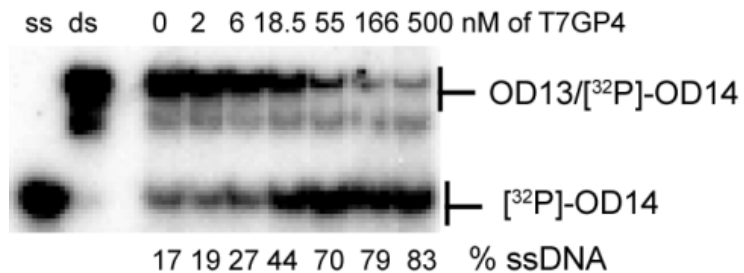
Figure D.2 Concentration dependent unwinding of OD13/[^{32}P]-OD14 duplex DNA by T7GP4. Preannealed OD13/[^{32}P]-OD14 (10 nM) was incubated with dTTP (1 mM) in buffer (40 mM Tris-HCl pH 7.5, 10 mM MgCl$_2$, and 50 mM potassium glutamate) and increasing monomer concentrations of T7GP4 (0, 2, 6, 18.5, 55, 166, and 500 nM) for 10 min at 37 °C. Reactions were quenched with EDTA (40 mM) and combined with bromophenol blue and xylene cyanol in 30% glycerol. Products were separated by 10% native PAGE and visualized by phosphorimagery. Yields are reported as the band intensity relative to the total signal in each lane.

Shane Byrne

2821 Saint Paul St.   (978)-424-5542
Baltimore, MD 21218   sbyrne9@jhu.edu

EDUCATION:

Johns Hopkins University   Baltimore, MD   **Sept. 2015-Oct. 2019**
- Ph.D candidate in the Chemistry-Biology Interface (CBI) Program.

Johns Hopkins University   Baltimore, MD   **Sept. 2015-June 2017**
- Master of Science, Chemical Biology

Boston College   Chestnut Hill, MA   **Aug. 2011-May 2015**
- Bachelor of Science, Chemistry
- Minor in Hispanic Studies
- Studied abroad at the Universidad Complutense de Madrid (Madrid, Spain) from Sept.- Dec. 2013

RESEARCH EXPERIENCE:

Dedon Laboratory, Massachusetts Institute of Technology   **Will begin in Jan. 2020**
Postdoctoral Researcher
- Advisor: Dr. Peter C. Dedon
- Project title: Exploration of DNA Phosphorothioate Modifications in the Human Gut Microbiome

Rokita Laboratory, Johns Hopkins University   **Feb. 2016-Oct. 2019**
Ph.D Candidate
- Advisor: Dr. Steven E. Rokita
- Thesis title: How DNA Packaging and Processing Proteins Affect Dynamic DNA Crosslinking
- Synthesized quinone methides and investigated their alkylation of DNA and interactions with DNA repair enzymes and polymerases
- Mentored 2 undergraduate students, 5 graduate rotation students, and 1 graduate student

Liu Laboratory, Boston College   **Jan. 2014-May 2015**
Undergraduate research student
- Advisor: Dr. Shih-Yuan Liu
- Project title: Olefin-bearing 1,2-azaborines: Precursors to polycyclic BN-antiaromatics
- Synthesized and characterized various olefin-bearing 1,2-azaborine substrates for ring closing metathesis reactions

Nazario Martín Laboratory, Universidad Complutense de Madrid   **Sept.-Dec. 2013**
Visiting undergraduate research assistant
- Advisor: Dr. Nazario Martín

- Worked with a graduate student to synthesize precursors to fullerenes and tetrathiafulvalenes

PUBLICATIONS:
1. Byrne, S.R.; Yang, K.; Rokita, S.E.; Effect of nucleosome assembly on alkylation by a dynamic electrophile. *Chem. Res. Toxicol.* **2019**, 32 (5), 917-925. DOI:10.1021/acs.chemrestox.9b00057
2. Byrne, S.R.; Rokita, S.E.; When biological machines encounter reversible crosslinks in duplex DNA. *In preparation.*
3. Hutchinson, M.A.; Deeyaa, B.; Byrne, S.R.; Williams, S.; Rokita, S.E.; Directing Quinone Methide-Dependent Alkylation and Cross-Linking of Nucleic Acids with Quaternary Amines. *In preparation.*

PRESENTATIONS:
Oral Presentations:
1. Byrne, S.R.; Rokita, S.E.; When biological machines encounter reversible crosslinks in duplex DNA. Gordon Research Seminar- Nucleosides, Nucleotides, and Oligonucleotides; **2019 June 22**; Newport, RI.
2. Byrne, S.R.; Rokita, S.E.; Effect of Nucleosome assembly on alkylation by a dynamic electrophile. Chromatin and Chromosomes Workshop; **2018 Dec. 17**; Johns Hopkins University Medical School, Baltimore, MD.
3. Byrne, S.R.; Yang, K.; Rokita, S.E.; Repair and processing of DNA lesions formed by a dynamic electrophile. 256th National Meeting of the American Chemical Society; **2018 Aug. 20**; Boston, MA.

Poster Presentations:
1. Byrne, S.R.; Rokita, S.E.; When biological machines encounter reversible crosslinks in duplex DNA. Gordon Research Conference- Nucleosides, Nucleotides, and Oligonucleotides; **2019 June 23-28**; Newport, RI.
2. Byrne, S.R.; Rokita, S.E.; When biological machines encounter reversible crosslinks in duplex DNA. Gordon Research Seminar- Nucleosides, Nucleotides, and Oligonucleotides; **2019 June 22-23**; Newport, RI.
3. Byrne, S.R.; Rokita, S.E.; When biological machines encounter reversible crosslinks in duplex DNA. 12th Frontiers at the Interface of Chemistry and Biology Symposium; **2019 May 3**; Bethesda, MD
4. Byrne, S.R.; Rokita, S.E.; When biological machines encounter reversible crosslinks in duplex DNA. Johns Hopkins Chemistry Department Recruitment Weekend; **2019 March 8**; Baltimore, MD.
5. Byrne, S.R.; Yang, K.; Rokita, S.E.; Effect of nucleosome assembly on alkylation by a dynamic electrophile. Chromatin and Chromosomes Workshop; **2018 Dec. 17**; Johns Hopkins University Medical School, Baltimore, MD.
6. Byrne, S.R.; Yang, K.; Rokita, S.E.; Effect of DNA processing on dynamic alkylation. Johns Hopkins University Chemistry-Biology Interface Program Annual Retreat; **2018 Sept 22**; Baltimore, MD.

7. <u>Byrne, S.R.</u>; Yang, K.; Rokita, S.E.; Processing DNA lesions formed by a dynamic electrophile. 11th Frontiers at the Interface of Chemistry and Biology Symposium; **2018 May 5**; Philadelphia, PA.
8. <u>Byrne, S.R.</u>; Yang, K.; Rokita, S.E.; Processing DNA lesions formed by a dynamic electrophile. Johns Hopkins Chemistry Department Recruitment Weekend; **2018 March 23**; Baltimore, MD.
9. <u>Byrne, S.R.</u>; Yang, K.; Rokita, S.E.; Effect of nucleosome assembly on alkylation by a dynamic electrophile. Johns Hopkins University Chemistry-Biology Interface Program Annual Retreat; **2017 Sept 23**; Towson, MD.
10. <u>Byrne, S.R.</u>; Hutchinson, M.A.; Rokita, S.E.; Reversible alkylation of nucleosomes by quinone methides. 10th Frontiers at the Interface of Chemistry and Biology Symposium; **2017 May 6**; Newark, DE.
11. <u>Byrne, S.R.</u>; Hutchinson, M.A.; Eller, A.L.; Weeks, R.A.; Rokita, S.E.; Migration of bifunctional quinone methides along DNA. Johns Hopkins Chemistry Department Recruitment Weekend; **2017 March 17**; Baltimore, MD.

SKILLS:
- Nucleic acid chemistry and biochemistry: ^{32}P-radiolabeling of DNA, analytical and preparative gel electrophoresis, chemical modifications of oligonucleotides, DNA sequencing, DNA-protein interactions, nucleosome reconstitution
- Organic synthesis: product purification via extractions, column chromatography, and recrystallization, and air-free synthetic techniques
- Analytical techniques: NMR, UPLC-MS, fluorescence, and UV-Vis spectroscopy
- Protein expression and purification: affinity and gel filtration chromatography
- Analysis of small molecule modifications of proteins using UPLC-MS/MS
- Fluent in the Spanish language

TEACHING EXPERIENCE:
Johns Hopkins Dean's Teaching Fellow   **Sept.- Dec. 2019**
- Awarded a fellowship to teach a new undergraduate course that I proposed, entitled "Nucleic Acids in Chemistry and Biotechnology"

Johns Hopkins University
Teaching Academy   **July 2018-Oct. 2019**
- Participated in a multi-phase program designed to train graduate students and post-docs as instructors and provide them with useful skills for their potential future faculty positions. I attended 6 workshops that discussed various topics of pedagogy, participated in a 3 day teaching institute, and will complete at least 6 hours of classroom teaching
Teaching Assistant
Chemical Biology I (Graduate course)   **Fall 2016, Fall 2018**
- Course Director: Dr. Steven E. Rokita
- Attended lectures, held weekly office hours and review sessions, and wrote problem sets

Chemical Biology II (Graduate course)   **Spring 2017**
  - Course Director: Dr. Steven E. Rokita
  - Attended lectures, held weekly office hours and review sessions, and wrote problem sets

Summer Institute for the Gifted   **July 2015**
Instructor
University of California, Los Angeles, CA
  - Designed and taught a three week chemistry course (Chemistry: The Essential Element) for gifted 11-12 year old students
  - Planned daily lessons that included a combination of lectures, class discussions, and laboratory experiments
  - Supervised a teaching assistant that helped with the course
  - Wrote detailed performance evaluations for each student at the end of the course

ACADEMIC LEADERSHIP:
CBI Student Invited Speaker Co-organizer   **June 2018-June 2019**
  - Led the nomination and voting process among the students of the CBI program to choose both a speaker from within Johns Hopkins and a speaker from outside of Johns Hopkins, and organized the schedule and logistics of the speakers' visits to Johns Hopkins

Chemistry Department Student Liaison Committee   **May 2017-Dec. 2019**
Chair
  - Organized monthly department happy hours within a defined budget, and established a bimonthly student lunch group to promote inclusion and support for students within the department

Homewood Grievance Committee   **Nov. 2017-May 2019**
  - Nominated by the chemistry department to serve on two ad hoc committees to hear and evaluate cases filed by graduate students in the Schools of Arts and Sciences and Engineering

Chemistry Department Student Safety Committee   **Dec. 2016-May 2019**
  - Attended monthly meetings to discuss safety concerns and initiatives in the department, and monitored safety issues in the Rokita lab

CONFERENCES AND SYMPOSIA ATTENDED:
  - Gordon Research Conference- Nucleosides, Nucleotides, and Oligonucleotides; Newport, RI, **2019 June 23-28** (poster presenter)
  - Gordon Research Seminar- Nucleosides, Nucleotides, and Oligonucleotides; Newport, RI, **2019 June 22-23** (speaker and discussion leader)
  - 11th Frontiers at the Interface of Chemistry and Biology Symposium, National Institute of Health, **2019 May 3** (poster presenter)
  - Chromatin and Chromosomes Workshop, Johns Hopkins University Medical School, Baltimore, MD, **2018 Dec 17** (speaker and poster presenter)

- 256th National Meeting of the American Chemical Society, Boston, MA, **2018 Aug 19-23** (speaker)
- 11th Frontiers at the Interface of Chemistry and Biology Symposium, University of Pennsylvania, **2018 May 5** (poster presenter)
- 8th Baltimore Area Repair Symposium, University of Maryland, Baltimore, **2018 March 12**
- 10th Frontiers at the Interface of Chemistry and Biology Symposium, University of Delaware, **2017 May 6** (poster presenter)
- 9th Frontiers at the Interface of Chemistry and Biology Symposium, Johns Hopkins University, **2016 May 14**

SOCIETY MEMBERSHIPS:
- American Chemical Society   **2018-present**
    - Division of Chemical Toxicology
    - Division of Biological Chemistry

AWARDS:
- Johns Hopkins 2019-2020 Dean's Teaching Fellowship   **Dec. 2018**
- Johns Hopkins Graduate Representative Organization Travel Grant   **Sept. 2018**
- ACS Division of Chemical Toxicology Outstanding Student Oral   **Aug. 2018**
  Presentation, Honorable Mention
- ACS Division of Chemical Toxicology Travel Award   **July 2018**
- CBI Travel Award   **July 2018, July 2019**
- Boston College Undergraduate Research Fellowship   **June & Sept. 2014, Jan. 2015**
- Boston College Dean's List (6 semesters)   **Dec. 2012-May 2015**